



Lehrstuhl für Biotechnologie der Nutztiere

Cre/loxP-mediated tissue specific activation
of oncogene expression in pigs

Érica Alessandra Schulze

Vollständiger Abdruck der von der Fakultät Wissenschaftszentrum Weihenstephan für Ernährung, Landnutzung und Umwelt der Technischen Universität München zur Erlangung des akademischen Grades eines

Doktors der Naturwissenschaften

genehmigten Dissertation.

Vorsitzende(r):

Prof. Dr. Wilhelm Windisch

Prüfer der Dissertation:

1. Prof. Angelika Schnieke, Ph.D.

2. Priv.-Doz. Dr. Günter Schneider

Die Dissertation wurde am 7.12.2017 bei der Technischen Universität München eingereicht und durch die Fakultät Wissenschaftszentrum Weihenstephan für Ernährung, Landnutzung und Umwelt am 16.03.2018 angenommen.

Table of Contents

1 Introduction.....	1
1.1 Cancer animal models.....	1
1.1.1 Mouse cancer models.....	1
1.1.2 Need for porcine cancer models.....	3
1.2 Generation of transgenic pigs.....	5
1.2.1 Genetically engineered porcine cancer models.....	6
1.2.2 Cre/ <i>loxP</i> recombination system.....	9
1.2.3 Modified <i>loxP</i> sites.....	11
1.3 Temporal and spatial control of Cre recombinase activity.....	13
1.3.1 Tissue-specific Cre recombinase.....	13
1.3.2 Inducible cre recombinase.....	25
1.4 Aim of this work.....	28
2 Material and Methods.....	29
2.1 Material.....	29
2.1.1 Buffers and solutions.....	29
2.1.2 Chemicals.....	29
2.1.3 Chemicals for Southern blot analysis.....	30
2.1.4 Disposables.....	31
2.1.5 Cell culture media.....	31
2.1.6 Cell culture antibiotics.....	32
2.1.7 Supplements, chemicals and solutions for cell culture.....	32
2.1.8 Bacterial and mammalian cells.....	33
2.1.9 Cloning vectors and plasmids.....	34
2.1.10 Kits for DNA, RNA isolation.....	34
2.1.11 Enzymes.....	35
2.1.12 Oligonucleotides.....	35
2.1.13 Miscellaneous.....	38
2.1.14 Equipment.....	38
2.1.15 Software.....	39
2.2 Methods.....	40
2.2.1 Tissue culture methods.....	40
2.2.2 Molecular biology methods.....	48
2.2.3 Microbiology methods.....	55
3 Results.....	56
3.1 Suitable tissue-specific promoters.....	56
3.1.1 Construction and tests of tissue-specific Cre vectors.....	57
3.1.2 Construction of gene targeting vectors for insertion of tissue-specific Cre at the <i>ROSA26</i> locus.....	63
3.2 Gene placement of pancreas-specific Cre constructs at the porcine <i>ROSA26</i> locus.....	65
3.2.1 Detection of PDX-Cre target cell clones by RT-PCR, PCR and Southern Blot.....	67
Southern blot analysis.....	69
3.2.2 Detection of correctly PDX-Cre R26 retarget cell clones by PCR.....	70

3.2.3 Somatic cell nuclear transfer.....	71
3.3 PDX-Cre R26 gene targeted piglet analyses.....	71
3.4 New strategies for directing colon and pancreas specific Cre expression.....	74
3.4.1 Construction of iCre vectors.....	74
3.4.2 Cre and improved Cre recombinase expression test.....	75
3.4.3 Modification of colon- and pancreas-specific Cre expression constructs.....	78
3.5 Generation of pancreas-specific Cre driver pig lines.....	86
3.6 Generation of colon-specific Cre driver pig lines.....	86
3.6.1 Detection of tissue specific recombination.....	88
3.7 <i>In vitro</i> inducible Cre expression.....	95
3.7.1 Comparison of pSV40-βG-Cre-ERT ² with pPGK-Cre-ERT ² vector.....	95
3.7.2 pPGK-Cre-ERT ² vector construction and leakiness test.....	96
3.7.3 Generation of Cre recombinase with two 4-OHT binding domains and functionality test in reporter cells.....	97
4 Discussion.....	100
4.1 Identification, isolation and characterization of suitable promoters to drive tissue-specific Cre expression in different organs.....	100
4.1.1 Assessment of promoter function <i>in vitro</i>	101
4.2 Gene placement and gene stacking at the porcine <i>ROSA26</i> gene.....	104
4.2.1 Construction of vectors for promoter trap gene targeting.....	104
4.2.2 Gene placement and targeting efficiency.....	106
4.3 <i>In vivo</i> characterization of Cre expression in transgenic pigs.....	108
4.3.1 Analysis of PDX-Cre targeted piglet.....	108
4.3.2 Optimisation and evaluation of vectors for pancreas- and colon-specific expression.....	109
4.3.3 Analysis of Villin-iCre piglet.....	110
4.4 <i>In vitro</i> inducible Cre expression.....	112
5 Final remarks and outlook.....	115
6 Abbreviations.....	116
7 References.....	122
8 Appendix.....	139
9 Acknowledgment.....	155
10 Curriculum Vitae.....	156

Abstract

The use of livestock animals to model human cancers depends on the ability to control expression of mutated oncogenes or tumour suppressor genes in a spatial- and temporal-specific manner. A powerful means for conditional gene expression in a target tissue is the Cre/loxP system, which is widely used in mice. Although the power of the technique is well recognized, the Cre/loxP system for inducible gene expression has not yet been extended to large animals, i.e. pigs.

In this work, different approaches to create pancreas-, lung- and gut-specific Cre-driver pig lines for cancer research were investigated. Several constructs for Cre expression under the control of pancreas- and lung-specific promoters were generated and inserted at the permissive porcine *ROSA26* locus in primary porcine cells by homologous recombination. PDX-Cre gene-targeted cell clones, were used for nuclear transfer and founder animals were obtained. Analysis of piglets indicated that they carried the construct at the targeted *ROSA26* locus and confirmed the integrity and structure of the transgene, but expression of Cre was not sufficient to excise a loxP-flanked lox-stop-lox cassette. Consequently, new vectors were created that carried a mammalian improved Cre recombinase (iCre) and in some constructs also PDX-1 enhancer element was included. Constructs carrying iCre driven by the PDX-1 or villin (gut specific) promoter were used to transfect porcine primary cells, which carried a dual-reporter cassette (floxed mTomato followed by mGFP), to visualize Cre activity. Transgenic cell pools were used for nuclear transfer and pregnancies were established. Three piglets carrying the villin-iCre construct were born but were not viable. Tissue samples were collected and showed expression of mGFP only in tissues which normally express the villin gene, e.g. intestinal crypt cells. In one animal, a malformation of the intestinal crypts was observed, indicating that high Cre expression might interfere with normal intestine development.

To enhance the utility of Cre/loxP system, to avoid possible embryonic lethality and to extend life expectancy, another approach was applied, aiming at controlling the Cre activity in a temporal manner. For this, two tamoxifen-inducible forms of Cre were compared in vitro (Cre-ER^{T2} and ER^{T2}-Cre-ER^{T2}). Efficient recombination without leaky effect was observed using the fusion protein containing Cre recombinase with two modified estrogen receptor ligand binding domains flanking the Cre protein. This can be combined with the villin promoter to enable gut specific, inducible expression of mutated oncogenes or tumour suppressor genes.

Zusammenfassung

Um menschliche Krebserkrankungen in Großtieren akkurat modellieren zu können, ist eine zeitlich und räumlich spezifische Gendeletion oder Expression von fundamentalem Nutzen. Das Cre/loxP-System, welches häufig in transgenen Mäusen eingesetzt wird, ermöglicht eine extrinsische Kontrolle über konditionelle Genexpression in ausgewählten Zielgeweben. Dieses international anerkannte System wurde trotz reger Verwendung in der Maus bisher noch nicht umfassend in Großtieren und besonders Schweinen etabliert.

In der vorliegenden Arbeit wurden verschiedene Ansätze durchgeführt und analysiert um Pankreas-, Lungen- und Kolongewebe-spezifische Cre-Rekombinase-Expression in Schweinen für die Krebsmodellierung zu generieren. Hierfür wurden DNA-Konstrukte mit Cre-Rekombinase gekoppelt mit bauchspeicheldrüsen- und lungenspezifischen Promotoren generiert welche via homologer Rekombination zielgerichtet in den *ROSA26*-Lokus primärer Schweinezellen stabil integriert werden sollten. Klone mit gezielter PDX-Cre-Integration im *ROSA26*-Lokus wurden für Nukleartransfer eingesetzt und führten zu der Geburt transgener Gründertiere. Die Ferkel trugen das Konstrukt im *ROSA26*-Lokus in erwarteter Struktur und Integrität, aber die Expression von Cre war nicht ausreichend, um eine loxP-flankierte Lox-Stop-lox-Kassette zu exzidieren. Daher wurden neue Vektoren hergestellt, die eine für Säugetierzellen verbesserte Cre-Rekombinase (iCre) unter der Kontrolle von PDX-1 oder Villin-Promotoren und in einigen Fällen zusätzlich ein *Enhancer*-Element enthielten. Mittels zufälliger Transgen-Integration wurden die Konstrukte dann in primäre porcine Reporter-Zellen eingebracht. Diese Reporter-Zellen, tragen ein duales Fluoreszenz-Reporter-System (Floxed mTomato gefolgt von mGFP), welches die Cre-Rekombinase-Aktivität und Exzision der mTomato durch mGFP-Expression visualisiert. Transgene Zellpools wurden für den Kerntransfer verwendet und es wurden Schwangerschaften etabliert. Drei totgeborene Ferkel trugen das Villin-iCre-Konstrukt in sich. Gewebeproben wurden gesammelt und zeigten mGFP-Expression ausschließlich in den Darmkrypten sowie in Villin spezifischen Geweben. Bei einem Ferkel wurde eine Fehlbildung der Darmkrypten beobachtet, was darauf hindeutet, dass eine hohe Cre-Expression die normale Darmentwicklung beeinträchtigen könnte.

Um die Verwendung des Cre/loxP-Systems zu verbessern, Totgeburten zu verhindern und die Lebenserwartung von Ferkeln zu verlängern, wurde nachfolgend an einer zeitlich begrenzten Cre-Aktivität gearbeitet. Zwei Tamoxifen-induzierbare Formen der Cre-Rekombinase wurden *in vitro* miteinander verglichen (Cre-ER^{T2} und ER^{T2}-Cre-ER^{T2}). Effiziente Rekombination wurde mit einer Cre-Rekombinase erzielt, die zuvor mit je einer modifizierten Estrogen-Rezeptor-Ligandenbindungsdomäne an beiden Enden fusioniert worden war. Dies kann mit dem Villin-Promotor kombiniert werden, um Darm-spezifische, induzierbare Expression von mutierten Onkogenen oder Tumorsuppressorgenen zu ermöglichen.

1 Introduction

1.1 Cancer animal models

Cancer is a leading cause of death and morbidity worldwide. In particular, lung cancer accounts for the highest number of cancer deaths in the world, followed by breast cancer in women, prostate cancer in men and colorectal and pancreatic cancers in both sexes (Jemal *et al.*, 2010).

To date, progress in cancer research has led to the possibility of early diagnosis of malignant tissue and some efficient treatments for neoplasia (Stracci, 2009). However, cancer remains a serious disease. Notably the chance of surviving with many forms of cancer decreases markedly if positive identification is delayed. Therefore it is important to develop methods of early diagnosis as well as early intervention. Modelling events that occur during human cancer in animals is a useful means of investigating novel diagnostics and therapeutics.

1.1.1 Mouse cancer models

Numerous murine models have been created to study human cancer pathogenesis. These models are not only used to investigate transformation of normal cells to malignant, invasive and metastatic tumor cells (Richmond and Su, 2008), but also to investigate cancer drug candidate efficacy and mechanism(s) of action (Singh and Johnson, 2006).

One widely used model to analyze drug response therapy is the xenograft model (Singh and Johnson, 2006). The two main types of human xenograft mouse models used are defined by the location of the implanted xenograft, with heterotopic (tumor fragment implanted into an unrelated area of the original tumor site) or orthotopic (the same location as the original tumor) implantation of human tumor cell lines or tumor biopsies (*ex vivo* xenograft model) in immunocompromised mice (Huynh *et al.*, 2011). However, these models are not able to recapitulate the full intra-tumor heterogeneity (Politi and Pao, 2011). Another difficulty when using xenograft models is failure to engraft after implantation, which can reach more than 90% depending on the type of cancer. These engraftment failures may be due to the lack of a niche consisting of stromal tissue that preferentially support the growth of tumor cells or due to heterotopic implantation (Herter-Sprie *et al.*, 2013). Despite the fact that orthotopic xenografts can be appropriately placed in an organ to suitably reproduce the necessary environment in which the tumor grows, it is more complicated to have an accurate representation of tumor microenvironment, being difficult to quantify the tumor growth. Also they still have other disadvantages as being expensive, technically challenging and time consuming (Richmond and

Su, 2008). In addition, the predictive utility of xenografts for human clinical trials has been limited (Singh and Johnson, 2006). To present, despite beneficial findings for a drug therapy in preclinical xenograft models, in clinical trials the same therapy shows only modest efficacy to no effect (Kerbel 2003). As follows, this provoked uncertainty of using such preclinical models for early stage *in vivo* preclinical drug testing. This situation demands better preclinical models for early stage *in vivo* drug testing. Therefore, to circumvent the above-mentioned drawbacks genetically engineered mouse models (GEMMs) are created to recapitulate genetic alterations occurred in human spontaneous tumors (Kerbel 2003).

To mimic spontaneous tumor formation in humans, one or more genes of GEM models are manipulated (mutated, deleted or over-expressed). By altering cancer-associated genes, it is possible to allow immune, inflammatory and angiogenic processes to interact with the developing tumor (Politi and Pao, 2011). Additionally, a pronounced influence on tumor development due to the presence of a functional innate immune system can be studied (Herter-Sprie *et al.*, 2013).

GEM models are being developed to study the molecular and cellular aspects of tumorigenesis in the early and late stages of development (Politi and Pao, 2011). It is possible to induce genetic abnormalities that are present in human tumors in a tissue-specific and time-controlled fashion (Richmond and Su, 2008). Although GEM models are useful systems for basic studies of many human diseases including cancer, they are still of limited value in preclinical studies. They differ considerably from humans in size, general physiology, anatomy and life span, as well as pharmacokinetics and toxicokinetics (Herter-Sprie *et al.*, 2013).

The prognostic usefulness of conventional mouse cancer models for human clinical trials has been limited as historically they proved to be poor predictors of clinical efficacy. Similarly GEM models cannot fully represent the genetic complexity of human tumors, even though being capable of dissect the effects of specific genomic alterations present in a tumor (Herter-Sprie *et al.*, 2013). Despite the extensive similarities between mouse and human organ systems, subtle physical and biological variations between the two species lead to differing responses to cancer, altering the tumor phenotype drastically. When germline mutations associated with several human cancer genes are introduced into the mouse genome, different tumor phenotypes are produced compared to the human (Rangarajan and Weinberg, 2003). Similarly, common spontaneous tumors are rare in mice compared to humans (Anisimov *et al.*, 2005) and the phenotype seen in many metastatic human cancers can be rarely recapitulate. Due to the fewer genetic and/or epigenetic alterations to the cell genome that are necessary to give rise to tumors in GEMMs than in humans. Moreover, tumors in GEMMs are engineered to progress rapidly, as a result the tumors increase very fast and frequently the animal need to be euthanized before metastatic tumors even appear. Furthermore, inherent differences between

both species may also provide absence of metastases in GEMMs (Politi and Pao, 2011).

Other discrepancies between the two species concern with the transformation of normal cells to malignant as well as spontaneous tumors regression. In humans more genetic mutations are necessary to induce malignant transformation compared to in mice (Rangarajan and Weinberg, 2003). Furthermore, spontaneous regression of tumors is rare in adult humans whereas it is frequent in adult mice (Anisimov *et al.*, 2005) and the life expectancy of mice is 30-50 times shorter than for humans, making an appropriate age-related translation challenging. Also the age-related cancers in both species are different and mice tend to develop tumors of mesodermal origin, whereas tumors in humans arise in epithelial cells layers (Rangarajan and Weinberg, 2003). Most of the mice used in research are rather young and murine tumor induction is initiated shortly after sexual maturity (6-12 weeks). However, in humans cancer are most common among the elderly.

Consequences in size differences in human *versus* mice is another concern. Assessment of tumor response to cytotoxic therapies mainly uses non-invasive imaging modalities like magnetic resonance imaging (MRI), positron emission tomography (PET) and/or computed tomography (CT). However, these sophisticated technologies are not always available or affordable for small animal imaging (Herter-Sprie *et al.*, 2013) and the small size of mouse can compromise their use for surgical procedures, imaging, radiation and chemotherapy (de Jong and Maina, 2009). Also sensitivity is often a limiting factor regarding appropriate radiation dose in small-animal imaging studies and thus, the radiation dose may be high in rodents, particularly when repetition of scans need to be performed over time.

Although in the past two decades, GEMMs have been used for cancer biology research and enormously contributed to understanding of distinct aspects and phases of tumorigenesis (Heyer *et al.*, 2010), their utility for reliably predicting human tumor behavior are still limited (Rangarajan and Weinberg, 2003).

Inconsistencies in the translation of basic science into effective clinical treatments could be overcome using animal models that precisely recapitulate the biology of the disease and response criteria that are more closely related between mouse and human (Herter-Sprie *et al.*, 2013). Large animal models play an important role as predictive models for human diseases, specially pigs have been the predominant choice when modeling human diseases (Rogers 2016).

1.1.2 Need for porcine cancer models

In the past two decades, transgenic pigs were generated for biomedical research (Luo *et al.*, 2012). This was accomplished by improving of genetic and proteomic tools for pigs (Lunney,

2007), whole-genome sequencing and annotation of advanced genome maps of the pig (Gün and Kues, 2014) and advances in techniques of gene transfer (Luo *et al.*, 2012). Likewise there is a rising interest in using pigs in both experimental and pharmaceutical research studies. Consequently, background data on pigs are becoming more available. The utility of the porcine model in experimental, toxicological and pathological research will continue to expand and are evident (Swindle *et al.*, 2012). Large animal species, preferentially pigs are the species of choice for translational medicine (Prather *et al.*, 2013). Translational research applies findings from fundamental research to enhance human health in many fields of biomedicine, such as cancer research (Flisikowska *et al.*, 2013).

Pigs are very similar to humans in terms of anatomy, genetics, immunology and physiology. They also share important similarities with humans with respect to the gastrointestinal, cardiovascular, reproductive, hepatic, urinary, musculoskeletal, endocrine, lymphatic, hematopoietic and central nervous systems. Additional anatomical similarities with humans include renal and respiratory morphology, eye structure and skin (Swindle *et al.*, 2012). As a consequence, the pig is one of the most important large animal models currently being used to study human genetic diseases (Kuzmuk and Schook, 2011), to understand the pathogenesis of human disease, for functional genomics studies, preclinical testing of novel therapeutic approaches, and regulatory toxicity testing (Luo *et al.*, 2012). Currently, they are already used in studies of spontaneous melanoma formation as an *in vivo* model (Adam *et al.*, 2007).

Pigs have immune system that more closely resembles the human immune system (Dawson, 2011). Pigs have similar reactions to human diseases and pathogens (Meurens *et al.*, 2011) and can metabolize drugs and develop tumors in a similar manner (Kuzmuk and Schook, 2011). Their large size facilitates surgery and procedural training (Kuzmuk and Schook, 2011), and to collect large amount of samples e.g. tissues and blood (Lunney, 2007). Therefore, there are many advantages to using a large mammalian model for cancer research. Similarity between body size, morphological structures and physiological processes are important to extrapolate the results from animal experiments to humans. Also an ideal cancer model should be subject to develop tumor that progress to cancer in a similar way to humans (Kuzmuk and Schook, 2011).

The tumorigenesis process in both species are conserved at the molecular level, as indicated by the suppression of telomerase in a number of tissues and reactivation during cancer (Stewart and Weinberg, 2000). In addition, the tumors in pigs can also reach sizes seen in humans. These large tumors could be grown in genetically defined porcine cancer models for *in vivo* cancer studies and are also relevant for many preclinical applications (Adam *et al.*, 2007).

At the practical level, pigs have well established animal husbandry, reach sexual maturity at six months, have a short gestation period and have more than two litters per year producing large

litters each (Meurens *et al.*, 2011). As a result, pig breeding for experimental cancer studies is economically viable (Adam *et al.*, 2007). These and other benefits of using pigs as a large animal to model cancers are detailed in Figure 1.

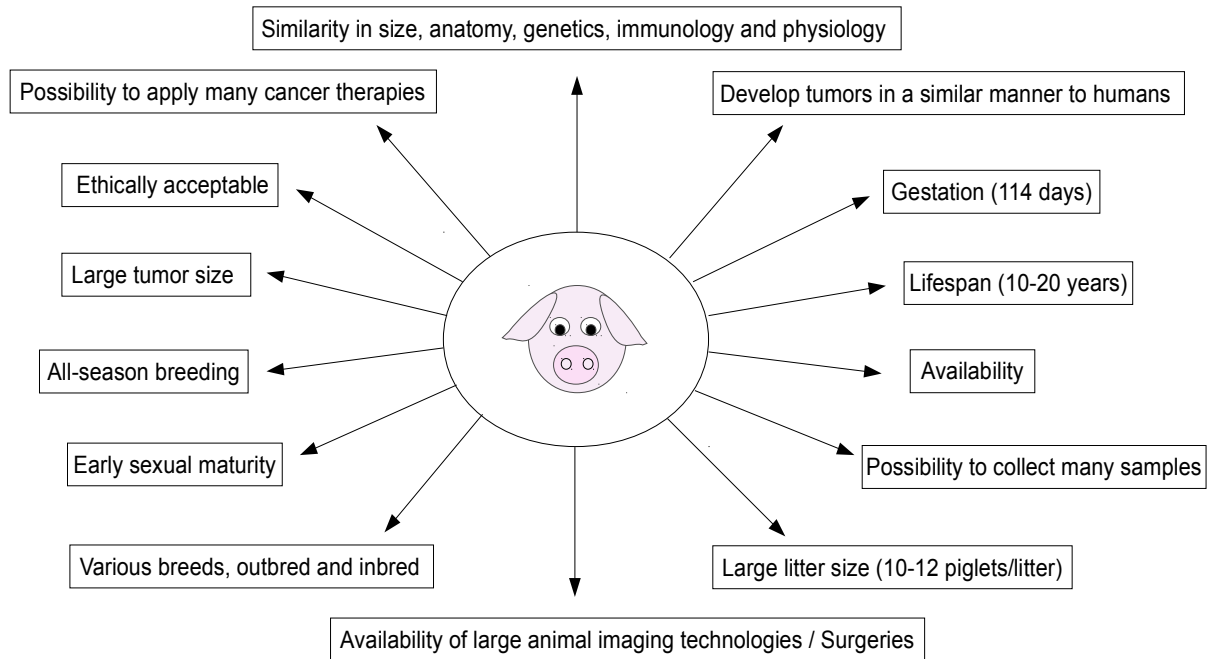


Figure 1: Advantages of the use of pigs as large animal models of cancer.

Some advantages of using porcine models are indicated in each box. Comparison of porcine size and immune system similarities were made with humans.

Adapted from Gün and Kues (2014) and Meurens *et al.* (2011).

As suggested there are many advantages that make the pig an attractive model system for studying cancer genetics and biology.

As pigs have a long lifespan, this contributes for observational studies for long periods of time under conditions that better recapitulate human tumors than in mice. This will allow modeling the effects of drugs on tumor progression, such as drug exposure and dose, tumor response, toxicity and drug resistant cells, as well as tumor remission (Flisikowska *et al.*, 2013).

1.2 Generation of transgenic pigs

Transgenic pigs can be generated by a variety of methods: nucleic acid transfer directly into embryos by either DNA injection (Hammer *et al.*, 1985) or viral transduction (Hofmann *et al.*, 2003; Whitelaw *et al.*, 2004), and cell-mediated DNA transfer method based on somatic cells (Li S. *et al.*, 2014; Fischer *et al.*, 2016). Currently the most important method of generating transgenic pigs is somatic cell nuclear transfer (SCNT) using genetically modified primary somatic cells. Various types of cells as donors in nuclear transfer has been successfully

employed (Fulka *et al.*, 1998), such as fetal fibroblasts (Niemann and Kues, 2000) and mesenchymal stem cells (Li S. *et al.*, 2014). The DNA sequence can be integrated into the genome of the cells transfected *in vitro* through random integration or into a specific locus by homologous recombination. The use of cultured cell populations for the production of animals by nuclear transfer permit the production of entire transgenic animals, in contrast of mosaic founder animals generated by microinjection (Schnieke *et al.*, 1997).

1.2.1 Genetically engineered porcine cancer models

The initiation of human tumors is determined by similar genetic alterations in a small set of genes (Futreal *et al.*, 2004). Thus, it should be possible to replicate different types of cancers by combining and activating defined oncogenic mutations in a tissue of preference (Flisikowska *et al.*, 2016). Our group is engaged in modelling human cancers in pigs, such as colorectal (CRC), pancreas and lung cancers. The most influential mutations in the development of colorectal cancer are known to occur within the tumor suppressor gene *APC* (adenomatous polyposis coli) and the proto-oncogene *KRAS* (Kirsten rat sarcoma viral oncogene homolog) (Worthley, 2007). Likewise disruption and somatic mutations of the tumor suppressor gene *TP53* contribute and are found in half of colorectal cancers and all tumors exhibiting mutation at this locus and germline mutations of the gene contribute to Li-Fraumeni syndrome (Olivier *et al.*, 2010). *KRAS* mutations are most frequently detected in pancreatic carcinomas and non-small-cell lung cancer (Pylayeva-Gupta *et al.*, 2011). Therefore, we have generated gene targeted pigs carrying a conditionally activatable mutant form of the key tumor suppressor p53, *TP53*^{R167H}, orthologous to human *TP53*^{R175H} and mouse *Trp53*^{R172H}, to model Li-Fraumeni syndrome and a number of other cancers (Leuchs *et al.* 2012). In addition, we also generated pigs with a Cre-dependent oncogenic *KRAS*^{G12D} mutation (Li S. *et al.*, 2015) and pigs carrying missense mutations of the *APC* gene at codons 1061 and 1311 (Flisikowska *et al.*, 2012), orthologous to germline mutations responsible for FAP (Familial adenomatous polyposis).

Wild-type p53 plays an important role in cancer biology and can be activated in response to various cellular stressors (Freed-Pastor and Carol Prives, 2012), to induce cell cycle arrest, DNA repair, senescence, and apoptosis (Rivlin *et al.*, 2011). The cancer-associated *TP53* mutations are usually produced by a nucleotide base substitution leading to a change in the amino acid coded (missense mutation) (Hollstein *et al.*, 1999). Although 87.9% of missense mutations occur between codons 125 and 300 and corresponds to the coding region for the DNA binding domain, outside this region, the majority of the mutations are nonsense or frameshift and missense mutations correspond about 40% (Olivier *et al.*, 2010).

Single missense mutations in the core domain of p53 can cause denaturation, disrupt local

structure or have little or no effect on folding. The vast majority of these mutations affect the thermodynamic stability of the p53 protein and thus, the ability of p53 to bind DNA and activate transcription of canonical p53 target genes (Bullock and Fersht, 2001).

APC is a negative regulator of the Wnt signalling pathway and believed to play a crucial role in suppressing intestinal neoplasia (Shaw and Clarke, 2007) by regulating cell differentiation, proliferation and apoptosis (Gregorieff and Clevers, 2005). Normal APC plays a role in binding and mediating the degradation of β -catenin, a positive regulator of the Wnt signalling pathway. Loss or reduction in this function through mutation or gene deletion facilitates carcinogenesis through uncontrolled Wnt signalling (Gregorieff and Clevers, 2005).

The protein K-RAS is a member of the family of GTPases which hydrolyse guanosine triphosphate (GTP). K-RAS participates in the regulation of numerous cellular events such as growth, differentiation and angiogenesis and its activity is controlled by GAPs (GTPase activating proteins) that bind to their target. Mutations of *KRAS* leads to proteins without binding sites for GAPs. This in turn results in constantly activated K-RAS and suppression of regulative cellular events (Deramaudt and Rustgi, 2005).

The evaluation of the founder *APC*¹³¹¹ pig generated by our group at age of 1-year revealed polyps in the colon and rectum, which are in accordance with the location and early onset of human FAP. Four more generations of *APC*¹³¹¹ pigs have been produced and they are being examined for tumor progression and metastasis (Flisikowska *et al.*, 2016). Sieren *et al.* (2014) developed a genetically modified porcine model of cancer carrying the *TP53*^{R167H} mutation, which is the same mutation we used to create a Cre-dependent pig. They reported that homozygous pigs developed lymphomas and osteogenic tumors, which accord with tumor types observed in human *TP53*^{R175H} and mouse *Trp53*^{R172H}, whereas pigs heterozygous for this mutant allele were reported to be free of tumors. Recently, Schook *et al.* (2015) created a Cre-dependent pig line encoding *KRAS*^{G12D} and *TP53*^{R167H} and demonstrated transformation and tumorigenesis after Cre activation of the latent transgenes with adenovirus encoding Cre (AdCre). In addition to the pigs with a Cre-dependent *TP53*^{R167H} mutation, we have also generated pigs with a Cre-dependent oncogenic *KRAS*^{G12D} mutation and we will generate transgenic pig lines expressing both, the *KRAS*^{G12D} mutation and the *TP53*^{R167H} mutation, after crossing them.

The pig cancer model program in our group is based on a cell/tissue-specific expression of Cre recombinase, a site-specific recombinase (SSR). Over the last ten years, site-specific recombinases have become an important tool for *in vivo* manipulation of mouse genomic sequences (Feil and Metzger, 2007). The exchange of chromosome segments during homologous recombination maintains the order of the genes. On the contrary, site-specific recombination can change gene order and also provides the insertion of new genetic

information in order to modify the genome (Walker and Rapley, 2009). Therefore, SSRs brings genetic manipulation to another level to better understand gene function (Sauer, 2002), as well as modelling cancers or other diseases *in vivo*.

Site-specific recombinases can perform rearrangements of DNA segments between short recognition sites (Feil and Metzger, 2007). As a result, site-specific recombination mediated by Cre/*loxP* system has been extensively used to create GEMMs for cancer research (Gould *et al.*, 2015). Cre/*lox* recombination is an advanced genetic engineering technique (Sauer, 2002) that allows for the activation of mutant proto-oncogenes or loss of tumor suppressors (Gould *et al.*, 2015) in a defined spatial (Li *et al.*, 2009) and temporal (Indra *et al.*, 1999) manner.

Controlling gene expression by Cre-mediated recombination is based on a two-component system (Sauer, 2002). For example, a latent oncogenic allele silenced by a transcriptional stop signal flanked by *loxP* sites can be activated by Cre-mediated excision of the stop signal. This can be achieved *in vivo* by mating animals carrying the latent allele with a second transgenic line that expresses Cre recombinase in a tissue-specific manner, resulting in offspring carrying both components. Appropriate choice of promoter to drive Cre and conditionally activated gene can enable tissue-specific expression of mutant oncogenes, and mimic the spontaneous somatic oncogenic mutations responsible for human neoplasia (see Figure 2).

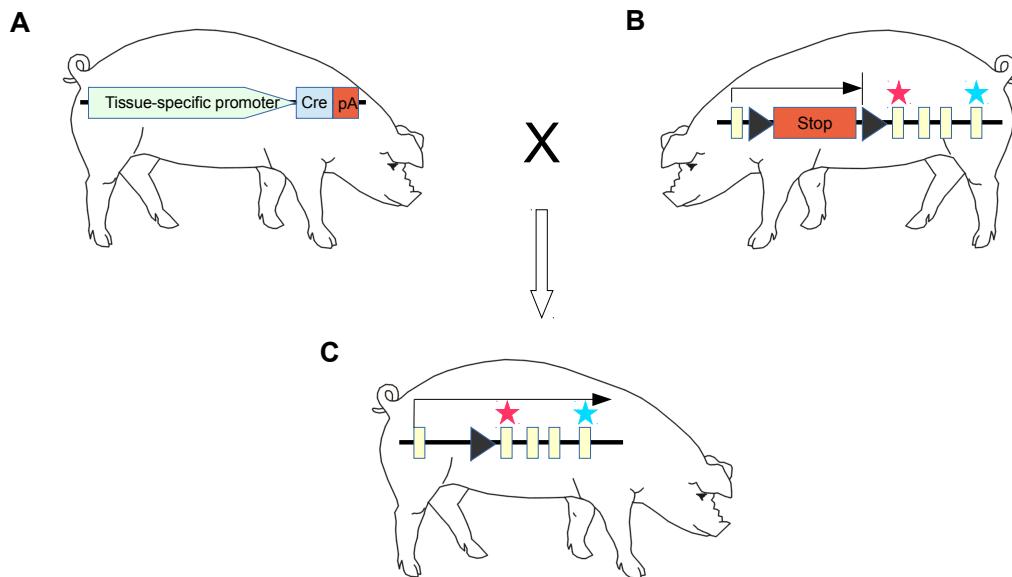


Figure 2: Scheme for tissue-specific activation of mutant proto-oncogenes or loss of tumor suppressors in pigs using the Cre/loxP recombination system.

The introduction of a point mutation and removal of selection markers can be made by crossing the transgenic pig that express Cre recombinase under the control of a tissue-specific promoter with another pig that contains *loxP* sites flanking a selection marker and transcription stop cassette. (A) A transgenic pig expressing Cre under control of a tissue-specific promoter. (B) A floxed transcriptional stop cassette in intron 1 prevents the activation of a proto-oncogene (e.g. $KRAS^{G12D}$ with a point mutation into exon 2 - pink star) or loss of tumor suppressor expression (e.g. $TP53^{R167H}$ with a point mutation into exon 5 - blue star). (C) Upon Cre-mediated excision of the floxed region a targeted activation of the $KRAS^{G12D}$ proto-oncogene or interruption of tumor suppressor $TP53^{R167H}$ expression can be obtained. Exons are indicated as yellow boxes and *loxP* sites as black triangles. The pink star indicates point mutation in exon 2 of porcine *KRAS* locus. The blue star indicate point mutation in exon 5 of porcine *TP53* locus. Abbreviations: pA: polyadenylation signal.

Another way to activate Cre recombinase and catalyse Cre-mediated recombination is delivery Cre locally as permeable fusion protein (Will, 2002) or using viral vectors (Pfeifer *et al.*, 2001; Silver *et al.*, 2001 and Saunders *et al.*, 2012).

Another SSR used in conditional gene targeting is the Flp (short for flippase) recombinase from yeast (*Saccharomyces cerevisiae*). As well as Cre, Flp recombinase recognises two identical 34 bp FRT (short for flippase recognition target) sites, and mediate site-specific recombination reactions between these two sites (Albert *et al.*, 1995). Combination of both the Cre/*loxP* and Flp/FRT systems allows greater targeting vector versatility for genome engineering applications (Maizels, 2013).

1.2.2 Cre/*loxP* recombination system

The site-specific DNA recombinase Cre (short for cyclization recombination), obtained from the bacteriophage P1 (Sternberg and Hamilton, 1981; Hoess and Abremski, 1984), catalyses the recombination of DNA at *loxP* target sites.

The Cre recombinase is a 38kDa enzyme that consists of four subunits and two domains, the N-terminal domain responsible for binding DNA and a C-terminal catalytic domain (Gibb, 2010), which contains all of the active site residues (Guo *et al.*, 1997). The enzyme binds to two distinct, specific sequences, called *loxP* sites (short for locus of x-over of P1) (Albert *et al.*, 1995). These are 34 bp long recognition sequences consisting of two 13 bp inverted repeats flanking an 8 bp asymmetrical core or spacer region (Sauer, 2002), which indicates the orientation of the *loxP* sites (see Figure 3) (Langer *et al.*, 2002).

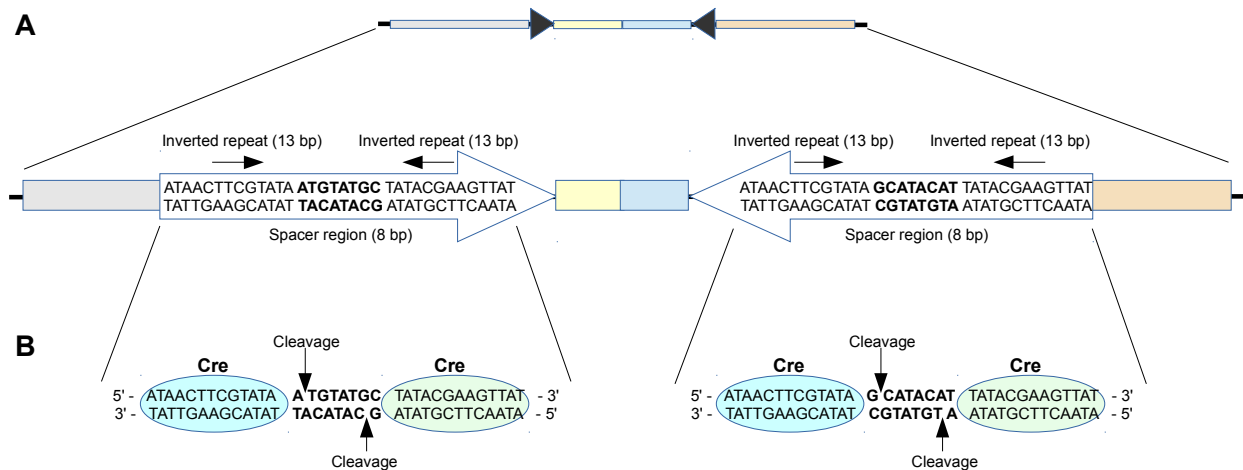


Figure 3: Sequence and organization of the *loxP* site and binding of Cre subunits to *loxP* sites.

DNA sequence containing two directly repeated *loxP* sites (black triangles) oppositely orientate. (A) The large arrows indicate the directionality of the *loxP* sites, which are defined by the asymmetric central spacer region. The small arrows show the inverted repeats, surrounding the central 8 bp spacer region (bold font). (B) Two Cre subunits specifically recognize and bind each *loxP* inverted repeat sequence, that serves as binding sites for the Cre recombinase. The positions of cleavage by Cre are indicated by vertical arrows.

Adapted from Araki *et al.* (2010) and Guo *et al.* (1997).

Cre/LoxP recombination technology is used to catalyse recombination between the two recognition sites. This leads to the generation of chromosomal deletions, inversions and translocations depending on the orientation of the *loxP* sites (Feil and Metzger, 2007) and based on the asymmetry of the spacer region to provide directionality to the recombination reaction (Langer *et al.*, 2002). Figure 4 shows Cre-mediated recombination between two *loxP* sites on the same DNA molecule or on separate DNA molecules.

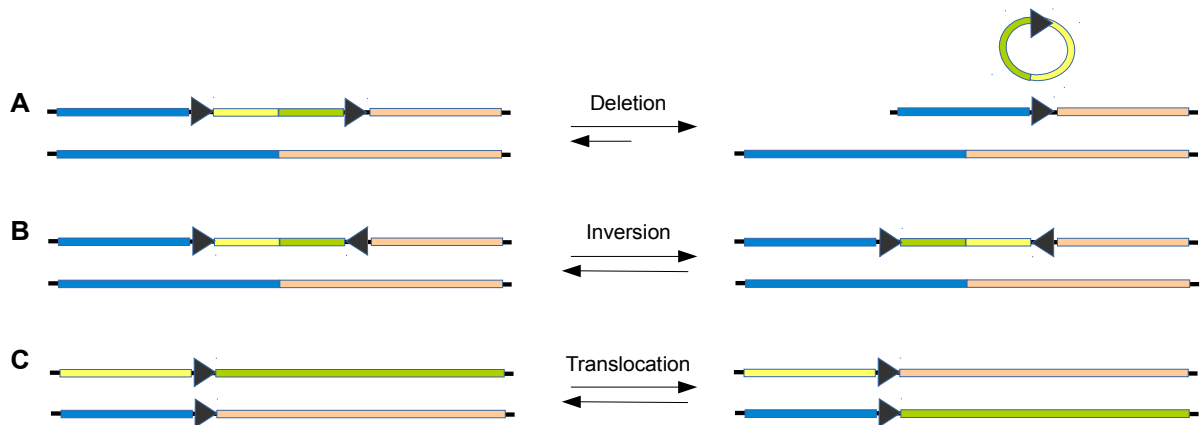


Figure 4: Schematic Cre/loxP site-specific recombination.

Depending on the orientation and location of the *loxP* sites different types of recombination occurs. (A) Deletion of DNA occurs when two directly repeated *loxP* sites are orientated in the same direction. This DNA will be excised as a circular loop and one *loxP* site remains in the genome. (B) Inversion of DNA occurs when two directly repeated *loxP* sites are oppositely orientated. (C) Translocation of DNA occurs when the *loxP* sites are on different chromosomes. Adapted from Feil and Metzger (2007).

In all cases, presented in Figure 4, the reactions are reversible but the excision of the DNA between the directly repeated *loxP* sites is kinetically favoured over integration (Feil and Metzger, 2007). Although the mechanism involved in Cre-mediated recombination does not conform to a simple kinetic model (Shoura *et al.*, 2012), intramolecular recombination (circularization) is more efficient than intermolecular recombination. In addition, the circular excised product can be quickly degraded, making this reaction essentially unidirectional (Feil and Metzger, 2007).

The Cre/*loxP* system has been successfully applied in yeasts, plants, mammalian cell cultures and mice (Albert *et al.*, 1995; Araki *et al.*, 1997). Our group is currently utilizing the Cre/*loxP* system to create pigs with conditionally-activatable *KRAS*^{G12D} and *TP53*^{R167H} mutants. Dual fluorescent reporter pigs (Li S. *et al.*, 2014) have been generated to provide an indication of Cre recombinase activity *in vivo*. With the help of tissue-specific Cre-activatable dual fluorescent reporter pigs, simultaneous expression of mutant *KRAS*^{G12D} and *TP53*^{R167H} alleles to induce cellular changes leading to cancer could be accomplished.

1.2.3 Modified *loxP* sites

Many alternative *lox* recognition sites for Cre recombinase (e.g. *lox551*, *lox2272*, *lox5171*, *lox66* and *lox71*) have been developed (Branda and Dymecki, 2004).

Modified *lox* recognition sites can be separated into two classes, spacer variants and inverted-repeat variants. The first class contains nucleotide mutations within the 8 bp spacer sequence (Langer *et al.*, 2002) and even one single nucleotide substitution can dramatically reduce

recombination with the wild-type (wt) sequence, but still renders efficient recombination with homologous *lox* sites (Hoess *et al.*, 1986). Examples of modified *loxP* sequences carrying mutations within the spacer region include *lox511* (Hoess *et al.*, 1986), *lox2272* and *lox5171* (Lee and Saito 1998).

The *lox511* carries a single point mutation in the 8 bp spacer region and therefore can still recombine with wt *loxP* sites at low frequencies (Lee and Saito 1998; Kolb, 2001). Therefore, during mutation analysis Lee and Saito (1998) synthesized many mutants with two substitutions in the 8 bp spacer region. After many recombination analysis they found that two mutants the *lox2272* and *lox5171* were the most efficient *in vitro*, and they yielded good amounts of recombination products with the identical mutants. Others also demonstrated the successfully use and exclusivity of these *lox* mutants to recombine with itself in embryonic stem (ES) cells (Kolb, 2001).

The second class of modified *lox* recognition sites, the inverted-repeat variants, were generated through nucleotide substitutions within the inverted repeats. These mutant sites carry 5 bp substitutions in the distal end of either the left (*lox66*) or the right (*lox71*) inverted repeats. The substitutions in the left or right elements of the inverted repeats are called LE and RE, respectively (Oberdoerffer *et al.*, 2003). Recombination products between LE and RE sites result in a wild-type *loxP* and one with two mutated inverted repeats (*lox72*). The latter is an inefficient substrate for Cre recombinase (Albert *et al.*, 1995). This strategy has typically been used to increase the frequency of Cre-mediated insertion of DNA at a predefined chromosomal locus (Branda and Dymecki, 2004). Araki *et al.* (2010) have demonstrated that recombination using *lox71/66* sites favoured integration over excision in ES cells and Oberdoerffer *et al.* (2003) have used *lox71/66* to induce unidirectional Cre-mediated inversion.

Table 1 summarizes the sequences differences between the *lox* sites variants cited above.

Table 1: Wild-type *loxP* site sequence and mutated *lox* sequences commonly used for site-specific recombination.

Name	Sequence (two 13 bp inverted repeats and an 8 bp core sequence)	Specificity	References
Wild-type <i>loxP</i> *	ATAACTTCGTATA ATGTATGC TATACGAAGTTAT	Self and <i>lox511</i>	Hoess <i>et al.</i> (1982)
Mutant <i>lox</i> sites <i>lox511</i> <i>lox66</i> <i>lox71</i> <i>lox2272</i> <i>lox5171</i>	ATAACTTCGTATA ATGTATaC TATACGAAGTTAT ATAACTTCGTATA ATGTATGC TATACGAAccgta taccgTTCGTATA ATGTATGC TATACGAAGTTAT ATAACTTCGTATA AaGTATcC TATACGAAGTTAT ATAACTTCGTATA ATGTgTaC TATACGAAGTTAT	Self and <i>loxP</i> <i>lox71</i> <i>lox66</i> Exclusive Exclusive	Hoess <i>et al.</i> (1986) Albert <i>et al.</i> (1995) Albert <i>et al.</i> (1995) Lee and Saito (1998) Lee and Saito (1998)

*The wild-type sequence is referred as a reference and the small caps in the mutant *lox* sequences indicate differences with the corresponding wild-type sequence.

The use of different *lox* sites at different genomic locations has the advantage that only the desired target is eliminated by Cre and no undesired inter-locus recombination can occur (Sauer, 1996).

1.3 Temporal and spatial control of Cre recombinase activity

Precise temporal and spatial regulation of Cre recombinase expression can be used to control the gene of interest in a tissue- and time-specific manner, thus overcoming embryonic lethality and developmental defects (Branda and Dymecki, 2004). In addition, it can be used to study the function of genes and acquisition of oncogenes or loss of tumor suppressors specifically in the tissue of interest at specific times (Gould *et al.*, 2015). Therefore, it facilitates the investigation of the molecular basis of tumorigenesis *in vivo* (Walrath *et al.*, 2010).

1.3.1 Tissue-specific Cre recombinase

The Cre/*loxP* system can act in a selective manner in which tissue-specific promoters are used to drive Cre recombinase (Gould *et al.*, 2015). Thus, after crossing one animal carrying the Cre recombinase under control of a tissue-specific promoter with another carrying the gene of interest flanked by *loxP* sites, the target gene will be altered during development exactly where the promoter chosen to drive the expression of Cre is activated (Walrath *et al.*, 2010) (see Figure 2).

Many promoters have been well characterized and have permitted to localize expression within specific tissues or cells, along with the immune, reproductive and central nervous systems, liver, heart, skin, mammary gland, pancreas (Ashizawa *et al.*, 2004; Rose *et al.*, 2001), lung (Singh *et al.*, 1988; Wert *et al.*, 1993) and colon (Pinto *et al.*, 1999).

1.3.1.1 Lung-specific promoter

The most widely used promoters to target expression to the respiratory tract epithelium are derived from the Clara cell secretory protein (CCSP, also known as *CC10* gene) and the surfactant protein C (*SFTPC* gene) (Singh *et al.*, 1988; Perl *et al.*, 2002). The two genes are expressed in different regions of the respiratory epithelium, CCSP in the larger airway and proximal epithelial cells of the lung and the SFTPC in the distal type II alveolar epithelial cells (Baron *et al.*, 2012).

To target alveolar epithelial cells type II transgene expression, a 3.7 kb human (Wert *et al.*, 1993) and 4.8 kb mouse (Kelly *et al.*, 1996) region from the SFTPC promoter upstream from the ATG codon has been widely used in mice (Perl *et al.*, 2009; Glasser *et al.*, 2004). For Clara cell-

specific expression in mice, a 2.3 kb rat CCSP promoter region upstream from the ATG codon has been widely used (Perl *et al.*, 2009).

Surfactant protein C

Pulmonary surfactant is a complex mixture of lipids and proteins (A, B, C, and D) synthesized and secreted by epithelial cells type II in the lung alveolus (Figure 5), which serves to reduce surface tension at the air-liquid interface of the lung (Korfhagen *et al.*, 1990).

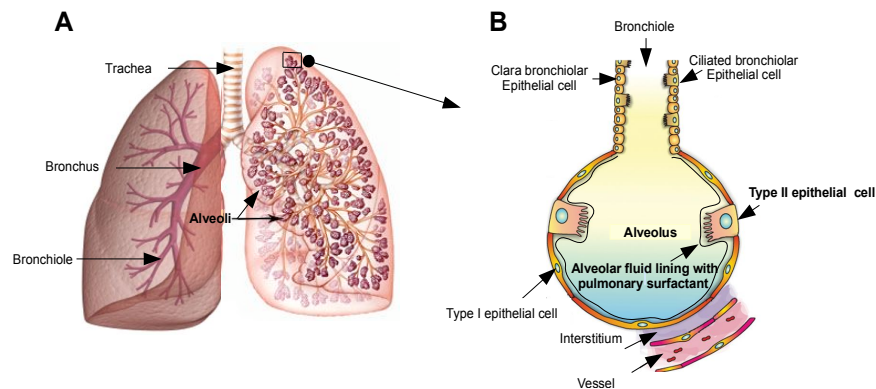


Figure 5: Schematic diagram of lung anatomy and an alveolus showing the terminal bronchiole, alveolar sac, locations of different epithelial cell types and surfactant layer.

The diagram shows the intrathoracic airway anatomy, which includes the trachea, the bronchus, bronchioles and alveoli. One alveolus is swollen and shows the locations of alveolar type I and II pneumocytes cells, clara and ciliated epithelial cells, as well as the surfactant layer. (A) The intrathoracic airway includes the trachea, the bronchus, bronchioles and alveoli. (B) Bronchiolar and alveolar regions. Bronchiolar clara cells and ciliated cells are shown in the bronchiole terminal. Alveolar type I cells, which facilitate gas exchange, form the structure of the alveolus. Alveolar type II cells secrete pulmonary surfactant (indicated by a black line) and thus, protect the inner lining of the alveoli by reducing alveolar surface tension.

Adapted from Boggaram (2009) and Rasmussen (2009).

According to sequencing comparisons between several mammals, both genomic and cDNA sequences of the *SFTPC* showed high levels of conservation in the coding region and at the 5' flanking regions (Hatzis *et al.*, 1994), and there is a considerable similarity between the porcine and the human *STPFC* gene regarding the length of exons and introns, except for the beginning of exon 5 (Cirera *et al.*, 2006). The human *SFTPC* gene codes for a hydrophobic peptide of 3.7 kDa, is located on chromosome 8 and consists of six exons (Korfhagen *et al.*, 1990). The porcine gene is located on chromosome 14 and according with Cirera *et al.* (2006) has two possible transcripts, one containing six and the other five exons. Agreement with human expression data (Rawlins and Perl, 2012) the porcine gene is very lung specific and expression in other organs is not common (Cirera *et al.*, 2006).

Porcine *SFTPC* mRNA appears in 50-day-old foetus and increases during lung development (Cirera *et al.*, 2006). Khor *et al.* (1994) detected *SFTPC* mRNA in distal airways cells of human fetuses and newborns starting at 15 weeks of gestation and increasing expression during

advanced gestational age. In the mouse and rat, SFTPC mRNA was detected on gestational days 11-12 and 17, respectively (Schellhase *et al.*, 1989; Wert *et al.*, 1993).

Regulation of SFTPC promoter

The activity of the SFTPC promoter depends on *cis*-acting regulatory elements that confer lung epithelial cell expression of the *SFTPC* gene (Wert *et al.*, 1993).

Glasser *et al.* (2000) tested *cis*-acting regions of the human *SFTPC* gene required to drive tissue and cell-specific expression in lung *in vivo*. They observed that 3.7 kb of DNA upstream from the transcription start site (+21 of exon 1 to -3686) were sufficient to produce gene expression specifically in bronchiolar and alveolar cells of the lung in transgenic mice. It was also demonstrated that regions at positions -3.7 kb and -1.9 kb of the *SFTPC* gene contain enhancer sequences and that the region -215 to +1 bp contains consensus binding sites for the TTF-1 (thyroid transcription factor-1) an important regulator of SFTPC expression in the lung (Glasser *et al.*, 2000). Consequently, mutations in the TTF-1 binding sites of the proximal and distal elements of the SFTPC promoter region considerably decrease lung-specific transcriptional regulation and gene expression (Whitsett and Glasser, 1998).

To generate lung-specific expression in transgenic mice, Kelly *et al.* (1996) reported that 4.8 kb fragment upstream of the transcription start site of the mouse SFTPC promoter is necessary. Bachurski *et al.* (1997) showed that the nuclear factor I (NF-I) binding sites were required for mouse SFTPC promoter activity in lung epithelial cell-derived line (MLE-15). NF-I family members regulate SFTPC expression independently of TTF-1, as they bind to sites on the proximal promoter region (-230 to +18 bp) and -318 to -230 bp region (Bachurski *et al.*, 1997).

Figure 6 summarizes the *cis*-acting regulatory target sequences of TTF-1 and NF-1 transcription factors in mouse SFTPC promoter sequence.

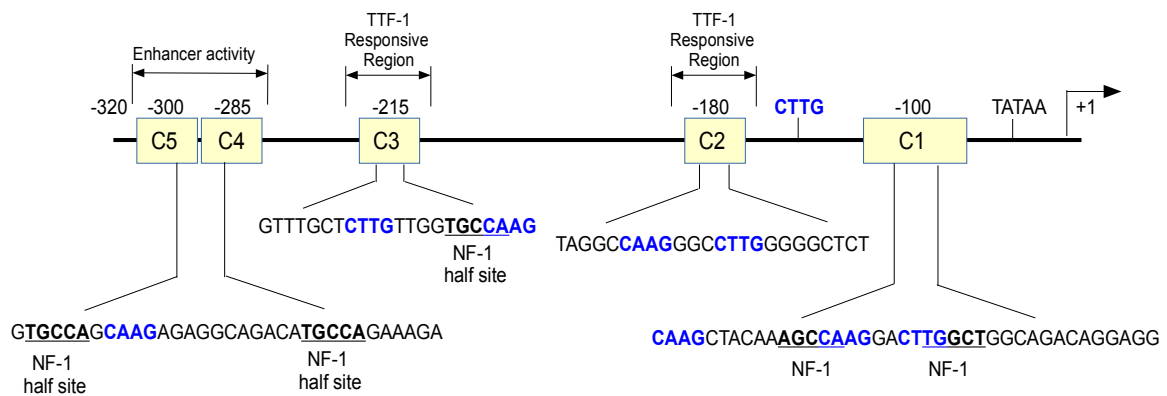


Figure 6: Mapping of NF-1 and TTF-1 cis-acting response elements in murine SFTPC promoter sequence.

Regulation of SFTPC transcription is due to multiple protein to DNA interaction on the proximal SFTPC promoter region. Boxed regions labeled C1 to C5 which denote sites of protein-DNA interaction as well as known *cis*-active regulatory elements are diagramed relative to the transcription start site indicated by an arrow and +1. NF-1-responsive fragments are underlined, and blue sequences correspond to the minimal TTF-1 motifs. The arrows followed by brackets indicate TTF-1 regulatory regions (responsive and cell selective enhancer regions). Adapted from Whitsett and Glasser (1998); Kelly *et al.* (1996).

Kelly *et al.* (1996); Bachurski *et al.* (1997) and Whitsett and Glasser (1998) identified five distinct regions (C1 to C5 see Figure 5) of protein-DNA interactions by DNase I footprint analysis of the proximal region (320 bp) of the mouse SFTPC promoter, contributing to transcription and regulation.

Furthermore, the authors reported that the region between -318 and -76 contains four binding sites for NF-I family members (footprints C1, C3, C4 and C5) and nine binding sites for the thyroid transcription factor-1.

NF-I site in footprint C1 and NF-I half site in C3 as well as TTF-1 site in C2 are necessary for regulation of basal SFTPC promoter activity (Whitsett and Glasser, 1998; Kelly *et al.*, 1996).

1.3.1.2 Gut-specific promoter

Several promoters have been used to drive a target gene in the gastrointestinal tract to achieve cell-specific expression. Some of them are listed in Table 2.

Table 2: Intestinal- and gastrointestinal-specific promoters.

Promoter	Abbreviation	Expression	References
human mucin-2	MUC2	expressed in epithelial cells (goblet cells) of the distal small intestine, colon and airways	Gum <i>et al.</i> (1999) Jany <i>et al.</i> (1991)
cytokeratin 19	K19	expression is restricted to villi of small intestine, surface of colonocytes, isthmus cells of the stomach and ductal cells of the pancreas	Brembeck <i>et al.</i> (2001)
villin-1	VIL-1	expressed in the absorptive cells of the small and large intestines, in the duct cells of pancreas and biliary system, and in the cells of kidney proximal tubules	Robine <i>et al.</i> (1985)
human, mouse and rat sucrase-isomaltase	SI	expressed exclusively in small intestine enterocytes	Wu <i>et al.</i> (1992) James <i>et al.</i> (1986) Chandrasena <i>et al.</i> (1992)
human and rat intestinal fatty acid binding protein	I-FABP	high expressed in epithelial cells (mature enterocytes) of small intestine and moderate expression in the duodenum. Also expression observed in small intestine goblet cells	Auinger <i>et al.</i> (2010) Sweetser <i>et al.</i> (1988)
mouse and rat liver fatty acid binding protein	L-FABP	high expressed in enterocytes located in the distal jejunum. Also expression in hepatocytes and in villus-associated enterocytes, as well as in proliferating and nonproliferating epithelial cells located in small intestine and colonic crypts. Inappropriate expression in the proximal tubular epithelial cells of the nephron	Sweetser <i>et al.</i> (1988) Simon <i>et al.</i> (1993)
human and rat intestinal trefoil factor	ITF	selectively expressed in goblet cells of the small and large intestinal mucosa	Ogata <i>et al.</i> (1998) Kanai <i>et al.</i> (1998)

After identification of intestine cell-specific genes and their promoter regions necessary for gene expression in human, mouse, and/or rat, some of them have been used to generate gut specific mouse cancer models, as KR19, MUC2, ITF and VIL-1 (Harada *et al.*, 1999; Gum *et al.*, 1999; Gum *et al.*, 2004; Janssen *et al.*, 2002). For example Harada *et al.* (1999) used the mouse K19 promoter to drive Cre recombinase in murine intestine (Ck19-cre). After crossing these mice with mice, in which the third exon of the murine β -Catenin gene was floxed [$Catnb^{+/\text{lox}(\text{ex}3)}$ or $Catnb^{\text{lox}(\text{ex}3)/\text{lox}(\text{ex}3)}$], the resulting offspring developed adenomatous intestinal polyps resembling those found in $Apc^{\Delta 176}$ knockout mice. The results suggest that the polyposis is caused by transcriptional regulation through the Wnt signaling pathway and its activation in the gut can lead to tumorigenesis. The same authors also used the rat *Fabpl* gene to drive cre expression and to generate mutants carrying the *Fabpl*-cre transgene. They crossed these mice with $Catnb^{+/\text{lox}(\text{ex}3)}$ or $Catnb^{\text{lox}(\text{ex}3)/\text{lox}(\text{ex}3)}$ mice. In both types of compound heterozygous offspring (generated with the *Fabpl*-cre or Ck19-cre transgenic mice), polyps started to form at young ages (approximately 2 weeks after birth). In the case of *Fabpl*-cre offsprings, polyps developed in smaller numbers than Ck19-cre offsprings and most mice died within 4-5 weeks after birth due fatty degeneration of their livers. In contrast the mutants carrying Ck19-cre transgene died

at about 3 months of age, in a similar way then *Apc*^{Δ716} heterozygotes do (due anemia and cachexia) (Harada *et al.*, 1999). Others tried to use the mouse MUC2 promoter to drive the SV40 Tag oncogene. The authors found that the oncogene was expressed in the small intestine goblet cells of the transgenic mice. Unfortunately, the cells did undergo apoptosis instead proliferation which is required for cancer cell continuation. They conclude that inappropriate goblet cell growth is blocked by apoptosis, which supports the considered role of apoptosis as an antineoplastic "agent" (Gum *et al.*, 2001). To generate tumor in the intestinal epithelium, specially in goblet cells, they used another intestine-specific promoter (ITF) to express the SV40 Tag oncogene. The use of ITF provoked tumor formation in the proximal colon that were rapidly growing, multifocal, and invasive. The developed ITF-Tag tumors were similar of human small cell carcinomas of the colon, implying that its occurrence could be due enteroendocrine cell lineage as well (Gum *et al.*, 2004).

Villin-1

Villin is a Ca²⁺ regulated actin-binding protein and a major component of the microvillus border of intestinal epithelial cells and kidney proximal tubules (Maunoury *et al.*, 1988), with a molecular mass of 92.5 kDa (Robine *et al.*, 1985). It is responsible to hold together actin filaments and supports the microvillus membrane forming the brush border as illustrated in Figure 7 (Maunoury *et al.*, 1992).

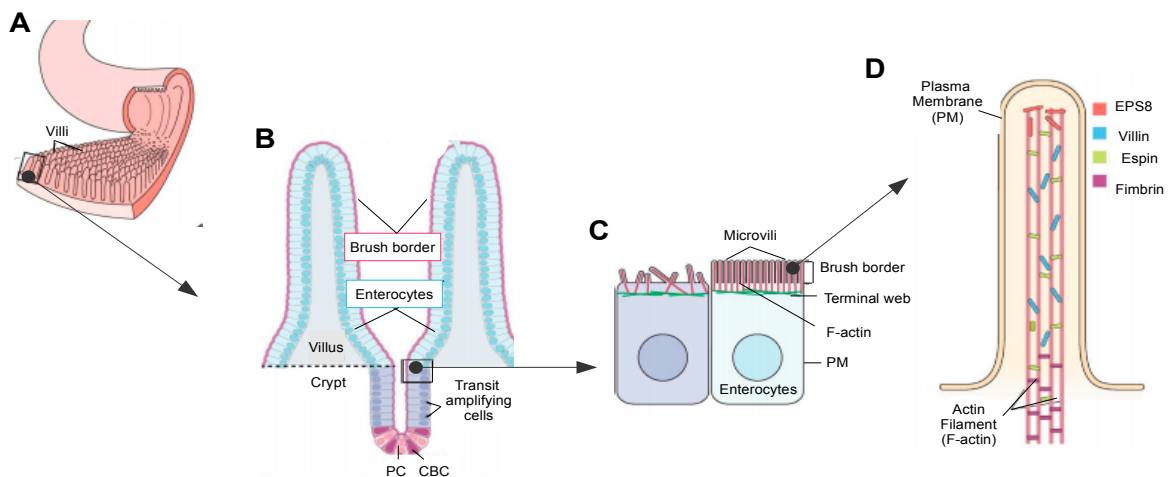


Figure 7: Architecture of the small intestinal epithelium and villin location in adults.

The intestinal epithelium is composed from villi (finger-like projections) that increase the internal surface area of the intestinal walls for nutrients absorption. Each villus (singular from villi) contains enterocytes cells that has many microvilli projections, that collectively form the brush border. The villin is located in the microvillus and it is a major component of the actin bundles that support the microvilli of the brush border and its expression increases as the cells differentiate and move from the crypt to the tip of the villi. (A) The small intestinal epithelium is characterized by ubiquitous finger-like projections known as villi. (B) The simple columnar epithelium lining the villus consists of primarily enterocytes that are generated in a stem cell niche composed of crypt base columnar (CBC) cells and flanking Paneth cells (PC). CBC cells differentiated into enterocytes and then exit the crypt through the crypt-villus axis. (C) Enterocytes before and after differentiation contain different brush border microvilli apical surface organization, packed in tight, hexagonal arrays, composed of F-actin. The brush border is composed of two interconnected regions, the microvillus assembly and the terminal web area. (D) Microvillus. A bundle of parallel actin filaments, held together by the actin-bundling proteins villin, fimbrin, espin and ESP8, forms the core of a microvillus. Adapted from Crawley *et al.* (2014).

Biological functions regulated by villin in an epithelial cell are cell migration, cell invasion, cell morphology, and cell death (Khurana and George, 2008).

Villin-1 is expressed early during embryonic development in both human and mice (Lacroix *et al.*, 1984; Robine *et al.*, 1985; Maunoury *et al.*, 1988). Robine *et al.* (1985) detected villin-1 expression in the intestinal tube of an 8-week-old human foetus, which coincides with the first outgrowth of villi (Lacroix *et al.*, 1984). Also between 9 and 11 weeks of gestation apical brush borders were composed of microvilli, and in a 16-week-old foetus both small and large intestines expressed villin (Robine *et al.*, 1985). The same results were observed by Lacroix *et al.* (1984), who observed that between 10 to 14 weeks of gestation the height of villi increase and a typical "finger-like" projections appears. Therefore, within 16 weeks of gestation, a differentiated brush border is obtained. Others reported that in mouse embryos, villin could be detected in the primitive endoderm at day 6, then in the extra-embryonic yolk sac until full term of gestation, where villin concentrates in the brush border of the epithelium surrounding the villi (Maunoury *et al.*, 1988; Maunoury *et al.*, 1992). Thus, at the moment that intestinal crypts are established, villin is expressed in all cells of the crypt-villus axis and increases as the cells differentiate and migrate from the crypt until they reach the tip of the villus (Maunoury *et al.*, 1992).

Villin expression is limited to absorptive cells and/or cells that exhibit well-developed microvilli at their surfaces (Robine *et al.*, 1985). Accordingly, villin is highly expressed in intestinal and kidney proximal tubule cells, which are specialized absorptive cells of the brush border, and it shows low expression in other gut derivatives, as biliary and pancreatic cells (Maunoury *et al.*, 1992).

Regulation of VIL-1 promoter

To analyse the promoter activity and tissue specificity of the mouse *villin* gene, Pinto *et al.* (1999) used an extended genomic region of this gene. They first determined the location of the transcription start site (TSS) of the mouse *villin* gene, and revealed that it was separated from the translation start site by a 5.5 kb intronic region. Thus, they could map elements localized 5' and 3' of the transcription start site, by DNase I-hypersensitive sites assays, that improve the levels of transgenic expression in the intestinal epithelium. The authors found four distinct sites (I to IV). The hypersensitive sites I and II were found at +5.5 kb and +3 kb downstream from the transcription start site (+1). The site I was detected in liver, kidney and intestine and site II just in intestine. The hypersensitive sites III and IV were found at -0.5 kb and -1 kb, respectively and both were observed in intestinal tissue, whereas site III was also detected in kidney (Figure 8).

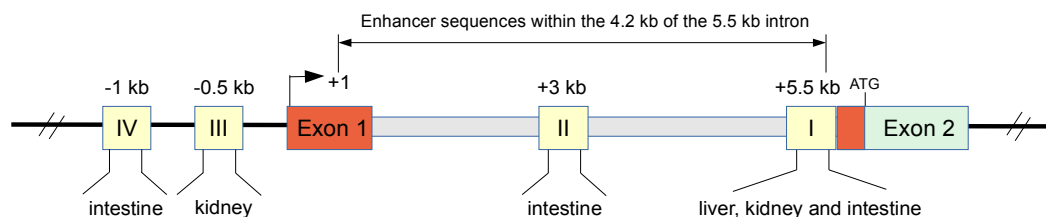


Figure 8: Schematic representation of the endogenous villin locus and the organization of the sites responsible for tissue-specific control of villin expression.

Four major distinct DNase I-hypersensitive sites (I to IV) were shown to be present in the region extending from -1 kb to +5.5 kb in respect to the transcription start site. They are responsible for distinct tissue-specific expression, as indicated. The orange boxes represent the untranslated exon, and the green box represents the first coding exon. The transcription start site is indicated in exon 1 (+1) as well as the initiation codon (the ATG codon) in exon 2. The size of the intron is indicated and 4.2 kb region of the first intron revealed the presence of one or more enhancers.

In addition, the same authors found two other hypersensitive sites at -10 kb (V) and -15 kb (VI), but they were only detected in liver tissue. They were not further investigated, because they were located faraway from the TSS and the authors concluded that these could belong to an adjacent gene. Therefore, only the hypersensitive sites I to IV were subcloned to investigate their roles in controlling villin expression in the intestine.

Nine different combinations of sequences containing one or more sites were sub-cloned upstream of a promoter-less *LacZ* gene. They were then transfected into two cell lines (Caco-2 and LLCPK1) which express villin and into a control epithelial cell, in which no villin expression

is detected. The most efficient transcription of the LacZ reporter gene, in both intestine-derived cell lines, was obtained with the 9 kb construct (containing -3.5 kb to +5.5 kb from the start site of transcription). Also in both cell types when the hypersensitive site II or the region upstream from this site was removed, a dramatic decrease of the β -galactosidase reporter gene expression level was observed. Taking together, these results indicated that 9 kb of the mouse *villin* genomic region contains the necessary promoter/enhancer elements to generate enterocyte-specific activity. According to Madison *et al.* (2002) the generation of transgenic mice, using the 12.4 kb promoter fragment from the mouse *villin* gene (harbouring 6.7 kb 5' of the transcriptional start site until the first 65 base pairs of exon 1), directed expression of LacZ reporter gene and Cre recombinase in the large and small intestines of transgenic mice. No position-effect variegation was observed, indicating that the transgene contains a *cis*-acting promoter element that recruits chromatin-remodeling enzymes and facilitates position-independent expression.

Many functions of villin such regulating actin dynamics, cell structure, cell morphology, cell motility and cell death have been well studied *in vitro* and *in vivo* (Khurana and George, 2008). However the underlying molecular mechanisms affecting the regulation of the *villin* gene, identification of transcription regulatory factors and *cis*-regulatory DNA sequences and its binding sites involved in promoting villin transcription, have not been further investigated.

1.3.1.3 Pancreas-specific promoter

There are four categories of pancreas-specific promoters, which are distinguished by genes based on the cell type of origin and cell type specific expression: endocrine, acinar, ductal and pancreatic progenitor cells. They have been successfully used to produce Cre-driver lines, which have been used in studies of pancreas development and/or function when crossed with mice harbouring the gene of interest flanked by *loxP* sites (Magnuson and Osipovich 2013). Table 3 contains a number of different pancreas-specific promoters used to generate Cre driver lines.

Table 3: Pancreas-specific promoters and Cre driver lines*

Cell specific	Gene name	Common Name	Species	Expression site(s) in pancreas
Endocrine	Ins2	RIP-Cre	rat	β -cells
		HIP-Cre	human	
		PIP-iCre	porcine	
		MIP-CreER	mouse	
	Gck	Gck-Cre	mouse	
	Slc2a2	pGlut2-Cre	mouse	
	Sst	Sst-Cre/CreER	mouse	δ -cells
	Gcg	Glu-Cre	rat	α -cells
	Ppy	PP-Cre	rat	PP-cells
Ghrl	Ghrl-Cre-GFP	mouse	ϵ -cell	
Acinar	Amy2	Amy-Cre	mouse	acinar cells
	Ela1	Ela-Cre/CreER ^I	rat	
	Vil	Vil-Cre/CreER	mouse	
	Cpal	Cpal-CreER ^T	mouse	pre-pancreatic endoderm, acinar cells
Ductal	Krt 1	CK19-CreER ^T	mouse	ductal cells
	CA2	Call-Cre/CreER ^T	human	
	Muc1	Muc1-CreER ^{T2}	mouse	acinar, ductal cells
Progenitor	Foxa2	Foxa2-Cre/CreER Foxa2-T2AiCre	mouse	endoderm
	Foxa3	Foxa3-Cre	mouse	
	Sox17	Sox17-Cre-GFP	mouse	
	Cldn6	Cldn6-CreER	mouse	
	Pdx-1	Pdx1-Cre/CreER	mouse	pre-pancreatic endoderm
	Ptfla	Ptfla-Cre	mouse	pre-pancreatic endoderm, acinar cells
	Sox9	Sox9-Cre/CreER Sox9-CreER ^{T2}	mouse	pre-pancreatic endoderm, ductal cells
	Neurog3	Ngn3-Cre/CreER/ER ^T	mouse	pre-endocrine cells
	Nkx2-2	Nkx2-2-Cre/CreER	mouse	pre-pancreatic endoderm, p-cells
	Isl1	Isl1-Cre/CreER ^T	mouse	endocrine cells
Pax4	Pax4-Cre/CreER	mouse		

*Table 3 was adapted from (Magnuson and Osipovich 2013).

In this work the promoter of the pancreatic duodenal homeobox 1 (PDX-1) gene was used to direct Cre recombinase expression to the porcine pancreas. The PDX-1 promoter has been successfully used to generate transgenic mice containing 5.5 kb upstream of the transcription start site (Gu *et al.*, 2002), as well as 4.5 kb 5' upstream (Herrera, 2000; Gannon *et al.*, 2000; Hingorani *et al.*, 2003) and also a distal enhancer element in combination with regulatory regions (areas I and II) that are important for PDX-1 expression (Wiebe *et al.*, 2007).

PDX-1

PDX-1 is one of the earliest transcription factors that are expressed in the prospective pancreatic regions and is required for pancreatic development (Jonsson *et al.*, 1994; Shih *et al.*, 2013), including duodenal differentiation and β -cell maturation (Afelik *et al.*, 2006). Thus, homozygous deletion of *PDX-1* in the mouse (Jonsson *et al.*, 1994), as well as its mutation in humans result in pancreas development failure.

PDX-1 is expressed in pancreatic progenitor cells, that give rise to endocrine, exocrine, and duct pancreatic tissue (see Figure 9), and its detection in mice starts on embryonic day 8.5 in the part of the ventral and dorsal bud that later fuse to form the definitive pancreas (Melloul *et al.*, 2002). Between embryonic days 9.5 and 12.5, duct progenitors cells express elevated levels of PDX-1 (Gu *et al.*, 2002), but in ductal and exocrine cells PDX-1 expression decrease after late embryonic development, and reappears later mainly in β -cells (Wu *et al.*, 1997; Stoffers *et al.*, 1999).

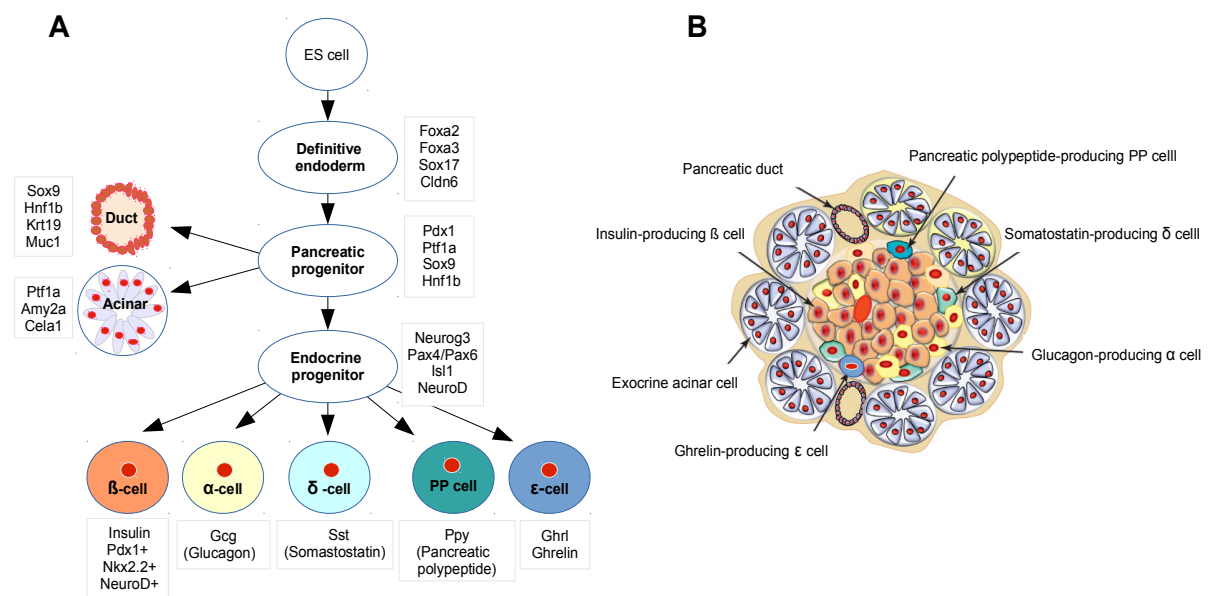


Figure 9: Simplified scheme of pancreas development and pancreatic islet.

(A) The pancreas is derived from definitive endoderm (DE) that develops from pluripotent cells in the early embryo (ES). The DE gives rise to pancreatic multipotent progenitor cells, which have the capacity to differentiate in acinar, ductal or endocrine cell lineages. The endocrine progenitors then may differentiate into five types of islet cells, α -, β -, δ -, ϵ - and PP. Some genes that have been used to drive Cre expression to distinct cell types or lineages are indicated in the right and left sides. (B) An overview of an islet of Langerhans, consisting in a conglomerate of cells of α -, β -, δ -, ϵ - and PP cells. The α -cells secrete the hormone glucagon, the β -cells secrete insulin, the delta δ -cells secrete somatostatin, the PP cells secrete pancreatic polypeptides and the ϵ -cells secrete ghrelin. Adapted from Magnuson and Osipovich (2013); Efrat and Russ (2012); Vetere *et al.* (2014).

As shown in Figure 9, the four major pancreatic islet cell types (α , β , δ and PP cells) synthesize specific hormones and are distributed throughout the exocrine tissue. PDX-1 expression becomes confined to adult β -cells of the islets of Langerhans (Guz *et al.*, 1995).

Diverse Cre-driver mouse lines directed by the human or mouse PDX-1 promoter were created and have successfully shown Cre recombination in the pancreas when crossed with mice containing the gene of interest flanked by *loxP* sites (Magnuson and Osipovich 2013). Transgenic pigs have been also generated to direct gene expression of fluorescent Venus protein to the pancreas using the mouse PDX-1 promoter (6.5 kb of the mouse PDX-1 promoter) (Matsunari *et al.*, 2014). Interestingly, when using the mouse PDX-1 promoter to generate transgenic pigs, PDX-1 expression was only detected in pancreas, but not in other tissues known to express PDX-1 during early stages of mouse embryogenesis, as subpopulations of duodenal and gastric enteroendocrine cells (Gannon *et al.*, 2000). However, in transgenic mice it has been observed that expression of lacZ under control of the 5'-proximal 4.6 kb of the PDX-1 promoter resulted in detection not only in the exocrine and endocrine pancreatic tissue, but also in the intestinal epithelium of the duodenum, pyloric glands of the distal stomach, Brunner's glands, common bile and cystic ducts, and the spleen (Stoffers *et al.*, 1999). In the adult mouse PDX-1 expression was detected in the exocrine pancreas (Wu *et al.*, 1997), endocrine pancreas (mostly in β -cells) (Guz *et al.*, 1995), antral stomach (Larsson *et al.*, 1996) and duodenum (Guz *et al.*, 1995; Offield *et al.*, 1996). Others reported Cre recombination in tissues other than pancreas, such as inner ear, hypothalamus, and in non-serotonergic neurons of the caudal hindbrain containing 5.5 kb of upstream mouse PDX-1 promoter (Honig *et al.* 2010), as well as duodenum and antral stomach (4.5 kb) (Gannon *et al.*, 2000), when Cre recombinase was driven by 4.5 kb of 5'-proximal mouse PDX-1 promoter. Expression of PDX-1 in parts of the nervous system could be due to a common cascade of transcription factor expression that both serotonergic neurons and pancreatic insulin-producing β -cells share during development (Honig *et al.*, 2010).

Regulation of PDX-1 promoter

The activity of the human PDX-1 promoter is regulated by several responsible elements and regulatory regions. The *PDX-1* gene is TATA-less and it utilizes three principal transcription start sites or E-boxes (enhancer box). These sequences are highly conserved among the rat, mouse, and human genes (Melloul *et al.*, 2002).

It is known that 6.5 kb upstream of the transcription start site of the PDX-1 promoter confer β -cell specific expression *in vitro* (Melloul *et al.*, 2002) and *in vivo* (Sharma *et al.*, 1996; Melloul *et al.*, 2002). This gene segment contains important control regions for PDX-1 expression, denominated as areas I, II and III (Gerrish *et al.*, 2000) and are highly conserved between the mouse and the human (Melloul *et al.*, 2002). Also, a distal enhancer element (area IV) (Gerrish *et al.*, 2004), regulates the expression levels of PDX-1 in pancreatic-cells (Eto *et al.*, 2007). Figure 10 shows a schematic structure of *PDX-1* gene and its transcriptional control regions.

Factors binding and regulating the transcriptional activity of the human and mouse PDX-1 promoter are hepatocyte nuclear factor (HNF)-3 β , HNF-1 α , specificity protein (SP)1/3, and PDX-1 itself (Melloul *et al.*, 2002). It was revealed that HNF-3 and PDX-1 transcription factors cooperate with another and HNF-3 plays an important role in the expression of the mouse PDX-1 (Marshak *et al.*, 2001). Furthermore, another conserved region was found to bind members of the USF-1 (upstream stimulatory factor) family of transcription factors near the E-box motive (Melloul *et al.*, 2002). Others reported that in the region between -3.7 and -3.4 kb upstream of the transcription initiation site of the human *PDX-1* gene binding sequences for the transcription factors SP1/3 and HNF-1 α /HNF-3 β were found. These factors up-regulate the transcriptional activity of the PDX-1 gene (Melloul *et al.*, 2002; Marshak *et al.*, 2001).

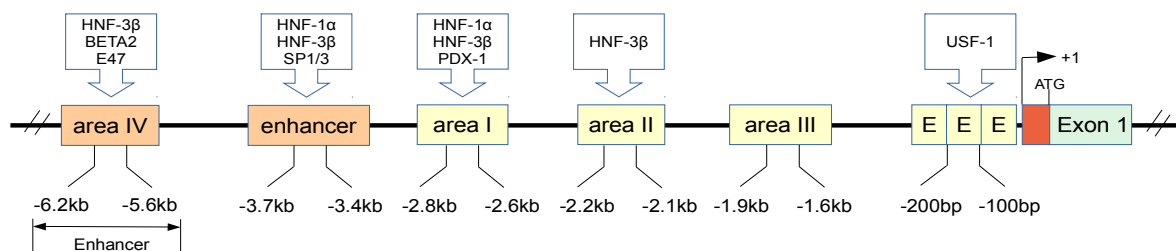


Figure 10: Schematic representation of the endogenous mouse and human *PDX-1* locus and the enhancer/promoter regions.

Cis-acting regulatory elements of the PDX-1 5'-flanking sequences are indicated as yellow boxes. The *PDX-1* gene is TATA-less and utilizes three principal transcription initiation sites (E-boxes motives indicated as "E"), followed by a short 5' untranslated sequence of approximately 100 nucleotides (indicated as a red box). There are three regions denominated area I, II, III in the gene region located at -2.8 kb to -1.6 kb relative to transcription start site +1 (TSS). A proximal and distal (Area IV) enhancer element are indicated as orange boxes. The positions relative to the TSS of the human *PDX-1* gene are indicated as numbers at the bottom. Transcription factors binding to the regulatory elements are indicated above each box.

Adapted from Melloul *et al.* (2002); Ashizawa *et al.* (2004).

As seen in Figure 10 the distal enhancer element (area IV), consists of binding sites for the transcription factors; HNF-3 β , beta-cell E-box trans-activator 2 (BETA2) and the E-box binding protein E47 factor (Sharma *et al.*, 1997). It is known that the factors HNF-3 β and BETA2 act together to induce PDX-1 expression (Melloul *et al.*, 2002). This 530 bp segment contains transcriptional control elements (Gerrish *et al.* 2004; Ashizawa *et al.*, 2004), which regulate the expression levels of PDX-1 in pancreatic cells (Eto *et al.*, 2007) and is important for islet cell-specific activity (Ashizawa *et al.*, 2004).

1.3.2 Inducible cre recombinase

Conditional expression systems that control Cre expression temporally are powerful tools to study gene function, to control gene inactivation, expression of mutated genes, and to analyse the effects of altered gene expression at precise times (Baron *et al.*, 2012). Furthermore, to

mimic spontaneous tumorigenesis in humans it is preferable to induce development of tumours in adult tissues instead during embryonic development (Politi and Pao, 2011). Two of the most widely used systems are those induced by tamoxifen (Indra *et al.*, 1999) or tetracycline (Heyer *et al.*, 2010).

The tamoxifen-inducible system is a fusion between a mutated ligand binding domain of the human estrogen receptor (ER) and Cre recombinase (Feil *et al.*, 1997; Rawlins and Perl, 2012). Two types of mutant ER have been generated, a single-point mutation in the ligand binding domain, G521R (called ER^T), or a triple mutation G400V, M543A, and L544A (called ER^{T2}) (Feil *et al.*, 1997, Indra *et al.*, 1999). The mutations prevent binding of the estrogen receptor to its natural ligand, but confer high affinity to a synthetic anti-estrogen, 4-hydroxy-tamoxifen (4-OHT). The triple mutant, ER^{T2}, results in a 10-fold enhanced sensitivity to the 4-hydroxy-tamoxifen, as compared to the ER^T (Indra *et al.*, 1999).

In the absence of tamoxifen, the Cre-ER^{T/T2} fusion protein binds to heat-shock proteins such as Hsp90 that is located in the cytoplasm (Zhang *et al.*, 2012). Hsp90 is a highly conserved, abundant and ubiquitously expressed protein that is associated with steroid receptors in cytosol extracts (Smith *et al.*, 1993). Hsp90 interacts with the estrogen receptor domain in the cytosol and prevents DNA recombination (Ristevski, 2005). In the presence of tamoxifen, Hsp90 is released from ER, which exposes the nuclear localization signal (NLS) of the ER (Zhang *et al.*, 2012). NLS serves as recognition sites for NLS receptor proteins, which import proteins into the cell nucleus (Smith *et al.*, 1993). Under the guidance of the NLS, the Cre recombinase, fused to a mutant estrogen ligand-binding domain, moves to the nucleus, where recombination may occur (Zhang *et al.*, 2012) (see Figure 11-A for a detailed illustration of this mechanism). Therefore, Cre expression under specific times/conditions can be controlled by delivering tamoxifen or by its absence (Walrath *et al.*, 2010).

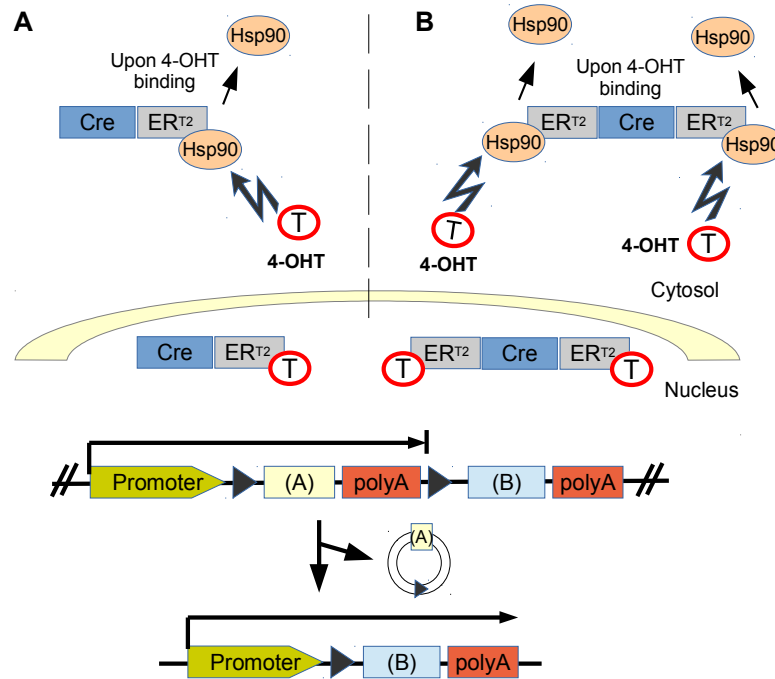


Figure 11: Outline of the Cre/LoxP-inducible systems, containing single or double tamoxifen-binding domains of triple mutated estrogen receptor (ER^{T2}).

The tamoxifen-inducible system is fusion of the Cre recombinase gene to one (A) or two (B) mutated ligand-binding domain(s) of the human estrogen receptor (ER) that is specifically activated by the synthetic ligand 4-hydroxytamoxifen (4-OHT). In the absence of 4-OHT, the inducible Cre recombinase binds to heat-shock proteins (Hsp90) and interacts with the estrogen receptor domain in the cytosol and prevents DNA recombination. In the presence of 4-OHT, upon binding to tamoxifen, the inducible Cre is translocated to the nucleus, where it mediates site-specific recombination. Thus, Cre will excise the floxed transgene A cassette (DNA sequence flanked by two *loxP* recognition sites) and transgene B will be transcript.

Abbreviations: polyA: polyadenylation signal; (A) or (B): vector containing two distinct transgenes; Hsp90: heat-shock protein; T: tamoxifen receptor.

Adapted from Ouvrard-Pascaud *et al.* (2003).

Cre-ER^{T2} is now the most popular and reliable way to temporally regulate recombination by ligand administration (Anastassiadis *et al.*, 2009). However, many authors reported basal expression of the ER and thus, Cre recombination in the absence of the ligand 4-OHT (known as "leaky effect") (Feil *et al.*, 1997; Hayashi and McMahon, 2002), given that the ER is endogenously expressed. Therefore, a Cre-ER system that does not undergo cytoplasmic translocation of Cre-ER^{T2} in the absence of 4-OHT induction has been developed to provide tighter control over recombinase activity. This is based on a modified version of tamoxifen-inducible Cre recombinase protein (ER^{T2}-Cre-ER^{T2}), composed of Cre recombinase and two tamoxifen-binding domains of triple mutated estrogen receptor (ER^{T2}), one at each end of the Cre recombinase (see Figure 11-B) (Verrou *et al.*, 1999; Kam *et al.*, 2012; McCarthy *et al.*, 2012). This ensures efficient binding of ER^{T2}-Cre-ER^{T2} to 4-OHT and maintaining maximal Cre activity (Kam *et al.*, 2012). The Cre double fused (ER^{T2}-Cre-ER^{T2}) may have a higher affinity for Hsp90 to form a stable complex. Degradation of the estrogen receptor possibly generates "active Cre" lacking the regulatory domain, whereas ER^{T2}-Cre-ER^{T2} is still inactive even after losing one regulatory domain (Matsuda and Cepko, 2007).

1.4 Aim of this work

The main goal of this work was to generate pigs predisposed to cancers of particular organs, notably the gut, pancreas, or lung. This was done by producing pigs carrying a latent form of an oncogenic mutant gene, known to be a cancer driver in humans, and then inducing its expression in a specific tissue. Work towards the first line of pigs had already started, resulting in inducible mutant pigs (*TP53*^{R167H}, *KRAS*^{G12D}) (Leuchs *et al.*, 2012; Li S. *et al.*, 2015, respectively). Therefore, the aim of this project was to generate Cre driver pig lines. This required four steps:

- 1) identification, characterisation and selection of appropriate promoters to drive tissue-specific Cre expression in gut, pancreas and lung;
- 2) assessment of promoter function *in vitro*;
- 3) construction of tissue-specific Cre vectors and gene placement at the porcine *ROSA26* locus, or by random transgene integration;
- 4) *in vivo* characterisation of Cre expression in transgenic pigs.

To visualise Cre-activity *in vitro* and *in vivo* the tissue-specific Cre constructs were to be introduced into porcine cells carrying a CAG promoter-directed floxed mTomato/mGFP dual reporter cassette (Li S. *et al.*, 2014). This would be accomplished by placement of the tissue specific Cre constructs into porcine *ROSA26* 'stacked' adjacent to the dual reporter to avoid transgenes segregation or by Cre transgene random integration to achieve multiple Cre copy number.

2 Material and Methods

2.1 Material

2.1.1 Buffers and solutions

Buffers and solutions	Composition or Source
Gel loading buffer (5x)	5 ml glycerol; 4 ml EDTA (0.5 M); point of a spatula Bromphenol blue; filled up with ddH ₂ O to 10 ml
DNA lysis buffer	0.1M Tris; 5mM EDTA; 0.2% (w/v) SDS; 0.2M NaCl; 100 µg/ml Proteinase K (before use)
Flow cytometer buffer	1 % BSA in D-PBS; 2 mM EDTA
Miniprep solution I	5 mM sucrose; TRIS (pH 8.0); 10 mM EDTA
Miniprep solution II	1% SDS; 0.2 N NaOH
Miniprep solution III	3 M sodium acetate (pH 5.3)
Rnase Away	Roth, Karlsruhe, Germany
TAE buffer (50x)	2 M Trisbase; 50 mM EDTA (0.5 M); 57.1 ml glacial acetic acid; filled up with ddH ₂ O to 1 l
TBE buffer (10x)	0.9 M Trisbase; 20 mM EDTA; 0.9 M boric acid; filled up with ddH ₂ O to 1 l
TTE buffer	20 mM Trisbase (pH 8.3); 2 mM EDTA (pH 7.8); Triton-x 1% filled up with ddH ₂ O to 40 ml

2.1.2 Chemicals

Chemicals	Source
Acetic acid	Fluka Laborchemikalien GmbH, Seelze, Germany
Boric acid	Fluka Laborchemikalien GmbH, Seelze, Germany
Bovine serum albumin (BSA)	PAA, Pasching, Austria
Bromphenol blue	Sigma, Steinheim, Germany
Calcium chloride	Merck KGaA, Darmstadt, Germany
Chloroform	Sigma, Steinheim, Germany
Dimethyl sulfoxide (DMSO)	Sigma, Steinheim, Germany
Ethanol absolute	Riedel-de-Haen, Seelze, Germany
Ethidium bromid solution	Sigma, Steinheim, Germany
Ethylenediamintetraacetic acid (EDTA)	Sigma, Steinheim, Germany
Formalin	Sigma, Steinheim, Germany

Chemicals	Source
GenAgarose L.E.	Genaxxon Bioscience GmbH, Biberach, Germany
Glacial acetic acid	Fluka Laborchemikalien GmbH, Seelze, Germany
Glutaraldehyde	Fluka Laborchemikalien GmbH, Seelze, Germany
Glycerol	Carl Roth GmbH, Karlsruhe, Germany
Glycine	Carl Roth GmbH, Karlsruhe, Germany
Isopropanol (2-Propanol)	Carl Roth GmbH, Karlsruhe, Germany
Magnesium chloride-hexahydrate	Merck KGaA, Darmstadt, Germany
Methanol	Sigma, Steinheim, Germany
Saccharose	Sigma, Steinheim, Germany
Sodium chloride	J.T. Baker, Deventer, Holland
Sodium citrate tribasic dihydrate	Sigma, Steinheim, Germany
Sodium thiosulfate	Sigma, Steinheim, Germany
Sodium acetate	Roth, Karlsruhe, Germany
Sodium dodecyl sulfate (SDS)	Sigma, Steinheim, Germany
Sucrose	Sigma, Steinheim, Germany
Trizma base (Tris base)	Sigma, Steinheim, Germany
Tris hydrochloride (Tris HCl)	Sigma, Steinheim, Germany
Trizol	Invitrogen, Karlsruhe, Germany
Tween 20	Sigma, Steinheim, Germany

2.1.3 Chemicals for Southern blot analysis

Chemicals for Southern blot	Source
Anti-Digoxigenin-AP, Fab fragments	Roche Diagnostics GmbH, Mannheim, Germany
Blocking Reagent	Roche Diagnostics GmbH, Mannheim, Germany
CDP-Star	Roche Diagnostics GmbH, Mannheim, Germany
DIG Easy Hyb Granules	Roche Diagnostics GmbH, Mannheim, Germany
Digoxigenin-11-2'-deoxy-uridine- 5'-triphosphate, alkaline-labile (DIG-labelled UTP)	Roche Diagnostics GmbH, Mannheim, Germany
DNA molecular weight marker VII, Digoxigenin-labelled	Roche Diagnostics GmbH, Mannheim, Germany

2.1.4 Disposables

Disposable	Source
Bacterial culture 14 ml Polypropylene Round-Tube	Becton, Dickinson GmbH, Sparks, USA
0.5 ml, 1.5 ml and 2.0 ml EP tubes	Brand, Wertheim, Germany
Cell culture flasks (25, 75, 150 cm ²)	Corning Inc., New York, USA
Cell culture plates (6-, 12-, 24-well)	Corning Inc., New York, USA
Centrifugation tubes (15-, 50 ml)	Corning Inc., New York, USA
Costar stripettes 1, 2, 5, 10, 25 ml	Corning Inc., New York, USA
CryoTubes	Nunc, Wiesbaden-Biebrich, Germany
Electroporation cuvettes, 2 mm	Peqlab, Erlangen, Germany
Electroporation cuvettes, 4 mm	Peqlab, Erlangen, Germany
Glass transfer pipettes	Brand, Wertheim, Germany
Glassware (bottles, flasks)	Marienfeld GmbH, Lauda-Königshofen, Germany
PCR-reaction tube	Brand, Wertheim, Germany
Petri dish (10 cm)	Brand, Wertheim, Germany
Photometer Cuvettes	Eppendorf, Hamburg, Germany
Pipette tips	Brand, Wertheim, Germany
Plugged pipette tips (2, 20, 200 and 1000 µl)	Mettler Toledo GmbH, Dreieich, Germany
Rainin pipette tips (2, 20, 200 and 1000 µl pipettes)	Mettler Toledo GmbH, Dreieich, Germany
Rotilabo [®] blotting paper (1mm)	Carl Roth GmbH, Karlsruhe, Germany
Sterile plastic pipettes 1 - 25 ml	Corning Inc., New York, USA
Syringes (BD Discardit [™])	Becton, Dickinson GmbH, Sparks, USA
Sterile syringe filter (0.22 µm)	Sartorius Biotech, Göttingen, Germany

2.1.5 Cell culture media

Mammalian cell culture medium	Source
Advanced Dulbecco's Modified Eagle's Medium (Advanced DMEM)	Gibco BRL, Paisley, Scotland
Dulbecco's Modified Eagle's Medium (DMEM), high glucose (4.5 g/l)	Sigma, Steinheim, Germany

Mammalian cell culture medium	Source
Opti-MEM Reduced Serum Medium modification of MEM (Eagle's)	Gibco BRL, Paisley, Scotland
RPMI 1640 with L-Glutamine	Sigma, Steinheim, Germany

Bacterial cell culture medium	Source
Difco Luria broth Agar, Miller	Becton Dickinson and Company, Sparks, USA
Difco Luria Broth Base	Becton Dickinson and Company, Sparks, USA

2.1.6 Cell culture antibiotics

Bacterial cells antibiotics	Supplier	Working concentration
Ampicillin	Sigma, Steinheim, Germany	100 µg/ml
Kanamycin	Sigma, Steinheim, Germany	30 µg/ml

Mammalian cells antibiotics	Supplier	Working concentration
For selection		
Blasticidin	Germany	2-16 µg/ml
Geneticin	Sigma, Steinheim, Germany	250-800 µg/ml
For primary cell isolation		
Amphotericin B	Sigma, Steinheim, Germany	0.25 µg/ml
Penicillin/streptomycin	Sigma, Deisenhofen, Germany	100 IU/ml and 100 µg/ml

2.1.7 Supplements, chemicals and solutions for cell culture

Supplements, chemicals and solutions	Source
Accutase	PAA, Pasching, Austria
Bovine pituitary extract	PromoCell GmbH, Heidelberg, Germany
β-mercaptoethanol	Sigma, Steinheim, Germany
Cell Culture Water, EP-grade	PAA, Pasching, Austria
Collagen R (type I)	Serva, Heidelberg, Germany
Collagenase Type I and IV	Sigma, Steinheim, Germany
Dexamethasone (water-soluble)	Sigma, Steinheim, Germany
Dimethyl sulfoxide (DMSO)	Sigma, Steinheim, Germany
Dulbecco's PBS, w/o Ca & Mg	PAA, Pasching, Austria
Epidermal Growth Factor Human	Sigma, Steinheim, Germany
Epinephrine	Sigma, Steinheim, Germany

Supplements, chemicals and solutions	Source
Ethanolamine	Sigma, Steinheim, Germany
Ferrous sulfate	Sigma, Steinheim, Germany
Fetal calf serum (FCS)	PAA, Pasching, Austria
GlutaMAX	Gibco BRL, Paisley, Scotland
HEPES	Invitrogen, Karlsruhe, Germany
Human Fibroblast Growth Factor	Genaxxon, Biberach, Germany
Hydrocortisone	Sigma, Steinheim, Germany
Hypoosmolar Buffer	Eppendorf, Hamburg, Germany
Lipofectamine 2000	Invitrogen, Karlsruhe, Germany
Insulin solution human	Sigma, Steinheim, Germany
Non-essential amino acids (NEAA)	Sigma, Steinheim, Germany
Nanofectin solution	PAA, Pasching, Austria
Nucleofector solution	Lonza, Cologne, Germany
O-Phosphorylethanol-amine	Sigma, Steinheim, Germany
Passive Lysis Buffer	Promega, Mannheim, Germany
Retinoic acid	Sigma, Steinheim, Germany
Selenium	Sigma, Steinheim, Germany
Sodium pyruvate	Sigma, Steinheim, Germany
Transferrin	Sigma, Steinheim, Germany
T3 Triiodothyronine	Sigma, Steinheim, Germany
Zinc sulfate	Sigma, Steinheim, Germany

2.1.8 Bacterial and mammalian cells

Table 4: Mammalian cell lines

Cell lines	Organism	Description	Source
Caco-2	Human	Colorectal adenocarcinoma	Chair of Livestock Biotechnology
Calu-3	Human	Lung adenocarcinoma	
INS-1	Rat	Pancreatic islets tumor	
HEK-293	Human	Embryonic kidney	
HT1080	Human	Fibrosarcoma	
NIH-3T3	Mouse	Embryonic fibroblast	
NTERA-2	Human	Pluripotent embryonal carcinoma	
Panc-1	Human	Epithelial carcinoma	
PM86	Pig	Porcine melanoma	
SW-480	Human	Colorectal adenocarcinoma	

Table 5: Mammalian primary cells

Primary cells	Organism	Description	Source
pAdMSCs	Pig	Adipose-derived mesenchymal stem cells, different isolations	Chair of Livestock Biotechnology or isolated during this work
rEAF	Rat	Ear Fibroblast	
pKDNF	Pig	Kidney fibroblast, different isolations	
pLEC	Pig	Lung epithelial cells, different isolations	Isolated during this work

Table 6: Strains and genotype of Escherichia coli (E. coli)

Bacterial strain	Genotype	Supplier
DH10B	F ⁻ mcrAΔ(mrr-hsdRMS-mcrBC) Φ80dlacZΔM15, ΔlacX74 deoR recA1 araD139 Δ(ara, leu)7697 galU galK rpsL endA1 nupG	Invitrogen, Karlsruhe, Germany

2.1.9 Cloning vectors and plasmids

Cloning vectors	Source
pJET1.2/blunt	Invitrogen, Karlsruhe, Germany
pGEM-T Easy Vector System	Promega, Mannheim, Germany
pSL1180	Amersham Bioscience, New Jersey, USA
Plasmids	Source
paavCAG-iCre	Addgene, Cambridge, USA
pBS-Villin-CrehGHpA	Kind gift of Dr. Sylvie Robine
pGEMT-ROSA26-CAG-mTmG-BS	Chair of Livestock Biotechnology
pL452-infBSinfK	Chair of Livestock Biotechnology
pPGK-Cre	Chair of Livestock Biotechnology
pPGK-neo	Chair of Livestock Biotechnology
pMouseROSA26-mTmG	Addgene, Cambridge, USA
psiCHECK-2	Promega, Mannheim, Germany
pSL1180-LSL-PdxeH-CreP	Chair of Livestock Biotechnology

2.1.10 Kits for DNA, RNA isolation

Kits	Source
Direct-zol TM RNA Miniprep	Zymo Research, Irvine, USA
Nucleo Bond, Xtra Midi and Maxi	Macherey-Nagel GmbH & Co. KG, Düren, Germany
Rneasy mini kit	Quiagen GmbH, Hilden, Germany

Kits	Source
Turbo DNA-free	Ambion, Huntingdon, UK
GenElute Mammalian Genomic DNA Miniprep Kit	Sigma, Steinheim, Germany
Wizard SV gel and PCR clean-up System	Promega, Mannheim, Germany

2.1.11 Enzymes

Enzymes for cloning	Source
Calf Intestinal Alkaline Phosphatase (CIP)	New England Biolabs, Frankfurt, Germany
DNA Polymerase I, Large (Klenow) Fragment	New England Biolabs, Frankfurt, Germany
Proteinase K	Sigma, Steinheim, Germany
Restriction endonuclease BglII	Fermentas, St. Leon-Rot, Germany
Restriction Endonucleases	New England Biolabs, Frankfurt, Germany
RNase A solution	Sigma, Steinheim, Germany
T4 DNA Ligase	New England Biolabs, Frankfurt, Germany

2.1.12 Oligonucleotides

Table 7: Oligonucleotides for sequencing

Oligonucleotides for sequencing	Sequence 5' - 3'
Cre F	ATACCGGAGATCATGCAAGC
ERT2 F.	GTCAGTGCCTTGTTGGATGC
ERT2 R.	ACAGTAGCTTCACTGGGTGC
ERT2 F2.	CGGGCTCTACTTCATCGCAT
R1 ERT2	TCTGGTAGGATCATACTCGGAAT
F.PDX PH1	TCTGAAACCACCGAGGAAGAC
F.PDX PH2	TGGAAGCAAATGAAGCATCG
F.PDX PH3	ATGCCCTTGCTGTCACCGAA
F.PDX Ebox	TCTTTCCCCCTCGCTGTATTG
F1 SFTP-C	GTTTCCCAGTCACGACGTT
F2 SFTP-C	TGCTCAGTGGGTTAGGGATT
F3 SFTP-C	AGAGCGACAGCCTGAGAAAG
F4 SFTP-C	TGGGGAGTAGTGTGGACCTC
F5 SFTP-C	TTGAAGTTCCTGGGTTTTGG

Oligonucleotides for sequencing	Sequence 5' - 3'
F.hGH-pA Villin	TTCAAGCGATTCTCCTGCCT
Reverse Villin	CAGATCCGAATTCGATATCAAGC
Villin_R_start	ACAAAGGTTTCATGTAGCTG
rb β g-EcoRI-iCre F	GGGACACAGCATTGGAGTCA
iCre_SV40_R	GGGACACAGCATTGGAGTCA
T7	TAATACGACTCACTATAGGG

Table 8: Oligonucleotides for cDNA amplification

Oligonucleotides for cDNA amplification	Specie and Gene	Sequence 5' - 3'
F. Pig PDX Ex.1 R. Pig PDX Ex.2	Pig; PDX-1	TGAAGTCTACCAAGGCTCACG CGCTTCTTGTCTCCTCCTTT
F. rat-PDX Ex.1 R. rat-PDX Ex.2	Rat; PDX-1	TTCCCGAATGGAACCGAGAC TCTTCCACTTCATGCGACGG
F.hPDX- primer 3 R.hPDX- primer 3	Human; PDX-1	AAGTCTACCAAAGCTCACGC GTTCAACATGACAGCCAGCT
F.vil-1 HS mRNA R.vil HS mRNA	Human; Villin-1	GGCACCTCCCGAATAACAA ATCCAGAAGTTGGCTGGCTC
F.Vil-1 pig mRNA R.Vil-1 pig mRNA	Pig; Villin-1	GAACAAGAACCACCGAGGCA AGCTGACCCTTGAAGATGGC
SP-C Forw.1 SP-C Rev.1	Pig; SFTP-C	GTCACACTTGGGGATGAGCA CCACGACAAGAAGGCGTTTG
F.SPC Calu-3 R.SFC Calu-3	Human; SFTP-C	GAGCCAGAAACACACGGAGA CGATCAGCAGCTGGTAGTCAT
Cre_F Cre_R	Bacteriophage; Cre	GCATTTCTGGGGATTGCTTA TCAATACCGAGATCATGCA
F. GAPDH R. GAPDH	Pig; GAPDH	TGGTGAAGGTCGGAGTGAAC GGAAGGCCATGCCAGTGAGC
F. rat GAPDH R. rat GAPDH	Rat and Human; GAPDH	TCATTGACCTCAACTAC GTAGTTGAGGTCAATGA
hPolR2A F hPolR2A R	Pig, Rat and Human; hPolR2A	GCACCACGTCCATGACAT GTGCGGCTGCTTCATAA

Table 9: Oligonucleotides for gene targeting PCR detection

Oligonucleotides for gene targeting PCR detection	Sequence 5' - 3'
<i>Rosa26</i> I1 F2	TATGGGCGGGATTCTTTTGC
<i>Rosa26</i> Loc 2R	CTTTACGGTATCGCCGCTCC
<i>Rosa26</i> I3 R2	CAGGTGGAAAGCTACCCTAGCC
<i>Rosa26</i> I1 R3	CTTGGGTTTCCTGTGCAAAC
<i>Rosa26</i> E1F1	CGCCTAGAGAAGAGGCTGTGC
targ_SA_R	GAAAGACCGCGAAGAGTTTG

Table 10: Oligonucleotides for Cre recombination PCR detection

Oligonucleotides for Cre recombination PCR detection	Sequence 5' - 3'
Screen F pdx-Cre	ATGCTTCTGATTTGGTGGCC
Screen R pdx-Cre	TGCTGGGATGGTAGAACAGG

Table 11: Oligonucleotides for villin-1 piglet PCR detection

Oligonucleotides for villin-1 piglet PCR detection	Sequence 5' - 3'
F3 Villin	AGGGAGGTCGAGGCTAAAGAA
R_Col_PCR_iCre	TGACTCCAATGCTGTGTCCC

Table 12: Oligonucleotides for DIG-labeled for Southern Blot

Oligonucleotides DIG-labeled for Southern Blot	Sequence 5' - 3'
PR neo F	GCCACCATGATTGAACAAGA
probe_neo R3	AAGGCGATAGAAGGCGATG

Table 13: Oligonucleotides for Gibson Assembly

Oligonucleotides for Gibson Assembly	Sequence 5' - 3'
R26short_F_pSL (F1)	agcttaagtctagagttaaactTTTGTGTCGCAATTCCTG
R26short_R_pSL (R1)	actagcgtaccgtttGGCCACCAAATCAGAAGC

lowercase: Overhang for cloning; UPPERCASE: oligonucleotide for porcine *ROSA26*

2.1.13 Miscellaneous

Miscellaneous	Source
dNTPs	Biomers.net GmbH, Ulm, Germany
DualGlo Luciferase-Assay	Promega, Mannheim, Germany
Ladder (100 bp; 1 kb; 2 Log)	New England Biolabs, Frankfurt, Germany
RNase away	Roth, Karlsruhe, Germany
RNase free water	Quiagen, Hilden, Germany
TRIZOL reagent	Invitrogen, Karlsruhe, Germany

2.1.14 Equipment

Equipment	Source
+4°C fridge	Beko Technologies, Dresden, Germany
-20°C freezer	Liebherr International, Bulle, Switzerland
-80°C freezer (Therma Forma)	Thermo Electron GmbH, Dreieich, Germany
Agarose gel electrophoresis, classic CSSU78 / CSSU1214	Thermo Electron GmbH, Dreieich, Germany
Analytical balance, 440-33N	Kern, Balingen, Germany
AxioCAM MRc and HR	Zeiss AG, Oberkochen, Germany
Bio imaging System Gene Genius	Bio Imaging System Gene Genius, Syngene, Cambridge, UK
BioPhotometer 6131	Eppendorf, Hamburg, Germany
Countess automated cell counter	Invitrogen, Karlsruhe, Germany
Centrifuge 5810 and miniSpin	Eppendorf, Hamburg, Germany
Centrifuge Mikro200	Hettich Zentrifugen, Tuttlingen, Germany
Coolable centrifuge 1-15K and 4K-15C	Sigma, Osterode, Germany
Digital Graphic Printer UP-D895MD	Syngene, Cambridge, UK
Freezing Container	Nalgene, Rochester, USA
Flow Cytometer BD LSR II	Becton Dickison, Mountain View, USA
Heating block	Gefran Deutschland, Seligenstadt, Germany
Ice maker	Eurfrigor, Lainate, Italy
Incubator CO ₂	Forma Scientific Inc., Marietta, Ohio, USA
Luminometer, Glomax 20/20	Turner Biosystems, Mannheim, Germany
Membrane high pure water	Membranepure, Bodenheim, Germany
Microscope, Axiovert 40 CFL	Zeiss Microimaging GmbH, Göttingen, Germany

Equipment	Source
Microscope, Axiovert 40 CFL	Zeiss Microimaging GmbH, Göttingen, Germany
Microscope, Axiovert 200M	Zeiss Microimaging GmbH, Göttingen, Germany
Microwave MDA MW12M706	Haushaltswaren GmbH, Barsbüttel, Germany
Minispin	Eppendorf, Hamburg, Germany
Mini trans-blot electrophoretic transfer cell	BioRad, Luton, United Kingdom
Multiporator	Eppendorf, Hamburg, Germany
Nano Drop Lite	Thermo Scientific, Karlsruhe, Germany
Nucleofector™	Lonza, Cologne, Germany
PCR Unit	MJ Research PTC Thermal Cycler, GMI, Inc., USA
Pipetman Ultra U2 0.2 - 2 µl	Gilson, Bad Camberg, Germany
Pipetman P20, P200, P1000	Gilson, Bad Camberg, Germany
Sterile Cabinets class II HERAsafe	Heraus Instruments, Munich, Germany
Shaker, Forma orbital shaker	Thermo Electron Corporation, Dreieich, Germany
Sterile-Cycle CO ₂ incubator	Thermo Electron Corporation, Dreieich, Germany
Trans-Blot Module	BioRad, Luton, UK
UV-Transilluminator NU72K	Benda, Wiesloch, Germany
Vortex Mixer	VELP Scientifica, Usmate, Milano, Italy
Waterbath Haake C10	Thermo Electron GmbH, Dreieich, Germany

2.1.15 Software

Software	Source
AxioVision	Zeiss AG, Oberkochen, Germany
Basic local alignment search tool	http://www.ncbi.nlm.nih.gov/blast/Blast.cgi
BD FACSDiva	Becton Dickison, Mountain View, USA
ClustalW	http://www.ebi.ac.uk/Tools/clustalw2
Ensembl Genome Browser	http://www.ensembl.org
EveryVector	http://www.everyvector.com
Finch TV	http://www.geospiza.com/finchtc
GenBank	http://www.ncbi.nlm.nih.gov
Image J	National Institute of Healthy, USA
New England BioLabs	http://www.neb.com
Primer- BLAST	http://www.ncbi.nlm.nih.gov/tools/primer-blast
Reverse Complement	http://www.bioinformatics.org/sms/rev_comp.html
UCSC Genome Browser	http://www.genome.ucsc.edu
VectorNTI	Invitrogen, Karlsruhe, Germany

2.2 Methods

2.2.1 Tissue culture methods

2.2.1.1 Cultivation of mammalian cell lines

Cell lines were cultivated in 25, 75 or 150 cm² T-flasks, with a total volume of 5, 20 or 30 ml of culture medium (see Table 14), respectively. They were maintained at 37°C in a humidified, 5% enriched CO₂ incubator. Cells were subcultured twice per week to maintain the cells in exponential growth. To subculture the cells, the medium was removed and cells were washed once with D-PBS and detached by adding 1, 3 or 5 ml Accutase, followed by incubation at 37°C for 5 min. Accutase was inactivated using a double amount of medium containing 10% FCS (v/v). Cell densities and viability were determined by hemocytometer counts or by automated cell counter (Countess™) using trypan blue stain. The cell suspension was transferred into a new culture flask for subculturing or directly used for experiments.

Table 14: Mammalian cells and culture growth medium

Mammalian cell	Growth medium
Primary cells:	
pAdMSCs	Advanced DMEM (4.5 g/l glucose); 2 mM GlutaMAX; 1 x Non essential amino acids; 10% (v/v) FCS
pLEC	DMEM (4.5 g/l glucose); 2 mM GlutaMAX; 1 x Non essential amino acids; 1 mM Sodium pyruvate; 4% (v/v) FCS; 10 µg/ml Bovine pituitary extract; 0.5 mg/ml BSA; 1.1x10 ⁻⁴ M Calcium Chloride; 0.5 - 25 ng/ml Epidermal Growth Factor; 2.7 µM Epinephrine; 0.5 µM Ethanolamine; 1.5x10 ⁻⁸ Ferrous Sulfate; 6x10 ⁻⁴ Magnesium Chloride; 0.5 µM Phosphorylethanol-amine; 5x10 ⁻⁸ Retinoic acid; 3.0 µM Selenium; 0.125 µM Transferrin; 0.01 µM Triiodothyronine; 3.0 µM Zinc Sulfate
poFF	DMEM (4.5 g/l glucose); 2 mM GlutaMAX; 1 x Non essential amino acids; 1 mM Sodium pyruvate; 10% (v/v) FCS
pKDNF	
rEAF	
Cell Lines:	
Caco-2	DMEM (4.5 g/l glucose); 2 mM GlutaMAX; 1 x Non essential amino acids; 1 mM Sodium pyruvate; 20% (v/v) FCS
INS-1	RPMI; 2 mM GlutaMAX; 12 mM HEPES; 1 mM Sodium pyruvate 10% (v/v) FCS
Calu-3	DMEM (4.5 g/l glucose); 2 mM GlutaMAX; 1 x Non essential amino acids; 1 mM Sodium pyruvate; 10% (v/v) FCS
HEK-293	
HT1080	
NIH-3T3	
NTERA-2	
Panc-1	
PM86	
SW-480	

2.2.1.2 Isolation and cultivation of primary porcine AdMSCs

Primary porcine adipose tissue derived mesenchymal stem cells (pAdMSCs) were isolated from a male reporter Landrace pig at the age of 11 months. The neck fat tissue was disinfected with 80% ethanol and transported at 37°C in a sterile tube containing a sterile solution made from D-PBS supplemented with 1 x Penicillin/Streptomycin and 2.5 µg/ml Amphotericin B. The fat tissue was then washed 3 times with the same sterile solution and transferred to petri dishes. Afterwards the tissue was minced with a sterile scalpel and mechanically and enzymatically digested. The tissue was mixed with a D-PBS solution containing 10 ml Collagenase type I A (1 mg/ml) and transferred to a flask with a magnetic stir bar and incubated on a magnetic stirrer at 37°C for 30 min. In order to remove remaining undigested tissue the suspension was filtered through a 100 µm cell strainer. The cell suspension was mixed with an equal volume of pAdMSCs medium, centrifuged for 10 min at 1000 x *g*. The pellet was resuspended in pAdMSCs medium supplemented with 1 x Penicillin/Streptomycin and 2.5 µg/ml Amphotericin B and plated onto T150 cm² flasks. For five days medium was changed daily. Thereafter the cells were cultured in pAdMSCs medium without antibiotic and anti-mycotic for additional three days to perform mycoplasma tests.

2.2.1.3 Isolation and cultivation of primary porcine KDNFs

Primary porcine kidney fibroblasts (pKDNF) were isolated from a male reporter Landrace pig at the age of 11 months. The kidney was washed with a sterile solution made from D-PBS supplemented with 1 x Penicillin/Streptomycin and 2.5 µg/ml Amphotericin B and transported at 4°C in a sterile tube containing the sterile solution. Fat and necrotic tissue were removed and pieces of the tissue were then washed 3 times with the same sterile solution and transferred to petri dishes. Afterwards the tissue was minced with a sterile scalpel and mixed with a D-PBS solution containing 10 ml Collagenase type II (with higher tryptic activity), in a flask with a magnetic stir bar, at 37°C for 30 minutes. Subsequently, the digested mixture was mixed with an equal amount of pKDNF medium supplemented with 1 x Penicillin/Streptomycin and 2.5 µg/ml Amphotericin B and centrifuged at 300 *g* for 10 minutes. The cell pellet was washed once more with pKDNF medium and plated onto T150 cm² flasks. For seven days medium has been changed daily. Thereafter cells were cultured in pKDNFs medium without antibiotic and anti-mycotic for additional three days to perform mycoplasma tests.

2.2.1.4 Isolation and cultivation of primary porcine lung epithelial cells

Porcine lung epithelial cells (pLEC) both from wild type Göttinger minipigs and Landrace pigs, as well from reporter Landrace pigs were isolated and cultured *in vitro* on 0.5 mg/ml collagen type I

coated plates and pLEC medium (see Table 14). The lung surface and main bronchus cannula were washed, with sterile D-PBS containing 1 x Penicillin/Streptomycin and 2.5 µg/ml Amphotericin B, using a 5 ml plastic syringe. Alveolar ducts and alveolar sacs were excised with a sterile scissor and scalpels. The tissue was transferred to petri dishes filled with the same sterile D-PBS solution as above. Then the tissue was transferred to a new petri dish and finely minced with the help of sterile scissors and scalpels. The minced tissue was transferred to a 50 ml Falcon tube containing the sterile D-PBS supplemented with antibiotics/antimycotics and centrifuged at 300 x g for 5 min. This procedure was repeated 3-5 times until the suspension turned clear. The cell pellet was resuspended in D-PBS containing 1mg/ml Collagenase type I A and transferred to a 50 ml shaker flask. The tissue was incubated for 30 min at 37°C with shaking. Medium containing 10% FCS was added to the cell suspension in order to stop the collagenase activity. The cell suspension was pelleted at 300 x g for 5 min, washed with D-PBS and centrifuged again. The cell pellet was resuspended in pLEC medium containing 1 x Penicillin/Streptomycin and 0.25 µg/ml Amphotericin B and plated onto collagen coated 6 well plates and 25 cm² T-flasks. The medium was changed daily for ten days. On the tenth day, antibiotics/antimycotics were removed and after three days 100 µl from the supernatant was used for mycoplasma test.

2.2.1.5 Immortalisation of primary porcine lung epithelial cells

To avoid culture induced senescence of primary porcine LEC, half of the isolated cells were immortalised using a plasmid that expresses a full-length cDNA of human telomerase reverse transcriptase (hTERT). Porcine LEC cells were plated at a confluence of 90% into 6 wells and transfected using nanofectin. LEC medium was removed and each well was washed with D-PBS supplemented with antibiotics/antimycotics. Cells were transfected with 2 µg of plasmid DNA (hTERT) and 6.4 µl of nanofectin solution according to the manufacturer's instructions. Twelve hours after transfection medium was changed. Expression of hTERT was confirmed by RT-PCR (reverse transcriptase polymerase chain reaction) after RNA isolation and cDNA synthesis.

2.2.1.6 Cell counting

Cell numbers, density and viability were determined either by the use of hemocytometer chamber or by automated cell counter using trypan blue as a stain. Detached cells were mixed 1:1 with trypan blue and counted. In the case of hemocytometer chamber use, four squares were counted and the cell number/ml was determined according to the formula:

$$\text{number of cells per ml} = \text{number of cells in four squares} / 4 \times \text{dilution factor} \times 10^4$$

2.2.1.7 Freezing and thawing mammalian cells

For cells freezing, the cells were detached from the culture vessel using Accutase (see Section 2.2.1.1). Thereafter the cells were counted (see Section 2.2.1.6) and the desired amount of cells was centrifuged at 300 x g for 5 min. After centrifugation cells were resuspended in sterile filtered Cryopreservation medium (60% FCS; 30% medium and 10% DMSO) and transferred into 2 ml cryotubes. The cryotubes were placed in a freezing container and stored at -80°C to ensure gradual cooling of -1°C per minute. After 3-7 days, cells were transferred into a liquid nitrogen tank.

To thaw cells, the cryotube was incubated at 37°C in a water bath until cell suspension become liquid and then mixed with 10 ml of the pre-warmed cell culture medium and centrifuged at 300 x g for 5 min. The cell pellet was resuspended in an appropriate volume of medium and plated on suitable culture vessel.

2.2.1.8 Transfection methods

Different transfection methods were employed for each primary cell or cell line used, as follows:

Electroporation: A total of 1×10^6 cells were resuspended in pre-warmed hypoosmolar buffer containing sterile plasmid DNA. Then cells were transferred to an eletroporation cuvette and pulsed at 1200V for 85 μ s in an Eppendorf Multiporator. Cells were allowed to recover for 10 min at RT and then they were transferred to two 25 cm² T-flasks each containing 5 ml pre-warmed medium.

Lipofection: One day prior to lipofection 0.25 to 8×10^5 cells per well of a twelve or six well plate were plated. They were transfected according to the manufacturer's instructions. Medium was changed four-six hours after transfection.

Nanofection: One day before nanofection 1 or 2×10^5 cells were plated per well into twelve or six well plates, respectively. Cells were transfected according to the manufacturer's instructions and medium was changed four hours post-transfection.

Nucleofection: In the case of nucleofection 0.5 to 1×10^6 cells were pelleted by centrifugation at 300 x g for 5 min and resuspended in 100 μ l nucleofection solution containing sterile plasmid DNA. The cell suspension was transferred to a nucleofection cuvette and pulsed using a specific program per cell preparation (see Table 15). Approximately 500 μ l medium were added to the cuvette and the cell suspension was transferred either to a 6 well plate or a 25 cm² T-flask depending on the cell line transfected.

A more detailed overview of the different transfection methods used for each primary cell or cell line used is showed in the Table 15.

Table 15: Primary cells, cell lines, plasmid DNA concentration, reagents and programs used for each transfection method.

Mammalian cells	Transfection method	pDNA (µg)	Reagent (µl)	Kit	Program
Primary cells:					
pAdMSCs	Eletroporation	10	800	Eppendorf	1200 V - 85 µs
	Nucleofection	2-3	100	Amaxa MSC	C-017
rEA	Nucleofection	2-3	100	Primary Fibroblast	U-023
poFF	Eletroporation	5	800	Eppendorf	1200 V - 85 µs
pKDNF	Nucleofection	2-3	100	Primary Fibroblast	U-012
pLEC	Nanofection	2-3	6.4-9.6	Nanofectin	None
Cell Lines:					
Caco-2	Lipofection	3	10	Lipofectamine 2000	None
	Nucleofection	2-3	100	Amaxa MSC	B-024
Calu-3	Nucleofection	2	100	Primary Fibroblast	U-023
INS-1	Lipofection	3	10	Lipofectamine 2000	None
HEK-293	Lipofection	3	10	Lipofectamine 2000	None
	Nucleofection	2-3	100	Amaxa V	Q-001
NIH-3T3	Nucleofection	2-3	100	Primary Fibroblast	U-023
Panc-1	Nucleofection	2	100	Primary Fibroblast	U-023
PM86	Nucleofection	2	100	Primary Fibroblast	C-017
SW-480	Nucleofection	2-3	100	Amaxa V	L-023

2.2.1.9 Generation of stable cell clones and lines

To generate stable cell clones or cell lines, 48 h post-transfection the cells were split at a ratio of 1:8 onto 150 mm dishes or split at a ratio of 1:10 onto 150 cm² T-flasks, respectively. The selection medium was changed every 2-3 days until un-transfected cells, served as a negative control, were dead.

Individual single cell colonies were pick using cloning cylinders, detached using Accutase and transferred to single wells of 12 well plates. Pool of cells were also detached using Accutase and then transferred onto 25, 75 or 150 cm² T-flasks. They were cultured in the presence of selective medium. When the cells reached confluence they were expanded and frozen.

2.2.1.10 Cre transduction experiments

The Cre protein was produced in the laboratory according to the method used by Peitz *et al.*

(2002) and Müntz *et al.* (2009). One day before cre transduction, 4×10^4 cells were seeded in a 24 well plate and 5 μ M Cre recombinase was added into the culture medium containing only 0.5% serum for 8 and 16 h (Leuchs *et al.*, 2012). Afterwards, medium was replaced with standard medium and culture continued.

2.2.1.11 Generation/isolation of double fluorescent reporter cells

To monitor the activity of tamoxifen inducible Cre, as well as iCre expression the double fluorescent reporter construct (pCAG-mT/mG) was used for randomly transfection into different cells by nucleofection (pDNA concentration, program and kit used can be visualised in Table 15). This reporter construct carries a cassette in which CAG promoter directs the expression of a floxed *mTomato* (mT) fluorescent protein gene upstream of a *mGFP* (mG) fluorescent protein gene. Mouse NIH-3T3 (embryonic fibroblast cells); rat AdMSC (adipose mesenchymal-derived stem cells) and EAF (ear fibroblast cells); human SW-480 and Caco-2 (both colorectal adenocarcinoma cells), human Panc-1 (epithelial carcinoma cells), and human HEK-293 (embryonic kidney cells) were transfected with the double reporter construct. Two days post-transfection G418 selection started and resistant colonies were polled for further experiments. Table 16 indicates the antibiotic concentration used for each transfected cell and their respective name after transfection.

Table 16: Concentration of G-418 resistance gene used for selection in each cell after transfection

Cell used	Cell named after transfection/selection	Specie	G418 concentration (μ g/ml)
HEK-293	HEK-293 mT/mG	human	600
SW-480	SW-480 mT/mG		800
Caco-2	Caco-2 mT/mG		700
Panc-1	Panc-1 mT/mG		700
AdMSC	AdMSC mT/mG	rat	500
EAF	rEAF mT/mG		500
NIH-3T3	NIH-3T3 mT/mG	mouse	300

2.2.1.12 Tamoxifen inducible Cre expression

To induce expression of tamoxifen inducible Cre vectors (see Table 17) transfected pKDNF_mT/mG, NIH-3T3_mT/mG, rEAF_mT/mG and SW-480_mT/mG cells were cultured in 1 ml of medium, supplemented with 4-hydroxy-tamoxifen (4-OHT) (Sigma Aldrich), using a 12 well plate.

Table 17: Vectors used for transfection of double reporter fluorescent cells

Vectors	pPGK-Cre; pSV40-βG-Cre-ER ^{T2} ; pPGK-Cre-ER ^{T2} ; pPGK-ER ^{T2} -Cre-ER ^{T2}
---------	---

First, for optimization of 4-OHT concentration, pKDNF_mT/mG cells were cultured in presence of 1μM, 100nM, 10nM and 1nM of 4-OHT and cell morphology, as well recombination were examined, 24 to 144 hours post-induction.

To express *Cre* stably or transiently two different experiments were performed:

- 1) For stable transfection 1×10^6 NIH-3T3_mT/mG cells were co-transfected at a ratio of 1:10 vector to resistance gene. The co-transfected cells were selected with 6 mg/ml blasticidin and induced with 100nM of 4-OHT in 1 ml of medium, using a 12 well plate.
- 2) To express *Cre* transiently 5×10^5 mT/mG cells (pKDNF_mT/mG; NIH-3T3_mT/mG; rEAF_mT/mG and SW-480_mT/mG), were transfected using each of the vectors from Table 17. Two days post-transfection, cells were plated into a 6 well plate and expression of the *Cre* gene was induced one day after with 100nM of 4-OHT in the medium.

2.2.1.13 Flow cytometry analysis

Flow cytometry analysis were carried out with a Becton-Dickson LD II flow cytometer equipped with a 488 nm argon-ion laser. For all experiments at least 1×10^4 cells were resuspended into 1000 μl cold flow cytometer buffer (PBS - Ca⁺⁺/Mg⁺⁺ free and containing 3 mM EDTA and 1% BSA) and left on ice until further analysis. Then, this aliquot of 1000 μl was transferred into a cytometer glas tube and the FITC and PE/or DsRed fluorescence were measured though a FL-1 filter (530 nm) and a FL-2 filter (575 or 585 nm), respectively, and at least 10.000 events were acquired by Flow Cytometer.

2.2.1.14 Cryosectioning tissues

After 3 months of pregnancy, many fresh tissues from the stillborn Villin-rbβG-iCre transgenic piglet were sampled. They were inserted in a suitable tissue mold and embedded in OCT (optimum cutting temperature). Subsequently the tissues were put on dry ice to freeze down and stored at -80°C. The embedded tissues were then sliced into 5 μm sections by a cryostat and transferred to microscope slices. The slices were stored at -80°C for further analysis.

2.2.1.15 Microscopy

The AxioVert 40CFL und AxioVert 200M inverted microscopes were used to routinely observe

the morphology of mammalian cells. They were also used to verify the expression of membrane-targeted tdTomato (mT) and enhanced green fluorescent protein (mG) from different cells. The mT and mG expression were visualized after excitation at 554 nm and 484 nm and emission at a wavelength of 581 nm and 510 nm, respectively. Cells were photographed with an AxioCam MRc and AxioCam HRm camera.

2.2.1.16 Somatic cell nuclear transfer (SCNT)

Transgenic pigs were generated by nuclear transfer. To this end, cells were plated, at a confluence of 70-80%, in one or two wells of a 12 well plate. To induce cell cycle synchronisation cells were cultured in starvation medium, which contained only 0.5% FCS. SCNT and embryo transfer were carried in collaboration with the group of Professor Eckhart Wolf (LMU).

2.2.1.17 Dual-Luciferase Assay

In order to investigate the activity of the tissue-specific constructs, the SFTPC promoter drove the expression of *Renilla* Luciferase. Each experiment was performed in triplicate. Per experiment $2-4 \times 10^5$ cells were seeded per well of a 12 well plate and transfected with 5 μg (Calu-3 and pLEC cells) or 4 μg (H441 and LCLC cells) of the distinct expression constructs. Promoter activity was investigated using the Dual Luciferase Assay (Promega) according to manufacturer's instructions.

Briefly, two days after transfection cells were lysed with 250 μl Passive Lysis buffer and incubated for 15 min at RT. The lysed cell was transferred into 1.5 ml reaction tubes and centrifuged for 5 min at $16.000 \times g$ to remove cell debris. From the cleared lysate 75 μl were mixed with 75 μl Dual-Glo Reagent and incubated at RT for 15 min. The *firefly* luciferase luminescence was measured with a GloMAX 20/20 Luminometer with an integration time of 2 s. Subsequently, 75 μl Dual-Glo Stop & Glo solution was added and incubated for 15 min at RT. The *Renilla* luciferase luminescence was determined as described for the *firefly* luciferase. The promoter activity was calculated by normalization of relative light units (RLU) by *Renilla* with *Firefly*, with the results expressed as the ratio of *Renilla* to *firefly* activity (Rluc/Fluc).

2.2.2 Molecular biology methods

2.2.2.1 DNA isolation of plasmid DNA from *E. coli*

Plasmid DNA was isolated by alkaline lysis method. An overnight culture of *E. coli* was prepared for small-scale (5 ml, mini) or large-scale (100 ml, midi) preparations, and the bacteria was pellet by centrifugation at 4500 rpm for 15 minutes.

Miniprep: The bacterial pellet was resuspended in 100 µl miniprep solution I and lysed for 5 min at RT with 200 µl miniprep solution II. The lysis reaction was stopped by addition of 150 µl miniprep solution III followed by incubation on ice for 30 min. The suspension was centrifuged for 10 min at 12.000 x *g* and the supernatant was transferred to a new reaction tube. The suspension, containing plasmid DNA was washed with 1 ml of 95% ethanol and centrifuged. The supernatant was discarded and the pellet was washed with 500 µl of 80% ethanol, centrifuged and washed again with 95% ethanol. The DNA pellet was then air-dried and after 20-30 min dissolved in 50 µl ddH₂O.

Midiprep: The bacterial pellet was treated according to manufacturer's instructions (NucleoBond Xtra Midi/Maxi kit). Genomic DNA (gDNA) from mammalian cells as well from tissue was isolated with Sigma's GenElute Mammalian Genomic DNA Miniprep Kit according to manufacturer's instructions.

2.2.2.2 Phenol-Chloroform

Phenol-Chloroform method was used when higher amounts of DNA were need. Cell pellet or small pieces of tissue were mixed in 500-1500 µl DNA lysis buffer, supplemented with 10 mg/ml of RNAse A and 10 mg/ml Proteinase K, and incubated overnight (O/N) at 55°C. An equal volume of phenol:chloroform:isoamyl alcohol (25:24:1) was added to the sample and then mixed by inversion. The mixture was incubated at RT for 10 min and then centrifuged for 15 min at 16.000 x *g*. The upper aqueous phase was removed and transferred to a fresh tube. An equal volume of chloroform was added, thoroughly mixed and centrifuged for 10 min at 16.000 x *g*. Again, the aqueous phase was removed and transferred into a new tube. Subsequently isopropanol to a final concentration of 70% was added and the mixture centrifuged at 16.000 x *g* to pellet the genomic DNA. The gDNA pellet was washed with 1 ml of 70% EtOH and centrifuged for 10 min at 16.000 x *g*. The gDNA pellet was air dried at room temperature, dissolved in 50-100 µl TE-buffer and stored at 4°C.

2.2.2.3 Isolation of RNA from mammalian cells and tissues

Either Direct-zol™ or RNase Mini Kit were used to isolate RNA from mammalian tissues or cells, according to manufacture's instructions. To remove any DNA contamination from RNA isolation, the TURBO DNA-free kit was used according to the supplier's instructions. RNA integrity was checked by denaturing agarose gel method for RNA electrophoresis and RNA was stored at -80°C.

2.2.2.4 Determination of nucleic acids concentration

Photometry: The BioPhotometer 6131 was used to determine DNA and RNA concentration. Samples were diluted 1/50 - 1/100 and optical density (OD) was measured at a wavelength of 260nm. Water was used as a blank. Concentrations were calculated according to the equations shown below:

$$\text{DNA } [\mu\text{g}/\mu\text{l}] = (\text{OD}_{260} \times 50 \times \text{dilution factor})/1000$$

$$\text{RNA } [\mu\text{g}/\mu\text{l}] = (\text{OD}_{260} \times 40 \times \text{dilution factor})/1000$$

Nano Drop Lite: The Nano Drop Lite was also employed to quantitate DNA and RNA. For calibration 1 µl of water was used. An equal volume of DNA or RNA was loaded. Depending on the program dsDNA (factor: 50) or RNA (factor: 40) was chosen, and the concentration of each sample was automatically measured and displayed on the screen.

2.2.2.5 Precipitation of plasmid DNA

Ethanol precipitation was used as a method to obtain purified plasmid DNA for transfection. DNA solution was mixed with 1/10th volume of 3 M NaAc and 2 volumes of ice cold 100% ethanol and incubated either for 2 hours at -80°C or O/N at -20°C. After centrifugation for 10 min at 16.000 x g the pellet was rinsed with 70% ethanol, centrifuged for 5 min at 16.000 x g and air dried. The DNA was resuspended in low-Tris EDTA (10 mM Trizma-HCl, 0.1 mM EDTA) under sterile conditions.

2.2.2.6 Agarose gel electrophoresis

Agarose gel electrophoresis was used to separate nucleic acids according to their size and varied between 0.8-2% agarose, depending on the size of the expected DNAs fragments. The agarose powder was heated with either TAE (Tris-Acetate-EDTA) or TBE (Tris-Borate-EDTA) buffers until the agarose was completely melted. After cooling 0.4 µg/ml of ethidium bromide

(EtBr) was added that allowed visualization of DNA fragments, by UV light at a wavelength of 254-366 nm, using the Gene Genius Bioimaging System. Samples were mixed with 5 x gel loading buffer, before loading into the gel combs. Molecular weight markers (100 bp, 1 kb and 2 Log) were used to determine the size of the DNA bands. Gels were run at a voltage of 5 V/cm.

2.2.2.7 DNA extraction and purification from agarose gels

To excise desired DNA fragments from agarose gels, an ethidium bromide stained TAE gel was quickly exposed to UV light and a scalpel was used to cut around the DNA band of interest. The excised band was placed in a 1.5 ml eppendorf tube. DNA purification was performed using the Wizard SV Gel and PCR Clean-Up System according to manufacturer's instructions and the DNA was eluted in 30 µl of nuclease free water.

2.2.2.8 Restriction enzyme digestion of DNA

For analytical digests up to 1 µg DNA was digested and for preparative digests 3 to 40 µg DNA were digested using 3-5 U/µg of DNA according to manufacturer's instructions.

2.2.2.9 Ligation

Ligation of DNA fragments was performed using T4 DNA ligase in T4 DNA ligase buffer, in a total volume of 20 µl. An 1:3 molar ratio of vector:insert was used, with 100 ng vector DNA. Ligations were either incubated for 1 h at RT, 4°C or 16°C O/N (overnight).

2.2.2.10 Fill-in reaction of stick ends

To create blunt ends of either 5' or 3' DNA overhangs the DNA Polymerase I, Large (Klenow) was used according to the manufacturer's instructions.

2.2.2.11 Desphosphorylation of plasmid DNA

In order to avoid/prevent recircularization of plasmid DNA, linearized plasmid DNA was treated with Antarctic Phosphatase, which removes 5' and 3' phosphate groups. The reaction was performed according to manufacturer's instructions.

2.2.2.12 DNA sequencing

For sequencing purposes, purified plasmid DNA (100 ng/μl) or purified PCR product (10 ng/μl) were mixed with 10 pmol/μl of the appropriate primer and nuclease free water to a final volume of 18 μl and sent to Eurofins MWG Operon (Ebersberg).

In the case that non-purified PCR products were sent for sequencing, 10 μl was treated with 0.4 μl of NEB Antartica Phosphatase and 0.2 μl of NEB Exonuclease I to degrade un-incorporated dNTPs. The reaction was incubated at 37°C for 30 min, followed by an incubation step at 80°C for 15 min.

2.2.2.13 Polymerase chain reaction (PCR)

PCR was conducted for *in vitro* DNA amplification and for screening of (gene-)targeted cell clones. As template 20 ng of plasmid DNA or 200 ng of genomic DNA were used, respectively. The primer pairs used were supplied by Eurofins MWG Operon and diluted in TE buffer to get a final concentration of 100 pmol/μl (stock solution). A 10μM primer stocks was used after 1:10 dilution into ddH₂O. GoTaq DNA polymerase, PCR Extender System (5 Prime) and Phusion polymerase were used according with supplier's instructions. Table 18 describes the components of the PCR master mixes and program conditions.

Table 18: Components of PCR reactions and cycling conditions

Component	Final concentration		Program		
GoTaq PCR					
5x Green buffer	1 x		Initial denaturation	95°C	2 min
dNTPs	200 μM per dNTP		Denaturation	95°C	30 s
Forward primer	200 nM	x 35	Annealing	58-60°C	30 s
Reverse primer	200 nM		Elongation	72°C	1 min/kb
Polymerase	1.25 U		Final elongation	72°C	5 min
H ₂ O	up to 50 μl		Hold	8°C	forever
5 Prime PCR					
10x HF buffer	1 x		Initial denaturation	94°C	2 min
dNTPs	200 μM per dNTP		Denaturation	94°C	30 s
Forward primer	200 nM	x 35	Annealing	58-62°C	30 s
Reverse primer	200 nM		Elongation	72°C	45 s/kb
Polymerase	2 U		Final elongation	72°C	5 min
H ₂ O	up to 50 μl		Hold	8°C	forever

Component	Final Concentration	Program			
5 Prime Long Range PCR					
10X Tuning buffer	1 x		Initial denaturation	93°C	3 min
dNTPs	500 µM per dNTP		Denaturation	93°C	30 s
Forward primer	400 nM	x 40	Annealing	62-64°C	1 min
Reverse primer	400 nM		Elongation	68°C	10 cycles: 1 min/kb each additional cycle: + 20 s
Polymerase	2 U		Final elongation	68°C	4 min
H ₂ O	up to 50 µl		Hold	8°C	forever
Phusion PCR					
5x phusion HF buffer	1 x		Initial denaturation	98°C	30 s
dNTPs	200 µM per dNTP		Denaturation	98°C	10 s
Forward primer	500 nM	x 35	Annealing	63°C	30 s
Reverse primer	500 nM		Elongation	72°C	30 s/kb
Polymerase	1 U		Final elongation	72°C	10 min
DMSO	3%		Hold	8°C	forever
H ₂ O	up to 50 µl				

2.2.2.14 SFTPC promoter amplification by PCR-reaction

A 4.4 kb region of the SFTPC promoter, based on the Ensembl (Gene ID ENSSSCG0000009619; Location 14:6877790-6880769:1), was amplified by PCR in four overlapping fragments, 1.9 kb, 1.1 kb, 1.5 kb and 509 bp (*SFTPC1*, *SFTPC2*, *SFTPC3*, *SFTPC4*), that were then ligated. All primers were designed using the Primer3 Web Interface and purchased from Eurofins MWG Operon. PCR reactions were carried out following the manufacturer's protocol (5 PRIME Manual PCR Extender System). Amplified fragments were subsequently subcloned into the pJET1.2 (Fermentas) vector.

2.2.2.15 Colony PCR

Colony PCR was used to determine the presence or absence of insert DNA in plasmid constructs directly from bacterial colonies. This procedure uses PCR and primers designed to specifically target the insert DNA and the vector. To derive a backup each individual colony, grown on an agar plate, was pick with a sterile toothpick and streaked onto another agar plate containing the appropriate antibiotic. The plate was incubated ON at 37°C. Thereafter the same toothpick was used to dip into each reaction tube containing either 30 µl of TTE buffer or 50 µl of GoTaq PCR reaction kit. The reaction tube was lysed with a short heating step (90°C - 10 min) or used directly for the PCR reaction and lysed during the initial heating step. Table 20

shows the colony PCR reaction and conditions used.

Table 19: Colony PCR reaction and cycling condition

Reagent	Final Concentration	Program		
GoTaq PCR				
5x Green buffer	1 x	Initial denaturation	95°C	5 min
dNTPs	200 µM per dNTP	Denaturation	95°C	30 s
Forward primer	200 nM	x 35	Annealing	58°C
Reverse primer	200 nM		Elongation	72°C
GoTaq polymerase	1.25 U		Final elongation	72°C
Template	N/A		Hold	8°C
H ₂ O	up to 50 µl			forever

2.2.2.16 Reverse Transcriptase Polymerase Chain Reaction (RT-PCR)

RT-PCR reactions were performed with GoTaq DNA polymerase, to quantify the expression of different genes, in accordance with manufacture's instructions. For the cDNA synthesis either Bio&Sell or SuperScript III RT-PCR System kit were used with 200 to 500 ng of mRNA, according to the supplier's instructions (see Table 21).

Table 20: Components of RT-PCR reactions and cycling conditions using Bio&Sell or SuperScript III RT-PCR

Components	Final Concentration	Program	
Bio&Sell			
Random primer	100 µM	70°C for 5 min and 15 min at 4°C, then the followed components were added and the follow program was used:	
RNA template	500 ng		
RNase free H ₂ O	up to 10 µl		
dNTPs	500 nM per dNTP		
Scriptum first buffer complete	1 x	42°C	10 min
Scriptum first reverse transcriptase	100 U	55°C	1 h
RNase free H ₂ O	up to 20 µl	8°C	forever
SuperScript III RT-PCR			
Random primer	100 µM	65°C for 5 min and then immediately chilled on ice. After 5 min the followed components were added and the follow program was used:	
RNA template	200 ng		
RNase free H ₂ O	up to 10 µl		
dNTPs	500 nM per dNTP		
buffer	1 x	25°C	10 min
SuperScript III reverse transcriptase	100 U	50°C	50 min
RNase free H ₂ O	up to 20 µl	8°C	forever

2.2.2.17 Southern Blot analysis

Southern blot was used to isolate and identify gene targeting fragments after cleavage of the genomic DNA by restriction enzymes.

Preparation of DIG-labeled probe

For the preparation of DIG (digoxigenin-11-2'-deoxy-uridine-5'-triphosphate)-labeled neomycin probe (NEO probe), the oligonucleotides Prob neo F and probe_neo R3 were used. PCR was performed with GoTaq polymerase. Additionally a PCR reaction without labeled-UTPs was set up to compare the shift in molecular weight between the labeled and unlabeled probe by gel electrophoresis. The incorporation of DIG into DNA during PCR leads to a larger DIG-labeled and it migrated in a gel more slowly than the corresponding unlabeled piece of DNA. The DIG-labeled probe was cut out from the gel and purified using Wizard SV Gel and PCR Clean-Up System and stored at -20°C.

Southern blot

For southern blot analysis 8-10 µg of gDNA were digested using 32 U of SbfI and BlnI restriction enzymes for 5 hours. Thereafter samples were size-fractionated by agarose gel electrophoresis, in a 0.8% TAE gel without EtBr, at 33 volts O/N. As size controls two markers were used, 4 µl DIG-labeled molecular weight marker VII and 6 µl of the 1 kb size marker. The next day, the gel lane with the 1 kb marker was then cut off the gel, stained with ethidium bromide for 30 min and the DNA marker visualized with UV light by the Bio Imaging System Gene Genius. This was done because according to the separation of the marker, some parts of the gel were cut off to minimize the gel area for blotting.

All blotting steps were performed according to DIG Application Manual for Filter Hybridization from Roche. Briefly, to denature the two DNA strands in the gel, into single strands by alkaline treatment, they were transferred to a nylon membrane by capillary transfer method. For pre-hybridization and hybridization, the membrane was put in a roller bottle and incubated with 10 ml of pre-warmed DIG Easy Hyb buffer at 47.5°C (NEO probe) for 1h with gentle rotation. During this time, 7.5 µl DIG-labeled probe were diluted in ddH₂O to a final volume of 50 µl and denatured for 5 min at 95°C. After cooling down, the hybridization solution was prepared by adding this denatured probe into 5 ml of pre-warmed DIG Easy Hyb and the pre-hybridization solution was then replaced by the hybridization solution. Hybridization took place at 47.5°C O/N. After the hybridization procedure, the membrane was washed twice, with gentle shaking, for 15 min in low stringency buffer, then in 68°C pre-heated high stringency buffer and finally in washing buffer for 2 min. The blocking was done using 1x Blocking Solution for 1h at RT. Labeled DNA

could be located on the blot using antibodies against digoxigenin (anti-digoxigenin-AP Fab fragment), diluted 1:1000 in 1x Blocking Solution for 30 min at RT with gentle agitation. Then the membrane was washed twice for 15 min at RT with washing buffer and then equilibrated in detection buffer for 3 min at RT. The membrane was put into a plastic wrap and the chemiluminescence substrate CDP-Star diluted 1:100 in detection buffer, was added drop wise to the membrane and the blot was sealed. Visualization was followed by exposition in X-ray film after 50 minutes at 37°C.

2.2.3 Microbiology methods

2.2.3.1 Cultivation of *E. coli*

E. coli liquid cultures were used for plasmid amplification and subsequent purification, as a liquid culture, or single clone cultivation on a freshly streaked selection plate.

For plasmid amplification, a single colony or a starter culture was used to inoculated LB medium containing the appropriate selective agent (100 µg/ml ampicillin or 30 µg/ml kanamycin) and grown O/N at 37°C with 220 rpm (rotation per minute) shaking.

E. coli was also cultured on LB agar plates, containing ampicillin or kanamycin, upon transformation and plates were incubated O/N at 37°C. If blue-white screening could be performed, agar plates were coated with 20 µl X-Gal (40 mg/ml in DMF) and 40 µl IPTG (100 mM in H₂O) per plate prior to spreading the bacteria containing the plasmid of interest.

2.2.3.2 Transformation of electrocompetent *E. coli*

DH10B electrocompetent cells (50 µl) were thawed on ice and 2-5 µl of a ligation mixture was added and gently mixed by pipetting up and down. The mixture was placed into a pre-cooled electroporation cuvette. Cells were pulsed once at 2500 V for 5 ms in an Eppendorf Multiporator. Immediately 500 µl of pre-warmed LB medium was added and the tube incubated at 37°C for 30 min with shaking (220 rpm). Afterwards 10 to 200 µl of the cells and ligation mixture were spread onto selection agar plates and incubated O/N at 37°C.

2.2.3.3 Storage of *E. coli*

E. coli agar plates and liquid cultures were kept at 4°C for short term storage. For long term storage 500 µl of the *E. coli* liquid culture were mixed with 500 µl sterile 99% glycerol and frozen at -80°C in Eppendorf tubes.

3 Results

The generation of pigs predisposed to cancers of particular organs e.g. pancreas, gut or lung can be done by conditional or inducible activation of gene expression using Cre recombination. Therefore, to specifically activate a mutant gene, known to be a cancer driver in humans, two lines of pigs are necessary: 1) Pigs carrying a mutant gene(s), such as *TP53*^{R167H}, *KRAS*^{G12D} (Leuchs *et al.*, 2012 and Li S. *et al.*, 2015, respectively) in a latent form by inclusion of a stop cassette flanked by *loxP* sites (both already produced in our group); 2) Pigs expressing Cre recombinase specifically in pancreas, gut, or lung. Additionally, a recently established fluorescent dual reporter pig (Li S. *et al.*, 2014) facilitates the monitoring of expression and activity of Cre recombinase in specific-tissues *in vivo*. In these pigs one reporter gene (membrane-targeted tandem dimer Tomato – mTomato) is flanked by *loxP* sites expressed ubiquitously prior to Cre-mediated recombination. Upon application of Cre recombinase it is excised and a second marker gene (membrane-targeted tandem dimer GFP – mGFP) is activated.

3.1 Suitable tissue-specific promoters

The use of a tightly-regulated and well-characterised promoter is important in directing recombination to the intended target tissue without undesirable recombination in non-target tissues. Firstly, appropriate promoters were identified and selected that would allow tissue-specific Cre expression in specific organs.

The human PDX-1 promoter was selected to induce conditional pancreas-specific oncogene expression. *In vitro* investigations carried out by M.Sc. Jana Treter and M.Sc. Heiko Guggemos had indicated its functionality. To induce colon-specific oncogene expression, the murine colon-specific (VIL-1) promoter (a kind gift from Dr. El Marjou) was chosen since it showed colon-specific Cre expression in mice (Pinto *et al.*, 1999 and El Marjou *et al.*, 2004). For lung-specific expression the SFTPC promoter was selected, since literature indicated that the surfactant protein C promoter is suitable for lung-specific expression of different genes *in vitro* and *in vivo* (Wert *et al.*, 1993 and Glasser *et al.*, 2000). Therefore, these three tissue-specific promoters were used to direct Cre expression to the pancreas, colon and lung, respectively.

3.1.1 Construction and tests of tissue-specific Cre vectors

3.1.1.1 Porcine SFTPC promoter

Isolation of the porcine SFTPC promoter

The 3.7 kb fragment of the human SFTPC promoter was widely used to direct Cre expression specifically in epithelial cells such as the alveolar cells type II (Okudo *et al.*, 2005; Mura *et al.*, 2010). SFTPC is expressed mainly in the lung and rarely in other organs (Rawlins and Perl, 2012). Based on high sequence homology between human and pig *SFTPC* genes (Cirera *et al.*, 2006), a 4.4 kb upstream of the transcription start site of the porcine SFTPC promoter was amplified by PCR as four overlapping fragments. These were ligated together and subcloned into pJET1.2 (pJET1.2_STFPC). Next, the SFTPC promoter was cloned into pSL1180 vector backbone (pSL1180_SFTPC) to obtain more restriction sites (see appendix for cloning details).

SFTPC expression in mammalian cells

To test the functionality of the constructed porcine lung SFTPC promoter *in vitro*, several different lung cell types were investigated for the expression of SFTPC in collaboration with the Comprehensive Pneumology Center at the Ludwig Maximilian University and Helmholtz Zentrum München by quantitative PCR. *GAPDH* gene was selected as a reference gene and as a reference cell line the murine transformed cell line (MLE-12), which it is known to express *SFTPC* in low passages number. Figure 12 depicts SFTPC expression levels normalized to *GAPDH* expression and the reference cell line, MLE-12.

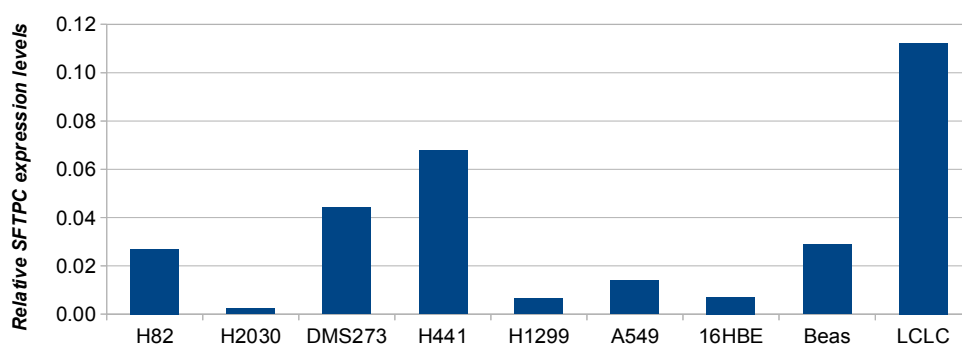


Figure 12: SFTPC expression measured by qPCR in human lung cells relative to a transformed murine lung cells known to express SFTPC.

Nine human lung cell lines were used: H82: human small cell lung - carcinoma; H2030: human non-small cell lung - adenocarcinoma; DMS273: human small cell lung - carcinoma; H441: human cell lung - adenocarcinoma; H1299: human non-small cell lung - carcinoma; A549: human lung - carcinoma; 16HBE: human bronchial cells; Beas: human bronchial virus transformed cells; LCLC: human large cell lung - carcinoma. Relative SFTPC expression levels in human lung cell lines. *GAPDH* was used as a reference gene for the qPCR. The human lung cell line LCLC shows the highest expression of SFTPC (fold-change of 0.11) followed by the H441 cell line (fold-change of 0.07).

The relative expression levels obtained (Figure 12) represent the change in expression of the SFTPC between the human lung cell lines tested and the MLE-12 reference cell line. The

results show, that LCLC has the highest expression of SFTPC (change-fold: 0.11), followed by H441 and DMS273 with change-fold of 0.07 and 0.04, respectively. The other cell lines examined showed low expression (change fold: from 0.01-0.03).

In addition, two other lung cell types were tested for SFTPC expression, a human adenocarcinoma cell line (Calu-3) and a primary porcine alveolar epithelial cells (pLECs). The latter was isolated from Göttingen minipigs and cultured *in vitro*. Since primary cells undergo only a limited number of cell divisions, before they undergo replicative senescence, half of the isolated and expanded cells were immortalised using a plasmid, encoding for a full-length cDNA of human telomerase reverse transcriptase (hTERT). Expression of hTERT was confirmed by RT-PCR after RNA isolation and cDNA synthesis (data not shown). After that the pLECs and the Calu-3 cell line were analysed for the expression of SFTPC using RT-PCR. Figure 13 shows SFTPC expression in pLECs.

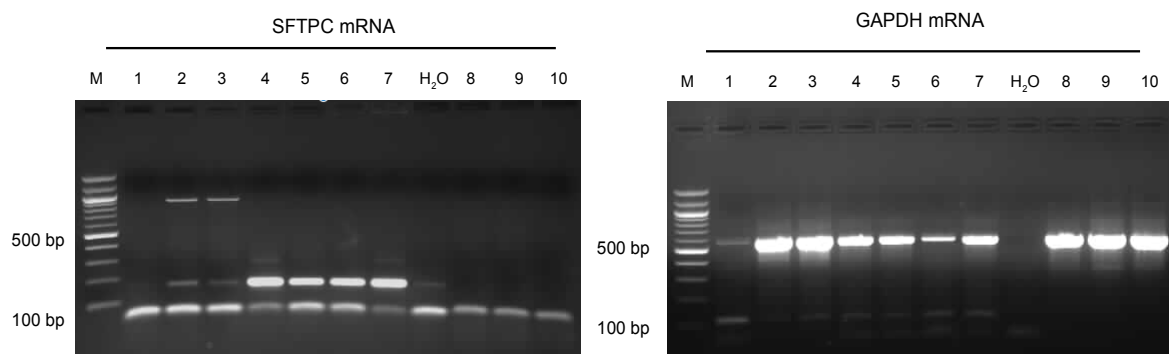


Figure 13: RT-PCR to detect SFTPC expression in porcine cells.

The expression of porcine and human *SFTPC* was detected by RT-PCR by a 160 bp and 142 bp PCR fragment, respectively. GAPDH was used as a loading control and detected by a 591 bp RT-PCR fragment. SFTPC expression was detected by a 160 RT-PCR fragment (lanes 2-7) in porcine primary cells and porcine lung tissues, but not in the negative controls.

Abbreviations: M: 1 kb DNA ladder. (1) mRNA from lung landrace porcine cells. (2) mRNA from porcine immortalised primary lung epithelial cells. (3) mRNA from porcine primary lung epithelial cells. (4) Positive control: mRNA from lung landrace pig tissue. (5-6) Positive control: mRNA from lung mini-pig tissues. (7) Positive control: mRNA from lung duroc pig tissue. (8-10) Negative controls: mRNA from mammary epithelial HC11 cells; embryonic kidney HEK-293 cells and WT landrace porcine cells, respectively. H₂O: water control.

Similar to the porcine lung tissues, a 160 bp fragment could be amplified from the two pLECs. These findings indicated SFTPC expression in those cells. In these samples an 899 bp PCR fragment was also detected, indicating gDNA contamination. Since a faint band was seen in the H₂O control, the two 160 bp PCR fragment originating from the pLECs were cut out of the gel and purified before sequencing with SFTPC specific primers. Sequencing alignment of these 2 samples with the *SFTPC* cDNA from the *Sus scrofa* sequence (Ensembl gene ID: ENSSSCG00000009619) revealed 98% identity.

RT-PCR analysis of Calu-3 cells showed an expected band by 142 bp and sequencing indicated that the fragment obtained was part of the *SFTPC* cDNA. Taken together, pLECs, Calu-3, and LCLC cells could be use to quantify the SFTPC promoter activity. Although these

cell lines were positive for SFTPC expression, the expression level were relatively low. Nevertheless, these cells were used in dual luciferase reporter assays to prove the activity of the porcine SFTPC promoter.

SFTPC functionality test by dual luciferase assay

Dual luciferase assay is commonly used as a reporter for characterization of promoter activity (Fan and Wood, 2007). It comprises the luciferase gene (*Renilla* luciferase, *hRluc*) under the control of a promoter of interest, while the other luciferase (firefly luciferase) is under the control of the constitutively active HSV-TK promoter.

As the original psiCHECK2 vector (Promega) contains promoters for both luciferase genes, it was necessary to replace the SV40 promoter driving *Rluc* with SFTPC promoter. This was done in two cloning steps. First additional restriction sites were added in front of the *hRluc* gene. Then the reporter genes *hluc+* and *hRluc* of psiCHECK2 (Promega) vector were cloned into the polylinker of pSL1180 (Amersham) vector (pSL1180_psiCHECK2.) The SFTPC promoter fragment, already subcloned into pSL1180 vector, was ligated with the pSL1180_psiCHECK2 vector. The design of the final vectors are shown in Figure 14 (for cloning details see appendix section).

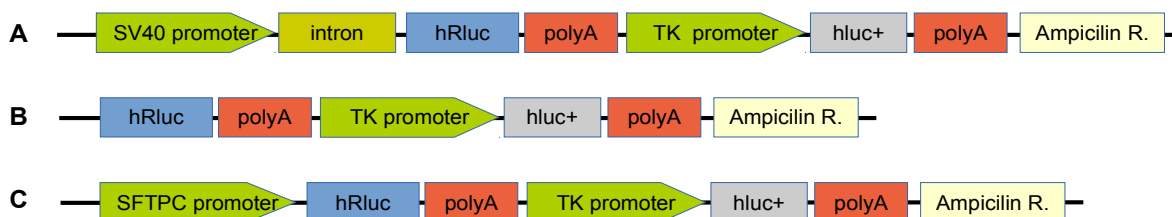


Figure 14: Structures of pSL1180_psiCHECK2 and pSL1180_psiCHECK2_SFTPC vectors.

(A) The original psiCHECK2 vector containing the reporter genes *hluc+* and *hRluc* (which are under the control of the TK and SV40 promoters, respectively). (B) The pSL1180_psiCHECK2 vector contains the multiple cloning sites of the pSL1180 vector placed upstream of the *hRluc* reporter gene. (C) The multiple cloning sites from pSL1180_psiCHECK2 vector enabled insertion of the SFTPC promoter, generating the pSL1180_psiCHECK2_SFTPC vector.

Abbreviations: *hRluc*: *Renilla* luciferase; *hluc+*: firefly luciferase; SFTPC: surfactant protein C promoter; TK: thymidine kinase; SV40: simian virus 40; polyA: polyadenylation signal; Ampicilin R: ampicilin resistance.

To evaluate SFTPC promoter activity by dual luciferase assay, the human lung LCLC and Calu-3 cell lines, as well as the porcine primary lung epithelial cells, were transfected with the following three plasmids (Figure 14): A) psiCHECK2, luciferase reporter plasmid containing SV40 promoter and enhancer driving *Renilla* luciferase cDNA as a positive control; B) pSL1180_psiCHECK2, luciferase reporter plasmid without an upstream promoter to drive *Renilla* luciferase cDNA served as a negative control and C) pSL1180_psiCHECK2_SFTPC, luciferase reporter plasmid containing the SFTPC promoter driving *Renilla* luciferase cDNA. Two days after transfection cells were lysed and transient expression of *Renilla* luciferase was

analysed (see Figure 15).

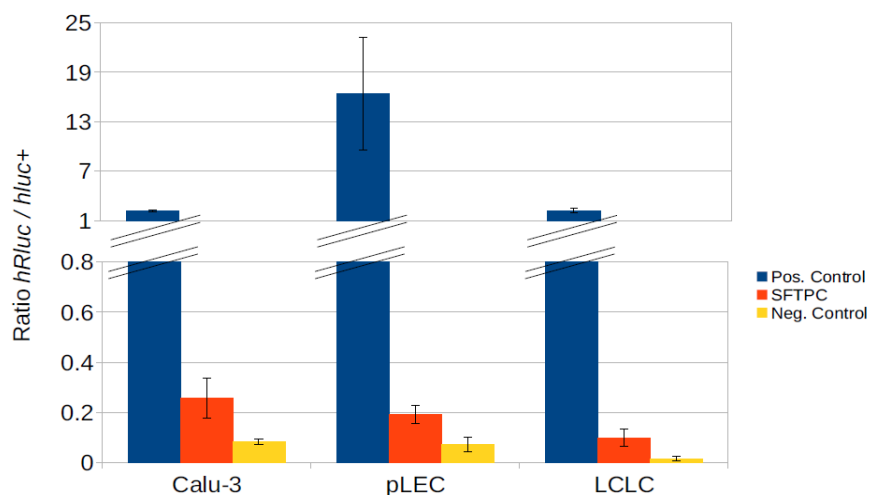


Figure 15: Dual luciferase assay to test the functionality of SFTPC promoter in different lung cells.

Activity of SFTPC promoter is shown as a function of the internal control promoter (ratio *hRluc* activity to *hLuc+* activity) 48 hours after transfection. Comparison of SFTPC expression shows that Calu-3 had higher expression. Error bars represent standard errors of triplicate samples.

Abbreviations: Pos. Control: positive control - psiCHECK2 vector; Neg. Control: negative control - pSL1180_psiCHECK2 vector; SFTPC: pSL1180_psiCHECK_ SFTPC vector; Calu-3: human cell lung - adenocarcinoma; pLEC: primary porcine lung epithelial cells; LCLC: human large cell lung - carcinoma.

Very low SFTPC-driven *hRluc* expression was detected in all cell lines tested and *hRluc* expression directed by the SV40 promoter (positive control) was much higher than SFTPC promoter activity. In pLEC, Calu-3 and LCLC cells the SFTPC directed expression was 2.6, 3 and 5.9 fold higher than the negative control respectively.

The cultivation of lung alveolar epithelial cells are time-consuming, labor intensive and expensive (Barkauskas *et al.*, 2013) and do not always succeed, due to weak ability to maintain proper conditions to cultivate lung epithelium *in vitro* (Clement *et al.*, 1990). In addition, Fuchs *et al.* (2003) reported that the time of *in vitro* culture of human alveolar type II cells (HAEPcs) potently affected the levels of SFTPC expression. On day 4 SFTPC levels decreased slightly and disappeared on latter cultures (day 8). Thus, an *in vitro* cell model that posses the relevant qualities of the alveolar epithelium *in situ* is definitely needed. This situation also emphasizes the importance of using *in vivo* models to test and define specific regulatory sequences that can recapitulate gene expression. Therefore, without a suitable cell to test the SFTPC promoter activity *in vitro*, and to allow to monitor the expression and activity of Cre recombinase in the lung *in vivo*, I decided to generate a SFTPC "gene stacking" construct to place SFTPC-Cre into the porcine *ROSA26* locus adjacent to the double reporter construct (see section 3.1.2). The latter had been inserted into the porcine locus by homologous recombination.

3.1.1.2 Human PDX-1 promoter

Human PDX-1 promoter construction

The activity of the human PDX-1 promoter is regulated by several responsive elements and regulatory regions (see Figure 16). The human PDX-1 promoter, was amplified by PCR in two steps. First, M.Sc. Christin Ruoff amplified by PCR 5.5 kb upstream of the transcription start site of the *PDX-1* gene. This gene segment contains important control regions for PDX-1 expression, denominated as areas I, II and III (see Figure 16 that correspond to important control regions for PDX-1 expression) (Gerrish *et al.*, 2000). Second, a distal enhancer element, termed as area IV, consisting of binding sites for the transcription factor Egr-1 (early growth response-1) that is known to regulate the expression levels of PDX-1 in pancreatic-cells (Eto *et al.*, 2007), was amplified by PCR by M.Sc. Jana Treter. The amplified 819 bp DNA fragment contained the 502 bp transcriptional control region area IV of the human *PDX-1* gene (Gerrish *et al.*, 2004). After several cloning steps the vector (pSL1180_hEnhPDX-1) was assembled containing the distal enhancer element upstream of the 5.5 kb human PDX-1 promoter. Figure 16 shows the structure of the vector (for further cloning details see appendix).

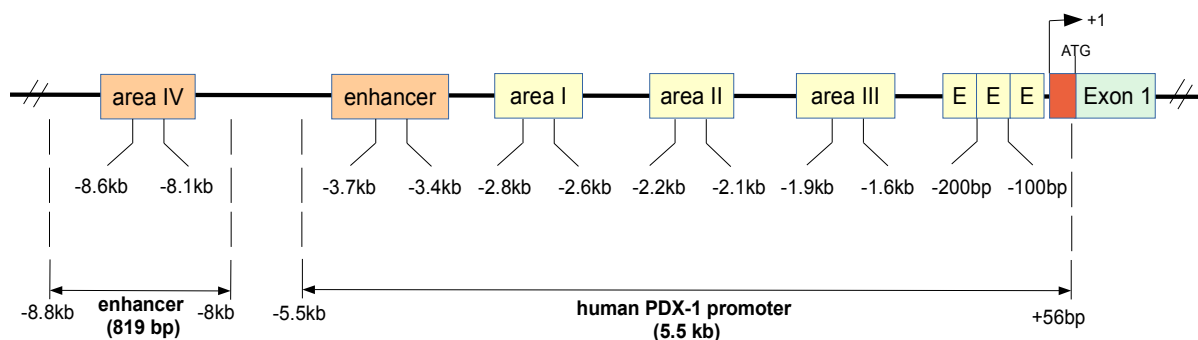


Figure 16: Schematic representation of the endogenous human *PDX-1* locus and its enhancer/promoter regions.

Cis-acting regulatory elements of the *PDX-1* 5'-flanking sequences are indicated as yellow boxes. The *PDX-1* gene is TATA-less and utilizes three principal transcription initiation sites (E-boxes motifs indicated as "E"), followed by a short 5' untranslated sequence of approximately 100 nucleotides (indicated as a red box). There are three regions denominated area I, II, III in the gene region located at -2.8 kb to -1.6 kb relative to transcription start site +1 (TSS). A proximal and distal enhancer elements (Area IV) are indicated as orange boxes. The positions relative to the TSS of the human *PDX-1* gene are indicated as numbers at the bottom. The vector pSL1180_hEnhPdx1 is approximately 6.4 kb, containing the *PDX-1* distal enhancer element (area IV) and part of the promoter region of the *PDX-1* gene. Abbreviations: 5' UTR: 5' untranslated region; Ampicilin R: ampicillin resistance. Adapted from Melloul *et al.* (2002); Ashizawa *et al.* (2004).

PDX-1 functionality test by dual luciferase assay

To test the functionality of the human PDX-1 promoter (hEnhPDX-1) a dual luciferase assay was performed. To test the activity of the 6.4 kb human PDX-1 promoter, a construct with *hRluc* under the hEnhPDX-1 promoter was generated. To this end, M.Sc. Heiko Guggemos digested the plasmid pSL1180_psiCHECK-2 with *PmlI* and *NheI* to isolate the *hRluc* reporter gene and the *hluc+* reporter gene, which is under the control of the TK promoter. The

pSL1180_hEnhPDX-1 vector was digested with *PmeI* and *SpeI* restriction enzymes. Both fragments were ligated to generate the pSL1180 Reverse psiCHECK-2 - hPdx1-Enh vector (Figure 17).



Figure 17: Structure of pSL1180 Reverse psiCHECK-2 - hPdx1-Enh vector.

The pSL1180 Reverse psiCHECK-2 - hPdx1-Enh vector contains the human PDX-1 promoter with an upstream enhancer element driving *Renilla* luciferase. The reporter gene *hLuc+* is under the control of the TK promoter.

Abbreviations: *hRluc*: *Renilla* luciferase; *hLuc+*: *firefly* luciferase; *enh*: enhancer element of the *PDX-1* gene; PDX-1: human pancreatic and duodenal homeobox 1 promoter; TK: *thymidine kinase*; SV40: simian virus 40; polyA: polyadenylation signal; Ampicilin R: ampicilin resistance.

This pSL1180 Reverse psiCHECK-2-hPdx1-Enh vector was tested by dual luciferase assay in rat insulinoma cells. This INS-1 cell line is known to express PDX-1 (see Figure 39).

M.Sc. Heiko Guggemos transfected INS-1 and HEK-293 cells with equimolar amounts of three plasmids: A) the psiCHECK2 vector, served as a positive control; B) the pSL1180_psiCHECK2 vector, served as a negative control without promoter in front of *Rluc* (see Figure 14) and C) pSL1180 Reverse psiCHECK-2 - hPdx1-Enh vector (Figure 17), containing the human PDX-1 promoter with its own enhancer element driving *Renilla* luciferase cDNA. Two days after transfection, the cells were lysed and transient expression of *Renilla* luciferase was analysed (see Figure 18).

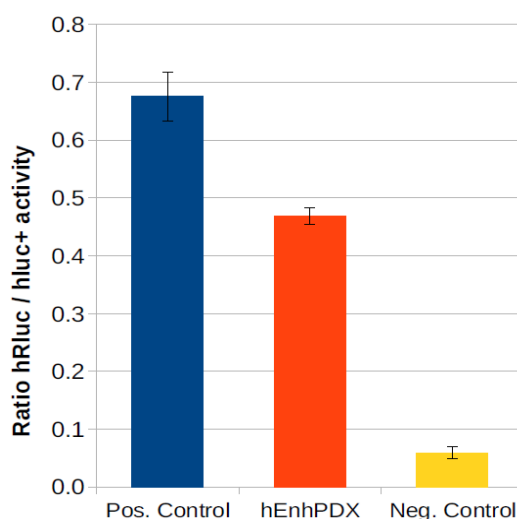


Figure 18: Dual luciferase assay to test the functionality of PDX-1 promoter in INS-1 cells.

Activity of PDX-1 promoter is shown as a function of the internal control promoter (ratio *hRluc* activity to *hLuc+* activity) 48 hours after transfection. Using the pSL1180 Reverse psiCHECK-2-hPdx1-Enh construct PDX-1 expression was 8 fold higher than the negative control and compared to the positive control 1.4 fold expression was detected. Error bars represent standard errors of triplicate samples.

Abbreviations: Pos. Control: positive control (psiCHECK2 vector); Neg. Control: negative control (pSL1180_psiCHECK2 vector); hEnhPDX: human PDX-1 promoter with its own enhancer element driving *Renilla* luciferase cDNA (pSL1180_psiCHECK2_hEnhPDX vector).

Figure 18 shows that the human PDX-1 promoter containing the distal enhancer element had 8 fold higher expression than the negative control and was nearly as effective as the positive control, where Renilla expression is direct by the strong SV40 promoter. Collectively, the data indicate that the 5'-flanking region of human PDX-1 has a strong promoter activity and may direct Cre expression in pancreatic cells *in vivo*.

3.1.2 Construction of gene targeting vectors for insertion of tissue-specific Cre at the *ROSA26* locus.

In mice, the *Rosa26* (reversed orientation splice acceptor 26) locus is widely used to insert transgenes for ubiquitous expression (Nyabi *et al.*, 2009; Perez-Pinera *et al.*, 2012). The disruption of this locus by gene insertion does not provide any adverse side-effects or consequences on mouse viability or cell phenotype (Perez-Pinera *et al.*, 2012). Our group has identified and characterized the porcine *ROSA26* locus, which has shown identical properties as the murine *Rosa26* locus and serves as a permissive locus for transgene expression (Li S. *et al.*, 2014).

Targeting vectors carrying Cre recombinase driven by the lung SFTPC and pancreas-specific PDX-1 promoters were constructed to place them into the porcine *ROSA26* locus by homologous recombination either by conventional cloning methods or based on the Gibson assembly (Gibson *et al.*, 2009). Several cloning steps were necessary to generate *ROSA26* gene targeting constructs (see appendix). The structure of the PDX-Cre *ROSA26* targeting construct is illustrated in Figure 19.



Figure 19: Structure of PDX-Cre *ROSA26* gene targeting construct.

The *ROSA26* gene targeting construct (pPDX_Cre_LSL_*ROSA26*) consists of a floxed splice acceptor (SA)- neomycin (neo) resistance cassette followed by Cre recombinase under the control of *PDX-1* promoter flanked by left homologous arm (LHA) and right homologous arm (RHA) of the porcine *ROSA26* (*R26*). *Lox2272* sites are indicated as triangles.

Abbreviations: enh: enhancer element of the *PDX-1* gene; PDX-1: human *pancreatic and duodenal homeobox 1* promoter; polyA: polyadenylation signal; Ampicilin R ampicillin resistance.

Before use, a functionality test of the mutant *lox2272* site (Figure 19) was done (see Figure 21 and 22). The functionality test of wild-type *loxP* sites (Figure 20) was already performed by Li S. *et al.* (2014).

In parallel to my project transgenic dual fluorescent reporter pigs were generated by Shun Li (Li S. *et al.*, 2014). These pigs carry at the *ROSA26* locus a highly expressed dual fluorochrome mTomato/mGFP cassette that switches expression after Cre-recombination, from mTomato (red fluorescence) to mGFP (green fluorescence). They can be used to visualise tissue-specific Cre

recombinase activity *in vivo*. Therefore it was decided to also generate constructs for a “gene stacking” strategy at the *ROSA26* locus (tissue-specific Cre + Cre reporter). For this, the promoter trap targeting vectors were designed to insert the PDX-1 or SFTPC–Cre recombinase upstream of mTomato/mGFP cassette (see Figure 24). Figure 20 shows the structure of SFTPC and PDX-1 gene stacking constructs (see appendix for further cloning details).

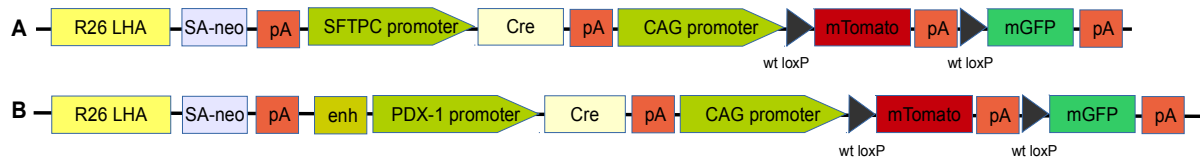


Figure 20: Structure SFTPC-Cre and PDX-1-Cre *ROSA26* gene stacking constructs.

(A) Porcine *SFTPC*-Cre *ROSA26* gene stacking construct (pSA-neo-SFC-Cre-R26-mT/mG), consists of left homologous arm (LHA) of the porcine *ROSA26* (*R26*); splice acceptor (SA)- neomycin (neo) resistance cassette followed by Cre recombinase under the control of *SFTPC* promoter and a right homologous arm of the target R26 mT/mG (carrying additionally a cassette in which CAG promoter directs the expression of a floxed mTomato (mT) fluorescent protein gene upstream of a mGFP (mG) fluorescent protein gene). (B) Human *EnhPDX*-Cre *ROSA26* gene stacking construct (pSA-neo-EnhPDX-Cre-R26-mT/mG), consists of left homologous arm (LHA) of the porcine *ROSA26* (*R26*); splice acceptor (SA)- neomycin (neo) resistance cassette upstream of *PDX-1* promoter driving Cre recombinase and a right homologous arm of the target R26 mT/mG.

Abbreviations: enh: enhancer element of the *PDX-1* gene; PDX-1: human *pancreatic and duodenal homeobox 1* promoter; *SFTPC*: *surfactant protein C promoter*; pA: polyadenylation signal.

LoxP sites functionality test

To ensure that the *lox2272* recombination sites of the PDX-1 gene targeting vector (Figure 19) were functional the plasmid vector was excised using *BsrGI* and *BlnI* restriction enzymes and then incubated with a commercial Cre recombinase. As a positive control the linearised 3.6 kb pLox2+ vector (NEB) was used (see Figure 21).

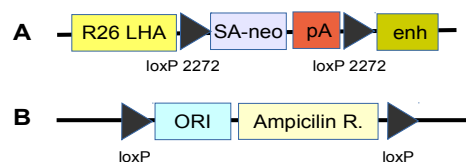


Figure 21: Vectors used for *loxP* site functionality test.

(A) The 3.2 kb pPDX_Cre_LSL_ROSA26 vector contains part of the left homologous arm (LHA) of the *ROSA26* (*R26*) porcine locus, the human PDX-1 distal enhancer element (enh) and a floxed splice acceptor (SA)- neomycin (neo) resistance cassette followed by a polyadenylation signal (pA). (B) The 3.6 kb positive control pLox2+ vector contains a floxed origin of replication (ORI) followed by a *ampicilin* (Ampicilin R.) resistance gene. *LoxP* sites are indicated as triangles.

The results from the reaction are illustrated in Figure 22.

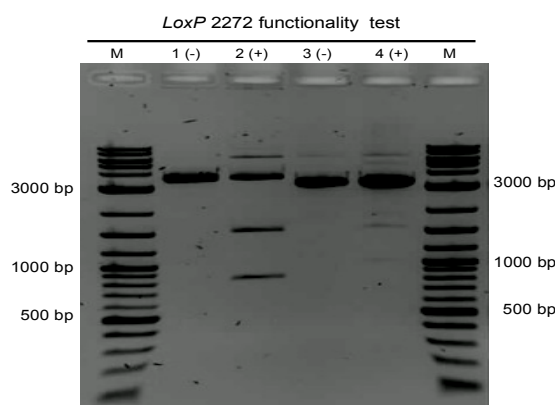


Figure 22: Functionality test of *lox2272* sites using Cre recombinase.

Here, the linear 3.6 kb positive control pLox2+ vector, as well as the excised/linear 3.2 kb pPDX_Cre_LSL_ROSA26 vector (lanes 1 and 3, respectively) are shown. After incubation with Cre recombinase for 30 minutes, Cre-mediated deletion of the floxed cassette occurred. The circular DNA fragments generated migrate differently. The circular 2.8 kb DNA from the pLox2+ plasmid migrated at 1.7 kb (lane 2) and the circular 1.6 kb DNA from the pPDX_Cre_LSL_ROSA26 plasmid migrated at 1.1 kb (lane 4). The linear DNA from the pLox2+ plasmid migrated at 850 bp and the linear DNA from the pPDX_Cre_LSL_ROSA26 plasmid migrated at 1.5 kb (lanes 2 and 4, respectively).

Abbreviations: M: 2-log DNA ladder.

In Figure 22 (lanes 1 and 3) no Cre recombinase was used (served as a negative control), and a 3.6 kb band for the pLox2+ plasmid and a 3.2 kb band for pPDX_Cre_LSL_ROSA26 plasmid were showed, respectively. After Cre treatment (lanes 2 and 4), Cre-mediated excision of the floxed cassette occurred. Although similar DNA fragments sizes were obtained after Cre-mediated deletion of part of the pPDX_Cre_LSL_ROSA26 linear vector (lane 4), the migration of circular forms of DNA are distinct. Thus, an excised, circular 1.6 kb splice acceptor-neomycin resistant cassette (which migrates at approximately 1.1 kb on the agarose gel) and a linear 1.5 kb DNA were observed. In the positive control (pLox2+ vector - lane 2) a circular 2.8 kb ampicillin resistant plasmid (which migrates at approximately 1.7 kb on the agarose gel) and a linear 850 bp DNA were observed after recombination. This data proves the functionality of the mutant *lox2272* sites.

3.2 Gene placement of pancreas-specific Cre constructs at the porcine *ROSA26* locus

After testing that PDX-1 promoter, as well as that the *lox2272* sites, were functional, the Cre constructs were to be inserted into the porcine *ROSA26* locus. A diagram of the gene placement strategy is shown in Figure 23, for gene stacking see Figure 24.

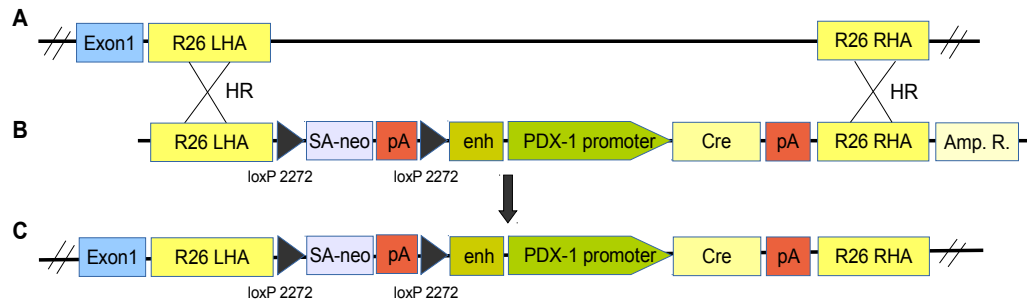


Figure 23: Diagram of gene targeting strategy with PDX-Cre vector before and after homologous recombination (HR).

(A) Porcine wild-type *ROSA26* locus, with left (LHA) and right (RHA) homologous arms of the porcine *ROSA26* locus. (B) pPDX_Cre_LSL_ROSA26 targeting construct consists of left homologous arm (LHA) of the porcine *ROSA26* locus; floxed splice acceptor (SA)- neomycin (neo) resistance cassette followed by Cre recombinase under the control of PDX-1 promoter and a right homologous arm (RHA) of the porcine *ROSA26* locus. (C) Porcine targeted *ROSA26* locus after homologous recombination. *Lox2272* sites are indicated as triangles.

Abbreviations: enh: enhancer element of the *PDX-1* gene; *PDX-1*: human *pancreatic and duodenal homeobox 1* promoter; Amp. R: ampicillin resistance; pA: polyadenylation signal.

As indicated in Figure 23, our promoter trap vector contains a promoter-less floxed splice acceptor-*neo* resistance cassette, followed by the Cre recombinase driven by the PDX-1 promoter, flanked by homology arms to facilitate insertion into the first intron of the porcine *ROSA26* gene. In addition, splice acceptor (added in front of the *neo* resistance gene) and polyA elements were placed upstream of the tissue-specific promoter for the termination of the *neo* gene transcript.

For gene placement by homologous recombination at the porcine *ROSA26* locus, the PDX-Cre gene targeting vector (pPDX_Cre_LSL_ROSA26) as well as the PDX-Cre gene stacking vector (pSA-neo-PDX-Cre-R26-mT/mG) were linearised. Adipose-derived mesenchymal stem cells (pAdMSCs) were isolated from wild-type Landrace pig (for transfections with PDX-Cre R26) and pKDNFCs were isolated from a dual fluorescent reporter pig (for gene stacking with PDX-Cre R26 mT/mG). A diagram of gene placement of PDX-Cre (gene stacking) at the porcine *ROSA26* locus is indicated in Figure 24.

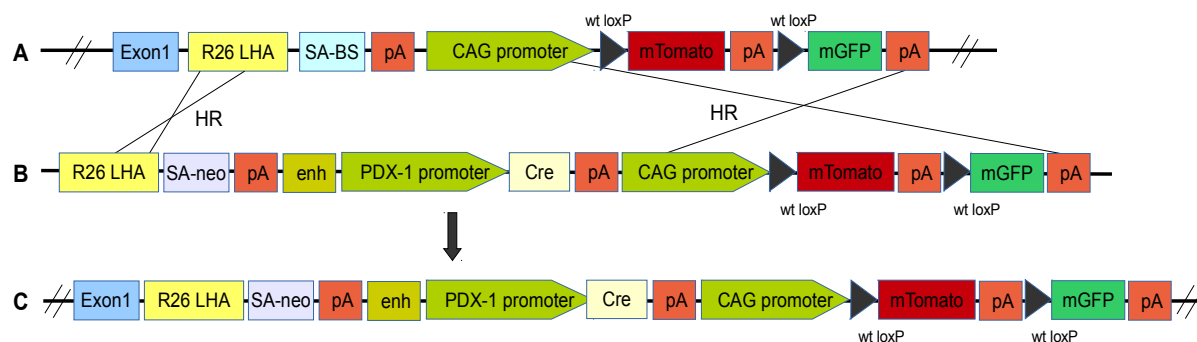


Figure 24: Diagram of gene stacking strategy with PDX-Cre vector before and after homologous recombination (HR).

(A) Porcine *ROSA26* targeted locus, consisting of a splice acceptor (SA), Blasticidin (BS) resistance cassette followed by a dual fluorescent (mTomato/mGFP) reporter cassette, being mTomato floxed, under the control of the CAG promoter. (B) pSA-neo-PDX-Cre-R26-mT/mG targeting construct consists of left homologous arm (LHA) of the porcine *ROSA26* locus; splice acceptor (SA)- neomycin (neo) resistance cassette followed by Cre recombinase under the control of PDX-1 promoter and a right homologous arm of the target *ROSA26* locus. (C) Porcine retargeted *ROSA26* locus after homologous recombination. *LoxP* sites are indicated as triangles.

Abbreviations: enh: enhancer element of the *PDX-1* gene; *PDX-1*: human *pancreatic and duodenal homeobox 1* promoter; Amp. R: ampicillin resistance; pA: polyadenylation signal.

3.2.1 Detection of PDX-Cre target cell clones by RT-PCR, PCR and Southern Blot

Two days post-transfection, with the targeting vectors, selection was applied using G418 (*neomycin - Neo*). Seventy *Neo* resistant cell clones, obtained from pAdMSCs transfected with pPDX_Cre_LSL_ROSA26 targeting construct and 31 cell clones, obtained from pKDNFCs R26-mT/mG cells retargeted with the pSA-neo-PDX-Cre-R26-mT/mG construct, were isolated and assessed for vector integration by homologous recombination.

First the seventy G418-resistant clones were screened for the targeting event by PCR across the 5' homology arm to a point outside the targeting vector. From those 70 cell clones, 28 cell clones were positive by 5' junction PCR. From those 28 positive clones further analysis such as 3' junction PCR and selectable cassette expression (*Neo*) by RT-PCR were possible to perform with just 11 clones, as the others 17 clones stopped dividing and growing.

For selectable cassette expression verification, RNA samples isolated from the 11 cell clones were tested for the presence of RNA transcribed from the *ROSA26* promoter extending from exon 1 spliced to the *Neomycin* gene (see Figure 25-A). The RT-PCR results are shown in Figure 25-A'.

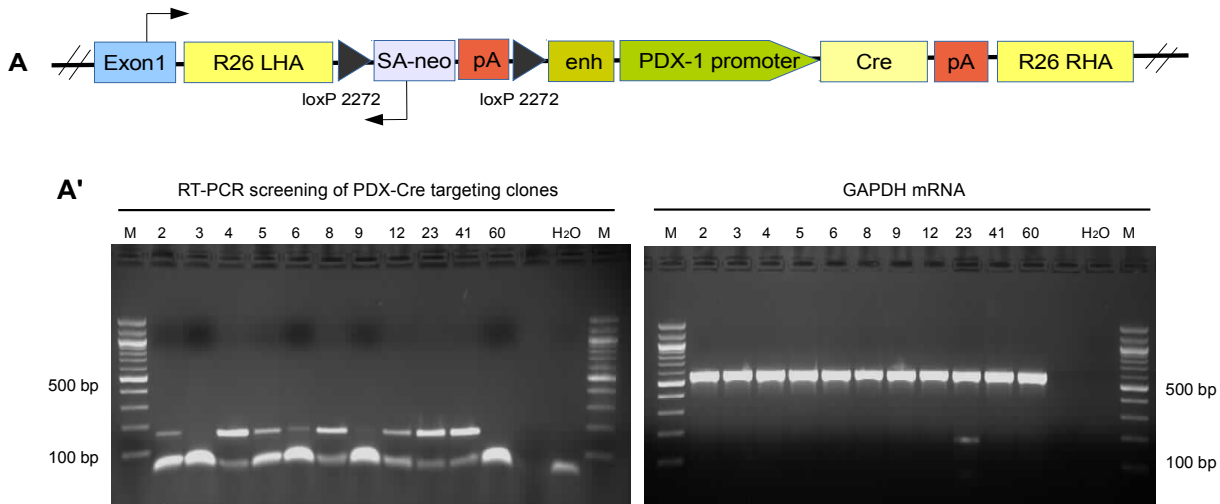


Figure 25: Schematic location of primers and RT-PCR identification of PDX-Cre clones targeted at the porcine *ROSA26* locus.

(A) Schematic structure of the porcine *ROSA26* locus, showing the primer pair used for targeting RT-PCR amplification. (A') PDX-Cre *Neomycin* resistant single-cell clones (left) was detected by RT-PCR by a 158 bp PCR fragment. Porcine GAPDH (right), was used as a loading control, and detected by a 583 bp PCR fragment. *Neomycin* resistant single-cell clones numbers are showed at each lane. Eight of eleven single-cell clones are positive (clones 2, 4, 5, 6, 8, 12, 23 and 41). Abbreviations: M: 100 bp DNA ladder; H₂O: water control.

From the eleven clones screened by RT-PCR, eight were able to express *Neo* and could confirm that the *Neo* gene was expressed from the *ROSA* promoter (see Figure 25 A' clones 2, 4, 5, 6, 8, 12, 23 and 41). They were used for further screening for targeting event by 3' junction PCR.

Figure 26 shows a schematic location of the primer pairs used to detect targeting at the 5' and 3' junction PCR, as well as the endogenous control.

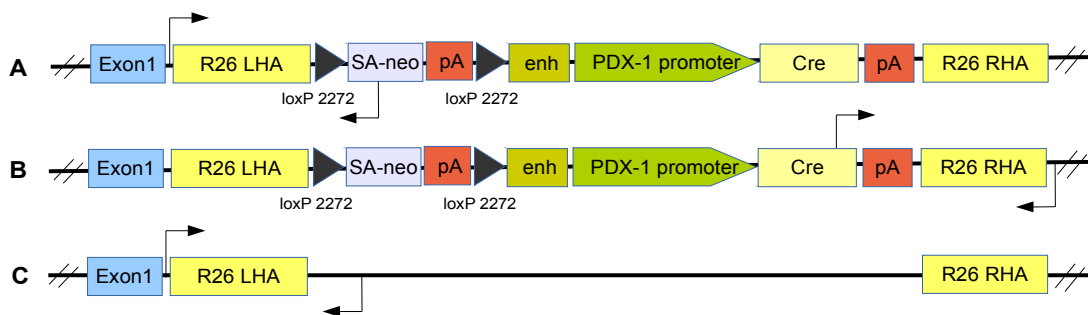


Figure 26: Schematic structure of primers and 5' junction PCR of PDX-Cre R26 targeting clones.

(A) Schematic structure of the porcine *ROSA26* locus, showing the primer pair used for 5' junction targeting PCR amplification or (B) 3' junction targeting PCR amplification. (C) Schematic structure of the porcine *ROSA26* locus, showing the primer pair used for endogenous PCR amplification.

Using a forward primer outside the targeting vector (in the *ROSA26* intron 1) and a reverse primer at the 5' homology arm (splice acceptor-neo cassette), several clones were positive (data not shown). However, from those only the 8 clones, positive for selectable neo cassette expression, were tested at the 3' homology arm to a point outside the targeting vector. The results showed that only three clones tested were positive (4, 5 and 23). The 5' and 3' junction PCR analyses for these three positive PDX-Cre R26 targeted cell clones are showed in Figure 27.

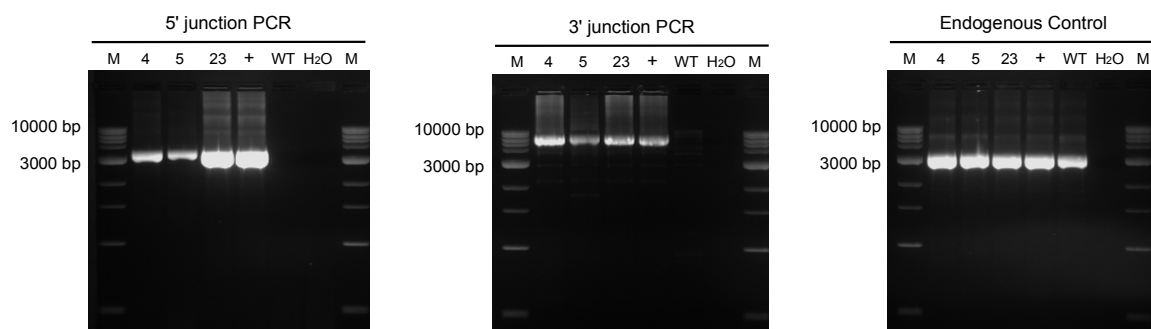


Figure 27: Endogenous control as well as 5' and 3' junction PCR of PDX-Cre R26 gene targeted clones. 5' junction targeting PCR (left) and 3' junction targeting PCR (middle) of PDX-Cre *Neomycin* resistant single-cell clones. A band by 3.3 kb and 5.5 kb is expected by positive 5' and 3' targeting PCR, respectively. Endogenous PCR (right) for PDX-Cre *Neomycin* resistant single-cell clones. A band by 3.1 kb is expected by endogenous PCR. *Neomycin* resistant single-cell clones numbers are showed at each lane. Positive control: genomic DNA of gene targeted construct at the porcine *ROSA26* locus (ECF#74 Konrad). Wild-type porcine genomic DNA and H₂O were used as negative control.

Abbreviations: M: 1 kb DNA ladder; +: Positive control; WT (wild-type); H₂O: water control.

To detect the presence of single or double PDX-Cre R26 targeted allele in all screened samples, an endogenous control PCR was used and these three clones amplified the endogenous fragment, indicating that only one *ROSA26* allele was targeted.

Southern blot analysis

Southern blot analysis was carried out to evaluate the structure of the targeted *ROSA26* alleles and to exclude random integrants. Therefore, the three PDX-Cre R26 targeted clones that were positive for 5' and 3' junction PCR, as well as by RT-PCR were analysed. Genomic DNA from those three positive clones as well from porcine wild-type was isolated, double digested using *SbfI* and *BlnI* restriction enzymes and size-separated by agarose gel electrophoresis. Figure 28 shows the DNA sequences detected and visualised after exposition in X-ray film.

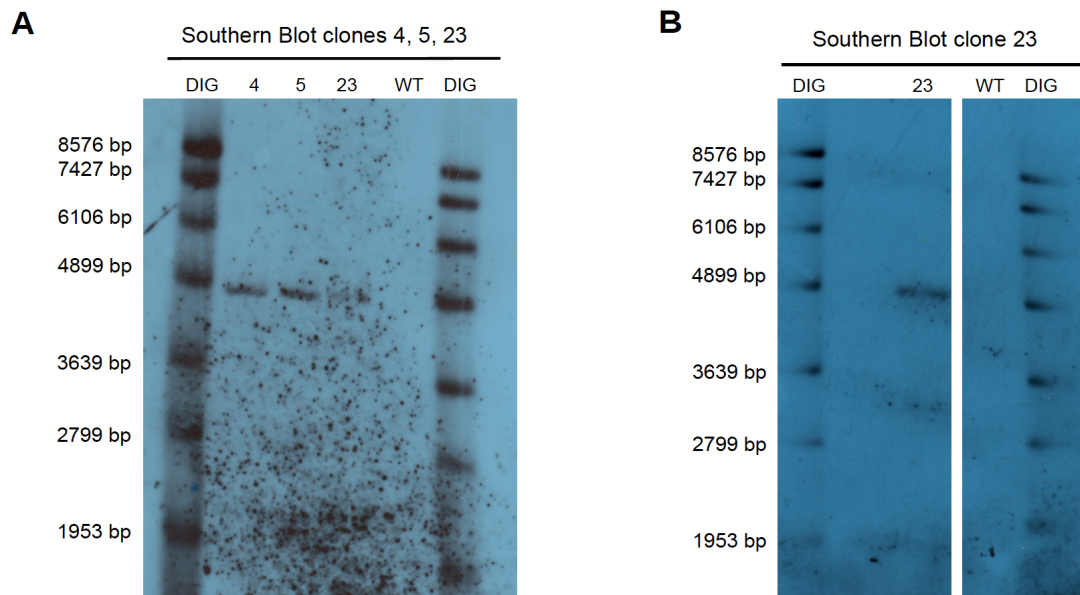


Figure 28: Southern blot X-ray film analysis from PDX-Cre R26 targeted cell clones.

The lanes shows genomic DNA from three PDX-Cre R26 targeted clones (numbers 4, 5 and 23) and from porcine wild-type that was double digested. The probe binds the *neomycin* cassette for a 4802 bp fragment. All three target clones are positive.

Abbreviations: DIG: DNA molecular weight marker VII, DIG-labeled, 0.081-857 kbp; WT: wild-type genomic DNA.

Southern blot using the genomic DNA from the PDX-Cre R26 cell clone number 23 was repeated for better visualisation of the results (Figure 28 - B). The specific DNA band sequence of 4.802 bp was detected with the *Neo* probe in each cell clone used (4, 5 and 23). The results indicated that in each of the three cell clones the *ROSA26* locus was correctly targeted and no random integration was observed.

3.2.2 Detection of correctly PDX-Cre R26 retarget cell clones by PCR

After transfection with pKDNFs R26-mT/mG cells using the pSA-neo-PDX-Cre-R26-mT/mG re-targeting vector, genomic DNA from 31 resistant G418 cell clones was isolated. They were screened for targeting event by PCR across the 5' homology arm a to point outside the targeting vector, using the same primer pair as shown in Figure 25. Here, 12 screened clones were positive and of these just five also amplified the endogenous fragment. Unfortunately all clones stopped proliferating, so it was not possible to get enough material for further screenings.

The transfection was repeated two more times using the same conditions. For each transfection about thirty resistant clones after G418 selection were screened for the targeting event by 5' junction PCR, but no positive clones were detected. To confirm that no exchange between the targeted porcine *ROSA26* locus and the PDX-Cre R26 gene stacking construct happened, another PCR was conducted. Thus, the same forward primer (in *ROSA26* intron 1) was used as indicate in Figure 25 and a reverse primer which hybridizes to the *Blasticin* resistance gene

cassette. The results confirmed that no homologous recombination took place, as indicated by the amplification of the DNA fragment consisting in the *Blasticidin* resistance cassette to a point outside the targeting vector. Although all the screened cell clones were resistant to G418, no homologous recombination between the target vector and the targeted porcine *ROSA26* locus occurred.

3.2.3 Somatic cell nuclear transfer

Due to lack of PDX-Cre R26 retargeted clones for further analysis, only PDX-Cre R26 targeted cell clones (4, 5 and 23), verified by PCR and Southern analysis and positive for gene targeting event, were used as a donors for nuclear transfer (NT). They were pooled and used for NT, which was carried in collaboration with the group of Professor Eckhart Wolf (LMU). Reconstructed porcine embryos were then transferred into recipient sows and two pregnancies were established.

3.3 PDX-Cre R26 gene targeted piglet analyses

Two healthy nuclear transfer PDX-Cre R26 transgenic piglets were born. Analysis of the piglets by 5' and 3' junction PCR and sequencing indicated that they carry the construct at the *ROSA26* locus, and integrity and structure of the transgene were confirmed. Figure 29 shows 5' junction PCR from both PDX-Cre R26 piglets (#331 and #357).

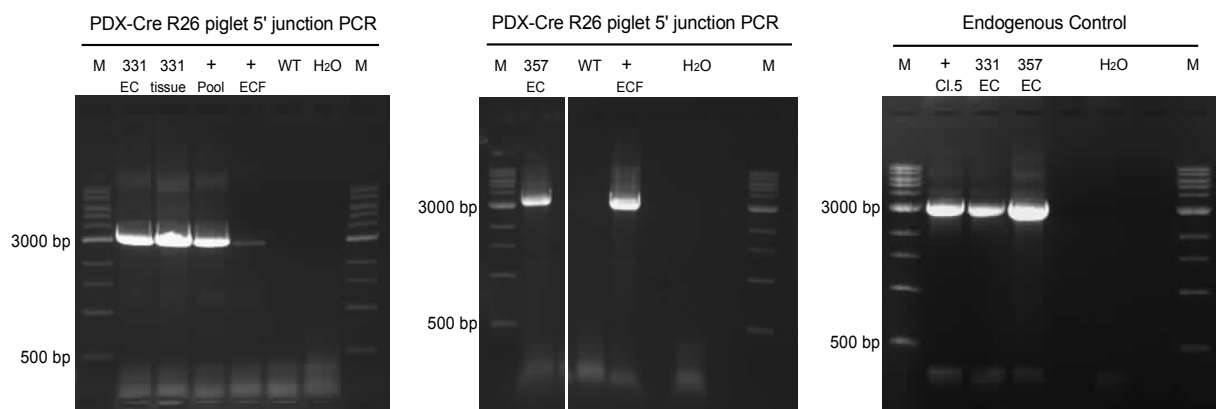


Figure 29: 5' junction PCR identification of PDX-Cre R26 piglets.

5' junction targeting PCR of the first (left) and the second (middle) birth to identify PDX-Cre R26 transgenic piglets. Endogenous control PCR (right) was also made. The identification of positive PDX-Cre R26 transgenic piglets was detected by PCR by a 3.3 kb PCR fragment and endogenous control was detected by PCR by a 3.1 kb PCR fragment. Piglets numbers are showed at each lane. Both transgenic piglets #331 and #357 amplified the 3.3 kb PCR fragment. Genomic DNA from ECF (ear clip fibroblast), ear clip (EC), tissue or cells were isolated for PCR analyses. Positive control ECF (left and middle): genomic DNA of gene targeted construct at the porcine *ROSA26* locus isolated from ECF (ECF#74 Konrad); Positive control Pool (left): genomic DNA isolated from PDX-Cre R26 cell clones number 4, 5 and 23 used for nuclear transfer; Positive control (right): genomic DNA isolated from PDX-Cre R26 cell clone number 5. Wild-type porcine genomic DNA and H₂O were used as negative control. Both fragments from the PCR at the middle position is originated from the same PCR.

Abbreviations: M: 1 kb DNA ladder; + Positive control; WT (wild-type); H₂O: water control.

To determine if the Cre recombinase was expressed specifically in the pancreas, one transgenic piglet was sacrificed (#357), and multiple organs were sampled. Genomic DNA and RNA from various tissues were extracted. Expression analyses of PDX-1 with all samples was performed. GAPDH was used as a control for measuring cDNA synthesis efficiency (see Figure 30).

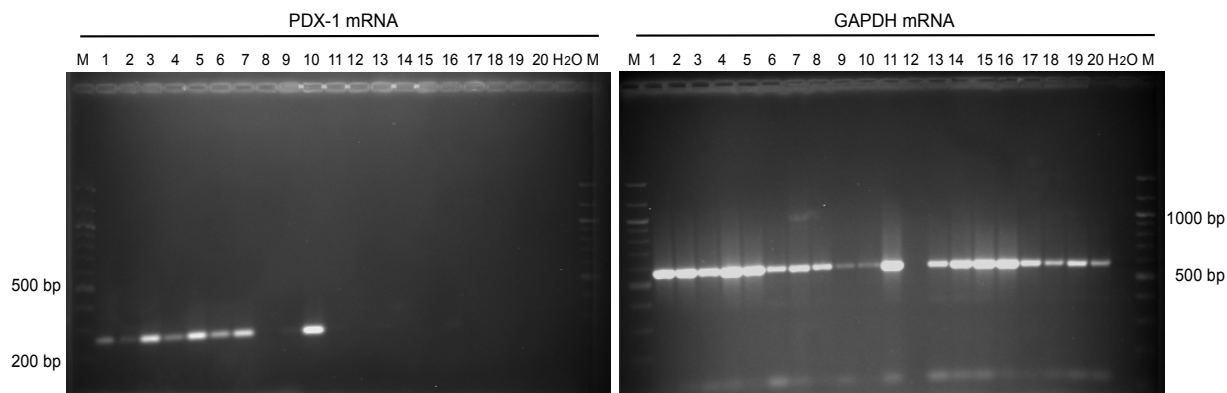


Figure 30: RT-PCR from PDX-Cre R26 piglet for detection of PDX-1 expression in different tissues and pancreas primary cells.

PDX-1 expression in PDX-Cre R26 piglet #357 (left) was detected by RT-PCR by a 262 bp PCR fragment. Porcine GAPDH (right), was used as a loading control, and detected by a 583 bp PCR fragment. Tissues and cells used for detection are showed at each lane: 1: pancreas primary acinar and islets cells; 2: pancreas primary cells; 3: small Intestine upper; 4: small intestine middle; 5: final part of duodenum; 6: upper part of duodenum; 7: middle part of duodenum; 8: stomach middle part; 9: antrum of the stomach; 10: pyloric gland; 11: large intestine lower; 12: large intestine upper; 13: large intestine middle; 14: lung; 15: heart; 16: liver; 17: muscle; 18: testis; 19: spleen; 20: kidney. H₂O was used as negative control.

Abbreviations: M: 100 bp DNA ladder; H₂O: water control.

The results obtained of PDX-1 mRNA show that pancreas, duodenum, antrum of the stomach, pyloric gland, bile duct, as well as the small intestine expressed endogenous PDX-1. It is known that in addition to the pancreas, PDX-1 is also expressed in other tissues. Therefore, these results are in accordance with those obtained by Hingorani *et al.* (2003) and Stoffers *et al.* (1999). These authors observed PDX-1 expression in pancreas, duodenum and stomach. PDX-1 was also detected in pyloric glands of the distal stomach and common bile and cystic ducts (Stoffers *et al.*, 1999). Others described that in the intestinal tract, PDX-1 is mostly and highly expressed in the duodenum with decreased expression in the small intestine (Guz *et al.*, 1995). All those results coincided with the expression of PDX-1 mRNA.

The same cDNA was further used for PCR to verify expression of Cre recombinase. As Cre recombinase does not get spliced DNA contamination had to be excluded. For this, additional PCR was performed with primers specific for genomic GAPDH (primers binding to intron 5). The PCR results showed amplification of Cre product and also intronic fragment of GAPDH in all analysed tissues, indicating DNA contamination in all RNA samples (data not shown). Two additional DNase treatments were done, but without completely elimination of the genomic DNA contaminants. Therefore, while still being detectable at the genomic level, no gene expression

of the Cre cDNA could be verified. For this reason another experiment was performed.

It is known that PDX1 expression occurs during early stages of mouse embryogenesis (Melloul *et al.*, 2002). It was therefore expected that, due to PDX-1 expression and Cre recombinase activation during pig pancreas development, the selectable cassette flanked by *lox2272* sites should be excised. Therefore, genomic DNA was used to identify the presence of cre-mediated recombination by PCR, with primers across the Lox-neo-Lox cassette. As a positive control genomic DNA from gene targeted cells derived from the PDX-Cre R26 #331 piglet after cre transduction was used (Figure 31 - A and B).

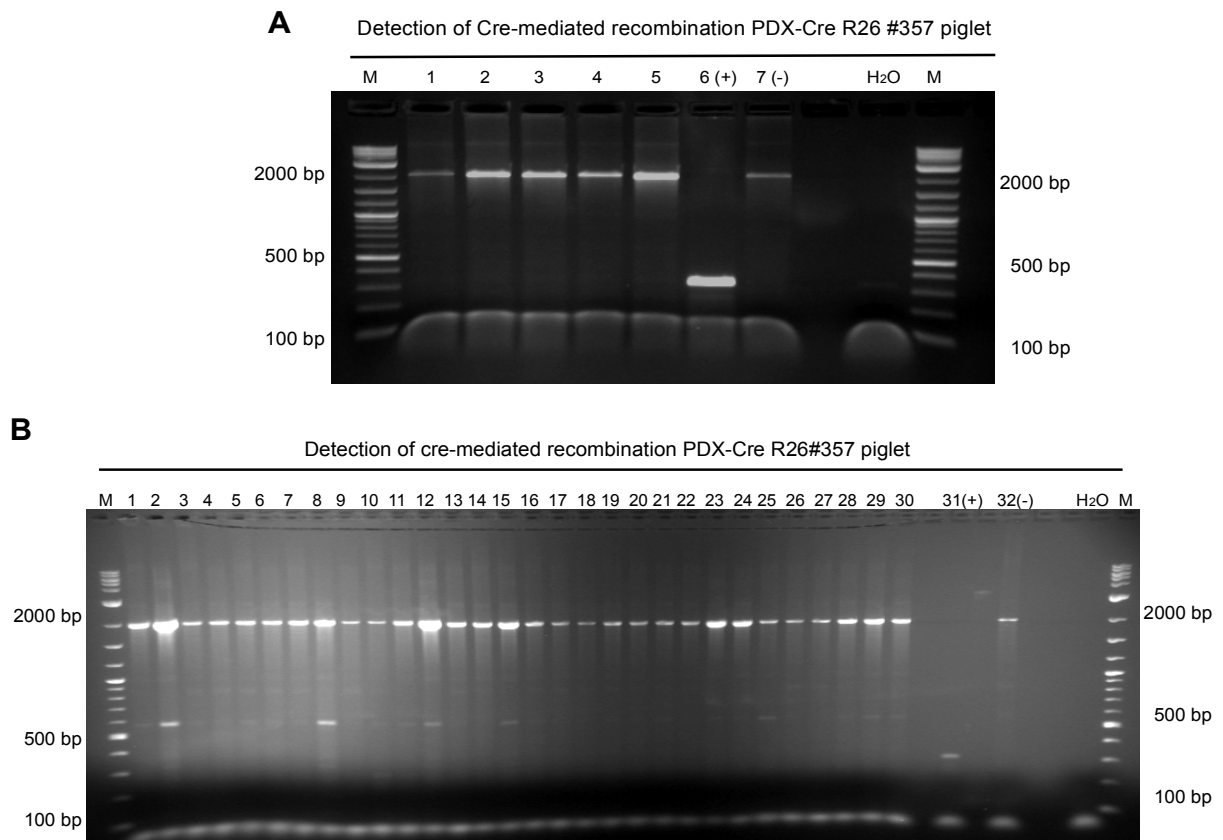


Figure 31: Identification of Cre-mediated recombination between *lox2272* sites from PDX-Cre R26 #357 piglet.

Site-specific recombination mediated by the Cre recombinase. Analysis of genomic DNA by PCR were done using specific primers for the *loxP* locus. Cre-mediated recombination between the two *lox2272* sites of the PDX-Cre R26 transgenic piglet would result in a 297 bp PCR fragment. If no deletion of the cassette flanked by *loxP* sites occurred detection by PCR by a 1964 bp PCR fragment was expected. No detection of *lox2272* deletion was observed in any tissues tested. Tissues used for detection are showed at each lane. (A) Tissues and cells used: 1: pancreas head piece 1; 2: pancreas head piece 1; 3: pancreas body; 4: pancreas tail piece 1; 5: pancreas tail piece 2; 6: Positive control: Positive control for Cre-mediated recombination: genomic DNA from porcine ear clip PDX-Cre R26 #331 piglet after cre transduction (16h); 7: Negative control for Cre-mediated recombination: genomic DNA from untreated porcine ear clip PDX-Cre R26 #331 cells. H₂O was used as negative control. (B) No detection of *lox2272* deletion was observed in any tissues or cells tested. Tissues and cells used: 1: pancreas tail piece A; 2: pancreas tail piece B; 3: pancreas body piece A; 4: pancreas body piece B; 5: pancreas head piece A; 6: pancreas head piece B; 7: pancreas head/end piece A; 8: pancreas head/end piece B; 9: pancreas; 10: stomach upper; 11: stomach middle; 12: pyloric gland; 13: duodenum upper; 14: duodenum middle; 15: duodenum final part; 16: small intestine upper; 17: small intestine middle; 18: large intestine middle; 19: large intestine upper; 20: large intestine lower; 21: skin; 22: lung; 23: heart; 24: liver; 25: muscle; 26: testis; 27: spleen; 28: kidney; 29: cortex frontal; 30: cerebellum; 31: Positive control for Cre-mediated recombination: genomic DNA from porcine ear clip PDX-Cre R26 #331 piglet after cre transduction (16h); 32: Negative control for Cre-mediated recombination: genomic DNA from untreated porcine ear clip PDX-Cre R26 #331 cells. H₂O was used as negative control.

Abbreviations: M: 100 bp DNA ladder; H₂O: water control.

Detection of Cre-mediated recombination between the two *lox2272* sites indicated that in all samples tested no Cre-mediated excision of the floxed cassette occurred (detection observed by a 1964 bp PCR fragment). Only in the positive control sample, due to Cre excision of the cassette flanked by *lox2272* sites, detection by a 297 bp PCR fragment was observed (see Figure 31 - A and B). This data indicate either the lack of Cre expression or deviation from *lox2272* consensus sequence. To exclude the possibility of mutation within *lox2272* sites the PCR spanning a fragment across Lox-neo-Lox cassette was sequenced. The PCR was performed with genomic DNA isolated from pancreas of PDX-Cre piglet #357 and from the targeting vector (used to generate this piglet). The sequencing results showed an insertion of 21 bp DNA fragment behind the intact left *lox2272* site (see Figure 75 in appendix). As the same insertion was also present in the targeting vector it can be concluded that the sequence was not introduced due to incorrect homologous recombination. In addition, the *in vitro* experiment to test the functionality of the *lox2272* sites (see Figure 22) showed that their were functional.

In all transgenic PDX-Cre driver mouse lines that were generated, pronuclear injection was used. Consequently, the transgene integrates as multiple copies into the genome. For this reason, while our data do not fully exclude that Cre recombinase was not expressed, our work strategy was changed.

3.4 New strategies for directing colon and pancreas specific Cre expression

The PDX-promoter had been tested in rat insulinoma cells where it was functional. But tranfection of the insulinoma cells resulted in multiple transgenes copies. Integration by homologous recombination into the *ROSA26* locus resulted in a single copy, which might not be sufficient for cre expression. Therefore the PDX-Cre transgene was transfected into primary porcine cells in order to achieve multiple copies. Also, we replaced the bacteriophage P1 Cre recombinase sequence for an improved Cre recombinase sequence (iCre). The sequence of iCre recombinase is a mammalian codon-optimized version of the original bacteriophage P1 Cre recombinase sequence with reduced CpG content in the coding sequence, that is predicted to reduce possible epigenetic silencing in mammalian cells. In some constructs a rabbit beta-globin (*rbβG*) intron was inserted between the tissue-specific promoter and iCre recombinase, since that intron was assumed to contain an enhancer element (Buchman and Berg, 1988).

3.4.1 Construction of iCre vectors

To compare the activity of the bacteriophage P1 Cre recombinase with the improved Cre recombinase, a new construct was generated to drive the expression of both recombinases by the PGK (phosphoglycerate kinase 1) promoter. The choice to use a PGK promoter was made

based on former results obtained by our group with the PGK-Cre construct, as the PGK promoter directed robust transgene expression. For this purpose the coding sequence of Cre was replaced by the improved Cre, using the PGK-Cre and the pAAV-CAG-iCre (Addgene) vectors. The iCre cDNA, obtained from the pAAV-CAG-iCre plasmid was isolated with *Bam*HI and *Hind*III restriction digest and placed under the control of the PGK promoter (see appendix section for cloning details).

As a positive control for cell culture experiments, the original pAAV-CAG-iCre plasmid was modified in order to eliminate the WPRE (woodchuck hepatitis virus post-transcriptional regulatory element) sequence. The WPRE sequence was used in a variety of viral vectors and was shown to induce higher transgene expression levels (Higashimoto *et al.*, 2007). However, the post-transcriptional regulatory element (PRE) of woodchuck hepatitis virus (WHV) might potentially contribute to tumorigenesis, based on data from WHV-associated hepatocellular carcinomas (Bouchard and Schneider, 2004). The WPRE element of the pAAV-CAG-iCre plasmid was excised by *Hind*III and *Sall* restriction enzymes digestion.

In Figure 32 a schematic structure of the original PGK-Cre, the PGK-iCre and CAG-iCre vectors is shown.

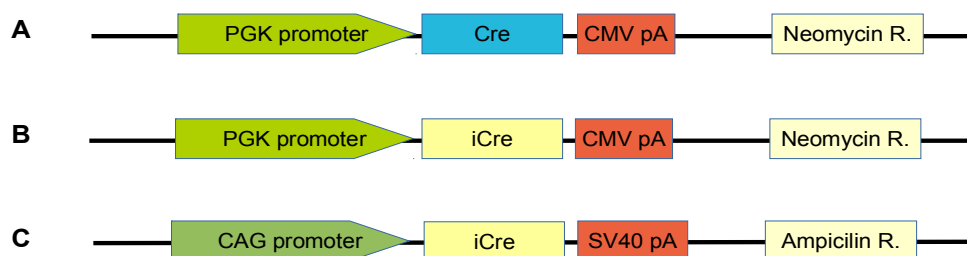


Figure 32: Design of the PGK-Cre, PGK-iCre and CAG-iCre constructs.

PGK promoter drives expression of Cre (A) or iCre (B) recombinase followed by a CMV polyadenylation signal (pA). The CAG promoter drives expression of iCre (C) recombinase followed by a SV40 polyadenylation signal (pA). Both Cre and iCre recombinase contain a Kozak sequence and an NLS of the simian virus 40 large T-antigen. Abbreviations: Neomycin or ampicilin R: resistance; SV40: simian virus 40; CMV: cytomegalovirus; iCre: improved Cre recombinase.

3.4.2 Cre and improved Cre recombinase expression test

Investigation of Cre and improved Cre recombinase activity were made using both PGK-Cre and PGK-iCre constructs as well as the CAG-iCre vector. They were transiently transfected into cell types from different species to compare cell/specie type specific activities. For that porcine KDNF R26-mT/mG, porcine AdMSC R26-mT/mG, human HEK-293 mT/mG, human SW-480 mT/mG, mouse NIH-3T3 mT/mG and rat EAF mT/mG reporter cells were used and visualised 72 and 96 h post-transfection. The use of reporter cell lines allowed for visualisation of Cre, since Cre mediates the excision of the flanked Tomato sequence leading to a fluorescence switch from red to green in recombined cells. The Figure 33 shows red and green fluorescence

96 h post-transfection, using porcine, human, mouse and rat reporter mT/mG cells.

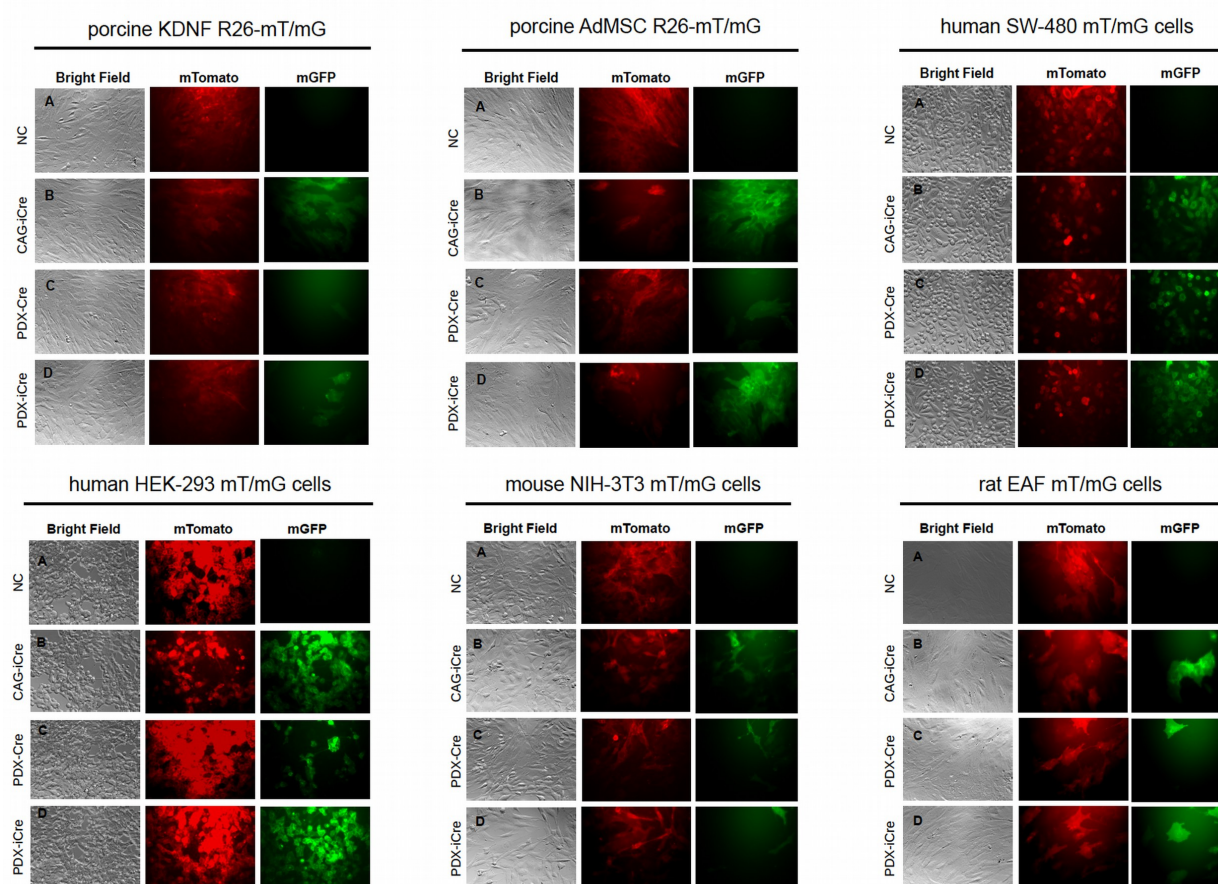


Figure 33: Activity comparison of improved Cre (PGK-iCre) and bacteriophage P1 Cre (PGK-Cre) recombinases using porcine, mouse, human and rat double reporter cells.

Cre mediates the excision of the flanked Tomato sequence leading to a fluorescence switch from red to green in recombined cells. The reporter mT/mG cells used for transfection and visualized after 96 hours were: porcine KDNF (kidney fibroblast); porcine AdMSC (adipose-derived mesenchymal stem cells); human SW-480 (colon adenocarcinoma cells); human HEK-293 (embryonic kidney cells); mouse NIH-3T3 (fibroblast) and rat EAF (ear fibroblast). (A) Negative control: untreated reporter cells. (B) Positive control: cells transfected with pCAG-iCre construct. (C) Cells transfected with pPGK-Cre vector and (D) pPGK-iCre vector. Magnification of 20x.

As illustrated in Figure 33, in all cells tested except, for the mouse NIH-3T3 mT/mG (where both recombinases had similar efficiency), the codon-improved Cre recombinase (Figure 33-D) shows an increased activity compared to the prokaryotic Cre (Figure 33-C).

To confirm the results obtained, fluorescent-activated cell sorting (FACS) was performed. Three out of the six double reporter cells used were chosen: porcine (KDNF R26-mT/mG), human (HEK-293 mT/mG) and mouse (NIH-3T3 mT/mG). Both PGK-Cre and PGK-iCre constructs, as well as the pmaxGFP vector (Lonza- as positive control), containing a CMV promoter and an intron to drive GFP expression, were used for transfection. Cells were visualised by microscopy 48, 72 and 96 h post-transfection to observe cre-mediated recombination (see Figure 34 - 48 h after transfection).

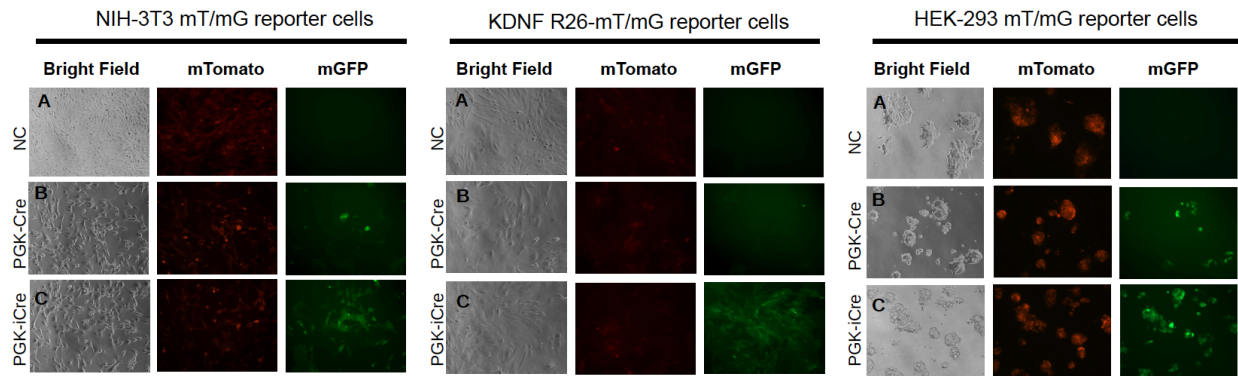


Figure 34: Activity comparison of improved Cre (PGK-iCre) and bacteriophage P1 Cre (PGK-Cre) recombinases using porcine, mouse and human double reporter cells.

Cre mediates the excision of the flanked Tomato sequence leading to a fluorescence switch from red to green in recombined cells. Fotos were taken 48 hours post-transfection from porcine KDNF (kidney fibroblast); human HEK-293 (embryonic kidney cells) and mouse NIH-3T3 (fibroblast) reporter mT/mG cells. (A) Negative control: untreated reporter cells. (B) Cells transfected with pPGK-Cre vector and (C) pPGK-iCre vector. Magnification of 10x.

Visualisation (2, 3 and 4 days post-transfection) confirmed a switch from red to green fluorescence in recombined cells after excision of the flanked Tomato sequence due cre-mediated recombination. Then, the cells were detached and resuspended in a flow cytometer buffer to be additionally used for quantification by FACS analysis. Figure 35 shows the quantification of red and green cells from porcine (KDNF R-26 mT/mG), human (HEK-293 mT/mG) and mouse (NIH-3T3 mT/mG) 48, 72 and 96 h post-transfection by FACS analysis.

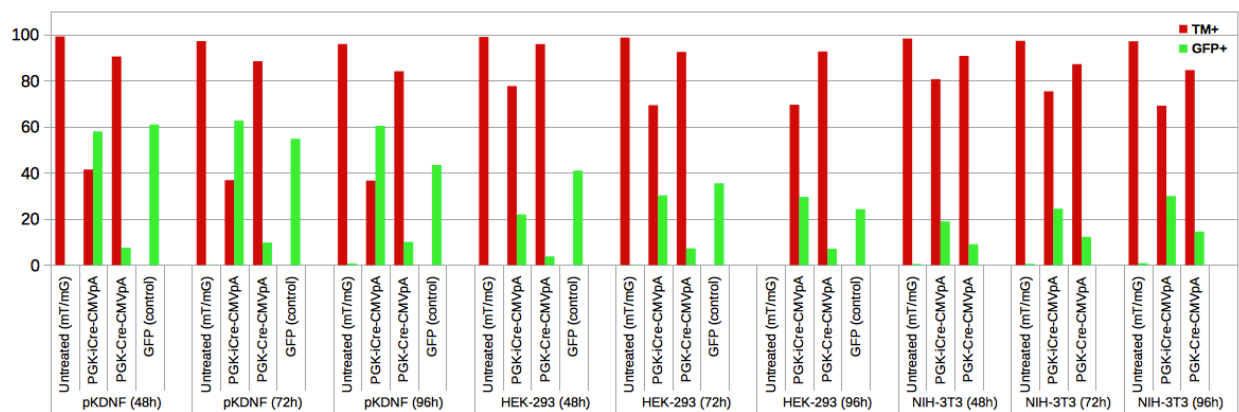


Figure 35: Quantification of improved Cre (PGK-iCre) and bacteriophage P1 Cre (PGK-Cre) recombinases activity using porcine, mouse and human double reporter cells by FACS.

Quantification of red and green cells after Cre recombination. The switch from red to green in recombined cells was measured by FACS analysis. 1): The reporter mT/mG cells used for transfection and visualized after 96 hours were: porcine KDNF (kidney fibroblasts); human HEK-293 (embryonic kidney cells) and mouse NIH-3T3 (fibroblasts). Untreated cells: no transfection was performed in the reporter cells. PGK-iCre-CMVpA or PGK-Cre-CMVpA: vector containing the improved iCre recombinase or the Cre recombinase driven by the PGK promoter. Control: GFP plasmid (pmaxGFP-Lonza) was used as a control of transfection and FACS analysis.

The results in Figures 34 and 35 demonstrate higher Cre recombinase activity from codon-optimized iCre compared to prokaryotic Cre. After 48 h an 7.7, 5.9 and 2.1 fold higher expression was observed in porcine KDNF, human HEK-293 and mouse NIH-3T3 reporter cells,

respectively. After 72 h the expression values detected were 6.4, 4.2 and 2 folder higher and after 96 h 6.1, 4.2 and 2.1 folder higher. These results confirm that the codon optimization provided higher efficiency in translation of the Cre protein. These results are in accordance with those reported by Shimshek *et al.* (2002) using HEK-293 and CV-1 (monkey kidney fibroblast) cell lines.

3.4.3 Modification of colon- and pancreas-specific Cre expression constructs

Based on the above findings the bacteriophage Cre recombinase coding sequence was substituted by the coding sequence of improved Cre in the colon- and pancreas-specific Cre expression constructs.

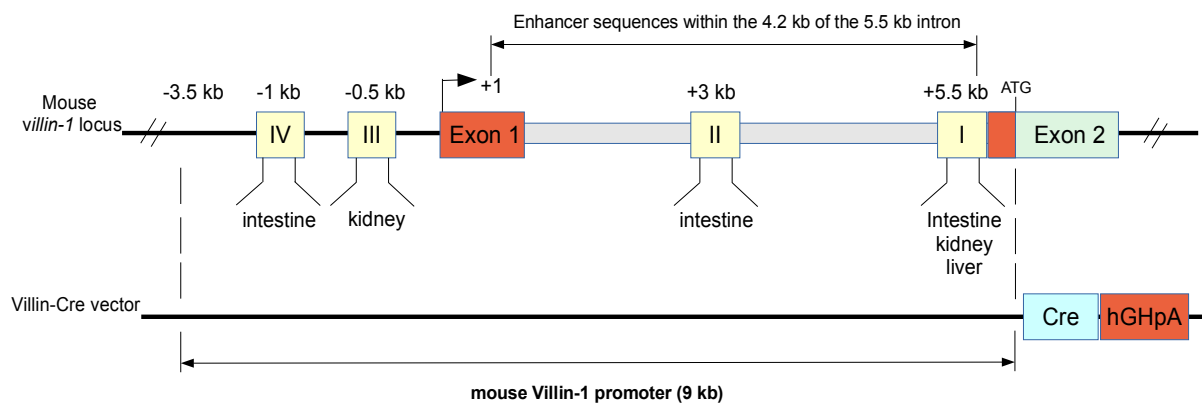


Figure 36: Schematic representation of the endogenous villin locus and the organization of the sites responsible for tissue-specific control of villin expression, as well as the villin-Cre vector.

Four major distinct DNase I-hypersensitive sites (I to IV) were shown to be present in the region extending from -1 kb to +5.5 kb in respect to the transcription start site in the mouse *villin-1* locus (upper Figure). They are responsible for distinct tissue-specific expression, as indicated. The orange boxes represent the untranslated exon, and the green box represents the first coding exon. The transcription start site is indicated in exon 1 (+1) as well as the initiation codon (the ATG codon) in exon 2. The size of the intron is indicated and 4.2 kb region of the first intron revealed the presence of one or more enhancers. The lower Figure represent the 9 kb villin-1 promoter (containing -3.5 kb to +5.5 kb from the start site of transcription) that drives expression of Cre recombinase followed by the human growth hormone polyadenylation signal (hGHpA).

The villin-Cre vector, consists of 9 kb of the villin-1 promoter region (-3.5 kb to +5.5 kb respective to the start site of transcription). It contains four distinct regions (I to IV) identified by Pinto *et al.* (1999) that are important to improve the levels of transgenic expression in the intestinal epithelium and are responsible for distinct tissue-specific expression in the villin-Cre vector (see Figure 36). The codon-improved Cre recombinase sequence was used to replace the bacteriophage Cre recombinase. In addition, the sequence of the rabbit beta-globin intron (rb β G) was also inserted into some constructs, between the villin-1 or the PDX-1 promoter and the iCre recombinase. Schematic representation of the final constructs are shown in Figure 37 (see appendix section for further cloning details).

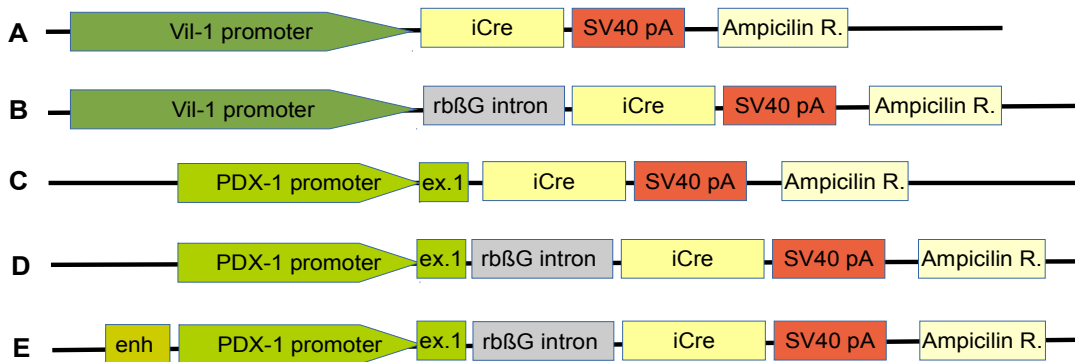


Figure 37: Schema of colon (villin-1) and pancreas (PDX-1) iCre vectors, with or without the rbβG intron.

The villin-1 promoter drives expression of iCre (A) or rbβG intron-iCre (B) recombinase followed by SV40 polyadenylation signal (pA). The PDX-1 promoter drives expression of iCre (C) or rbβG intron-iCre (D) recombinase followed by SV40 polyadenylation signal. The PDX-1 promoter containing an enhancer element drives expression of rbβG intron-iCre (E) recombinase followed by SV40 polyadenylation signal. A Kozak consensus sequence and an NLS of the simian virus 40 large T-antigen were included in front of iCre.

Abbreviations: rbβG: rabbit beta-globin; Vil-1: villin-1 promoter; pA: polyadenylation signal; iCre: improved Cre recombinase; enh: enhancer; ex.1: exon 1; SV40: simian virus 40; Ampicilin R: ampicilin resistance.

Colon- and pancreas-specific Cre expression constructs are functional

To find suitable cell lines to test the functionality and tissue specificity of the Cre expression vectors, several mammalian cell lines were analyzed for the expression of villin-1 (Figure 38) and PDX-1 (Figure 39).

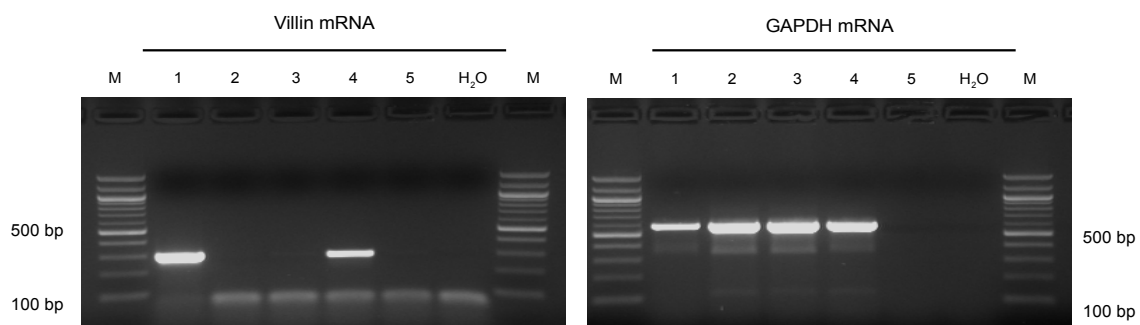


Figure 38: RT-PCR to detect villin-1 expression in different human cell lines.

The expression of villin-1 was detected by RT-PCR by a 284 bp PCR fragment. GAPDH, was used as a loading control and detected by a 591 bp PCR fragment. Villin-1 expression was detected in Caco-2 and NTERA-2 cells.

Abbreviations: M: 2-Log DNA ladder. (1) Caco-2 and (2) SW-480: human colorectal adenocarcinoma cells. (3) Panc-1: human epithelial carcinoma cells. (4) NTERA-2: human pluripotent embryonal carcinoma cells. (5) HEK-293: human embryonic kidney cells. H₂O: water control.

The results displayed in Figure 38 shows that Caco-2 and NTERA-2 cells express villin-1. PDX-1 (see Figure 39) was expressed in Caco-2, SW-480, Panc-1, HEK-293 and NTERA-2, in the positive control cells, rat insulinoma cells (INS-1), as well as weak expression in the human adipose-derived mesenchymal stem cells (hAdMSCs), used as negative control. Rat AdMSCs, also used as negative control, did not express any PDX-1 (see Figure 39).

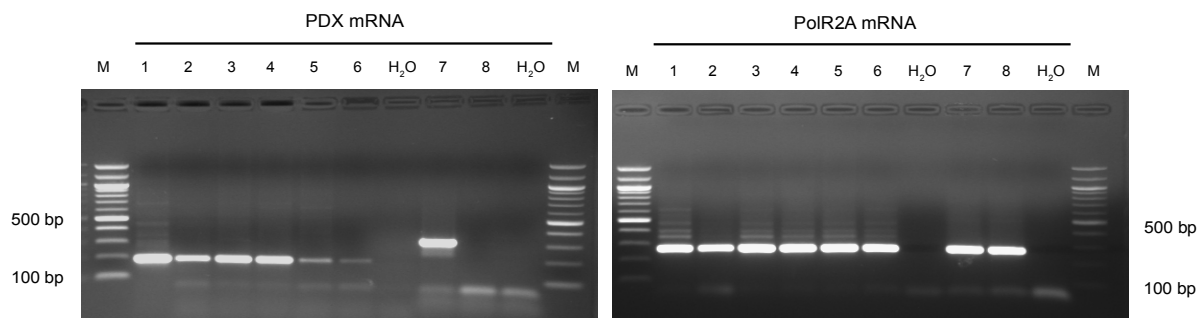


Figure 39: RT-PCR to detect PDX-1 expression in different human and rat cell lines.

The expression of porcine and rat PDX-1 was detected by RT-PCR by a 186 bp and a 312 bp PCR fragment, respectively. PolR2A, was used as a loading control, and detected by a 270 bp PCR fragment. In almost all cells tested PDX-1 expression could be detected, except for the rat AdMSC cells, used as negative control.

Abbreviations: M: 2-Log DNA ladder. (1) Caco-2 and (2) SW-480: human colorectal adenocarcinoma cells. (3) Panc-1: human epithelial carcinoma cells. (4) HEK-293: human embryonic kidney cells. (5) NTERA-2: human pluripotent embryonal carcinoma cells. (6) hAdMSC: human adipose-derived mesenchymal stem cells. (7) INS-1: rat insulinoma cells. (8) rAdMSC: rat adipose-derived mesenchymal stem cells. H₂O: water control.

Based on the above results following cell lines (carrying mT/mG reporter cassette) were used to test tissue specific Cre activity: Caco-2 for villin-1 and HEK-293 for PDX-1 expression constructs (for the constructs scheme see Figure 37).

Figure 40 depicts 96 h post-transfection results using the PDX- and villin-Cre expression vectors.

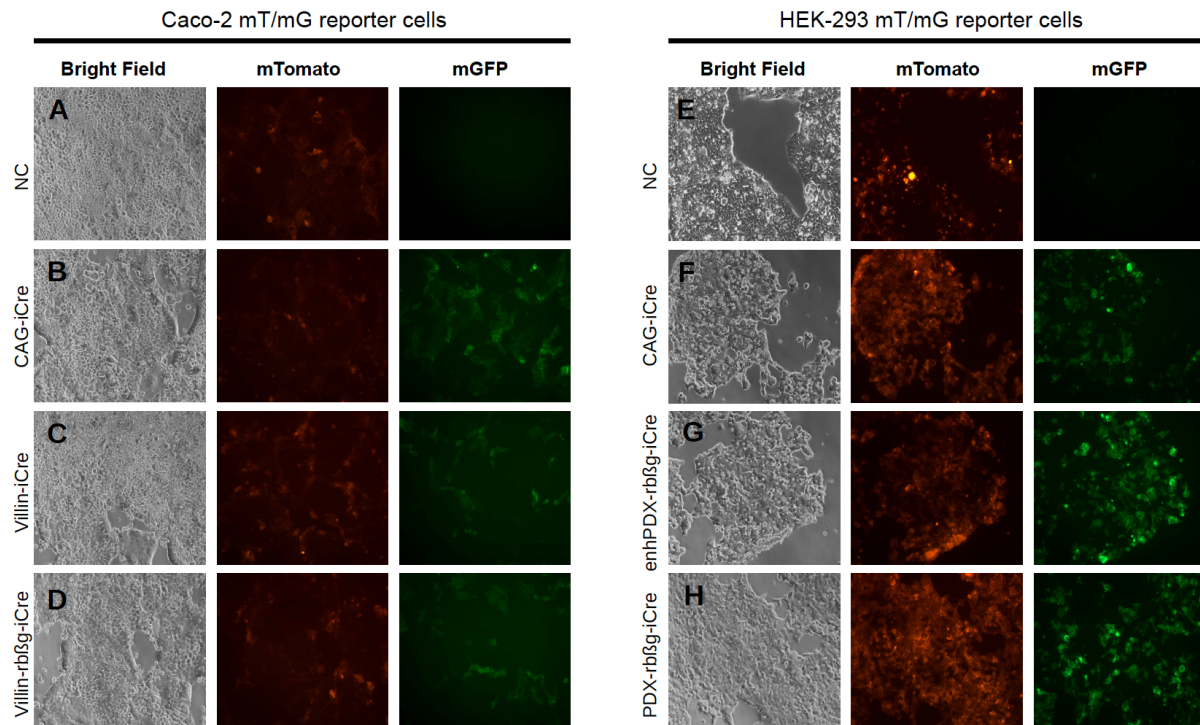


Figure 40: Functionality test of villin-1 constructs using Caco-2 mT/mG reporter cells and PDX-1 constructs using HEK-293 mT/mG reporter cells.

Pictures were taken 96 hours after transfection. After expression of villin-1 or PDX-1 the Cre protein mediated-recombination excised the mTomato cassette and the cells switched from red to green fluorescence. 1) Caco-2 reporter mT/mG cells (A) Negative control: un-transfected cells; (B) Positive Control: transfected cells using pCAG-iCreSV40pA; (C) Cells transfected with pVillin_iCreSV40pA; (D) Cells transfected with pVillin_rbβg_iCreSV40pA. HEK-293 mT/mG cells (E) Negative control: un-transfected cells; (F) Positive Control: transfected cells using pCAG-iCreSV40pA; (G) Cells transfected cells with pHEnhPDX-5'exon1_rbβg_iCreSV40pA; (H) Cells transfected cells with pHPDX-5'exon1_rbβg_iCreSV40pA. Magnification of 20x.

As depicted in Figure 40, mGFP fluorescence became evident in HEK-293 cells after PDX-1-iCre; and in Caco-2 cells after Vil-iCre constructs transfections. The number of mGFP positive cells for all transfections, including positive controls (CAG-iCre construct) was comparable, which proves that all tested promoters were functional. For quantification FACS analysis was performed including two cells lines used as negative controls, which showed no expression of Villin (INS-1-mT/mG) or PDX-1 (NIH-3T3-mT/mG). Cells were transfected with two different Vil-iCre constructs (see Figure 37 A and B) and two different PDX-1-iCre constructs (see Figure 37 D and E). FACS analysis was performed 96 h post transfection (see Figure 41).

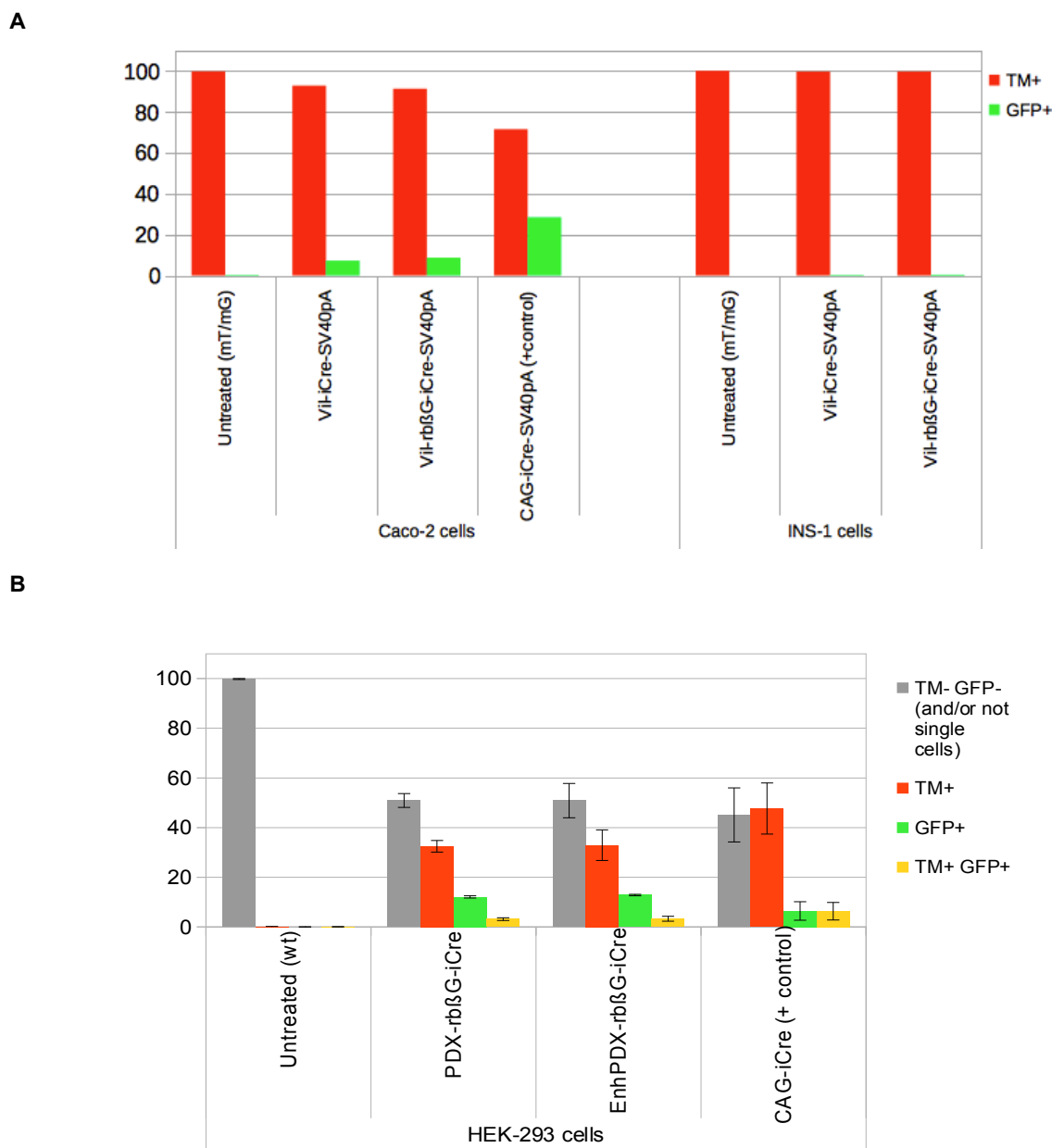


Figure 41: Quantification of red and green fluorescence cells by FACS analysis after transfection with villin-1 and PDX-1 constructs using Caco-2 and HEK-293 mT/mG reporter cells.

Measurements were made 96 hours after transfection. After expression of villin-1 or PDX-1 constructs the mTomato cassette is excised due Cre-mediated recombination and the cells switched from red to green fluorescence. (A) FACS analysis were done using Caco-2 reporter mT/mG cells, as well as INS-1 reporter mT/mG cells, as negative control for villin-1 analysis. Untreated cells: no transfection; Vil-iCreSV40pA: cells transfected with Villin_iCreSV40pA vector; Villin-rbβG-iCreSV40pA: cells transfected with pVillin_rbβG_iCreSV40pA vector. Positive Control: pCAG-iCreSV40pA vector used, in which the ubiquitously CAG promoter drive the expression of iCre recombinase. (B) For PDX-1 FACS analysis HEK-293 and SW-480 reporter mT/mG cells were used and NIH-3T3 reporter mT/mG cells as negative control. Untreated cells: wild-type HEK-293 or SW-480 cells; PDX-rbβG-iCre: cells transfected with phPDX-5'exon1_rβG_iCreSV40pA vector; EnhPDX-rbβG-iCre: cells transfected with phEnhPDX-5'exon1_rβG_iCre SV40pA vector. Positive Control: pCAG-iCreSV40pA vector used, in which the ubiquitously CAG promoter drive the expression of iCre recombinase. Error bars represent standard errors of triplicate samples.

The vector containing the constitutive CAG promoter, used as a positive control to drive iCre recombinase in Caco-2 cells, showed 3.9 and 3.3 folder higher expression in comparison with the villin-iCre and the villin-rbβG-iCre vectors (Figure 41-A). The negative control (INS-1 cells)

did not show any recombination events, as no green cells were either visualised by microscope or measured by FACS analysis. These results confirmed the functionality and tissue specificity of the villin-1 vectors.

As depicted in Figure 41-B, using HEK-293 mT/mG cells, a 2-fold higher expression was seen for both PDX-1 vectors compared to positive control CAG-iCre. The untreated, wild-type cells did show neither GFP nor tomato fluorescence, as expected. The grey bars represent mGFP / mTomato negative cells or cells that could not be counted as a single cell (approximately 50% of the HEK-293 cells and more than 50% of the NIH-3T3 mT/mG cells) were indicated in this category. The negative control (NIH-3T3 cells) did not show any recombination events (data not shown).

After confirmation of promoter functionality, it was decided to analyse the mRNA levels from both genes, *PDX-1* and *Vil-1*, in R26-mT/mG reporter pAdMSC and pKDNF cells, which could after be used as donors cells for SCNT, as well as other primary porcine cells (see Figure 42).

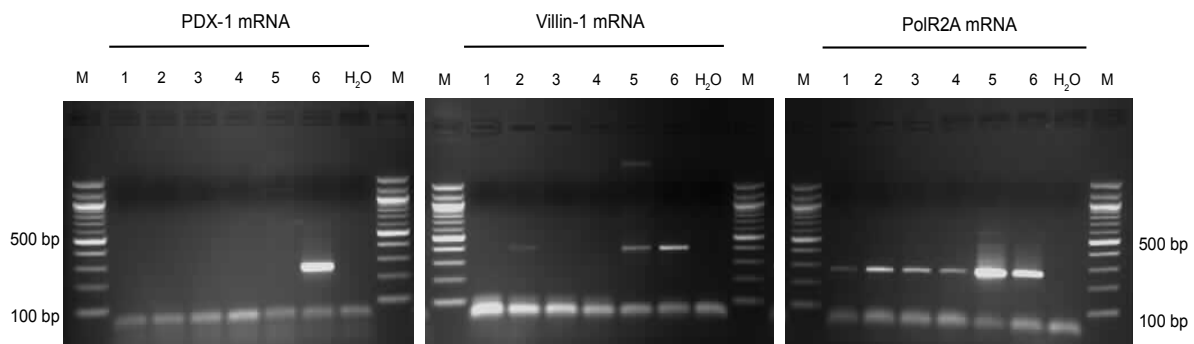


Figure 42: RT-PCR to detect PDX-1 and villin-1 expression in different primary porcine cells.

The expression of PDX-1 and villin-1 was detected by RT-PCR by a 262 bp and 407 bp PCR fragment, respectively. PolR2A, was used as a loading control, and detected by a 270 bp PCR fragment from both PDX-1 and VIL-1. Here, PDX-1 expression was not detected in any cells analysed, except for the positive control. On the other hand VIL-1 expression was detected in pKDNF and pEF cells.

Abbreviations: M: 2-Log DNA ladder. (1) pKDNF R26-mT/mG reporter cells: porcine kidney fibroblast from R26-mT/mG reporter foetus (ID 110713, foetus # 4). (2) pKDNF R26-mT/mG reporter cells: porcine kidney fibroblast from reporter pig #270. (3) pAdMSC R26-mT/mG reporter cells: porcine adipose-derived mesenchymal stem cells from reporter pig #270. (4) poFF: porcine fetal fibroblast. (5) pEF: porcine ear fibroblast. (6) Positive control Caco-2: human colon carcinoma cells. H₂O: water control.

Figure 42 shows that PDX-1 expression was only detected in the positive control, Caco-2 cells, and not in the primary porcine cells tested. However in Figure 39 (lane 6) PDX-1 was detected in the wild-type hAdMSCs at low level. Villin-1 expression was detected in the positive control Caco-2 cells, as well as in primary porcine kidney fibroblast and porcine ear fibroblast.

The detection of vil-1 expression in kidney cells was also observed by Kucherlapati *et al.* (2006), using the same 9 kb fragment of the villin-1 promoter. They reported that vil-1 was not only expressed in the epithelial cells of the mouse adult intestine but also in epithelial cells of the kidney proximal tubule. Thus our findings from the RT-PCR are consistent with those from

Kucherlapati *et al.* (2006). However, expression of PDX-1 in mice kidney was neither detected by Stoffers *et al.* (1997) or by Hingorani *et al.* (2003), using the mouse PDX-1 promoter. Therefore, it was decided to test both types of constructs, the PDX-iCre construct (pPDX-5'exon1_rbβG_iCre SV40pA) and the Vill-iCre construct (pVillin_rbβG_iCreSV40pA), in both pAdMSCs and pKDNF R26-mT/mG primary porcine reporter cells.

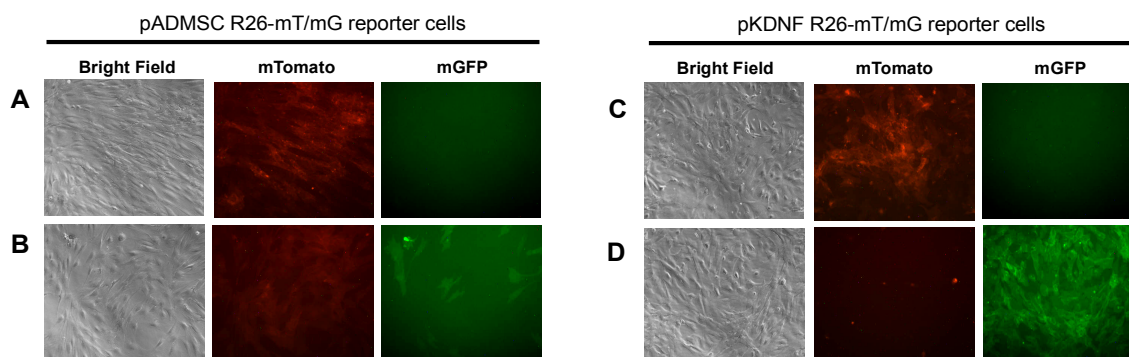


Figure 43: PDX-1 expression using pAdMSCs and pKDNF R26-mT/mG reporter cells.

R26 reporter mT/mG cells 10 days after transfection using the pPDX-5'exon1_rbβG_iCreSV40pA and pNEO vectors. Here, it is possible to distinguish the recombined, green cells after Cre excision, from the non-recombined red cells. pAdMSC R26-mT/mG cells: (A) Negative control: un-transfected cells; (B) Cells transfected with pPDX-5'exon1_rbβG_iCreSV40pA. pKDNF R26-mT/mG cells: (C) Negative control: un-transfected cells; (D) Cells transfected with pPDX-5'exon1_rbβG_iCreSV40pA. Magnification of 20x.

Surprisingly after selection, in Figure 43, an indication of PDX-Cre recombinase activity in both pKDNF and pAdMSC R26-mT/mG reporter cells was seen by the presence of green cells. It is evident that iCre under the control of the PDX-1 promoter and the enhancer element of the rbβG-intron mediated recombination between the *loxP* sites. Also similar recombination events were observed in both cells using the villin-1 construct, containing the villin-1 promoter and the rbβG intron (data not shown). Based on these results it was decided to evaluate if the rbβG intron alone could induce expression of Cre recombinase, due to elements that could provide similar promoter activity. Another experiment (performed by Dr. Anja Saalfrank) using HEK-293 mT/mG reporter cells, known to express the PDX-1 mRNA, was made. Table 21 below shows the different vectors used by Dr. Anja Saalfrank for transfection in HEK-293 mT/mG reporter cells.

Table 21: Plasmids used to transfect HEK-293 mT/mG reporter cells

Plasmid name	PDX-1 enhancer	PDX-1 promoter	rbβG intron (enhancer)	improved Cre
phEnhPDX-5'exon1_rbβG_iCre SV40pA	√	√	√	√
phPDX-5'exon1_rbβG_iCreSV40pA		√	√	√
phPDX-5'exon1_iCreSV40pA		√		√
prbβG_iCreSV40pA			√	√

In addition, three other vectors were used for the transfection experiments. Those were: positive control vector (expression of iCre is under the control of the constitutive active CAG promoter); the pPGK-eGFP vector functioned as a control vector to verify the transfection method and pPGK-*bsR* vector that encodes only the blasticidin resistance gene but not iCre. The results of transient versus stable transfection are shown in Figure 44.

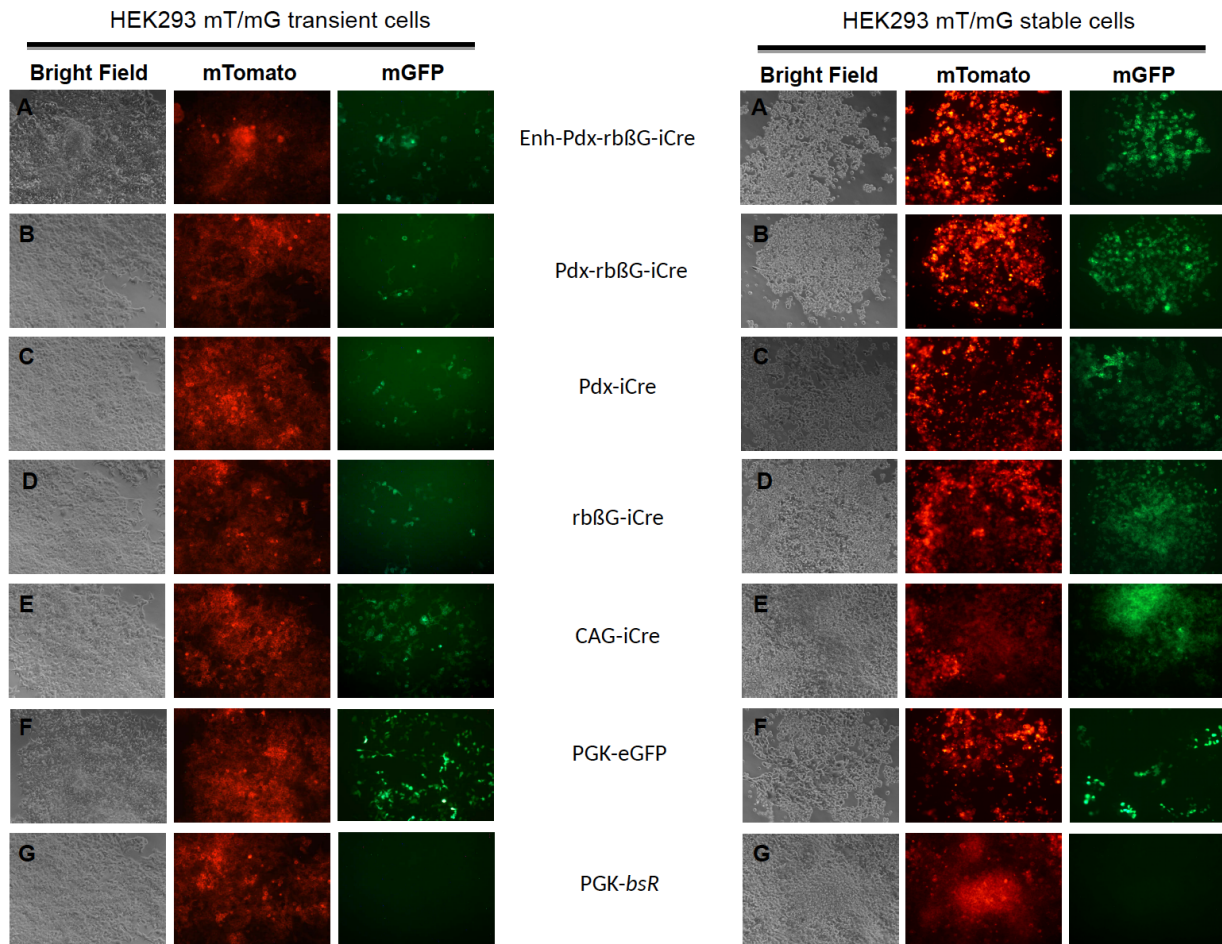


Figure 44: Expression test using vectors containing the $rb\beta G$ intron with or without the PDX-1 promoter in HEK-293 mT/mG cells.

Transient (2 days post-transfection) or stable transfection (12 days post-transfection) using HEK-293 mT/mG cells and different vectors. After Cre protein mediated recombination the mTomato cassette was excised and the cells switched from red to green fluorescence. (A) Cells transfected with phEnhPDX-5'exon1_ $rb\beta G$ _iCre SV40pA construct; (B) Cells transfected with phPDX-5'exon1_ $rb\beta G$ _iCreSV40pA construct; (C) Cells transfected with prb βG _iCreSV40pA construct; (E) Cells transfected with pCAG_iCreSV40pA construct; (F) Positive control: cells transfected with pPGK-eGFP construct; (G) Negative control: Cells transfected with pPGK-*bsR* construct. Magnification of 10x.

As expected, in both transient and stable transfection, using the HEK-293 mT/mG reporter cells, the PDX-1 promoters drove expression of iCre and recombination events. The recombination events were similar in all cases, with no differences between the PDX-1 constructs used. However even in the absence of the PDX-1 promoter recombination was observed as indicated by the presence of green cells. In both transient and stable transfections

using the rb β G-iCre construct, the recombination efficiency was comparable to the efficiency of the PDX-Cre constructs indicating promoter activity within the β -globin intron.

The constitutive CAG promoter, used as a positive control, showed higher recombination events in comparison with the PDX-1 and the rb β G vectors. The negative control did not show any recombination events.

Porcine AdMSCs showed low VIL-1 or PDX-1 expression of Cre vectors and were therefore chosen for further experiments. As the β -globin intron itself showed some promoter, as well as enhancer activity, iCre-expression vectors with or without the rb β G intron were included in the experiments.

3.5 Generation of pancreas-specific Cre driver pig lines

To create a pig where the pancreas promoter drives iCre recombinase the following PDX-1 constructs were used:

1. PDX-1 promoter, containing the rb β G intron, to drive iCre (phPDX-5'exon1_rb β G_iCre SV40pA);
2. PDX-1 promoter, without the rb β G intron, to drive iCre (phPDX-5'exon1_iCreSV40pA);

To derive cells for nuclear transfer pAdMSCs R26-mT/mG were transfected with one of the vectors described above. Selection was performed and Cre-mediated recombination was observed, as some cells turned green. Stable selected PDX-1-rb β G-intron transfectants and stable selected PDX-1 (without intron) transfectants were pooled for nuclear transfers.

Three rounds of nuclear transfer were performed in collaboration with the group of Professor Eckhart Wolf (LMU) and no pregnancy was established. Further tries are currently underway.

3.6 Generation of colon-specific Cre driver pig lines

In order to create colon-specific Cre driver pig lines Vil-1 constructs were used, as follows:

1. Vil-1 promoter containing the rb β G intron to drive iCre (pVillin_rb β G_iCreSV40pA);
2. Vil-1 promoter without the rb β G intron to drive iCre (pVillin_iCreSV40pA).

To derive cells for nuclear transfer, pAdMSCs R26-mT/mG were transfected. After selection, Cre recombination was detected as indicative by the presence of green cells in 10% of cells transfected with pVillin_iCreSV40pA vector. In the case of pVillin_rb β G_iCreSV40pA vector, 20% of cells were green.

Stable selected Vil-1-rb β G-intron transfectants and stable selected Vil-1 (without intron) transfectants were pooled and used for NT (pool 1). Since that cell pool consisted of red and

green cells, and we only want to have spatial control of villin expression *in vivo*, in the second attempt only stable selected red Vil-1 clones were picked, expanded and screened for the presence of the integrated vector construct (pool 2). Red, PCR positive single cell clones were pooled and used for NT in collaboration with the group of Professor Eckhart Wolf (LMU).

One live animal was obtained from pool 1 which died shortly after birth. As expected it was positive for mTomato fluorescence. Organs were collected for DNA and expression analysis and PCR was performed to verify the integration of the Vil-rb β G-iCre expression vector (Figure 45). Primers binding the *villin-1* gene and the improved Cre cDNA fragment were used.

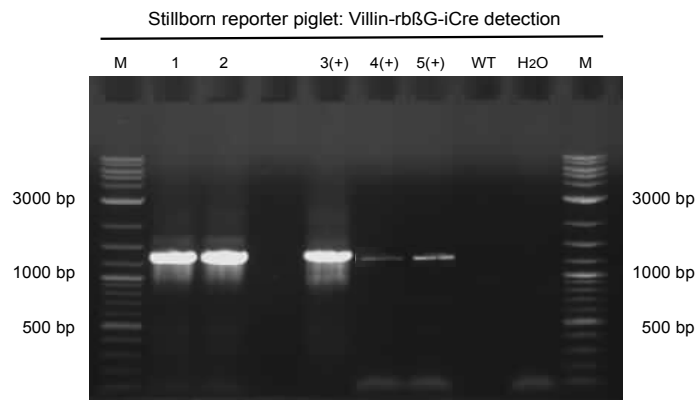


Figure 45: PCR analysis of stillborn Vil-rb β G-iCre piglet.

The gDNA isolated from the Vil-rb β G-iCre or from the positive controls were detected by PCR by a 1332 bp PCR fragment. Here, both gDNA isolated from the same Vil-rb β G-iCre stillborn piglet showed the same band as the positive controls used, indicating that the stillborn piglet contains the Vil-rb β G-iCre construct. (1) gDNA from stillborn piglet, isolated from KDNF tissue; (2) gDNA from stillborn piglet, isolated from KDNF tissue, from another gDNA isolation method; (3) positive control, plasmid DNA (pVillin-rb β G-iCre used for transfection); (4) positive control: gDNA from single cell clone #100 derived from transfection of pVillin-rb β G-iCre into pAdMSC#270; (5) positive control: gDNA from single cell clone #102 derived from transfection of pVillin-rb β G-iCre into pAdMSC#270. H₂O was used as a negative control.

Abbreviations: M: 2-Log DNA ladder; H₂O: water.

An expected 1332 bp PCR fragment was amplified from the positive control samples (3, 4 and 5, derived from a pVil-rb β G-iCre vector and single clones from Vil-rb β G-iCre pAdMSCs, respectively), as well as from the stillborn piglet samples (1 and 2). These results indicate that the stillborn piglet carried the Vil-rb β G-iCre construct. Next, gDNA from tissues of all three germ layers were isolated to verify iCre activity *in vivo*. In addition, the same tissue samples were embedded within OCT (Optimal Cutting Temperature compound) and fixed with formalin to paraffin embedding for further analysis (Table 22).

Table 22: Vil-rb β G-iCre stillborn piglet tissues isolated and its corresponding germ layers

Tissue	Corresponding germ layer
Tongue Oesophagus Stomach Duodenum Small intestine Middle gut Lower gut Caecum Pancreas Liver Lung	Endoderm
Kidney Heart Spleen Blood vessel Muscle	Mesoderm
Brain Skin	Ectoderm

3.6.1 Detection of tissue specific recombination

To detect recombination between the *loxP* sites, multiple organs from the reporter stillborn piglet were sampled (see Table 22 above). PCR was performed and primers were designed to amplify the regions just before and after the *loxP* sites from the gene targeted R26 mT/mG reporter porcine locus (see Figure 46 below for more details).

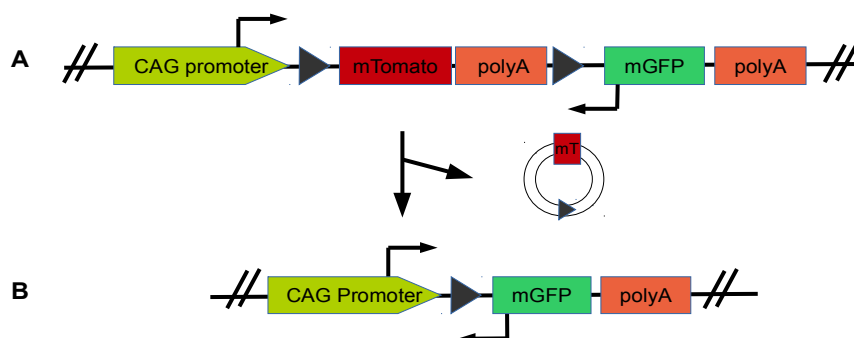


Figure 46: Schematic overview of the gene targeted R26 mT/mG reporter porcine locus and the primer pair used to detect recombination between the *loxP* sites.

The primer pair to detect recombination was designed to be close the *loxP* sites. (A) The forward primer binds in the 3' region of the CAG promoter and the reverse primer 5' in the mGFP fluorescence gene. All tissues of the Vil-rb β G-iCre stillborn piglet express mTomato prior to iCre-mediated excision. In that case, an un-recombined 2733 bp PCR fragment is amplified. (B) After Cre-mediated recombination the floxed mTomato cassette is excised from the gene targeted locus leading to a smaller recombined 327 PCR fragment.

Abbreviations: The two solid black triangles represent the *loxP* sequences, placed in the same orientation; CAG promoter (cytomegalovirus early enhancer/chicken β -actin promoter); mTomato/mT (membrane-targeted tandem dimer Tomato); mGFP (membrane-targeted green fluorescent protein); polyA (polyadenylation signal).

Using the primer pair described in Figure 47 two PCR fragments could be amplified. One from the un-recombined locus (Figure 46-A) and one from the recombined locus (Figure 46-B).

In Figure 46 the un-recombined PCR product with a size of 2733 bp was detected in samples 1-9, as well as in the negative control. These results indicate that Vil-1 is not active in these tissues. In contrast, for all samples isolated from kidney, pancreas, and stomach (lanes 10-12, respectively), as well as from gut (lanes 13-17) and liver (lane 3) the recombined and un-recombined PCR fragments are detectable. These findings indicate the excision of the floxed mTomato cassette and consequently the activity of iCre in these tissues.

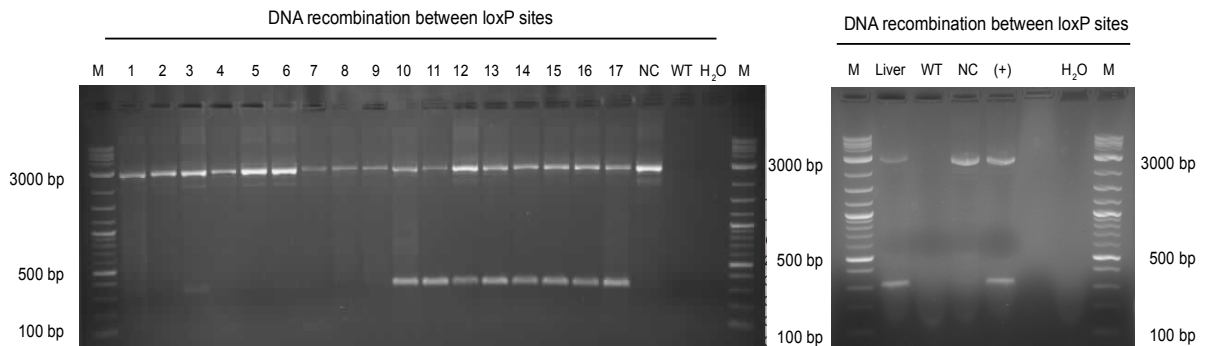


Figure 47: PCR amplification to detected DNA recombination between the *loxP* sites of the stillborn Vil-rb β G-iCre reporter piglet.

The gDNA recombination between the two *loxP* sites was detected by PCR by a 327 bp fragment. If no gDNA recombination occurred, a 2733 bp un-recombined PCR fragment was amplified. The Figure on the left side shows that in samples 1-9 no gDNA recombination occurred as the bigger 2733 bp un-recombined PCR fragment was amplified. The presence of the smaller recombined 327bp PCR fragment of samples 10-17 indicates the deletion of the floxed mTomato cassette. The Figure on the right side shows that recombination also occurred in liver tissue. Figure on the left: (1) lung; (2) muscle; (3) spleen; (4) skin; (5) blood vessel; (6) tongue; (7) oesophagus; (8) brain; (9) heart; (10) kidney; (11) pancreas; (12) stomach; (13) duodenum; (14) small intestine; (15) middle part of colon; (16) lower part of colon (17) caecum; (NC) Negative Control: gDNA from pAdMSC R-26 mT/mG #270; WT (wild-type): gDNA from WT pig #100809; H₂O: water control. Figure on the right: Liver; Wild-type (WT): gDNA from wild type pig #100809; Negative Control (NC): gDNA from pAdMSC R-26 mT/mG #270; Positive Control (+): gDNA from pAdMSC R-26 mT/mG transfected with iCre recombinase; H₂O: water control, water used as a template.

To confirm the PCR results cryosections were prepared from tissue of all three germ layers of the Vil-rb β G-iCre reporter piglet.

The use of a reporter cell line allowed us to visualize the activity of the Vil-rb β G-iCre construct, since iCre mediates the excision of the floxed mTomato sequence leading to a fluorescence switch from red to green in recombined cells.

Analysis of various tissues below (see Figure 48) revealed that approximately all cells expressed a marker gene, either mTomato or mGFP. In some cells in the lower part of the gut, kidney, liver and stomach mTomato and mGFP was co-expressed.

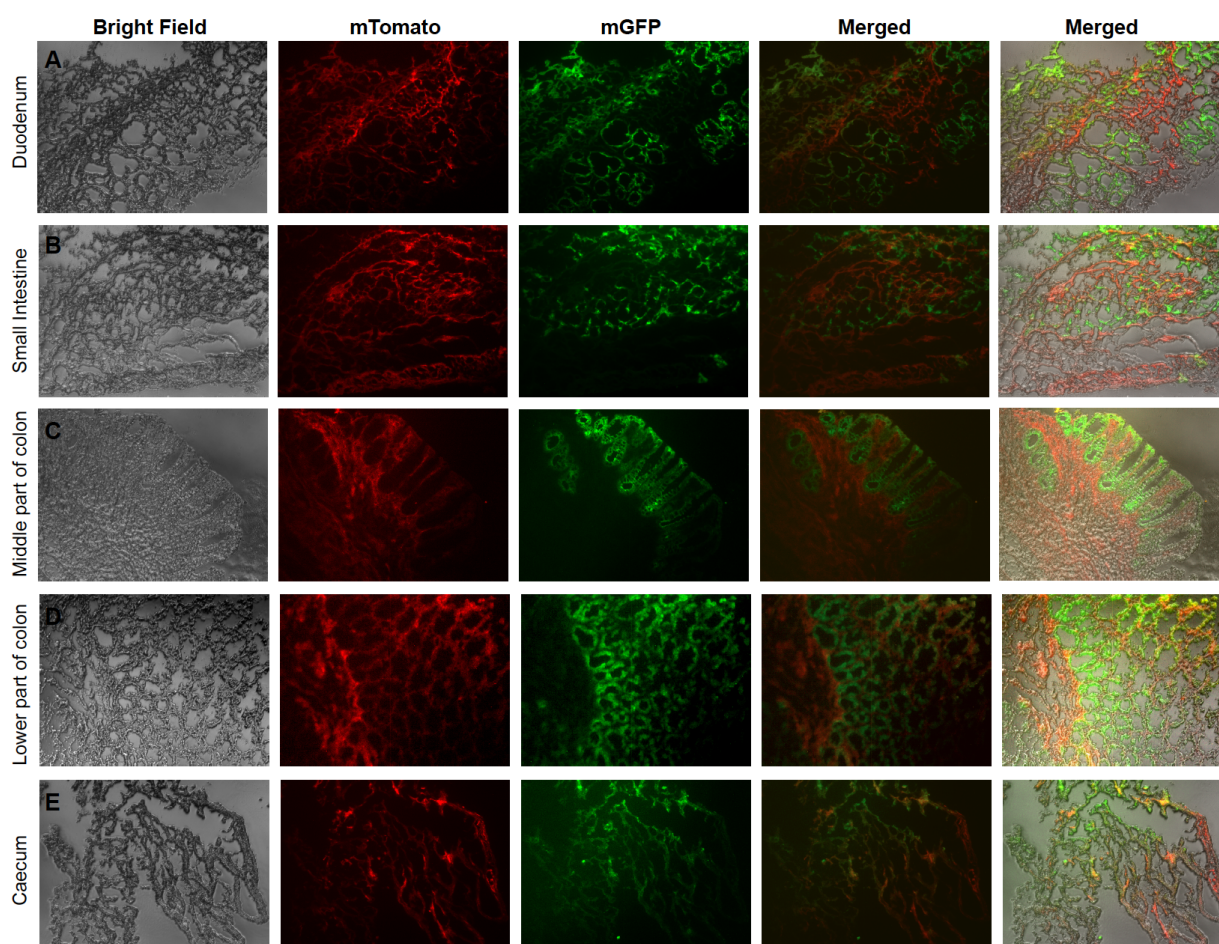


Figure 48: Fluorescence microscopy of gut cryosections from stillborn Villin-rb β G-icre reporter piglet, with villin expression observed in the epithelium.

Five tissue sections are shown here, four (A, B, D and E) were sliced across the long axes of the crypts and (C) sliced parallel to the long axes. All sections from gut tissues show mTomato as well as mGFP fluorescence. These findings indicate that the VIL-1 promoter directs colon-specific iCre expression, the cells express mTomato before iCre recombination and green fluorescent protein after iCre-mediated excision. Gut sections were divided into: duodenum (A); small intestine (B); middle part of colon (C); lower part of colon (D) and caecum (E). Merged: mTomato and mGFP superposed or bright field, mTomato and mGFP superposed. Slice cut at 5 μ m. Magnification of 10x.

Abbreviations: mTomato (membrane-targeted tandem dimer Tomato); mGFP (membrane-targeted green fluorescent protein).

The results in Figure 48 (A-E) shows frozen gut sections of the mucosa of duodenum, small intestine, middle and lower part of colon and caecum, respectively. In all these tissue sections examined mGFP fluorescence was visible in the epithelial cells of the crypts. These findings indicate that the VIL-1 promoter directs gut-specific expression of iCre *in vivo* in the pig.

Our results are in agreement with those of Maunoury *et al.* (1992) who reported that the villin-1 promoter has a specific activity in the epithelial cell lineages of the digestive and uro-genital tracts. As a tissue-specific actin-binding protein of the brush border, villin-1 is mainly expressed in epithelial cells (Kerneis *et al.*, 1996).

In Figure 48, panel/row C, the tissue section was sliced parallel to the long axes of the crypts, and a distinct mucosa structure is shown. No excision of the floxed mTomato is detectable in

the *lamina propria* (lamina that supports the epithelium) and the *lamina muscularis* (thin layer of smooth muscle that separates the *lamina propria* from the submucosa) since all cells are red. In contrast green cells are visible in the *lamina epithelialis*.

Additional cryosections were prepared from pancreas, kidney, stomach and liver tissues (Figure 49). These tissues were verified for the excision of the floxed mTomato cassette by PCR amplification.

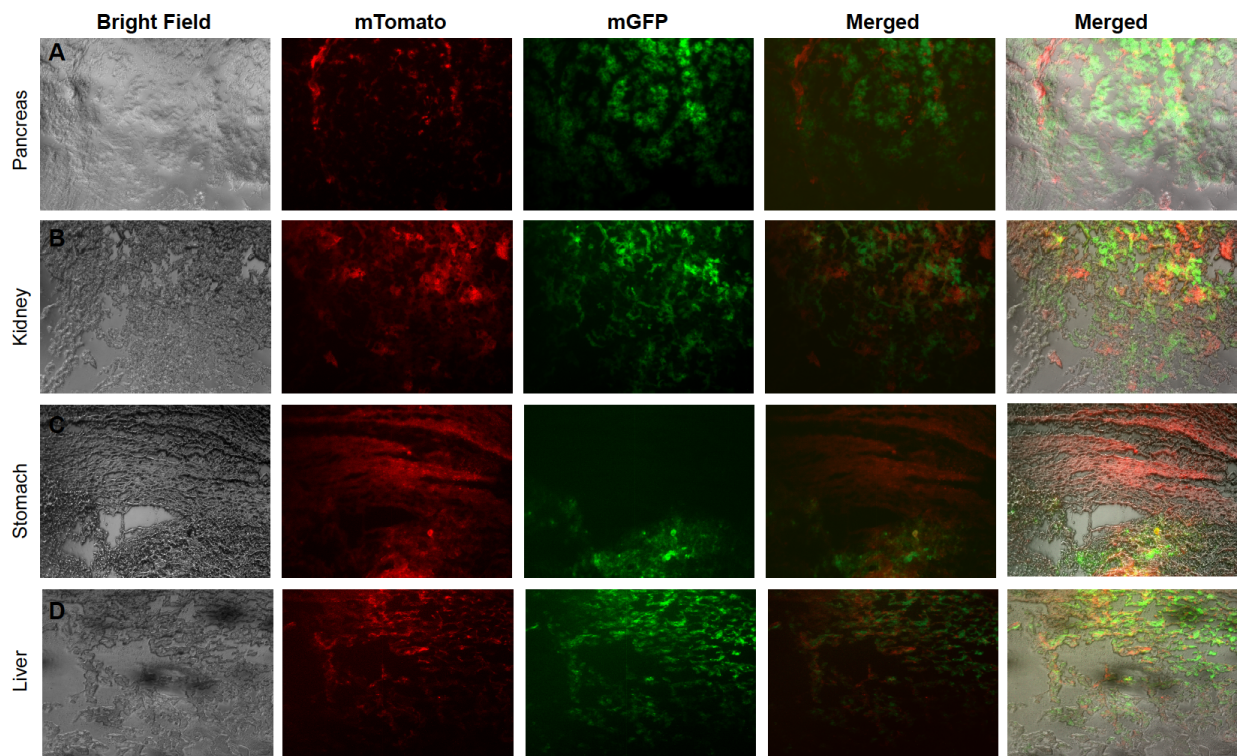


Figure 49: Fluorescence microscopy of pancreas, kidney, stomach and liver cryosections from stillborn Villin-rb β G-icre reporter piglet.

Positive tissues for VIL-1 expression: the cells express mTomato before iCre recombination and green fluorescent protein after iCre-mediated excision. Tissues cryosection were divided into: pancreas (A); kidney (B); stomach (C) and liver (D). Merged: mTomato and mGFP superposed or bright field, mTomato and mGFP superposed. Slice cut at 5 μ m. Magnification of 10x.

Abbreviations: mTomato (membrane-targeted tandem dimer Tomato); mGFP (membrane-targeted green fluorescent protein).

As shown in Figure 49 (A, B, C and D), mGFP protein expression was also evident in some cells of pancreas, kidney, stomach and liver tissues upon iCre-mediated recombination. These results are consistent with Robine *et al.* (1985), Maunoury *et al.* (1992), Pinto *et al.* (1999), Qiao *et al.* (2007) and Braunstein *et al.* (2002), who detected villin-1 expression in some of the epithelial cells of the above-mentioned tissues in mouse.

To confirm that no villin expression was detectable in additional tissues images were taken from other endodermal tissues, as well as ectodermal and mesodermal origin (Figure 50 and 51, respectively).

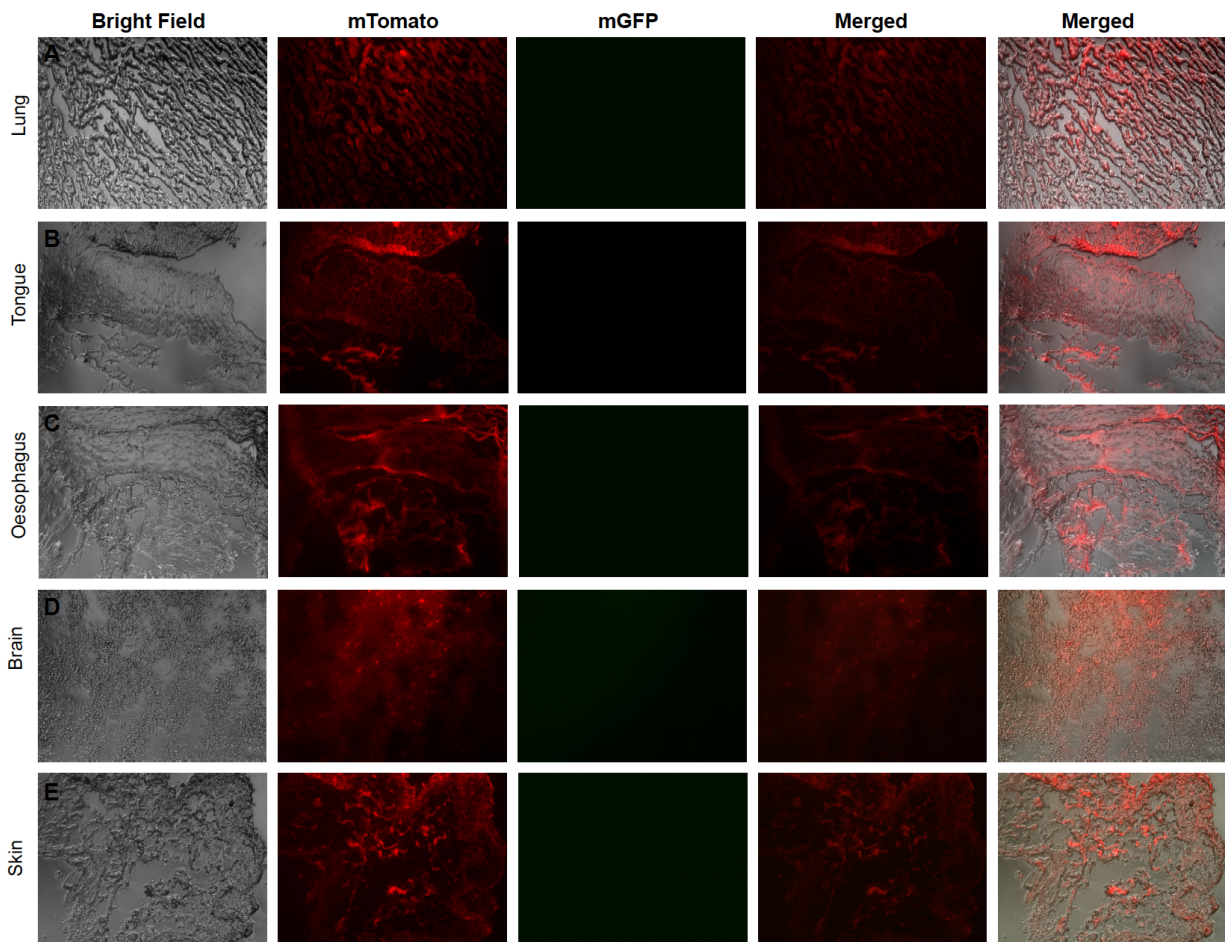


Figure 50: Fluorescence microscopy of ectodermal and endodermal tissues cryosections from stillborn Villin-rb β G-icre reporter piglet.

Prior to iCre-mediated recombination the cells express mTomato. Here, no recombination occurred then only the mTomato fluorescent protein was visible. Tissue cryosections were divided into: lung (A); tongue (B); oesophagus (C); brain (D) and skin (E). Merged: mTomato and mGFP superposed or bright field, mTomato and mGFP superposed. Slice cut at 5 μ m. Magnification of 10x.

Abbreviations: mTomato (membrane-targeted tandem dimer Tomato); mGFP (membrane-targeted green fluorescent protein).

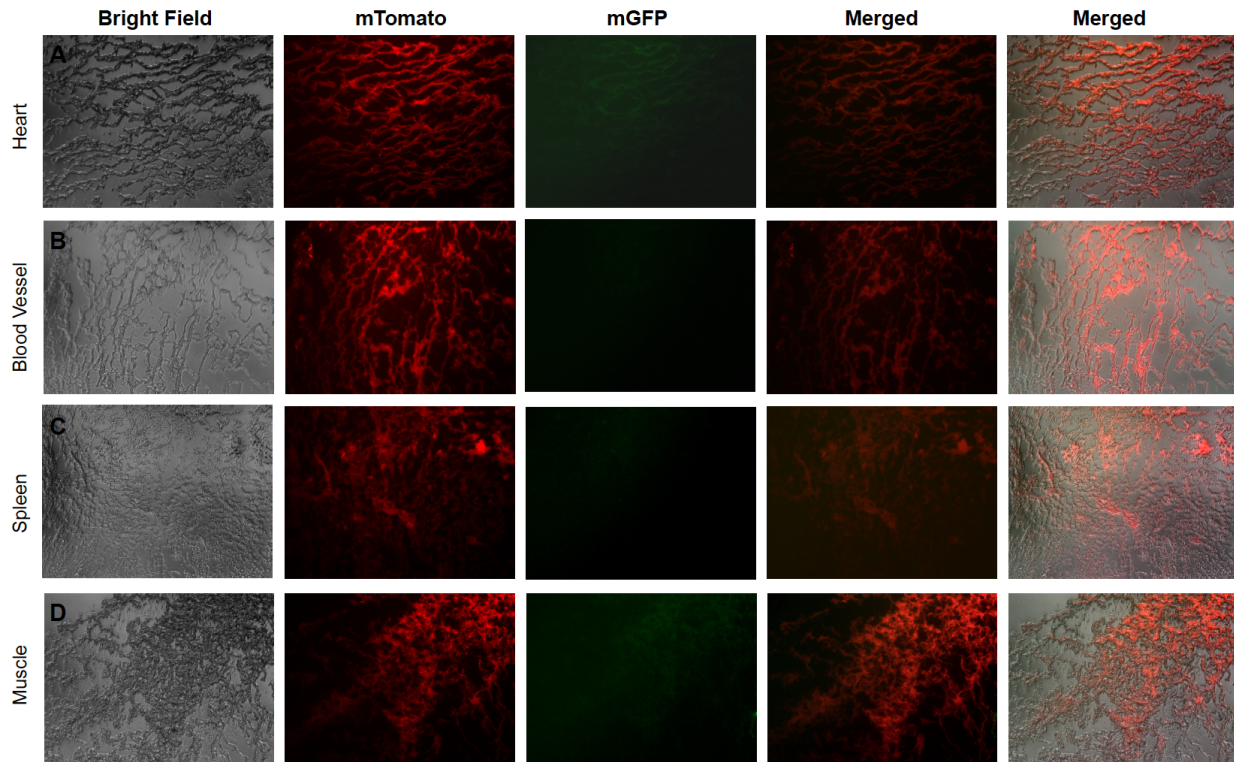


Figure 51: Fluorescence microscopy of mesodermal tissues cryosections from stillborn Villin-rb β G-icre report piglet.

Prior to iCre-mediated recombination the cells express mTomato and after recombination they express mGFP. Here, in heart and muscle green fluorescent protein was visible, but no green fluorescence was visible in spleen nor in blood vessel. Tissue cryosections were divided into: heart (A); blood vessel (B); spleen (C) and muscle (D). Merged: mTomato and mGFP superposed or bright field, mTomato and mGFP superposed. Slice cut at 5 μ m. Magnification of 10x.

Abbreviations: mTomato (membrane-targeted tandem dimer Tomato); mGFP (membrane-targeted green fluorescent protein).

Figure 50 and 51 show that no detectable mGFP fluorescence protein is visible in frozen tissue sections from lung, tongue, oesophagus, brain, skin, spleen and blood vessels specimen. These findings are consistent with previous PCR results. In contrast, mGFP fluorescent protein was weakly expressed in heart and muscle tissues (Figure 51). These results disagree with those obtained by PCR amplification and also by Pinto *et al.* (1999).

Thus, in order to investigate if the mGFP fluorescent protein detection from muscle and heart could be attributed to tissue background (auto-fluorescence), cryosections from those tissues were prepared from a wild-type pig (Figure 52).

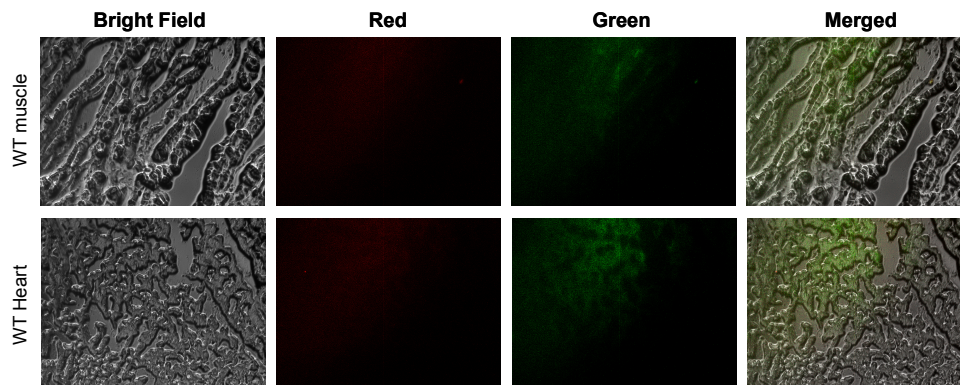


Figure 52: Fluorescence microscopy of heart and muscle cryosections from wild-type non fluorescent pig. Here, using the same conditions for fluorescence microscopy muscle and heart tissues showed auto-fluorescence. Merged: bright field, red and green fluorescence superposed. Slice cut at 5 μm . Magnification of 10x.

Figure 52 shows that a weak red and green fluorescence was seen in both muscle and heart samples analyzed from the wild-type pig.

Collectively, these findings show that the villin promoter is a suitable promoter to express iCre in the colon. Analysis of the stillborn vil-rb β G-iCre reporter piglet demonstrated that the iCre activity was only detectable in the intended tissues (gut, kidney, pancreas, distal stomach and liver).

To generate live pigs, pKDNF cells from the stillborn reporter piglet were isolated and denoted as pKDNF#191015 (Vil-rb β G-iCre reporter cells). These primary kidney fibroblasts consisted of red and green cells, as the villin promoter was shown to be active in cells of the kidney proximal tubules (Figure 49 - cryosections). A serial dilution was carried out to derive only red, un-recombined primary kidney fibroblasts that are suitable for NT. A pool of several red single cell clones was sent for SCNT. Again one non-viable animal was born. Due to this result no further NT experiments were carried out with these cells. In addition, further rounds of nuclear transfer were carried out with new pools from Vil-rb β G-iCre cells or Vil-rb β G-iCre reporter cell clones. One pregnancy was established and two Villin stillborn piglets were obtained. In both stillborn piglets colons mucosal edema and haemorrhage was detected, as well as failure in intestinal crypts formation (personal communication with Dr. Tatiana Flisikowska). It is well known that Cre has cell toxicity when it is expressed at high levels (Sharma and Zu, 2014) which presumably was the case in the porcine experiment described here.

Once a healthy Villin-iCre piglet will be born these founder animals can be mated with APC¹³¹¹/KRAS^{G12D} targeted animals. Transgenic offsprings with the desired genotype will allow to model the Cre progression in pigs.

3.7 *In vitro* inducible Cre expression

In order to induce tumours in adult tissues and to circumvent embryonic lethality, developmental abnormalities during embryo development, or short life expectancy after birth, as observed in this work, conditional expression systems that control Cre expression temporally can be used (Politi and Pao, 2011; Higashi *et al.*, 2009). To allow temporal control of Cre activity, tamoxifen-inducible Cre recombinases, Cre-ERT² and ER^{T2}-Cre-ER^{T2}, which are fusion proteins between Cre recombinase and a triple mutated ligand binding domain (LBD) of the human estrogen receptor (ER), were tested *in vitro* (Feil *et al.*, 1997; Rawlins and Perl, 2012). This triple mutation of the human ER LBD (G400V/L539A/ L540A) prevents binding of the estrogen receptor to its natural ligand, but it confers high affinity to the synthetic estrogen antagonist, 4-hydroxy-tamoxifen (4-OHT), enabling this drug to be used to induce Cre activation (Indra *et al.*, 1999).

3.7.1 Comparison of pSV40-βG-Cre-ERT² with pPGK-Cre-ERT² vector

To investigate the functionality of inducible Cre expression *in vitro*, double fluorescent reporter cells were used. In a first attempt, the functionality of the tamoxifen inducible Cre recombinase vector (pSV40-βG-Cre-ERT²), previously generated at our group, was investigated in mouse reporter cells. Therefore, NIH-3T3 mT/mG cells were co-transfected with pSV40-βG-Cre-ERT² (see Figure 53) and pL452-BS vectors carrying BS gene (for positive selection).



Figure 53: Structure of the SV40-βG-Cre-ERT2 construct.

Expression of the Cre-ERT² fusion protein is driven by the SV40 promoter fused with the β-globin intron. The Cre recombinase is fused to a cDNA encoding a mutated human ER LBD and polyadenylation site (polyA) from the SV40 (simian virus 40 early).

After co-transfection and selection the survived colonies were plated, pooled and induced 24h later, using 100nM of 4-OHT. The 4-OHT concentration was chosen according with Feil *et al.* (1997) and Hayashi and McMahon (2002). Figure 54 shows mGFP fluorescence at 72 hours post 4-OHT induction.

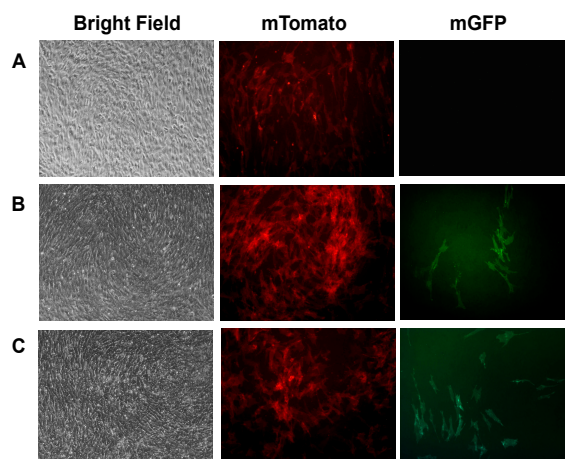


Figure 54: Functionality of the pSV40- β G-Cre-ERT² vector in NIH-3T3 mT/mG cells.

Illustration of untreated NIH-3T3_mT/mG cells or co-transfected with pSV40- β G-Cre-ERT² and pL452-BS vectors. After 4-OHT induction and Cre-mediated recombination the mTomato cassette should be excised and the cells switch from red to green fluorescence. Here, the co-transfected cells without 4-OHT induction showed a leaky effect. (A) Negative control: untreated pKDNF R26-mT/mG cells; (B) Negative control: transfected cells but without 4-OHT induction; (C) co-transfected cells 72 hours post 4-OHT induction (100nM). Magnification of 10x.

As illustrated in Figure 54 (B) the transfected cells showed mGFP expression in the absence of 4-OHT administration. This leaky effect was also observed in mice by Feil *et al.* (1997) using a similar SV40- β G-intron-Cre-ERT² construct and by Hayashi and McMahon (2002) also applying a similar construct (CAG- β G-intron-Cre-ERT²). Others have described that early versions of Cre-ERT² when expressed from a strong promoter are leaky (Rawlins and Perl, 2012). The authors suggested, that a weaker promoter could have low or even no leaky activity. Accordingly, the pSV40- β G-Cre-ERT² vector was modified to place the Cre gene under the control of the weaker mouse phosphoglycerate kinase 1 (PGK) promoter (Qin *et al.*, 2010).

3.7.2 pPGK-Cre-ERT² vector construction and leakiness test

To test if a weaker promoter will prevent the background from the Cre recombinase activity in the absence of 4-OHT, the Cre-ERT² fusion gene was placed downstream of the weaker PGK promoter. The Cre-ERT² coding sequence, isolated as an *EcoRI* and *SacI* restriction fragment from the pSV40- β G-Cre-ERT² vector, was placed under the control of the PGK promoter (see appendix section for cloning details). A schematic diagram of the final plasmid is presented in Figure 55.



Figure 55: Structure of pPGK-Cre-ERT² vector.

The pPGK-Cre-ERT² construct contains a Kozak consensus sequence and a SV40 Large T-antigen NLS in front of the start ATG in Cre. Here, the PGK promoter drives expression of 4-OHT-inducible Cre. Abbreviations: NLS (Nuclear Localization Signal); CMV polyA (cytomegalovirus polyadenylation signal).

Subsequently, to evaluate the leakiness potential of the pPGK-Cre-ER^{T2} vector mouse NIH-3T3 mT/mG reporter cells were used. Thus, the mouse cells were co-transfected using pPGK-Cre-ER^{T2} vector and pL452-BS vector (for positive selection) and induced with 100nM of 4-OHT. Figure 56 shows mGFP expression 72 h post 4-OHT induction.

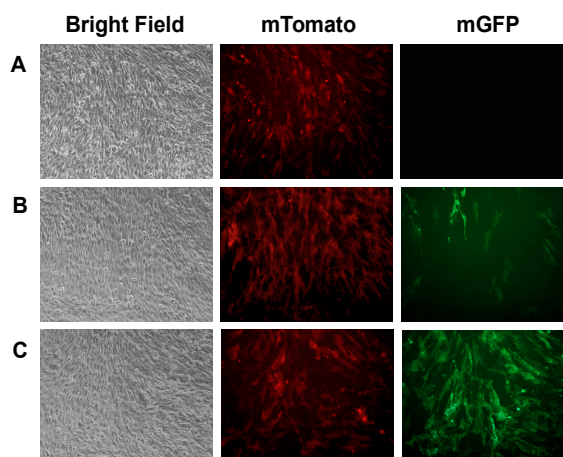


Figure 56: Test of leakiness effect of the pPGK-Cre-ERT2 construct in mouse reporter cells.

Untreated NIH-3T3 mT/mG cells or co-transfected cells with pPGK-Cre-ER^{T2} and pL452-BS vectors. After 4-OHT induction and Cre-mediated recombination the mTomato cassette should be excised and the cells switch from red to green fluorescence. Here, the co-transfected cells without 4-OHT induction showed a leaky effect. (A) Negative control: untreated NIH-3T3 mT/mG cells; (B) Negative control: transfected cells but without 4-OHT induction; (C) co-transfected cells 72 hours post 4-OHT induction (100nM). Magnification of 10x.

Figure 56 shows that even using the weaker PGK promoter Cre recombination also occurred in the absence of the ligand. Zhang *et al.* (1996) suggested that the leaky activity of Cre may be due to a cleavage of Cre and the ligand binding domain by intracellular proteases. To overcome this problem, they and others designed a Cre enzyme carrying a ligand binding domain of the human estrogen receptor at both of its termini.

3.7.3 Generation of Cre recombinase with two 4-OHT binding domains and functionality test in reporter cells

To obtain a Cre-ER system that does not undergo cytoplasmic translocation of Cre-ER^{T2} in the absence of 4-OHT induction, the PGK-Cre-ER^{T2} vector was modified by introducing another ER^{T2} at the N-termini of Cre coding sequence. The N-termini of ER^{T2} sequence was amplified by PCR and further required 5 cloning steps (see appendix for detailed procedure). The structure of the final construct, designated as pPGK-ER^{T2}-Cre-ER^{T2}, can be seen in Figure 57.

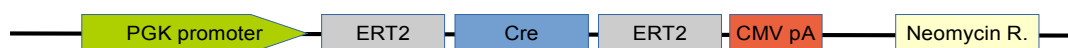


Figure 57: Structure of the PGK-ERT²-Cre-ERT² construct.

The Cre recombinase is fused to a cDNA encoding a mutated human ER LBD at both of its termini. The first ER LBD contains a Kozak consensus sequence, the second ER LBD is followed by a polyadenylation site (pA) from the CMV (human cytomegalovirus). The PGK promoter drives expression of ER^{T2}-Cre-ER^{T2} sequence. Abbreviation: CMV pA (human cytomegalovirus polyadenylation site).

To observe the effect of the Cre-ER^{T2} system in primary porcine cells after construction the pPGK-Cre-ER^{T2} vector was first used to test the better dose-dependent excision induced by 4-OHT. For that, primary porcine kidney cells derived from a transgenic porcine line (R26-mT/mG reporter) were transfected and induced with 1nM, 10nM, 100nM and 1 μ M of 4-OHT, respectively. One to five days post 4-OHT induction, cells were monitored for mGFP fluorescence expression. At all five visualized points (24, 72, 96, 120 and 144 hours) cells expressed mGFP. Nevertheless, using higher concentration of 4-OHT (1 μ M) did not improve Cre activity. On the contrary, the cells did not survive longer than 24 hours with 1 μ M of 4-OHT (data not shown). Using 1nM to 100nM of 4-OHT no toxicity was observed each day post 4-OHT administration. Cellular proliferation and morphology was similar to untreated control, where no 4-OHT was added. It was also apparent that induction with 100nM 4-OHT was more effective in inducing Cre recombination than 10nM or 1nM in all observed days (data not shown). These results are in accordance with those from Feil *et al.* (1997) and Hayashi and McMahon (2002).

In order to compare leakiness of the improved tamoxifen-inducible Cre, pPGK-ER^{T2}-Cre-ER^{T2} with those of the pPGK-Cre-ER^{T2} construct, porcine, mouse, human and rat reporter cells were transfected with these constructs. As positive control, cells were transfected with the constitutive active PGK-Cre vector. Two days after transfection, cells were induced with 100nM of 4-OHT. Figure 58 shows mGFP expression at 96 hours post-induction of porcine pKDNF R26-mT/mG and human SW-480 mT/mG. The results from mouse NIH-3T3 mT/mG and rat EAF mT/mG reporter cells are in Figure 59 (in appendix).

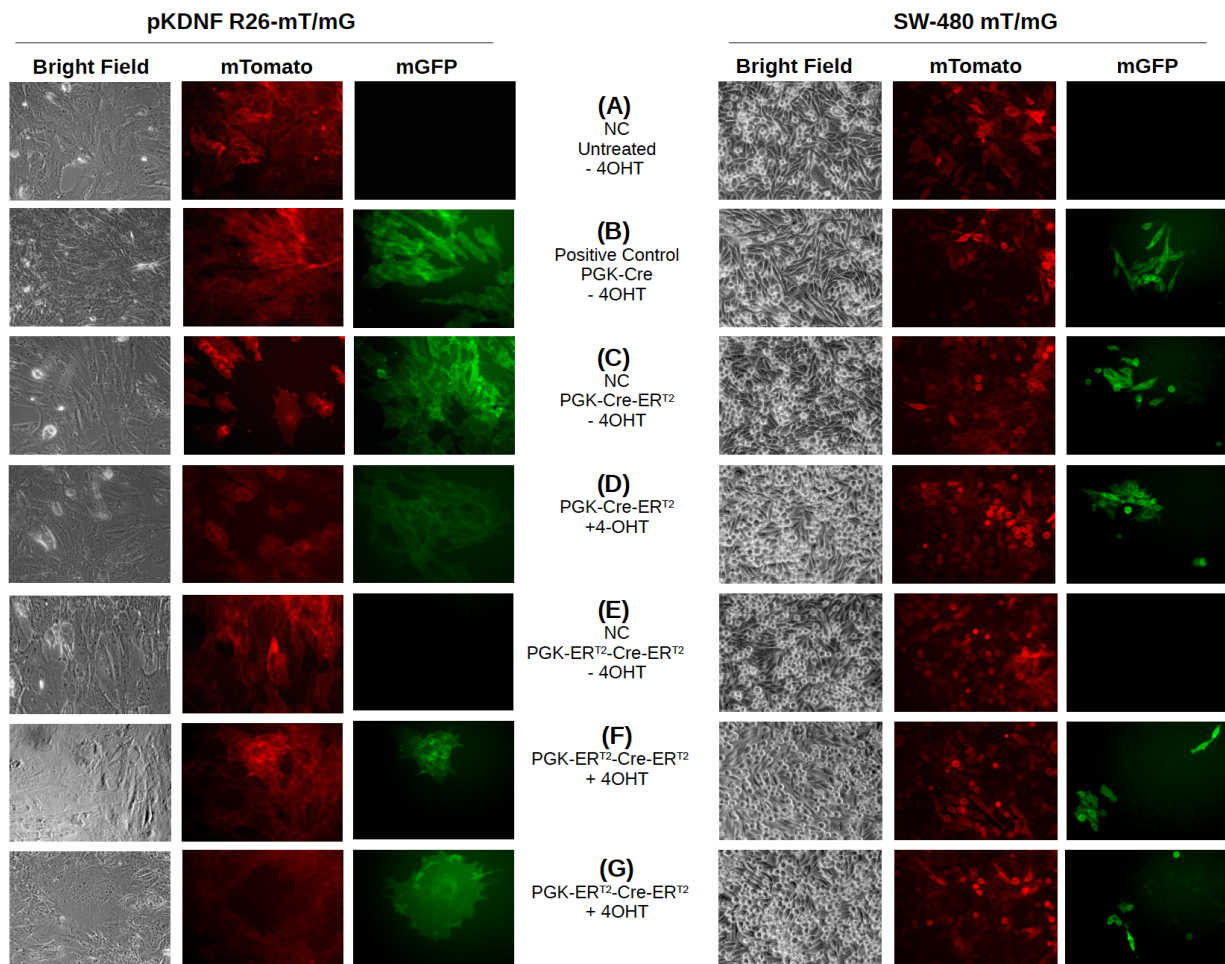


Figure 58: Functionality test of the pPGK-ERT²-Cre-ERT² and Cre-mediated recombination comparison between pPGK-Cre, pPGK-Cre-ERT² and PGK-ERT²-Cre-ERT² using porcine and human reporter cells.

The reporter cells used were: porcine KDNF and human SW-480 reporter cells. The cells express mTomato before 4-OHT induction, but after 4-OHT induction and Cre excision of the floxed mTomato sequence they express mGFP. Here, the pPGK-Cre-ERT² construct is leaky, and mGFP expression without 4-OHT induction was showed. In the other hand, the pPGK-ERT²-Cre-ERT² showed no background in the absence of the inducing agent. (A) Negative control: untreated cells; (B) positive control: transfected cells with pPGK-Cre; (C) transfected cells with pPGK-Cre-ERT² without 4-OHT induction; (D) transfected cells with PGK-Cre-ERT² and addition of 100nM of 4-OHT; (E): transfected cells with pPGK-ERT²-Cre-ERT² without 4-OHT induction; (F and G) transfected cells with pPGK-ERT²-Cre-ERT² and addition of 100nM of 4-OHT. Magnification of 20x.

In Figure 58 and in Figure 59 (see appendix section), similar GFP expression levels were detected in all cells transfected with pPGK-Cre-ER^{T2} without 4-OHT (Figure 58-C above and 59-C in appendix) and Cre alone (Figure 58-B above and 59-B in appendix), indicating leakiness of the Cre-ER^{T2} system. In contrast, the expression of ER^{T2}-Cre-ER^{T2} is strictly 4-OHT dependent, with no evidence of recombination in absence of the ligand (Figure 58-E above and 59-E in appendix). This construct is therefore suitable to control the Cre activity in a temporal manner and to regulate gene expression in the porcine cancer models.

4 Discussion

Regulation of gene expression by spatial and/or temporal control through conditional Cre activity using the Cre//oxP system is a powerful tool for analysing gene function. Also, in tumour research, to study the molecular mechanisms that drive tumorigenesis, as well as to provide animal models as a preclinical platform for new therapies and drug testing. This methodology, along with gene targeting techniques through homologous recombination (HR) allows precise targeted insertion of genetic information (Lai and Lien, 1999), enabling knock-in, conditional and inducible knockouts animals to be produced (Tong *et al.*, 2011). In mice, gene targeting to the *Rosa26* locus is widely used to place transgenes where expression can be well-controlled (Nyabi *et al.*, 2009; Perez-Pinera *et al.*, 2012). The disruption of this locus by gene insertion does not have any adverse consequences on mouse viability or cell phenotype (Perez-Pinera *et al.*, 2012). Our group has identified and characterised the porcine *ROSA26* locus, which has similar properties to the murine *Rosa26* locus and serves as a permissive locus for transgene expression (Li S. *et al.*, 2014). Others have also characterized the porcine *ROSA26* locus and, as well as the mouse, rat and human locus, is an ubiquitously expressed gene that has a high homologous recombination efficiency and also supports stable expression (Li *et al.*, 2014).

Targeting a transgene to a known locus by HR has many advantages. Similar levels of expression can be obtained in transgenic animals and the transgene can be inserted as a single copy (Chu *et al.*, 2016), avoiding silencing by methylation (Martienssen, 2003).

Currently the most important method of generating transgenic pigs is somatic cell nuclear transfer using genetically modified primary somatic cells, such as fetal fibroblasts (Niemann and Kues, 2000), or mesenchymal stem cells (Li S. *et al.*, 2014) as nuclear transfer donors. Thus, the DNA sequence can be integrated into the genome of the cells transfected *in vitro* through random integration or into a specific locus by homologous recombination.

4.1 Identification, isolation and characterization of suitable promoters to drive tissue-specific Cre expression in different organs

The utility of animal model systems to study tumorigenesis critically depends on the ability to control gene inactivation or expression in a spatial- and temporal-specific manner. Therefore, it is crucial to identify and characterize tissue-specific promoters to provide proper temporal- and/or spatial-specific gene expression using the Cre//oxP technology.

Complete genome sequences and correct database annotations for functional and repeat sequences for model organisms are crucial information for life science laboratories worldwide. Moreover, the availability of computational tools to analyze this sequence information greatly

facilitates the identification and understanding of transcriptional regulatory sequences that control gene expression (Yandell and Ence, 2012; Charoensawan *et al.*, 2010). Generally the transcriptional regulatory machinery in eukaryotes is very complex, typically a gene contains two different *cis*-acting transcriptional regulatory DNA elements; a promoter (consisting of a core promoter and proximal regulatory elements) and distal regulatory elements (such as enhancers, silencers, insulators, or locus control regions) (Maston *et al.*, 2006). Transcription factors (TFs) are key cellular components that control gene expression, because they recognize and bind proximal and distal regulatory regions on DNA, and the interaction between different TFs, in turn, activates or represses gene transcription (Maston *et al.*, 2006). Furthermore, isolated regulatory sequences are tested *in vitro* and *in vivo* to confirm their functional value in gene expression in various organisms.

4.1.1 Assessment of promoter function *in vitro*

In vitro transcription systems are used to identify DNA-binding proteins and their interactions with other regulatory proteins in mammalian cells (Dignam *et al.*, 1983; Parvin and Sharp, 1993), as well as to identify promoter or inhibitory elements that control transcription (Osborne *et al.*, 1987). Another method is to use the promoter/regulatory region of interest to drive expression of a reporter gene that allows the activity of the promoter to be monitored. Commonly used reporter genes are green fluorescent protein (GFP), which confers green fluorescence in cells when it absorb blue light (Chalfie *et al.*, 1994); luciferase, which catalyzes a reaction with luciferin leading to light production (de Wet *et al.*, 1985); red fluorescent protein from the gene *dsRed* (Matz *et al.*, 1999); improved monomeric red, orange and yellow fluorescent proteins derived from *dsRed* (Shaner *et al.*, 2004); and chloramphenicol acetyltransferase (CAT) (Gorman *et al.*, 1982), which catalyzes the acetylation of chloramphenicol. These have all been successfully used in mammalian cells (Gorman *et al.*, 1982; de Wet *et al.*, 1987; Kain *et al.*, 1995), as well as *in vivo* (Piatkevich *et al.*, 2010, Li S. *et al.*, 2014, Tiffen *et al.*, 2010) for monitoring gene expression in various organisms.

Lung-specific SFTPC promoter

To test the activity of the porcine SFTPC promoter, *Renilla luciferase* was used as a reporter protein and its detection and expression levels in the lung cells were correlated with SFTPC promoter activity. In all cell lines tested (Calu-3, H441 and LCLC cells), *hRluc* expression directed by the simian virus promoter was much higher than SFTPC promoter activity. The SV40 promoter is known to be very strong in many mammalian cells (Quin *et al.*, 2010) and the chimeric intron downstream of the promoter region increases the expression level from the

luciferase cDNA by threefold (Brondyk 1994). Despite the fact that the carcinoma lung cell lines Calu-3, H441 and LCLC cells express SFTPC, the level of reporter expression was relatively low. The activity of the SFTPC promoter depends on *cis*-acting regulatory elements that are critical for SFTPC expression in lung cells (Wert *et al.*, 1993). These can either enhance or repress transcription (Maston *et al.*, 2006).

Because the *in vitro* properties of the carcinoma lung cell lines (Calu-3, H441 and LCLC) do not fully represent the properties of normal lung epithelium, porcine primary alveolar epithelial (pAE) cells were isolated. Although such primary cell cultures can be used to mimic the physiological state of cells *in vivo*, they require suitable growth conditions (e.g. specific cytokines and growth factors) to maintain the characteristics of the tissue of origin. In addition, adult alveolar epithelial type 2 cells do not support as many rounds of cell division *in vitro* as do neonatal cells, and failed to increase in cell number after 24 h in culture, a fact also observed by Clement *et al.* (1990). We observed a similar effect and thus, half of the isolated pAE cells were immortalised and expression of hTERT was confirmed by RT-PCR. However, cell growth was arrested after some cell divisions and loss of SFTPC expression was detected. Clement *et al.* (1990) observed that by producing neonatal rat distal respiratory epithelial cells by transfection with the SV40 TAg (simian virus 40 large tumor antigen), the cells exhibited epithelial cell morphology for only 30-40 passages in culture. Also, lung epithelial cell lines have been generated by expressing SV40 TAg under the control the human SFTPC promoter in the lungs of transgenic mice (Wikenheiser *et al.*, 1993). The authors concluded that the expression of SFTPC can be significantly altered by the environment.

Cultivation of lung alveolar epithelial cells is time-consuming, labor-intensive and expensive (Barkauskas *et al.*, 2013) and does not always succeed (Clement *et al.*, 1990). Additionally, the poor growth rate of distal respiratory epithelial cells *in vitro* possibly contributed to the low efficiency of transfection in my experiments, and thus, could also be a limiting factor for acquiring conclusive data in the dual-reporter assays.

The DNA sequence of the porcine SFTPC promoter used for the dual-luciferase assay was determined and aligned to human and mouse homologs. This revealed no insertion, deletion or point mutations in the region -780 to +1 bp relative to the TSS from the porcine SFTPC promoter. In the regions from -4.4 kb to -780 bp a few point mutation were detected, but these can be also explained by the genetic variation within pig breeds (SanCristobal *et al.*, 2006; Groenen *et al.*, 2012), which cannot account for the low expression levels of *hRluc*.

Although in humans a stretch of 3.7 kb upstream of the TSS of the *SFTPC* gene is sufficient to generate lung specific expression in transgenic mice (Glasser *et al.*, 2000), in pigs 4.4 kb of the lung SFTPC promoter was not sufficient to drive expression of the reporter gene *hRluc* in the lung cells used in this work. In May 2016 the National Center for Biotechnology Information

updated the *SFTPC* gene sequence and the new sequence revealed that the transcription start site is actually located on exon 3, and also an additional transcript containing 8 exons compared to the known transcript with 5 and 6 exons.

Though bioinformatics tools for gene prediction are improving, it is impossible to exclude some annotation inaccuracy that leads to apparent fragmentation of genes, missing exons, retention of non-coding sequences in exons, and merges with neighbouring genes (Drăgan *et al.*, 2016). What is important here is that the porcine *SFTPC* gene sequence available at the beginning of this work in 2012 was different to the predicted sequence now available. This should also be considered in the luciferase assays results, as porcine regulatory regions possibly important for directing *SFTPC* expression were missing. It is known that 5' untranslated regions (5' UTR's) contain elements involved in transcription regulation (Pichon *et al.*, 2012). In addition, 5' UTRs contribute to the regulation of gene expression in cells and tissue types enhancing the expression of some genes (Cenik *et al.*, 2010).

The function of the human and mouse *SFTPC* gene has been well studied *in vitro* and *in vivo*, but functional *cis*-elements necessary to recapitulate expression of the porcine gene *in vivo* have so far not been identified. More testes need to be performed with new constructs containing different combinations of sequences able to drive expression of Cre recombinase in lungs *in vivo*. This situation illustrates the importance of using *in vivo* models to test and define specific regulatory sequences that can recapitulate gene expression, as well as to use the endogenous *SFTPC* gene for generating genetic modifications *in vivo*.

Pancreas-specific PDX-1 promoter

The 5' flanking region of the human PDX-1 promoter comprises the E-box motive and areas I, II and III, as well as the enhancer region in area IV (see Figure 10 for details). These are important control regions for PDX-1 expression in pancreas (both in adult as in developing pancreas). This promoter region was used in this work to drive activity in rat INS-1 cells (PDX-1 expressing cell line).

The dual-luciferase reporter expression results indicated that the human PDX-1 promoter region (spanning the region from -5.5 kb to the TSS with distal enhancer element) is sufficient to drive expression of the *hRluc* reporter gene. This is in accordance with the findings of Wu *et al.* (1997) and Gerrish *et al.* (2004). Wu *et al.* (1997) demonstrated that transgene reporter constructs containing area I, or all three areas were sufficient to drive mouse Pdx-1 expression *in vitro*. Gerrish *et al.* (2004) also used the same reporter assay to compare the activity of area IV of mouse Pdx-1 and concluded that area IV had similar properties as areas I/II, being also related with β -cell-specific activation and potentiated the activity of areas I/II. Others also

detected that area I potentiated the activity of area II, in cell line-based transfection assays (Van Velkinburgh *et al.*, 2005).

4.2 Gene placement and gene stacking at the porcine *ROSA26* gene

The *ROSA26* locus is a safe harbor site for targeting ubiquitous or controlled expression of genes of interest, as the insertion into this locus do not lead to abnormality and do not produce unwanted phenotype (Sadelain *et al.*, 2012). Moreover, this locus can be efficiently targeted, gene-silencing is typically not induced, and it shows broad expression in most cell types tested (Zambrowicz *et al.*, 1997; Kisseberth *et al.*, 1999; Irion *et al.*, 2007, Kong *et al.*, 2014). Since its discovery, many transgenic animals and cell lines have been successfully created and used with moderate and consistent gene expression of the transgene of interest (Zambrowicz *et al.*, 1997; Kisseberth *et al.*, 1999).

4.2.1 Construction of vectors for promoter trap gene targeting

No classical gene targeting procedure using targeted porcine ESC (embryonic stem cells) or iPSC (induced pluripotent stem cells) have been yet established, since definitive fully functional porcine ESC or iPSC have not yet been derived (Ezashi *et al.*, 2012). Thus, in this study, for gene targeting into the porcine *ROSA26* locus using primary somatic cells we used a "promoter trap" strategy. The promoter trap strategy depends on the endogenous promoter of the targeted gene to drive expression of a reporter or drug resistance gene for positive selection (Zambrowicz *et al.*, 1997; Friedel *et al.*, 2005). This helps eliminate non-specific insertions (Zhao *et al.*, 2015), as the expression of the drug resistance gene relies on insertion downstream of the promoter of the targeted gene (Friedrich and Soriano, 1991).

Others have generated promoter trap vectors, in which β -galactosidase, hPAP (human placental alkaline phosphatase) or GFP reporter genes were ubiquitously expressed by the mouse *Rosa26* promoter, when integrated into the first exon (Zambrowicz *et al.*, 1997; Kisseberth *et al.*, 1999). They demonstrated that this locus can be used for marking cells *in vitro*, as well as *in vivo* by directing reporter gene expression to a specific cell type or ubiquitously, depending on the promoter used. Kisseberth *et al.* (1999) also demonstrated the utility of the hPAP and GFP reporter genes for marking donor cells in transplantation studies. Since the identification of the porcine *ROSA26* locus, some authors have targeted a reporter gene into the first intron of the porcine *ROSA26* gene driven by the porcine endogenous *ROSA26* promoter and ubiquitous expression was obtained (Kong *et al.*, 2014; Li *et al.*, 2014, Li S. *et al.*, 2014).

We used two strategies to targeting genes into the porcine *ROSA26* locus. We first applied a traditional homologous recombination-mediated targeting strategy, to generate transgenic pigs carrying tissue-specific promoters driven by Cre recombinase. In addition, to introduce a Cre-dependent double reporter gene into the same porcine *ROSA26* locus sequential targeted gene placement or “gene stacking” was investigated.

To gene target or to retarget the porcine *ROSA26* locus by HR in this study, left and right homology arms were cloned based on the HR strategy used by our group (Li S. *et al.*, 2014 and Fischer *et al.*, 2016). For the gene targeting strategy, as Li S. *et al.* (2014), we used 2.1 kb left and 4.6 kb right homology arms of intron 1 of the porcine *ROSA26* locus, but instead to targeted expression of the *bsr* (blastidicin S resistance gene) selectable marker or the β -geo reporter gene using the endogenous porcine *ROSA26* promoter, targeted expression of the *neo* (neomycin resistance gene) selectable marker was made. Kong *et al.* (2014) used 1.5 kb left and 3.6 kb right arms homologous to intron 1 of the porcine *ROSA26* locus to target a GFP cassette by promoter trap strategy. For the retargeting (gene stacking) strategy in order to re-introduce transgenes into the same porcine *ROSA26* allele, the same 2.1 kb left homology arm and a right homology arm consisting of 5.3 kb of the targeted porcine *ROSA26* locus was used (see Figure 24). Fischer *et al.* (2016) also used gene stacking to place the human CD55 minigene 5' to the HO1 (heme oxygenase 1) cassette into the porcine *ROSA26* locus. Their retargeting vector consisted of 2.2 kb left homology arm and a 5 kb right homology arm. They used the ubiquitously expressed CAG promoter to drive the CD55 minigene.

To accomplish conditional and spatial control of gene expression Cre recombinase can be used under the control of a tissue-specific promoter. Cre/*loxP*-mediated recombination of the gene of interest, occurs only in the specific tissue expressing Cre recombinase. Therefore, pigs carrying a *loxP* flanked selectable marker/stop cassette (in which the *loxP* sites are on the same strand of DNA and in the same orientation) upstream of a conditional mutant allele (such as *APC*¹³¹¹, *KRAS*^{G12D} and/or *TP53*^{R167H}) can be crossed with pigs expressing Cre controlled by tissue-specific promoters to activate a marker such as GFP or a gene carrying a modification of interest such as an oncogenic mutation in the tissue of interest. To avoid undesired inter-locus recombination between *loxP* sites (after crossing animal lines containing *loxP* sites) a modified *lox2272* site was used in these constructs. Both *loxP* and *lox2272* sites are recognized by Cre; however, would not be able to recombine, due to their non-identical core sequences (Sauer, 1996). Only *lox* sites with identical core sequences are able to recombine with each other (Langer *et al.*, 2002). Other mutant versions of *loxP* could be also applied to allow more than one specific recombination event in a single system. In addition, Dre-rox system, another site-specific recombinase system (SSRs) from a P1-like transducing phage D6 isolated from *Salmonella oranienburg* (Sauer and McDermott, 2004), can be used together with the Cre

system, as no recombination between *Dre/loxP* or *Cre/rox* embryos has been detected (Sauer and McDermott, 2004; Anastassiadis *et al.*, 2009). The genes encoding Dre (D6 site-specific DNA recombinase) and Cre recombinases share only 39% sequence similarity (Herrmann *et al.*, 2012). In addition, Flp (another active SSRs) commonly used with Cre for removal of selectable marker genes and for achieving conditional mutagenesis (Tokunaga *et al.*, 2016) has been enhanced to increase its thermostability (Buchholz *et al.*, 1998). This enhanced variant of Flp, called Flpe, exhibited a 4-fold increase in recombinase activity compared with the wild-type Flp recombinase at 37 °C and 10-fold at 40 °C *in vitro* (Rodríguez *et al.*, 2000).

The use of different recombination systems, in combination allow sophisticated genetic modelling strategies and flexibility. They can be used for genome engineering, to generate large inversions, translocations or deletions and also for conditional mutagenesis, as they are completely independent of each other (Anastassiadis *et al.*, 2009; Tokunaga *et al.*, 2016).

4.2.2 Gene placement and targeting efficiency

The mouse and rat *Rosa26* loci can be easily targeted in ESC (embryonic stem cells) or iPSC (induced pluripotent stem cells) (Soriano, 1999; Kobayashi *et al.*, 2012). A human homolog has been identified, but targeting efficiency in human ES cells is lower than in rodent cells (Irion *et al.*, 2007). A targeting efficiency about 2.3% (2 of 88 clones) in human (Irion *et al.*, 2007), 34.7% (8 of 23 clones) in mouse (Soriano, 1999) and 36.6% (26 of 71 clones) in rat (Kobayashi *et al.*, 2012) detected by PCR was obtained by gene targeting in ES cells. The lower targeting frequency could be explained due locus-specific species differences, or technical problems using hESCs and the lack of homologous recombination optimization in these cells (Irion *et al.*, 2007). Also the efficiency of gene targeting in hES cells is extremely low, especially in adherent culture (Tokunaga *et al.*, 2016).

The newly identified and characterized porcine *ROSA26* locus has been targeted using a Cre-dependent reporter gene (Li *et al.*, 2014). The authors showed that the marker gene was ubiquitously expressed in all tissues examined. They and others also demonstrated that the *ROSA26* promoter was able to drive EGFP gene expression in all cell lines tested in a high and stable manner (Kong *et al.*, 2014; Li P. *et al.*, 2014; Li X. *et al.*, 2014). These results are similar to those seen in mice, rats and humans.

The aim of my study was to achieve Cre expression in the pancreas. To this end, a targeting vector carrying Cre recombinase driven by a pancreas-specific promoter, was used to target the porcine *ROSA26* locus in porcine AdMSCs. From 70 clones analysed, 28 clones were positive (40%) by 5' junction PCR. These results are in accordance with previous works obtained in our group. Li S. *et al.* (2014) showed that targeting porcine *ROSA26* in porcine AdMSCs was also

efficient, 48% GCROSA transfectants (β -Geo/mCherry construct, under the control of the endogenous porcine ROSA26 promoter) and 42% TGROSA transfectants (dual fluorochrome cassette under the control of the CAG promoter) identified were correctly targeted by screening PCR. In contrast Kong *et al.* (2014) targeted porcine MSCs and obtained just 0.25 % (1 out of 404) efficiency to targeting GFP, driven by the elongation factor 1a promoter, and 0.58 % (3 out of 516) when Fst (Follistatin), driven by Myostatin promoter, was targeted into the porcine ROSA26 locus by HR. The differences from our results is that these authors used smaller homology arms (1.5 kb 5' short arm and 3.6 kb 3' long arm), and a different site in the locus for the gene targeting. It is known that gene targeting frequency and the length of the 5' and 3' homology arms are strongly correlated (Deng and Capecchi, 1992). An increase in the extent of homology by 2-fold augments the gene targeting frequency by 20-fold (Thomas and Capecchi, 1987).

In the case of retargeting into the porcine ROSA26 locus using R26 reporter pKDNFs, from the first set of experiments with the PDX-1 driving Cre recombinase 5' upstream of mTomato/mGFP cassette construct (for selectable cassette exchange), screening of 31 clones by 5' junction PCR revealed 12 correctly targeted clones (targeting efficiency of 38.7%). The positive clones for the targeting event could not however be used for NT, as the cells stopped dividing after a few passages. Thus, a second and third experiment was conducted and screening of about 30 clones/experiment revealed no additional, correctly targeted clones. Here a longer 3' homology arm was used for the retargeting (5.3 kb instead of 4.6 kb), but did not increase the proportional targeted cell clones.

Fischer *et al.* (2016) carried out serial targeting of the porcine ROSA26 locus to insert multiple xenoprotective transgenes. They first targeted porcine MSCs to place a SV40-driven human HO1 (human heme oxygenase 1) cDNA into porcine ROSA26 locus by HR (with a 5% targeting efficiency) and the cell clones were used for NT. Then in order to retargeted the same locus, they isolated pKDNFs from the live born piglet obtained. The pKDNFs were used for retargeting the human CD55 minigene under the control of the CAG promoter to the HO1 cassette and thus, to exchange the selectable marker. During the gene stacking procedure they obtained a targeting efficiency of 11% and the cells were used for NT generating healthy piglets. All these results suggests that gene targeting/retargeting into the ROSA26 locus is efficient, however due to lack of PDX-Cre R26 retargeting clones for further analysis, only PDX-Cre R26 targeted cell clones were used as a donors for NT.

4.3 *In vivo* characterization of Cre expression in transgenic pigs

4.3.1 Analysis of PDX-Cre targeted piglet

Gene targeting vectors were generated to place the human PDX-1 promoter at the porcine *ROSA26* locus. Cells transfected with the PDX-Cre construct were used twice for nuclear transfer and piglets from two different pregnancies were generated. DNA analysis from both PDX-Cre piglets by PCR and sequencing confirmed the integrity, structure and correct *ROSA26* locus integration of the targeted transgene. Multiple organs from one piglet were collected. Unfortunately, however no Cre expression was detected in pancreas tissue. These results were in contrast to *in vitro* tests (see Figure 18 from results part), which demonstrated that the human PDX-1 promoter is active in INS-1 cells and could efficiently drive expression of the *Rluc* gene. Also, test of the mutated *lox2272* sites demonstrated correct functionality *in vitro*. Cre recombinase was sequenced after gene targeting and no mutations or insertions were detected in the Cre sequence, nor in the essential areas I, II and IV of the PDX-1 promoter (Gerrish *et al.*, 2000). Gerrish *et al.* (2000) tested the human and mouse Pdx-1 promoter and observed in transfected β -cells that pancreatic β cell-selective expression was shown to be controlled by area I or area II, but not area III in both species. Mouse and human Pdx-1 promoter areas, I, II, III share between 78 to 89% homology (Gerrish *et al.*, 2000) and area IV 82% homology (Gerrish *et al.*, 2004). The conserved areas I, II, and IV, could independently direct β -cell-selective reporter gene expression, but also mutually mediate appropriate developmental and adult cell-specific Pdx-1 expression (Gerrish *et al.*, 2004). The sequence approximately -6 kb upstream of the start codon of the *Pdx-1* gene (comprehending regions, I, II and III) showed islet-specific activity in transgenic mice (Melloul *et al.*, 2002). A transgene directed by areas I and II of the mouse Pdx promoter was expressed in β -cells *in vivo* (Wu *et al.*, 1997). Others have directed transgene expression in pancreatic β -cells *in vivo* using the mouse Pdx1 promoter areas I and II or I-III, as well as I-IV (Sharma *et al.* 1997; Gerrish *et al.*, 2004; Gannon *et al.*, 2001). Taken together, these results indicated that the length used in the human PDX-1 promoter to drive expression of Cre recombinase should have been adequate to generate pancreas-specific activity.

It is known that targeting into the porcine *ROSA26* locus does not lead to gene silencing effects (Kong *et al.*, 2014; Li S. *et al.*, 2014; Li *et al.*, 2014 and Fischer *et al.*, 2016), and the porcine *ROSA26* locus protects exogenous constructs from epigenetic silencing (Kong *et al.*, 2014). Also in mouse, human and rat, the *Rosa26* locus is not subject to gene-silencing effects (Kong *et al.*, 2014). Thus in this study gene silencing effect is probably not the cause of lack of expression in pigs. Although, this phenomenon should be further investigated. Cells isolated from the piglets could have been used to verify for selectable cassette expression (neo) by RT-PCR to show the presence of RNA transcribed from the *ROSA26* promoter extending from exon 1

spliced to the *Neomycin* gene.

One important issue to be considered is the Cre-mediated recombination efficiency using the Cre/*loxP* system. Many factors may affect Cre activity, such as the activity of the promoter driving Cre expression (Araki *et al.*, 1997) regulated by the activity of its regulatory elements (Sharma and Zu, 2014), that determine the efficiency of gene modification in a given cell type. Also intra-cellular Cre levels, the number of *loxP* sites in the genome (Cox *et al.*, 2012), as well as epigenetic modifications and DNA looping at the floxed gene (Sharma and Zu, 2014).

The genetic distance between *loxP* sites may also affect Cre recombination efficiency (Zheng *et al.*, 2000), and can be expected to decrease as the distances between the *loxP* sites increased, but in our work the *loxP* sites were only a few kilobases apart, which does not affect Cre deletion efficiency, as demonstrated by Zheng *et al.* (2000). They showed that Cre recombination efficiency was inversely proportional to the genetic distance between 2 and 60 cM (centimorgan) to the *loxP* sites.

The most reasonable explanations for the lack of PDX-1 directed expression failure to undergo Cre-mediated recombination *in vivo* could be the single copy number of the PDX-Cre transgene and the fact that the P1 bacteriophage-derived Cre used was not mammalian-codon optimized (Shimskek *et al.*, 2002). Transgene copy number has a strong influence on transgene expression level (Haruyama *et al.*, 2009; Kong *et al.*, 2009), except when the insertion of a transgene is directly into a transcriptionally inactive region in the genome (Haruyama *et al.*, 2009). However, the exact relationship between the intra-cellular Cre levels and the efficiency of recombination has not been yet established. In addition, the codon-optimized Cre (iCre) exhibits higher activity than regular Cre in mammalian cells, and thus, has been utilized to improve deletion efficiency (Shimskek *et al.*, 2002).

4.3.2 Optimisation and evaluation of vectors for pancreas- and colon-specific expression

Working on the basis that Cre expression and codon optimisation were the cause of failure we generated new constructs containing an improved form of Cre. The iCre is a codon-improved Cre, which also has reduced GpC content in its coding sequence, designed to prevent silencing by DNA methylation, and has been reported to increase the expression efficiency in mouse cells and *in vivo* (Shimskek *et al.*, 2002). Porcine cells isolated from the pR26 dual fluorescent reporter pig (Li S. *et al.*, 2014), as well as human and mouse cells, previously transfected with a vector containing the reporter cassette (CAG mT/mG), were used to investigate iCre/Cre-mediated recombination efficiency. Notably the recombination efficiency in porcine and human cells, measured by FACS, showed more than a 7- and 5-fold increase in GFP expression,

respectively, compared with 2-fold increase in mouse cells, after 48 h post-transfection, using the improved Cre recombinase version. These results are in accordance with those from Shimshek *et al.* (2002), who reported higher recombination activity of iCre compared to that of the prokaryotic Cre using HEK-293 and CV-1 (monkey kidney fibroblast) cell lines. After generating transgenic mice expressing iCre, some of the lines exhibited high iCre expression, and DNA excision was observed in all cells expressing iCre. Hobeika *et al.* (2006) showed that integration of the mammalian-optimised Cre recombinase into the *mb1* locus led to extremely high recombination efficiency (97-99%) of *loxP* sites in the B cell lineage. In addition to using iCre, we chose to include in some constructs (see Figure 37 in results part) a fragment of the rabbit beta-globin (*rbβG*) intron upstream of the iCre recombinase. Intronic sequences can enhance the expression of many genes in eukaryotes by a variety of mechanisms (Haddad-Mashadrizeh *et al.*, 2009) and the *rbβG* intron provides an enhancer element that increases transgene expression (Buchman and Berg, 1988).

To address the issue concerning use of a single copy transgene, we applied random integration, so that several copies of the transgene could randomly integrate. Dual fluorescent reporter cells were transfected with the new pancreas- and colon-specific constructs to generate cell clones that were used in NT. The use of dual-reporter cells facilitate the visualisation of Cre-mediated recombination. A double fluorescent reporter gene system is useful, as the non-recombined cells are also labeled (Muzumdar *et al.*, 2007), as the stop cassette behind mTomato prevents GFP gene expression in the absence of Cre, but when Cre is active GFP expression will be only driven in cells that express Cre.

4.3.3 Analysis of Villin-iCre piglet

A 9 kb region containing the mouse *villin* gene has the necessary regulatory elements to generate enterocyte-specific activity in transgenic mice (Pinto *et al.*, 1999; El Marjou *et al.*, 2004). Pinto *et al.* (1999) generated transgenic mice containing the 9 kb regulatory region, or with shorter regulatory sequences of the mouse villin promoter. They observed that *villin* expression was only restricted to epithelial cells along the crypt-villus axis of the intestine (duodenum, jejunum, ileum, proximal, and distal colon), as well as epithelial cells of the proximal kidney tubules. In addition, β -galactosidase expression using a construct that entirely lacks the first intron was only present in the small intestine of three of four transgenic mice. Thus, the intronic intestine-specific site II (see Figure 8 in results for more details), is able to restrict *in vivo* expression of the reporter gene to epithelial cells along the crypt-villus axis of the small intestine. El Marjou *et al.* (2004) also showed that transgenic mice harbouring either a 9 kb mouse villin-1 promoter fragment containing the same regulatory region achieved gut-specific expression. They generated a transgenic Vill-Cre mouse line that had a single copy of

the transgene, and then bred it with a Cre-responsive mouse Rosa reporter strain. The resulting double transgenic mice showed expression of the reporter gene specifically in the intestinal epithelium.

Therefore, iCre or rb β G-iCre constructs driven by the 9 kb mouse villin-1 promoter were used to transfect dual fluorescent pAdMSCs R26-mT/mG in this study. Analysis of various tissues revealed that nearly all cells expressed either mTomato or mGFP depending on VIL-1 expression. Only a few cells appeared yellow by fluorescent microscopy due to co-expression of mTomato and mGFP in the lower part of the colon, kidney, stomach and liver. This is due to membrane overlap or persistence of the mTomato protein (Muzumbar *et al.*, 2007), as some cells of these tissues have undergone Cre-mediated recombination (based on PCR results). In the intestinal epithelium, as well as in the proximal absorptive tubules of the kidney, mGFP fluorescence outlined the brush border due to villin-1 expression in this membrane structure. The *mTomato* gene deletion in the gut, demonstrated by tissue expression of mGFP, was confirmed by PCR and fluorescence microscopy of tissue cryosections. Cre-mediated recombination was also detected in other tissues where villin-1 is active, such as the kidney, liver, pancreas and antral part of the stomach. These results are consistent with the findings of Robine *et al.* (1985) and Maunoury *et al.* (1992) who detected villin expression at the luminal faces of many epithelial cells in adult mice. These authors observed villin-1 expression in all intestine epithelial cells, pancreas (duct cells), liver (bile ducts) as well as in the kidney (proximal tubules). Despite the lack of an organized brush border, as with the epithelial cells of the small intestine and kidney proximal tubules, these other cells line absorptive surfaces and share a common embryological origin with the cells from the gastrointestinal tract (Maunoury *et al.*, 1988). Pinto *et al.* (1999) used the same 9 kb regulatory region of the mouse *villin* gene and detected villin-1 expression in the kidney (epithelial cells of the proximal tubules). In accordance to our findings Qiao *et al.* (2007) reported rare villin expressing stem/progenitor cells in the pyloric region of the stomach in a villin transgenic mouse. Also Braunstein *et al.* (2002) suggest a possible epithelial compartment boundary between the distal stomach (pyloric antrum) and the intestine, using a villin/ β -galactosidase mouse model. They revealed that intense β -galactosidase staining in the intestinal region gradually decreases into the distal stomach.

Although no *Vil-1* gene expression is present in the heart and muscle, a faint green fluorescence was seen in those tissue samples. This is probably due to auto-fluorescence from the amount of collagen and elastin present in these tissues. Deliolanis *et al.* (2008) used human glioma cells expressing GFP and tdTomato and wild-type non fluorescing cells to serve as a control for tissue and cell auto-fluorescence. They observed that for all wavelengths used, a background signal from the wild-type cells was observed and was attributed to auto-fluorescence. To obtain an accurate fluorescent signal from cryosections from stillborn Villin-

rb β G-icre reporter piglet, it would be necessary to subtract the wild-type auto-fluorescence signal from the mGFP and mTomato fluorescent proteins fluorescence signals. Another way to overcome this problem would be to test the best excitation and emission wavelengths where tissue autofluorescence is significantly lower.

In addition, other piglets were generated using other cell clones derived from the pAdMSCs Villin-rb β G-iCre cells and not from the piglet analysed in this study. Two piglets were positive for villin expression, but unfortunately both were stillborn. Analysis of the colon of both stillborn piglets revealed mucosal edema and haemorrhage, as well as failure of intestinal crypts formation (personal communication with Dr. Tatiana Flisikowska). It is well known that the mammalian genomes contain cryptic (or pseudo) *loxP* sites (Schmidt *et al.*, 2000; Thyagarajan *et al.*, 2000) and the proximity of two cryptic *loxP* sites may have increased the possibility of Cre-mediated recombination (Semprini *et al.*, 2007). Although Cre-mediated recombination between these pseudo-*loxP* sites may occur with low efficiency (Thyagarajan *et al.*, 2000), when a mammalian codon-optimized Cre with a nuclear localization signal is highly expressed, cell toxicity and deletion efficiency is increased and has become a considerable issue (Sharma and Zu, 2014). Therefore, it is assumed that the abnormalities in the gut and distorted crypts formation in both stillborn piglets are probably due to high levels of Cre expression, obtained by random integration, leading to illegitimate DNA recombination in the genome, resulting in deletions or translocations damaging the genome and reducing viability (Schmidt *et al.*, 2000).

In case of random integration, the lack of control over the sites of integration in the genome, variable copy numbers and unpredictable expression levels may affect the phenotype of the animal (Gould *et al.*, 2015). There is also a possibility of disrupting the function of normal genes (Lai and Lien, 1999) and the transgene may be silenced by epigenetic mechanisms (Garrels *et al.*, 2011). In order to overcome these issues, targeting the insertion of transgenes to a defined genomic location by homologous recombination (McCreath *et al.*, 2000), such as the ubiquitously expressed porcine *ROSA26* locus is preferred.

4.4 *In vitro* inducible Cre expression

The use of *Cre//loxP* technology, combined with tissue-specific and inducible systems allows control of genetic modification of transgenic animals to bypass embryonic lethal phenotypes (Nagy 2000) and to mutate or activate tumour suppressor genes as well as oncogenes in a spatial and temporal manner (Deng, 2012). The tamoxifen-inducible Cre-ERT² system has a mutated LBD (ligand binding domain) with 1000-fold lower affinity for its natural ligand (17 β -oestradiol) than that of the wild-type receptor (Danielian *et al.*, 1993), but it has a higher affinity

and consequently activation by a synthetic anti-estrogen, 4-hydroxy-tamoxifen (4-OHT) (Indra *et al.*, 1999).

In this work the SV40 (simian virus 40 early) promoter and the β -globin intron was used to direct expression of Cre-ERT². To determine whether this vector functions effectively as an inducible system, mouse NIH-3T3 double fluorescent reporter mT/mGFP cells were used for the transfection experiments. The transfected cells showed mGFP expression in the absence of 4-OHT administration, also known as “leakiness” of the system. Feil *et al.* (1997) and Hayashi and McMahon (2002) using a similar SV40- β G-intron-Cre-ER^{T2} and CAG- β G-intron-Cre-ER^{T2} construct, respectively, detected a slight “leakiness” in embryonic and adult mice. This effect likely results from the use of strong promoters to drive early versions of Cre-ER^{T2} (Rawlins and Perl, 2012). In addition, the promoters used by those authors and in this work were followed by a β -globin intron, which is commonly used to enhance gene expression. Quin *et al.* (2010) compared six constitutive mammalian promoters to drive ectopic gene expression *in vitro* and *in vivo*. They demonstrated that the CAG promoter was consistently strong in all cell types tested and the SV40 promoter was fairly strong. By contrast, the mouse phosphoglycerate kinase 1 (PGK) promoter was consistently weak in all cell types. Considering that a weaker promoter may have less problems with leakiness, the strong SV40- β G promoter sequence was replaced with the weaker PGK promoter to drive Cre-ER^{T2} recombinase. However, after transfection in mouse NIH-3T3 double fluorescent reporter mT/mGFP cells, we still observed leaky activity of Cre-ER^{T2} without tamoxifen induction. These findings are consistent with those of Zhao (2010), who also observed a leaky effect of Cre-ERT² using a PGK promoter. Zhang *et al.* (1996) suggested that the residual Cre activity could be due to proteolytic cleavage between Cre and the fused ligand binding domain of the ER, resulting in uncontrolled Cre. To overcome this problem, they and others generated a Cre recombinase carrying two 4-OHT binding domains of the triple mutated estrogen receptor one at each end of Cre recombinase (Verrou *et al.*, 1999; Kam *et al.*, 2012; McCarthy *et al.*, 2012). Therefore, to control the Cre enzyme more tightly, the Cre-ER^{T2} system was modified to express a fusion protein in which a LBD of the human estrogen receptor was appended to both ends of the Cre enzyme.

To test the constructed expression vector, pPGK-ER^{T2}-Cre-ER^{T2}, for the induction of Cre activity, and to compare the tightness of this system with the pPGK-Cre-ER^{T2} vector, reporter cells of mouse, rat, human and porcine origin were used in transfection experiments. An enhanced control of gene expression was obtained with the pPGK-ER^{T2}-Cre-ER^{T2} vector in all cell used, as Cre activity was induced only after exposure to tamoxifen. In contrast, the pPGK-Cre-ER^{T2} vector was not strictly dependent on tamoxifen induction, as evidence of recombination in absence of the ligand was already noticed in all cells. A double LBD of the estrogen receptor has been shown to confer tight control with 4-OHT induction in mouse embryonic stem cells

(Verrou *et al.*, 1999), human carcinoma (Hela) cells (Kam *et al.*, 2012) and in transgenic mice (McCarthy *et al.*, 2012). These authors reported that successful induction occurred with 4-OHT treatment, but in the absence of 4-OHT no recombination was detected, indicating that this system is tightly regulated. In addition, Matsuda and Cepko (2007), tested the activities of steroid ligand-regulated forms of Cre (Cre-ER^{T2}, ER^{T2}-Cre and ER^{T2}-Cre-ER^{T2}) *in vivo* in rat retina and *in vitro* using 293T and mouse brain cells (embryonic day 14.5). They co-transfected those cells with Cre vectors, and a vector carrying a cassette in which the CAG promoter directs expression of a floxed GFP gene upstream of a DsRed gene. Cre-ER^{T2} and ER^{T2}-Cre showed very high background activity without 4-OHT. In contrast, in ER^{T2}-Cre-ER^{T2} no detectable recombination activity was observed in absence of the ligand. However, 24 hours after 4-OHT administration, in ER^{T2}-Cre-ER^{T2}, DsRed expression was clearly detectable. This indicates that the ER^{T2}-Cre-ER^{T2} system is tightly regulated. The reason is that the Cre protein fused to a ER mutated ligand binding domain at both of its termini may confer a higher affinity for the heat-shock protein Hsp90 that keeps Cre inactive since it is retained in the cytoplasm (Ristevski, 2005). However when only one ligand binding domain is used, possible degradation of the estrogen receptor generates active Cre lacking the regulatory domain. In contrast, ER^{T2}-Cre-ER^{T2} is still inactive even after losing one regulatory domain (Matsuda and Cepko, 2007). Then, in the presence of tamoxifen, which disrupts the interaction of ER^{T2}-Cre-ER^{T2} and Hsp90, the fusion protein translocates into the nucleus becomes active, and Cre carries out site-specific recombination between flanking *loxP* sites (Zhang *et al.*, 2012).

5 Final remarks and outlook

Cre/loxP technology, combined with tissue-specific promoters and/or inducible systems can be used to induce site-specific recombination, and has been widely used to generate animal models for spatial and/or temporal conditional control of gene expression. Despite the progress made in this project to generate pigs that express Cre recombinase in the gut epithelium, there is still further work to be done in generating pancreas and lung-specific porcine Cre-driver lines.

To achieve consistent and reliable expression of transgenes, it is essential to select appropriate promoters, as well as the transgene integration site. In many species, including pigs, gene targeting to the *ROSA26* locus by homologous recombination is commonly used to achieve ubiquitous and abundant transgene expression. The challenge is to use the porcine *ROSA26* locus to target and locally express Cre recombinase, by utilizing tissue-specific promoters to express Cre. This is preferable to random genomic integration, as disruption of normal gene expression profiles and improper activation of the Cre recombinase can occur. Additionally, the use of porcine somatic cells for SCNT to target transgenes to the *ROSA26* locus by HR is time consuming. Recently, other methods have been developed that facilitate targeted genome modification via double-strand break repair, such as zinc finger nucleases (ZFN), transcription activator-like effector nucleases (Talens) and the clustered regularly interspaced short palindromic repeat (CRISPR)/Cas9 system. Combined with these genetic editing tools, transgenes could be efficiently delivered to the porcine *ROSA26* locus where they can be driven by tissue-specific promoters to achieve a desired expression level of transgene at the *ROSA26* locus. Also, the expression of a tamoxifen-inducible version of Cre driven by a tissue-specific promoter can be used to spatially and temporally controlled site-specific somatic Cre expression in the pig to avoid embryonic lethality or the reduced life expectancy after birth. One limitation of this system is however the lower deletion efficiency in comparison to “normal” Cre. In this way, to improve the deletion efficiency, a possible approach can be the use of the estrogen receptor ligand-binding domain fused to the mammalian optimized Cre recombinase, which exhibits higher activity than regular Cre in mammalian cells.

Furthermore, characterization of tissue-specific Cre-expressing pig strains with dual fluorescent reporter pigs, permits *in vivo* monitoring of Cre-mediated recombination events in different tissues and developmental stages, providing a multipurpose indicator of Cre activity. These lines could be further used and crossed with pigs carrying the latent LSL-*TP53*^{R167H} and/or LSL-*KRAS*^{G12D} mutant alleles to monitor the proliferative status of tumours and tracing them. These multi-transgenic pigs will provide knowledge of important aspects of cancer biology that contributes to tumour initiation, promotion, and progression of different human cancer types, as well as serve as models to improve early diagnosis, tumour detection and intervention and investigating novel therapeutics.

6 Abbreviations

%	percent
°C	Degree Celsius
µg	Microgram
µl	Microliter
µM	Micromolar
µm	Micrometer
APC	Adenomatous polyposis coli
AdMSCs	Adipose-derived mesenchymal stem cells
bFGF	Basic fibroblast growth factor
bp	Base pair
<i>bsr</i>	Blasticidin S-resistance gene
β-globin	Enhancer element
CAG	Chicken beta-actin promoter and cytomegalovirus enhancer element
CAT	Chloramphenicol acetyltransferase
cDNA	Complementary DNA
cm ²	Square centimeter
CO ₂	Carbon dioxide
Cre	Causes recombination
CRISPR	Clustered regularly interspaced short palindromic repeats
ddH ₂ O	Double distilled water
DMEM	Dulbecco's Modified Eagle's Medium
DMSO	Dimethylsulfoxide
DNA	Desoxyribonucleic acid
dNTP	Deoxynucleotide triphosphate
DsRed	Red fluorescent protein cloned from <i>Discosoma coral</i>
<i>dUTP</i>	<i>Desoxyuridin-5'-triphosphate</i>
EDTA	Ethylenediaminetetraacetic acid
<i>E. coli</i>	<i>Escherichia coli</i>
EtOH	Ethanol
FAP	Familial adenomatous polyposis
FCS	Fetal calf serum
FITC	Fluorescein Isothiocyanate
g	Gram
<i>g</i>	Gravitational acceleration
GAPDH	Glyceraldehyde 3-phosphate dehydrogenase

GFP	Green fluorescent protein
G418	Geneticin
HR	Homologous recombination
KDNFs	Porcine kidney fibroblasts
KRAS	Kirsten rat sarcoma viral oncogene homolog
kDa	Kilodalton
L	Liter
MEM	Minimum Essential Medium
Min	Minute
ml	Milliliter
mGFP	membrane-bound form of GFP
mRNA	Messenger RNA
NaCl	Sodium chloride
NaOH	Sodium hydroxide
NaAC	Sodium Acetate
NEAA	Non-essential amino acids
<i>Neo</i>	Neomycin
O/N	Overnight
PBS	Phosphate buffered saline
PCR	Polymerase Chain Reaction
PDX-1	Pancreatic and duodenal homeobox 1 promoter (pancreas-specific)
PE	Phycoerythrin (red protein-pigment)
rpm	Revolutions per minute
RPMI	Roswell Park Memorial Institute medium
RT-PCR	Reverse transcriptase polymerase chain reaction
s	Second
SCNT	Somatic cell nuclear transfer
SDS	Sodium dodecyl sulfate
SFTPC	Surfactant protein C promoter (lung-specific)
SV40	Simian virus 40
TALENs	Transcription activator-like (TAL) effector nucleases
tdTomato/ mTomato	Membrane-targeted tandem dimer Tomato
TP53	Tumour protein 53
UV	Ultraviolet
VIL-1	Villin-1 promoter (colon-specific)
ZFN	Zinc finger nuclease

List of Figures

Figure 1: Advantages of the use of pigs as large animal models of cancer.....	5
Figure 2: Scheme for tissue-specific activation of mutant proto-oncogenes or loss of tumor suppressors in pigs using the Cre/loxP recombination system.....	9
Figure 3: Sequence and organization of the loxP site and binding of Cre subunits to loxP sites.....	10
Figure 4: Schematic Cre/loxP site-specific recombination.....	11
Figure 5: Schematic diagram of lung anatomy and an alveolus showing the terminal bronchiole, alveolar sac, locations of different epithelial cell types and surfactant layer.....	14
Figure 6: Mapping of NF-1 and TTF-1 cis-acting response elements in murine SFTPC promoter sequence.....	16
Figure 7: Architecture of the small intestinal epithelium and villin location in adults.....	19
Figure 8: Schematic representation of the endogenous villin locus and the organization of the sites responsible for tissue-specific control of villin expression.....	20
Figure 9: Simplified scheme of pancreas development and pancreatic islet.....	23
Figure 10: Schematic representation of the endogenous mouse and human PDX-1 locus and the enhancer/promoter regions.....	25
Figure 11: Outline of the Cre/LoxP-inducible systems, containing single or double tamoxifen-binding domains of triple mutated estrogen receptor (ERT2).....	27
Figure 12: SFTPC expression measured by qPCR in human lung cells relative to a transformed murine lung cells known to express SFTPC.....	57
Figure 13: RT-PCR to detect SFTPC expression in porcine cells.....	58
Figure 14: Structures of psL1180_psiCHECK2 and psL1180_psiCHECK2_SFTPC vectors.....	59
Figure 15: Dual luciferase assay to test the functionality of SFTPC promoter in different lung cells.....	60
Figure 16: Schematic representation of the endogenous human PDX-1 locus and its enhancer/promoter regions.....	61
Figure 17: Structure of psL1180 Reverse psiCHECK-2 - hPdx1-Enh vector.....	62
Figure 18: Dual luciferase assay to test the functionality of PDX-1 promoter in INS-1 cells.....	62
Figure 19: Structure of PDX-Cre ROSA26 gene targeting construct.....	63
Figure 20: Structure SFTPC-Cre and PDX-1-Cre ROSA26 gene stacking constructs.....	64
Figure 21: Linearised vectors used for loxP site functionality test.....	64
Figure 22: Functionality test of lox2272 sites using Cre recombinase.....	65
Figure 23: Diagram of gene targeting strategy with PDX-Cre vector before and after homologous recombination (HR).....	66
Figure 24: Diagram of gene stacking strategy with PDX-Cre vector before and after homologous recombination (HR).....	67
Figure 25: Schematic location of primers and RT-PCR identification of PDX-Cre clones targeted at the porcine ROSA26 locus.....	68
Figure 26: Schematic structure of primers and 5' junction PCR of PDX-Cre R26 targeting clones.....	68
Figure 27: Endogenous control as well as 5' and 3' junction PCR of PDX-Cre R26 gene targeted clones.....	69
Figure 28: Southern blot X-ray film analysis from PDX-Cre R26 targeted cell clones.....	70
Figure 29: 5' junction PCR identification of PDX-Cre R26 piglets.....	71
Figure 30: RT-PCR from PDX-Cre R26 piglet for detection of PDX-1 expression in different tissues and pancreas primary cells.....	72
Figure 31: Identification of Cre-mediated recombination between lox2272 sites from PDX-Cre R26 #357 piglet.....	73
Figure 32: Design of the PGK-Cre, PGK-iCre and CAG-iCre constructs.....	75
Figure 33: Activity comparison of improved Cre (PGK-iCre) and bacteriophage P1 Cre (PGK-Cre) recombinases using porcine, mouse, human and rat double reporter cells.....	76
Figure 34: Activity comparison of improved Cre (PGK-iCre) and bacteriophage P1 Cre (PGK-	

Cre) recombinases using porcine, mouse and human double reporter cells.....	77
Figure 35: Quantification of improved Cre (PGK-iCre) and bacteriophage P1 Cre (PGK-Cre) recombinases activity using porcine, mouse and human double reporter cells by FACS.....	77
Figure 36: Schematic representation of the endogenous villin locus and the organization of the sites responsible for tissue-specific control of villin expression, as well as the villin-Cre vector.	78
Figure 37: Schema of colon (villin-1) and pancreas (PDX-1) iCre vectors, with or without the rb β G intron.....	79
Figure 38: RT-PCR to detect villin-1 expression in different human cell lines.....	79
Figure 39: RT-PCR to detect PDX-1 expression in different human and rat cell lines.....	80
Figure 40: Functionality test of villin-1 constructs using Caco-2 mt/mG reporter cells and PDX-1 constructs using HEK-293 mt/mG reporter cells.....	81
Figure 41: Quantification of red and green fluorescence cells by FACS analysis after transfection with villin-1 and PDX-1 constructs using Caco-2 and HEK-293 mt/mG reporter cells.....	82
Figure 42: RT-PCR to detect PDX-1 and villin-1 expression in different primary porcine cells..	83
Figure 43: PDX-1 expression using pAdMSCs and pKDNF R26-mT/mG reporter cells.....	84
Figure 44: Expression test using vectors containing the rb β G intron with or without the PDX-1 promoter in HEK-293 mT/mG cells.....	85
Figure 45: PCR analysis of stillborn Vil-rb β G-iCre piglet.....	87
Figure 46: Schematic overview of the gene targeted R26 mT/mG reporter porcine locus and the primer pair used to detect recombination between the loxP sites.....	88
Figure 47: PCR amplification to detected DNA recombination between the loxP sites of the stillborn Vil-rb β G-iCre reporter piglet.....	89
Figure 48: Fluorescence microscopy of gut cryosections from stillborn Villin-rb β G-icre reporter piglet, with villin expression observed in the epithelium.....	90
Figure 49: Fluorescence microscopy of pancreas, kidney, stomach and liver cryosections from stillborn Villin-rb β G-icre reporter piglet.....	91
Figure 50: Fluorescence microscopy of ectodermal and endodermal tissues cryosections from stillborn Villin-rb β G-icre reporter piglet.....	92
Figure 51: Fluorescence microscopy of mesodermal tissues cryosections from stillborn Villin-rb β G-icre report piglet.....	93
Figure 52: Fluorescence microscopy of heart and muscle cryosections from wild-type non fluorescent pig.....	94
Figure 53: Structure of the SV40- β G-Cre-ERT2construct.....	95
Figure 54: Functionality of the pSV40- β G-Cre-ERT2 vector in NIH-3T3 mT/mG cells.....	96
Figure 55: Structure of pPGK-Cre-ERT2 vector.....	96
Figure 56: Test of leakiness effect of the pPGK-Cre-ERT2 construct in mouse reporter cells....	97
Figure 57: Structure of the PGK-ERT2-Cre-ERT2 construct.....	97
Figure 58: Functionality test of the pPGK-ERT2-Cre-ERT2 and Cre-mediated recombination comparison between pPGK-Cre, pPGK-Cre-ERT2 and PGK-ERT2-Cre-ERT2 using porcine and human reporter cells.....	99
Figure 59: Functionality test of the pPGK-ERT2-Cre-ERT2 and Cre-mediated recombination comparison between pPGK-Cre, pPGK-Cre-ERT2 and PGK-ERT2-Cre-ERT2 using mouse and rat reporter cells.....	139
Figure 60: Localization of the amplified SFTPC promoter fragments and ligation into pJET1.2 cloning vector to generate the pJET1.2_SFTPC vector.....	140
Figure 61: Schematic overview of psL1180_psiCHECK2 and psL1180_psiCHECK2_SFTPC vectors construction.....	141
Figure 62: Schematic overview of the cloning steps to generate the gene targeting psL1180_PDX-Cre_LSL_ROSA vector.....	142
Figure 63: Molecular cloning schematic overview of the steps to generate the pSA-neo-PDX-Cre-R26-mT/mG vector.....	143
Figure 64: Schematic diagram of the cloning steps necessary to create the pSA-neo-SFC-Cre-R26-mT/mG vector.....	144
Figure 65: Schematic overview from molecular cloning steps of pPGK-iCre vector and pAAV-	

CAG-iCre (w/o WPRE) vector.....	145
Figure 66: Schematic diagram of the cloning steps to create the pVillin_iCreSV40pA vector..	146
Figure 67: Schematic overview from molecular cloning steps of the pVillin_rbβG_iCre SV40pA vector.....	147
Figure 68: Schematic overview from molecular cloning steps of the pSL1180_Enh-hPDX-5'exon1_rbβG_iCre SV40pA vector.....	148
Figure 69: Schematic overview from molecular cloning steps of the pSL1180_hPDX-5'exon1_iCreSV40pA vector.....	149
Figure 70: Schematic overview from two molecular cloning steps to generate the pPGK-Cre-ERT2 vector.....	150
Figure 71: Schematic overview from four molecular cloning steps to generate the pPGK-ERT2-Cre-ERT2 vector.....	151
Figure 72: Localisation of the primers used for sequencing of the PDX-Cre #357 pig at the targeted porcine ROSA26 locus.....	152
Figure 73: DNasequence alignment of 3' junction of the of the targeted porcine ROSA26 locus from PDX-Cre pig.....	152
Figure 74: DNA sequence alignment of 5' junction of the of the targeted porcine ROSA26 locus from PDX-Cre pig.....	153
Figure 75: DNA sequence alignment of loxP 2272 (left) of the targeted porcine ROSA26 locus from PDX-Cre pig.....	153
Figure 76: DNA sequence alignment of lox2272 (right) of the targeted porcine ROSA26 locus from PDX-Cre pig.....	153
Figure 77: DNA sequence alignment of Cre (forward) of the targeted porcine ROSA26 locus from PDX-Cre pig.....	154
Figure 78: DNA sequence alignment of Cre (reverse) of the targeted porcine ROSA26 locus from PDX-Cre pig.....	154

List of Tables

Table 1: Wild-type loxP site sequence and mutated lox sequences commonly used for site-specific recombination.....	12
Table 2: Intestinal- and gastrointestinal-specific promoters.....	17
Table 3: Pancreas-specific promoters and Cre driver lines*.....	22
Table 4: Mammalian cell lines.....	33
Table 5: Mammalian primary cells.....	34
Table 6: Strains and genotype of Escherichia coli (E. coli).....	34
Table 7: Oligonucleotides for sequencing.....	35
Table 8: Oligonucleotides for cDNA amplification.....	36
Table 9: Oligonucleotides for gene targeting PCR detection.....	37
Table 10: Oligonucleotides for Cre recombination PCR detection.....	37
Table 11: Oligonucleotides for villin-1 piglet PCR detection.....	37
Table 12: Oligonucleotides for DIG-labeled for Southern Blot.....	37
Table 13: Oligonucleotides for Gibson Assembly.....	37
Table 14: Mammalian cells and culture growth medium.....	40
Table 15: Primary cells, cell lines, plasmid DNA concentration, reagents and programs used for each transfection method.....	44
Table 16: Concentration of G-418 resistance gene used for selection in each cell after transfection.....	45
Table 17: Vectors used for transfection of double reporter fluorescent cells.....	46
Table 18: Components of PCR reactions and cycling conditions.....	51
Table 19: Colony PCR reaction and cycling condition.....	53
Table 20: Components of RT-PCR reactions and cycling conditions using Bio&Sell or SuperScript III RT-PCR.....	53
Table 21: Plasmids used to transfect HEK-293 mT/mG reporter cells.....	84
Table 22: Vil-rb β G-iCre stillborn piglet tissues isolated and its corresponding germ layers.....	88
Table 23: Oligonucleotides for the amplification of the porcine SFTPC 4.4 kb promoter.....	140

7 References

- Adam, S. J., Rund, L. A., Kuzmuk, K. N., Zachary, J. F., Schook, L. B. and Counter, C. M.** 2007. "Genetic Induction of Tumorigenesis in Swine." *Oncogene* 26 (7): 1038–45.
- Afelik, S.** 2006. "Combined Ectopic Expression of Pdx1 and Ptf1a/p48 Results in the Stable Conversion of Posterior Endoderm into Endocrine and Exocrine Pancreatic Tissue." *Genes & Development* 20 (11): 1441–46.
- Albert, H., Dale, E. C., Lee, E. and DW., Ow.** 1995. "Site-Specific Integration of DNA into Wild-Type and Mutant Lox Sites Placed in the Plant Genome." *The Plant Journal* 7 (4): 649–59.
- Anastassiadis, K., J. Fu, C. Patsch, S. Hu, S. Weidlich, K. Duerschke, F. Buchholz, F. Edenhofer, and A. F. Stewart.** 2009. "Dre Recombinase, like Cre, Is a Highly Efficient Site-Specific Recombinase in E. Coli, Mammalian Cells and Mice." *Disease Models & Mechanisms* 2 (9-10): 508–15.
- Anisimov, V. N., Ukraintseva, S. V., and Yashin, A. I.** 2005. "Cancer in Rodents: Does It Tell Us about Cancer in Humans?" *Nature Reviews Cancer* 5 (10): 807–19.
- Araki, K., Imaizumi, T., Okuyama, K., Oike Y., and Yamamura., K.** 1997. "Efficiency of Recombination by Cre Transient Expression in Embryonic Stem Cells- Comparison of Various Promoters." *Journal of Biochemistry* 122: 977–982.
- Araki, K., Okada, Y., Araki, M., and Yamamura K.** 2010. "Comparative Analysis of Right Element Mutant Lox Sites on Recombination Efficiency in Embryonic Stem Cells." *BMC Biotechnology* 10 (1): 1.
- Ashizawa, S., Brunicardi, F. C. and Wang, X.-P.** 2004. "PDX-1 and the Pancreas." *Pancreas* 28 (2): 109–20.
- Auinger, A., U. Helwig, D. Rubin, J. Herrmann, G. Jahreis, M. Pfeuffer, M. de Vrese, et al.** 2010. "Human Intestinal Fatty Acid Binding Protein 2 Expression Is Associated with Fat Intake and Polymorphisms." *Journal of Nutrition* 140 (8): 1411–17.
- Bachurski, C. J., Kelly, S. E., Glasser, S. W., and Currier, T. A.** 1997. "Nuclear Factor I Family Members Regulate the Transcription of Surfactant Protein-C." *Journal of Biological Chemistry* 272 (52): 32759–66.
- Barkauskas, C. E., Cronce, M. J., Rackley, C. R., Bowie, E. J., Keene, D. R., Stripp, B. R., Randell, S. H., et al.** 2013. "Type 2 Alveolar Cells Are Stem Cells in Adult Lung." *Journal of Clinical Investigation* 123 (7): 3025–36.
- Baron, R. M., Choi, A. J. S., Owen, C. A., and Choi, A. M. K.** 2012. "Genetically Manipulated Mouse Models of Lung Disease: Potential and Pitfalls." *AJP: Lung Cellular and Molecular Physiology* 302 (6): L485–97.
- Boggaram, V.** 2009. "Thyroid Transcription Factor-1 (TTF-1/Nkx2.1/TITF1) Gene Regulation in the Lung." *Clinical Science* 116 (1): 27–35.
- Bouchard, M. J., and Schneider, R. J.** 2004. "The Enigmatic X Gene of Hepatitis B Virus". Genetically Manipulated Mouse Models of Lung Disease: Potential and Pitfalls." *Journal of Virology* 78 (23): 12725–12734.

- Branda, C. S., and Dymecki, S. M.** 2004. "Talking about a Revolution: The Impact of Site-Specific Recombinases on Genetic Analyses in Mice." *Developmental Cell* 6 (1): 7–28.
- Braunstein, E. M., Qiao, T. X., Madison, B., Pinson, K., Dunbar, L., and Gumucio, D. L.** 2002. "Villin: A Marker for Development of the Epithelial Pyloric Border." *Developmental Dynamics* 224 (1): 90–102.
- Brembeck, F. H., Moffett, J., Wang, T. C., and Rustgi, A. K.** 2001. "The Keratin 19 Promoter Is Potent for Cell-Specific Targeting of Genes in Transgenic Mice." *Gastroenterology* 120 (7): 1720–28.
- Brondyk, W. H.** 1994. "pCI and pSI Mammalian Expression Vectors." *Promega notes* 49 7–11.
- Buchholz, F., Angrand, P-O., and Stewart, A. F.** 1998. "Improved properties of FLP Recombinase Evolved by Cycling Mutagenesis." *Nature* 393 (7): 657–662.
- Bullock, A. N., and Fersht, A. R.** 2001. "Rescuing the Function of Mutant p53." *Nature Reviews Cancer* 1 (1): 68–76.
- Buchman, A. R., and Berg, P.** 1988 "Comparison of Intron-Dependent and Intron-Independent Gene Expression" *Molecular and Cellular Biology* 8 (10): 4395–4405.
- Benk, C., Derti, A., Mellor, J. C., Berriz, G. F., and Roth, F. P.** 2010. "Genome-Wide Functional Analysis of Human 5'untranslated Region Introns." *Genome Biology* 11 (3): 1.
- Chalfie, M., Tu, Y., Euskirchen, G., Ward, W. W., and Prasher, D. C.** 1994. "Green fluorescent protein as a marker for gene expression." *Science* 263 (5148): 802–5.
- Chandrasena, G., Sunitha, I., Lau, C., Nanthakumar, N. N., and Henning, S., J.** 1992. "Expression of sucrase-isomaltase mRNA along the villus-crypt axis in the rat small intestine." *Cellular and Molecular Biology* 38(3): 243–54.
- Charoensawan, V., D. Wilson, and S. A. Teichmann.** 2010. "Genomic Repertoires of DNA-Binding Transcription Factors across the Tree of Life." *Nucleic Acids Research* 38 (21): 7364–77.
- Chu, V. T., Weber, T., Graf, R., Sommermann, T., Petsch, K., Sack, U., Volchkov, P., Rajewsky, K., and Kühn, R.** 2016. "Efficient Generation of Rosa26 Knock-in Mice Using CRISPR/Cas9 in C57BL/6 Zygotes." *BMC Biotechnology* 16 (1).
- Cirera, S., Nygard, A. B., Jensen, H. E., Skovgaard, K., Boye, M., and Fredholm, M.** 2006. "Molecular Characterization of the Porcine Surfactant, Pulmonary-Associated Protein C Gene". *Genomics* 88: 659–668.
- Clement, A., Campisi, J., Farmer, S. R., and Brody, J. S.** 1990. "Constitutive Expression of Growth-Related mRNAs in Proliferating and Nonproliferating Lung Epithelial Cells in Primary Culture: Evidence for Growth-Dependent Translational Control." *Proceedings of the National Academy of Sciences* 87 (1): 318–22.
- Cox, B. C., Liu, Z., Mellado Lagarde, M. M., and Zuo, J.** 2012. "Conditional Gene Expression in the Mouse Inner Ear Using Cre-loxP." *Journal of the Association for Research in Otolaryngology* 13 (3): 295–322.
- Crawley, S. W., Mooseker, M. S., and Tyska, M. J.** 2014. "Shaping the Intestinal Brush

Border." *The Journal of Cell Biology* 207 (4): 441–51.

Danielian, P. S., R. White, S. A. Hoare, S. E. Fawell, and M. G. Parker. 1993. "Identification of Residues in the Estrogen Receptor That Confer Differential Sensitivity to Estrogen and Hydroxytamoxifen." *Molecular Endocrinology* 7 (2): 232–40.

De Jong, M., and Maina, T. 2010. "Of Mice and Humans: Are They the Same?--Implications in Cancer Translational Research." *Journal of Nuclear Medicine* 51 (4): 501–4.

De Wet, J. R., Wood, K. V., Helinski, D. R., and DeLuca, M. 1985. "Cloning of Firefly Luciferase cDNA and the Expression of Active Luciferase in Escherichia Coli." *Proceedings of the National Academy of Sciences* 82 (23): 7870–73.

De Wet, J. R., Wood, K. V, DeLuca, M., Helinski, D. R., and Subramani, S. 1987. "Firefly Luciferase Gene: Structure and Expression in Mammalian Cells." *Molecular and Cellular Biology* 7 (2): 725–37.

Deliolanis, N. C., Kasmieh, R., Wurdinger, T., Tannous, B. A., Shah, K., and Ntziachristos, V. 2008. "Performance of the Red-Shifted Fluorescent Proteins in Deep-Tissue Molecular Imaging Applications." *Journal of Biomedical Optics* 13 (4): 044008.

Deng, C., and Capecchi, M. R. 1992. "Reexamination of Gene Targeting Frequency as a Function of the Extent of Homology between the Targeting Vector and the Target Locus." *Molecular and Cellular Biology* 12 (8): 3365–71.

Deramautd, T., and Rustgi, A. K. 2005. "Mutant KRAS in the initiation of pancreatic cancer." *Biochimica et Biophysica* 2 (25): 97–101.

Dignam, J. D., Lebovitz, R. M. and Roeder, R. G. 1983. "Accurate Transcription Initiation by RNA Polymerase II in a Soluble Extract from Isolated Mammalian Nuclei." *Nucleic Acids Research* 11 (5): 1475–89.

Eto K., Kaur, V., and Thomas M. K. 2007. "Regulation of pancreas duodenum homeobox-1 expression by early growth response-1". *The Journal of Biological Chemistry* 282 (9): 5973–83.

Efrat, S., Russ, H. A. 2012. "Making b cells from adult tissues." *Trends in Endocrinology Metabolism* 23: 278–285.

El Marjou F., Janssen, K-P., Chang, B. H-J., Li, M., et al.. 2014. "Tissue-Specific and Inducible Cre-Mediated Recombination in the Gut Epithelium." *Genesis* 39: 186–193.

Ezashi, T., Telugu, B., and Rm Roberts. 2012. "Induced Pluripotent Stem Cells from Pigs and Other Ungulate Species: An Alternative to Embryonic Stem Cells?: iPS Cells from Domesticated Ungulates." *Reproduction in Domestic Animals* 47 (August): 92–97.

Feil, R., Jürgen, W., Metzger, D., and Chambon, P. 1997. "Regulation of Cre Recombinase Activity by Mutated Estrogen Receptor Ligand-Binding Domains" *Biochemical and Biophysical Research Communications* 237:752–757.

Feil, R., and Metzger, D. 2007. *Conditional Mutagenesis: An Approach to Disease Models*. Vol. 178. Springer.

Fischer, K., Kraner-Scheiber, S., Petersen, B. Rieblinger, B., et al. 2016. "Efficient Production of Multi-Modified Pigs for Xenotransplantation by 'combineering', Gene Stacking and Gene Editing." *Scientific Reports* 6 (June): 29081.

- Flisikowska, T., Merkl, C., Landmann, M., Eser, S., Rezaei, N., Cui, X., Kurome, M., et al.** 2012. "A Porcine Model of Familial Adenomatous Polyposis." *Gastroenterology* 143 (5): 1173–75.e7. doi:10.1053/j.gastro.2012.07.110.
- Flisikowska, T., Kind, A. and Schnieke.** 2013. "The New Pig on the Block: Modelling Cancer in Pigs." *Transgenic Research* 22 (4): 673–80.
- Flisikowska, T., Kind, A. and Schnieke., A.** 2016. "Pigs as Models of Human Cancers." *Theriogenology* 86 (1): 433–7.
- Freed-Pastor, W. A., and C. Prives.** 2012. "Mutant p53: One Name, Many Proteins." *Genes & Development* 26 (12): 1268–86.
- Friedel, R. H., Plump, A., Lu, X., Spilker, K., Jolicoeur, C., et al.** 2005. "Gene Targeting Using a Promoterless Gene Trap Vector ('targeted Trapping') Is an Efficient Method to Mutate a Large Fraction of Genes." *Proceedings of the National Academy of Sciences of the United States of America* 102 (37): 13188–93.
- Friedrich, G., and Soriano, P.** 1991. "Promoter Traps in Embryonic Stem Cells- a Genetic Screen to Identify, and Mutate Developmental Genes M Mice". *Genes & Development* 5:1513–1523.
- Fuchs, S., Hollins, A., Laue, M., Schaefer, U., et al.** 2003. "Differentiation of Human Alveolar Epithelial Cells in Primary Culture: Morphological Characterization and Synthesis of Caveolin-1 and Surfactant Protein-C." *Cell and Tissue Research* 311 (1): 31–45.
- Fulka, J. Jr., First, N. L., Loi, P., and Moor, R. M.** 1998 "Cloning by somatic cell nuclear transfer." *BioEssays* 20: 847–851.
- Futreal, P. A., Coin, L., Marshall, M., Down, T., Hubbard, T., et al.** 2004. "A Census of Human Cancer Genes." *Nature Reviews Cancer* 4 (3): 177–83.
- Gannon, M.** 2001. "Molecular genetic analysis of diabetes in mice." *Trends in Genetics* 17(10):S23–8.
- Gannon, M., Herrera, P-L., and Wright, C. V. E.** 2000. "Mosaic Cre-Mediated Recombination in Pancreas Using the Pdx-1 Enhancerpromoter." *Genesis* 26:143–144.
- Garrels, W., Mátés, L., Holler, S., Dalda, A., Taylor, U., Petersen, B., et al.** 2011. "Germline Transgenic Pigs by Sleeping Beauty Transposition in Porcine Zygotes and Targeted Integration in the Pig Genome." *PLoS ONE* 6 (8): e23573.
- Gerrish, K., Gannon, M., Shih, D., Henderson, E., Stofell, M., Wright, C. V., and Stein, R.** 2000. "Pancreatic Beta Cell-Specific Transcription of the Pdx-1 Gene. The Role of Conserved Upstream Control Regions and Their Hepatic Nuclear Factor 3beta Sites." *Journal of Biological Chemistry* 275 (5): 3485–92.
- Gerrish, K., Van Velkinburgh, J.C., and Stein. R.** 2004. "Conserved Transcriptional Regulatory Domains of the *pdx-1* Gene." *Molecular Endocrinology* 18 (3): 533–48.
- Gibb, B., Gupta, K., Ghosh, K., Sharp, R., Chen, J., and Van Duyne, G. D.** 2010. "Requirements for Catalysis in the Cre Recombinase Active Site." *Nucleic Acids Research* 38 (17): 5817–32.
- Gibson, D. G., Young, L., Chuang, R-Y., Venter, J. C., Hutchison, C. A., and Smith, H. O.**

2009. "Enzymatic assembly of DNA molecules up to several hundred kilobases." *Nature Methods* 6: 343–345.
- Glasser, S. W., Burhans, M. S., Eszterhas S. K., Bruno, M., D., and Korfhagen T. R.** 2000. "Human SP-C Gene Sequences That Confer Lung Epithelium-Specific Expression in Transgenic Mice." *AJP: Lung Cellular and Molecular Physiology* 278 (5): L933–45.
- Glasser, S. W., Eszterhas S. K., Detmer E. A., Maxfield M. D., and Korfhagen T. R.** 2004. "The Murine SP-C Promoter Directs Type II Cell-Specific Expression in Transgenic Mice." *AJP: Lung Cellular and Molecular Physiology* 288 (4): L625–32.
- Gorman, C. M., Moffat, L. F., and Howard, B. H.** 1982. "Recombinant Genomes Which Express Chloramphenicol Acetyltransferase in Mammalian Cells." *Molecular and Cellular Biology* 2 (9):1044–1051.
- Gould, S. E., Junttila, M. R., and J de Sauvage., F.** 2015. "Translational Value of Mouse Models in Oncology Drug Development." *Nature Medicine* 21 (5): 431–39.
- Gregorieff, A., Clevers, H.** 2005. "Wnt signaling in the intestinal epithelium: From endoderm to cancer". *Genes & development* 19 (8): 877–890.
- Groenen, M. A. M., Archibald, A. L., Uenishi, H., Tuggle, C. K., Takeuchi, Y., et al.** 2012. "Analyses of Pig Genomes Provide Insight into Porcine Demography and Evolution." *Nature* 491 (7424): 393–98.
- Gu, G., Dubauskaite, J., and Melton, D.** 2002. "Direct evidence for the pancreatic lineage-NGN3+cells are islet progenitors and are distinct from duct progenitors." *Development* 129: 2447–2457.
- Gum, J. R., Hicks, J. W., Gillespie, A-M., Carlson, E. J., et al.** 1999. "Goblet Cell-Specific Expression Mediated by the MUC2 Mucin Gene Promoter in the Intestine of Transgenic Mice." *American Journal of Physiology* 276 (3 Pt 1):G666–76.
- Gum J. R., Hicks J. W., Gillespie A. M., Rius J. L., Treseler P. A. , Kogan S. C., et al.** 2001. "Mouse intestinal goblet cells expressing SV40 T antigen directed by the MUC2 mucin gene promoter undergo apoptosis upon migration to the villi." *Cancer Research* 61: 3472–3479.
- Gum, J. R., Hicks, J. W., Crawley, S. C., Yang, S. C., et al.** 2004. "Mice Expressing SV40 T Antigen Directed by the Intestinal Trefoil Factor Promoter Develop Tumors Resembling Human Small Cell Carcinoma of the Colon." *Molecular Cancer Research* 2 (9):504–13.
- Gün, G., and Kues., W. A.** 2014. "Current Progress of Genetically Engineered Pig Models for Biomedical Research." *BioResearch Open Access* 3 (6): 255–64.
- Guo, F., Gopaul D., and Van Duyne, D.** 1997. "Structure of Cre Recombinase Complexed with DNA in a Sitespecific Recombination Synapse." *Nature* 389: 40–46.
- Guz, Y., Montminy, M. R., Stein, R., Leonard, J. et al.** 1995. "Expression of Murine STF-1, a Putative Insulin Gene Transcription Factor, in β Cells of Pancreas, Duodenal Epithelium and Pancreatic Exocrine and Endocrine Progenitors during Ontogeny." *Development* 121:11–18.
- Haddad-Mashadrizeh, A., Zomorodipour, A., Izadpanah, M., Sam, M. R., Ataei, F., Sabouni, F. and Hosseini, S. J.** 2009. "A Systematic Study of the Function of the Human B-Globin Introns on the Expression of the Human Coagulation Factor IX in Cultured Chinese Hamster Ovary Cells." *The Journal of Gene Medicine* 11 (10): 941–50.

- Hammer R.E., Pursel, V. G., Rexroad, C. E. Jr., Wall, R. J., Bolt, D. J., et al.** 1985. "Production of Transgenic Rabbits, Sheep and Pigs by Microinjection." *Nature* 315 (6021): 680–3.
- Harada, N., Tamai, Y., Ishikawa, T-o., Sauer, B., Takaku, K., Oshima, M. and Taketo M.** 1999. "Intestinal polyposis in mice with a dominant stable mutation of the beta-catenin gene." *The EMBO Journal* 18 (21): 5931–5942.
- Haruyama, N., Cho, A., and Kulkarni, A. B.** 2009. "Overview: Engineering Transgenic Constructs and Mice." In *Current Protocols in Cell Biology*, edited by Juan S. Bonifacino, Mary Dasso, Joe B. Harford, Jennifer Lippincott-Schwartz, and Kenneth M. Yamada. Hoboken, NJ, USA: John Wiley & Sons, Inc.
- Hatzis, D., Deiter, G., deMello, D. E., and Floros, J.** 1994. "Human Surfactant Protein-C: Genetic Homogeneity and Expression in RDS; Comparison with Other Species". *Experimental Lung Research* 20 (1): 57–72.
- Hayashi, S., and McMahon, A. P.** 2002. "Efficient Recombination in Diverse Tissues by a Tamoxifen-Inducible Form of Cre: A Tool for Temporally Regulated Gene Activation/Inactivation in the Mouse." *Developmental Biology* 244 (2): 305–18.
- Herrmann, S., T. Siegl, M. Luzhetska, L. Petzke, C. Jilg, E. Welle, A. Erb, P. F. Leadlay, A. Bechthold, and A. Luzhetskyy.** 2012. "Site-Specific Recombination Strategies for Engineering Actinomycete Genomes." *Applied and Environmental Microbiology* 78 (6): 1804–12.
- Herter-Sprue, G. S., Kung, A. L., and Wong, K-K.** 2013. "New Cast for a New Era: Preclinical Cancer Drug Development Revisited." *Journal of Clinical Investigation* 123 (9): 3639–45.
- Heyer, J., Kwong, L. N., Lowe, S. W., and Chin, L.** 2010. "Non-Germline Genetically Engineered Mouse Models for Translational Cancer Research." *Nature Reviews Cancer* 10 (7): 470–80.
- Higashi, A. Y., Ikawa, T., Muramatsu, M., Economides, A. N., Niwa, A., Okuda, T., Murphy, A. J., et al.** 2009. "Direct Hematological Toxicity and Illegitimate Chromosomal Recombination Caused by the Systemic Activation of CreERT2." *The Journal of Immunology* 182 (9): 5633–40.
- Higashimoto, T., Urbinati, F., Perumbeti, A., Jiang, G., Zarzuela, A., et al.** 2007. "The woodchuck hepatitis virus post-transcriptional regulatory element reduces readthrough transcription from retroviral vectors ". *Gene Therapy* 14: 1298–1304
- Hingorani, S.R., Petricoin, E.F., Maitra, A., Rajapakse, V., King, C.** 2003, "Preinvasive and invasive ductal pancreatic cancer and its early detection in the mouse". *Cancer Cell* 4: 437–50.
- Hobeika, E., Thiemann, S., Storch, B., Jumaa, H.,Nielsen, P.J., Pelanda, R., and Reth, M.** 2006. "Testing Gene Function Early in the B Cell Lineage in mb1-Cre Mice." *Proceedings of the National Academy of Sciences* 103 (37): 13789–13794.
- Hoess, R. H., Ziese, M., and Sternberg, N.** 1982. "Site-Specific Recombination- Nucleotide Sequence of the Recombining". *Proceedings of the National Academy of Sciences* 79: 3398–3402.
- Hoess, R. H., Abremski, K.** 1984. "Interaction of the bacteriophage P1 recombinase Cre with the recombining site *loxP*." *Proceedings of the National Academy of Sciences* 81 (4): 1026–9.

- Hoess, R. H., Wierzbicki, A., and Abremski, K.** 1986. "The Role of the *loxP* Spacer Region in PI Site-Specific Recombination." *Nucleic Acids Research* 14 (5): 2287–2300.
- Hofmann, A., Kessler, B., Ewerling, S., Weppert, M., Vogg, B., Ludwig, H., Stojkovic, M., et al.** 2003. "Efficient Transgenesis in Farm Animals by Lentiviral Vectors." *EMBO Reports* 4 (11): 1054–58.
- Hollstein, M., Hergenhahn, M., Yang, Q., Bartsch, H., Wang, Z-Q., Hainaut, P.** 1999. "New approaches to understanding p53 gene tumor mutation spectra." *Mutation Research* 431 (2): 199–209.
- Honig G., Liou, A., Berger, M., German, M. S., and Tecott, L. H.** 2010. "Precise Pattern of Recombination in Serotonergic and Hypothalamic Neurons in a Pdx1-Cre Transgenic Mouse Line." *Journal of Biomedical Science* 17: 82.
- Huynh, A. S., Abrahams, D. F., Torres, M. S., Baldwin, M. K., Gillies, R. J., and Morse, D. L.** 2011. "Development of an Orthotopic Human Pancreatic Cancer Xenograft Model Using Ultrasound Guided Injection of Cells." *PLoS ONE* 6 (5): e20330.
- Indra A. K., Warot X., Brocard J., Bornert J. M., Xiao J. H., Chambon P., and Metzger D.** 1999. "Temporally-Controlled Site-Specific Mutagenesis in the Basal Layer of the Epidermis-Comparison of the Recombinase Activity of the Tamoxifen-Inducible Cre-ER(T) and Cre-ER(T2) Recombinases." *Nucleic Acids Research* 27 (22): 4324–7.
- Irion, S., Luche, H., Gadue, P., Fehling, H. J., Kennedy, M., and Keller, G.** 2007. "Identification and Targeting of the ROSA26 Locus in Human Embryonic Stem Cells." *Nature Biotechnology* 25 (12): 1477–82.
- James P. S., Smith, M. W., Butcher G. W., Brown D., and Lund E. K.** 1986. "Evidence for a possible regulatory gene (Suc-1) controlling sucrase expression in mouse intestine." *Biochemical Genetics* 24 (3-4): 169–81.
- Janssen, K-P., El Marjou, F., Pinto, D., Sastre, X. Rouillard, D., Fouquet, C., Soussi, T., Louvard, D., and Robine S.** 2002. "Targeted Expression of Oncogenic K-Ras in Intestinal Epithelium Causes Spontaneous Tumorigenesis in Mice." *Gastroenterology* 123 (2): 492–504.
- Jany B. H., Gallup, M. W., Yan, P. S., Gum J. R., Kim, Y. S., and Basbaum, C.B.** 1991. "Human Bronchus and Intestine Express the Same Mucin Gene." *Journal of Clinical Investigation* 87(1): 77–82.
- Jemal, A., Siegel, R., Xu, J., Ward, E.** 2010. "Cancer Statistics, 2010." *CA: A Cancer Journal for Clinicians* 60 (5): 277–300.
- Jonsson, J., Carlsson, L., Edlund T., and Edlund H.** 1994. "Insulin-Promoter-Factor 1 Is Required for Pancreas Development in Mice." *Nature* 371 (6498): 606–9.
- Kain, S. R., Adams M., Kondepudi, A., Yang, T. T., Ward, W. W., and Kitts P.** 1995. "Green Fluorescent Protein as a Reporter of Gene Expression and Protein Localization." *Biotechniques* 19 (4): 650–5.
- Kam, M. K. M., Lee, K. Y., Tam, P. K. H., and Lui, V. C. H.** 2012. "Generation of NSE-MerCreMer Transgenic Mice with Tamoxifen Inducible Cre Activity in Neurons." Edited by Cesario V. Borlongan. *PLoS ONE* 7 (5): e35799.

- Kanai, M., Mullen, C., and Podolsky, D. K.** 1998. "Intestinal Trefoil Factor Induces Inactivation of Extracellular Signal-Regulated Protein Kinase in Intestinal Epithelial Cells." *Proceedings of the National Academy of Sciences* 95 (1): 178–182.
- Kelly, S. E., Bachurski, C. J., Burhans, M. S., and Glasser, S. W.** 1996. "Transcription of the Lung-Specific Surfactant Protein C Gene Is Mediated by Thyroid Transcription Factor 1." *Journal of Biological Chemistry* 271 (12): 6881–88.
- Kerbel, R. S.** 2003. "Human tumor xenografts as predictive preclinical models for anticancer drug activity in humans: better than commonly perceived-but they can be improved." *Cancer Biology & Therapy* 2 (4 Suppl 1): S134–9.
- Kerneis, S., Bogdanova, A., Colucci-Guyon, E., Kraehenbuhl, J-P., and Pringault, E.** 1996. "Cytosolic Distribution of Villin in M Cells From Mouse Peyer's Patches Correlates With the Absence of a Brush Border" *Gastroenterology* 110: 515–521.
- Khoor, A., Stahlman, M. T., Gray, M. E., and Whitsett, J. A.** 1994. "Temporal-Spatial Distribution of SP-B and SP-C Proteins and "As in Developing Respiratory Epithelium of Human Lung." *Journal of Histochemistry and Cytochemistry* 42 (9): 1187–99.
- Khurana, S., and George, S. P.** 2008. "Regulation of Cell Structure and Function by Actin-Binding Proteins: Villin's Perspective." *FEBS Letters* 582 (14): 2128–39.
- Kisseberth, W. C., Brettingen, N. T., Lohse, J. K., and Sandgren E. P.** 1999. "Ubiquitous Expression of Marker Transgenes in Mice and Rats." *Developmental Biology* 214 (1): 128-38.
- Kobayashi, T., Kato-Itoh, M., Yamaguchi, T., Tamura, C., Sanbo, M., Hirabayashi, M., and Nakauchi, H.** 2012. "Identification of Rat *Rosa26* Locus Enables Generation of Knock-In Rat Lines Ubiquitously Expressing *tdTomato*." *Stem Cells and Development* 21 (16): 2981–86.
- Kolb A. F.** 2001. "Selection-Marker-Free Modification of the Murine B-Casein Gene Using a lox2722 Site." *Analytical Biochemistry* 290 (2): 260–71.
- Kong, Q., Hai, T., Ma, J., Huang, T., Jiang, D., Xie, B., Wu, M., et al.** 2014. "*Rosa26* Locus Supports Tissue-Specific Promoter Driving Transgene Expression Specifically in Pig." Edited by Leighton R. James. *PLoS ONE* 9 (9): e107945.
- Kong, Q., Wu, M., Huan, Y., Zhang, L., Liu, H., Bou, G., Luo, Y., Mu, Y., and Liu, Z.** 2009. "Transgene Expression Is Associated with Copy Number and Cytomegalovirus Promoter Methylation in Transgenic Pigs." Edited by Joanna Mary Bridger. *PLoS ONE* 4 (8): e6679.
- Korfhagen, T. R., Glasser, S. W., Wert, S. E., Bruno, M. D., Daugherty, C. C., McNeish J. D., Stock, J. L., Potter, S. S., and Whitsett, J. A.** 1990. "Cis-Acting Sequences from a Human Surfactant Protein Gene Confer Pulmonary-Specific Gene Expression in Transgenic mice". *Proceedings of the National Academy of Sciences* 87 (16): 6122–6.
- Kucherlapati, M. H., Nguyen, A. A., Bronson, R. T., and Kucherlapati, R. S.** 2006. "Inactivation of Conditional Rb by Villin-Cre Leads to Aggressive Tumors Outside the Gastrointestinal Tract." *Cancer Research* 66 (7): 3576–83.
- Kuzmuk, K. N., and Schook, L. B.** 2011. "Pigs as a Model for Biomedical Sciences." In *The Genetics of the Pig*, edited by M. F. Rothschild and A. Ruvinsky, 426 2nd Edn.
- Lacroix, B., Kedinger, M., Simon-Assmann, P., and Haffen K.** 1984. "Early Organogenesis of Human Small Intestine- Scanning Electron Microscopy and Brush Border Enzymology." *Gut* 25

(9): 925–30.

Lai, L. W., and Lien, Y. H. 1999. “Homologous Recombination Based Gene Therapy.” *Experimental Nephrology* 7 (1): 11–4.

Langer, S. J., Ghafoori, A. P., Byrd, M., and Leinwand, L. 2002. “A genetic screen identifies novel non-copstible *loxP* sites.” *Nuclei Acids Research* 30 (14): 3067–3077.

Larsson, L.-I., Madsen, O. D., Seraph, P., Jonsson, J., and Edlund, H. 1996. “Pancreatic-Duodenal Homeobox 1 -Role in Gastric Endocrine Patterning.” *Mechanisms of Development* 00 175–184.

Lee, G., and Saito, I. 1998. “Role of Nucleotide Sequences of *loxP* Spacer Region in Cre-Mediated Recombination.” *Gene* 216 (1): 55–65.

Leuchs, S., Saalfrank, A., Merkl, C., Flisikowska, T. Edlinger, M., Durkovic, M., et al. 2012. “Inactivation and Inducible Oncogenic Mutation of p53 in Gene Targeted Pigs”. *PLoS ONE* 7 (10): e43323.

Li, L., Pang, D., Wang, T., Li, Z., Chen, L., Zhang, M., Song, N., et al. 2009. “Production of a Reporter Transgenic Pig for Monitoring Cre Recombinase Activity.” *Biochemical and Biophysical Research Communications* 382 (2): 232–35.

Li, P., Burlak, C., Estrada, J., Cowan, P. J., and Tector, A. J. 2014. “Identification and Cloning of the Porcine *ROSA26* Promoter and Its Role in Transgenesis.” *Transplantation Technology* 2 (1): 1.

Li, S., Flisikowska, T., Kurome, M., Zakhartchenko, V., Kessler, B., Saur, D., Kind, A., Wolf, E., Flisikowski, K., and Schnieke, A. 2014. “Dual Fluorescent Reporter Pig for Cre Recombination: Transgene Placement at the *ROSA26* Locus.” *PLoS ONE* 9 (7): e102455.

Li, S., Edlinger, M., Saalfrank, A., Flisikowski, K., Tschukes, A., Kurome, M., Zakhartchenko, V., Kessler, B., Saur, D., Kind, A., Wolf, E., Schnieke, A., and Flisikowska, T. 2015. “Viable pigs with a conditionally-activated oncogenic *KRAS* mutation”. *Transgenic Research* 24 (3): 509–517.

Li, X., Yang, Y., Bu, L., Guo, X., Tang, C., Song, J., Fan, N., et al. 2014. “*Rosa26*-Targeted Swine Models for Stable Gene over-Expression and Cre-Mediated Lineage Tracing.” *Cell Research* 24: 501–504.

Lunney, J. K. 2007. “Advances in Swine Biomedical Model Genomics.” *International Journal of Biological Sciences* 3 (3): 179–84.

Luo, Y., Lin, L., Bolund, L., Jensen, T. G., and Sørensen, C. B. 2012. “Genetically Modified Pigs for Biomedical Research.” *Journal of Inherited Metabolic Disease* 35 (4): 695–713.

Madison, B. B. 2002. “Cis Elements of the Villin Gene Control Expression in Restricted Domains of the Vertical (Crypt) and Horizontal (Duodenum, Cecum) Axes of the Intestine.” *Journal of Biological Chemistry* 277 (36): 33275–83.

Magnuson, M. A., and Osipovich, A. B. 2013. “Pancreas-Specific Cre Driver Lines and Considerations for Their Prudent Use.” *Cell Metabolism* 18 (1): 9–20.

Maizels, N. 2013. “Genome Engineering with Cre-*loxP*.” *The Journal of Immunology* 191 (1): 5–6.

- Marshak, S., Ben-Shushan, E., Shoshkes M., Havin, L., Cerasi, E., and Melloul, D.** 2001. "Regulatory Elements Involved in Human Pdx-1 Gene Expression." *Diabetes Suppl* 1:S37–8.
- Martienssen, R. A.** 2003 "Maintenance of heterochromatin by RNA interference of tandem repeats." *Nature Genetics* 35 (3): 213–4.
- Maston, G. A., Evans, S. K., and Green, M. R.** 2006. "Transcriptional Regulatory Elements in the Human Genome." *Annual Review of Genomics and Human Genetics* 7 (1): 29–59.
- Matsuda, T., and Cepko, C. L.** 2007. "Controlled Expression of Transgenes Introduced by in vivo Electroporation." *Proceedings of the National Academy of Sciences of the United States of America* 104 (3): 1027–1032.
- Matsunari, H., Kobayahi, T., Watanabe, M., Umeyama, K., et al.** 2014. "Transgenic Pigs with Pancreas-specific Expression of Green Fluorescent Protein." *Journal of Reproduction and Development* 60 (3): 230–237.
- Matz, M. V., Fradkov A. F., Labas, Y. A., Savitsky, A. P., Zraisky, A. G. Markelov, M. L., and Lukyanov, S. A.** 1999. "Fluorescent Proteins from Non bioluminescent Anthozoa Species." *Nature Biotechnology* 17 (10): 969–73.
- Maunoury, R., Robine, S., Pringault, E., Huet, C., Guénet J. L., Gaillard J. A., and Louvard D.** 1988. "Villin Expression in the Visceral Endoderm and in the Gut Anlage during Early Mouse Embryogenesis." *EMBO Journal* 7(11): 3321–9.
- Maunoury, R., Robine, S., Pringault, E., Léonard, N., Gaillard J. A., and Louvard D.** 1992. "Developmental Regulation of Villin Gene Expression in the Epithelial Cell Lineages of Mouse Digestive and Urogenital Tracts." *Development* 115 (3): 717–28.
- McCarthy, J. J., Srikuea, R., Kirby, T. J., Peterson, C. A., and Esser K. A.** 2012. "Inducible Cre transgenic mouse strain for skeletal muscle-specific gene targeting". *Skeletal Muscle* 2:8.
- McCreath, K. J., Howcroft, J., Campbell, K. H., Colman, A., Schnieke, A. E., and Kind, A. J.** 2000. "Production of Gene-Targeted Sheep by Nuclear Transfer from Cultured Somatic Cells." *Nature* 405 (6790): 1066–9.
- Melloul, D., Marshak, S., and Cerasi E.** 2002. "Regulation of Pdx-1 Gene Expression." *Diabetes* 51 (suppl 3): S320–S325.
- Meurens, F., Summerfield, A., Nauwynck, H., Saif, L., and Gerdtts, V.** 2012. "The Pig: A Model for Human Infectious Diseases." *Trends in Microbiology* 20 (1): 50–57.
- Münst B., Patsch C., Edenhofer F.** 2009. "Engineering cell-permeable protein." *Journal of visualized experiments* (34). pii: 1627.
- Muzumdar, M. D., Tasic, B., Miyamichi, K., Li, L. and Luo, L.** 2007. "A Global Double-Fluorescent Cre Reporter Mouse." *Genesis* 45 (9): 593–605.
- Nagy A.** 2000. "Cre Recombinase- the Universal Reagent for Genome Tailoring." *Genesis* 26 (2): 99-109.
- Niemann H., and Kues, W. A.** 2000. "Transgenic Livestock Premises and promises." *Animal Reproduction Science* 60-61: 277-93.
- Nyabi, O., Naessens, M., Haigh, K., Gembarska, A., Goossens, S., Maetens, M., De Clercq,**

- S., et al.** 2009. "Efficient Mouse Transgenesis Using Gateway-Compatible *ROSA26* Locus Targeting Vectors and F1 Hybrid ES Cells." *Nucleic Acids Research* 37 (7): e55–e55.
- Oberdoerffer, P., Otipoby, K. L., Maruyama, M., and Rajewsky, K.** 2003. "Unidirectional Cre-mediated genetic inversion in mice using the mutant loxP pair lox66/lox71". *Nucleic Acids Research* Vol. 31 (22): e140.
- Offield, M. F., Jetton, T. L., Labosky, P. A., Stein, R. W., Magnuson M. A., Hogan, B. L., and Wright, C. V.** 1996. "PDX-1 Is Required for Pancreatic Outgrowth and Differentiation of the Rostral Duodenum." *Development* 122 (3): 983–95.
- Ogata, H., Inoue, N., and Podolsky, D. K.** 1998. "Identification of a Goblet Cell-specific Enhancer Element in the Rat Intestinal Trefoil Factor Gene Promoter Bound by a Goblet Cell Nuclear Protein." *The Journal of Biological Chemistry* 273 (5): 3060–3067.
- Olivier, M., Hollstein, M. and Hainaut, P.** 2010. "TP53 Mutations in Human Cancers: Origins, Consequences, and Clinical Use." *Cold Spring Harbor Perspectives in Biology* 2 (1): a001008–a001008.
- Osborne, T. F., Gil, G., Brown, M. S., Kowal, R. C., and Goldstein, J. L.** 1987. "Identification of Promoter Elements Required for in Vitro Transcription of Hamster 3-Hydroxy-3-Methylglutaryl Coenzyme A Reductase Gene." *Proceedings of the National Academy of Sciences of the United States of America* 84(11): 3614 – 8.
- Ouvrard-Pascaud, A.** 2003. "Conditional Gene Expression in Renal Collecting Duct Epithelial Cells: Use of the Inducible Cre-Lox System." *AJP: Renal Physiology* 286 (1): F180F–187.
- Parvin, J. D., and Sharp, P. A.** 1993. "DNA Topology and a Minimal Set of Basal Factors for Transcription by RNA Polymerase II." *Cell* 73 v(3): v533–40.
- Peitz M., Pfannkuche K., Rajewsky K., Edenhofer F.** 2002. "Ability of the hydrophobic FGF and basic TAT peptides to promote cellular uptake of recombinant Cre recombinase: A tool for efficient genetic engineering of mammalian genomes." *Proceedings of the National Academy of Sciences of the United States of America* 99: 4489–4494.
- Perez-Pinera, P., Ousterout, D. G., Brown, M. T., and Gersbach, C. A.** 2012. "Gene Targeting to the *ROSA26* Locus Directed by Engineered Zinc Finger Nucleases." *Nucleic Acids Research* 40 (8): 3741–52.
- Perl, A.K., Zhang, L., and Whitsett, J. A.** 2009. "Conditional Expression of Genes in the Respiratory Epithelium in Transgenic Mice." *American journal of respiratory cell and molecular biology* 40(1):1–3.
- Pfeifer, A., Brandon, E. P., Kootstra, N., Gage F. H., and Verma, I.** 2001. "Delivery of the Cre Recombinase by a Self-Deleting Lentiviral Vector- Efficient Gene Targeting in Vivo." *Proceedings of the National Academy of Sciences* 98 (20): 11450–5.
- Piatkevich, K. D., Hult, J., Subach, O. M., Wu, B., Abdulla, A., Segall, J. E. and Verkhusha, V. V.** 2010. "Monomeric Red Fluorescent Proteins with a Large Stokes Shift." *Proceedings of the National Academy of Sciences* 107 (12): 5369–74.
- Pichon, X., Wilson, L. A., Stoneley, M., Bastide, A., King, H.A, Somers, J., and Willis A. E.** 2012. "RNA Binding Protein-RNA Element Interactions and the Control of Translation." *Current Protein & Peptide Science* 13 (4): 294–304.

- Pinto, D., Robine, S., Jaisser F., El Marjou, F. E., and Louvard, D.** 1999. "Regulatory Sequences of the Mouse Villin Gene That Efficiently Drive Transgenic Expression in Immature and Differentiated Epithelial Cells of Small and Large Intestines." *Journal of Biological Chemistry* 274 (10): 6476–82.
- Politi, K., and W. Pao.** 2011. "How Genetically Engineered Mouse Tumor Models Provide Insights Into Human Cancers." *Journal of Clinical Oncology* 29 (16): 2273–81.
- Prather, R. S., Lorson, M. Ross, J. W. Whyte, J. J., and Walters, E.** 2013. "Genetically Engineered Pig Models for Human Diseases." *Annual Review of Animal Biosciences* 1 (1): 203–19.
- Pylayeva-Gupta, Y., Grabocka, E., and Bar-Sagi, D.** 2011. "RAS Oncogenes: Weaving a Tumorigenic Web." *Nature Reviews Cancer* 11 (11): 761–74.
- Qiao, X. T., Ziel, J. W., McKimpson, W., Madison, B. B., Todisco, A., et al.** 2007. "Prospective identification of a multi-lineage progenitor in murine stomach epithelium." *Gastroenterology* 136 (6): 1989–1998.
- Qin, J. Y., Zhang, L., Clift, K. L., Hulur, I., Xiang, A. P., Ren, B-Z., and Lahn, B. T.** 2010. "Systematic Comparison of Constitutive Promoters and the Doxycycline-Inducible Promoter." Edited by Immo A. Hansen. *PLoS ONE* 5 (5): e10611.
- Rangarajan, A., and Weinberg, R. A.** 2003. "Comparative Biology of Mouse versus Human Cells- Modelling Human Cancer in Mice." *Nature Reviews Cancer* 3: 952–959.
- Rasmussen, J., 2009.** Lung Picture. Drawn by Julia Rasmussen and release into the public domain. Available at <http://soft-matter.seas.harvard.edu/index.php/User:Julia>. Accessed March 29, 2016.
- Rawlins, E. L., and Perl, A-K.** 2012. "The a'MAZE'ing World of Lung-Specific Transgenic Mice." *American Journal of Respiratory Cell and Molecular Biology* 46 (3): 269–82.
- Richmond, A., and Y. Su.** 2008. "Mouse Xenograft Models vs GEM Models for Human Cancer Therapeutics." *Disease Models and Mechanisms* 1 (2-3): 78–82.
- Ristevski, S.** 2005. "Making better transgenic models: conditional, temporal, and spatial approaches." *Molecular Biotechnology* 29 (2): 153–63.
- Rivlin, N., Brosh, R., Oren, M., and Rotter, V.** 2011. "Mutations in the p53 Tumor Suppressor Gene: Important Milestones at the Various Steps of Tumorigenesis." *Genes & Cancer* 2 (4): 466–74.
- Robine, S., Huet, C., Moll, R., Sahuquillo-Merino, C., Coudrier, E., Zweibaum, A., and Louvard, D.** 1985. "Can Villin Be Used to Identify Malignant and Undifferentiated Normal Digestive Epithelial Cells?" *Proceedings of the National Academy of Sciences* 82: 8488–8492.
- Rodríguez, C. I., Buchholz, F., Galloway, J., Sequerra, R., Kasper, J., Ayala, R., Stewart, F., and Dymecki, M.** 2000 "High-Efficiency Deleter Mice Show That FLPe Is an Alternative to Cre-loxP". *Nature Genetics* 25: 139–140.
- Rogers, C. S.** 2016. "Genetically engineered livestock for biomedical models." *Transgenic Research* 25 (3): 345–359.

- Rose, S. D., Swift, G. H., Peyton, M. J., Hammer, R. E., and MacDonald, R. J.** 2001. "The Role of PTF1-P48 in Pancreatic Acinar Gene Expression." *Journal of Biological Chemistry* 276 (47): 44018–26.
- Sadelain, M., Papapetrou, E. P., and Bushman, F. D.** 2012. "Safe harbours for the integration of new DNA in the human genome." *Nature Reviews Cancer* 12: 51–58.
- SanCristobal, M., Chevalet, C., Haley, C. S., Joosten, R., Rattink, A. P., Harlizius, B., Groenen, M. A. M., et al.** 2006. "Genetic Diversity within and between European Pig Breeds Using Microsatellite Markers." *Animal Genetics* 37 (3): 189–98.
- Sauer, B.** 1996. "Multiplex Cre/lox recombination permits selective site-specific DNA targeting to both a natural and an engineered site in the yeast genome." *Nucleic Acids Research* 24 (23): 4608–4613.
- Sauer, B.** 2002. "Cre lox One More Step in the Taming of the genome" *Endocrine* 19 (3): 221–8.
- Sauer, B.** 2004. "DNA Recombination with a Heterospecific Cre Homolog Identified from Comparison of the Pac-c1 Regions of P1-Related Phages." *Nucleic Acids Research* 32 (20): 6086–95.
- Sauer, B., and McDermott, J.** 2004. "DNA recombination with a heterospecific Cre homolog identified from comparison of the pac-c1 regions of P1-related phages." *Nucleic Acids Research* 32 (20): 6086–95.
- Saunders, A., Johnson, C. A., and Sabatini, B. L.** 2012. "Novel Recombinant Adeno-Associated Viruses for Cre Activated and Inactivated Transgene Expression in Neurons." *Frontiers in Neural Circuits* 6.
- Schellhase, D. E., Emrie, P. A., Fisher, J. H., and Shannon, J. M.** 1989. "Ontogeny of Surfactant Apoproteins in the Rat." *Pediatric Research* 26 (3): 167–74.
- Schmidt, E. E., Taylor, D. S., and Prigge, J. R.** 2000. "Illegitimate Cre-Dependent Chromosome Rearrangements in Transgenic Mouse Spermatids." *Proceedings of the National Academy of Sciences* 97 (25): 13702–13707.
- Schnieke A. E., Kind A. J., Ritchie W. A., Mycock K., Scott A. R., Ritchie M., Wilmut I., Colman A., Campbell K. H.** 1997. "Human Factor IX Transgenic Sheep Produced by Transfer of Nuclei from Transfected Fetal Fibroblasts." *Science* 278 (5346): 2130–3.
- Schook, L. B., Collares, T. V., Hu, W., Liang, Y., Rodrigues, F. M., Rund, L. A., Schachtschneider, K. M., et al.** 2015. "A Genetic Porcine Model of Cancer." *PLOS ONE* 10 (7): e0128864.
- Semprini, S., T.J. Troup, T.J., Kotelevtseva, N., King, K., Davis, J.R.E., Mullins, L.J., Chapman, K.E., Dunbar, D.R. and Mullins, J.J.** 2007. "Cryptic loxP Sites in Mammalian Genomes: Genome-Wide Distribution and Relevance for the Efficiency of BAC/PAC Recombineering Techniques." *Nucleic Acids Research* 35 (5): 1402–10.
- Shaner, N. C., Campbell, R. C., Steinbach, P. A., Giepmans, B. N. G., Palmer, A. E., and Tsien, R. Y.** 2004. "Improved Monomeric Red, Orange and Yellow Fluorescent Proteins Derived from *Discosoma* Sp. Red Fluorescent Protein." *Nature Biotechnology* 22 (12): 1567–72.
- Sharma, S., Leonard, J., Lee S., Chapman, H. D., Leiter, E. H., and Montminy, M. R.** 1996

“Pancreatic Islet Expression of the Homeobox Factor STF-1 Relies on an E-Box Motif That Binds USF.” *Journal of Biological Chemistry* 271 (4): 2294–9.

Sharma, S., Jhala, U. S., Johnson, T., Ferreri, K., Leonard, J., Lee S., and Montminy, M. R. 1997 “Hormonal Regulation of an Islet-Specific Enhancer in the Pancreatic Homeobox Gene STF-1.” *Molecular and Cellular Biology* 17 (5): 2598–2604.

Sharma, S., and Zhu, J. 2014. “Immunologic Applications of Conditional Gene Modification Technology in the Mouse: Conditional Gene Modification Technology.” In *Current Protocols in Immunology* 10.34.1–10.34.13.

Shaw, p., and Clarke, A. R. 2007. “Murine models of intestinal cancer: Recent advances.” *DNA repair* 6: 1403–1412.

Shih, H. P., Wang, A., and Sander M. 2013. “Pancreas Organogenesis: From Lineage Determination to Morphogenesis.” *Annual Review of Cell and Developmental Biology* 29 (1): 81–105.

Shimshek, D. R., Kim, J., Hübner, M. R., Spengel, D. J., Buchholz, F., Casanova, E., Stewart, A. F., Seeburg, P. H., and Sprengel, R. 2002. “Codon-Improved Cre Recombinase (iCre) Expression in the Mouse: Codon-Improved Cre.” *Genesis* 32 (1): 19–26.

Shoura, M. J., Vetcher, A. A., Giovan, S. M., Bardai, F., Bharadwaj, A., Kesinger, M. R., and Levene, S. D. 2012. “Measurements of DNA-Loop Formation via Cre-Mediated Recombination.” *Nucleic Acids Research* 40 (15): 7452–64.

Sieren, J. C., Meyerholz, D. K., Wang, X-J., Davis, B. T., Newell, J. D., and Hammond, E., Rohret, J. A., et al. 2014. “Development and Translational Imaging of a TP53 Porcine Tumorigenesis Model.” *Journal of Clinical Investigation* 124 (9): 4052–66.

Silver, D. P., and Livingston D. M. 2001. “Self-Excising Retroviral Vectors Encoding the Cre Recombinase Overcome Cre-Mediated Cellular Toxicity.” *Molecular Cell* 8 (1): 233–43.

Simon, T.C., Cho, A., Tso, P., and Gordon, J. I. 1993. “Use of transgenic mice to map cis-acting elements in the liver fatty acid-binding protein gene (Fabpl) that regulate its cell lineage-specific, differentiation-dependet, and spatial patterns of expression in the gut epithelium and in the liver acinus.” *Journal of Biological Chemistry* 268: 18345–58.

Smith, D. F., Sullivan, W. P., Marion, T. N., Zaitsu, K., Madden, B., McCormick, D. J., and Toft, D. O. 1993. “Identification of a 60-Kilodalton Stress-Related Protein, p60, Which Interacts with hsp90 and hsp70 and Toft 1993 Hsp90.” *Molecular and Cellular Biology* 13 (2): 869–876.

Singh, G., Singh, J., Katyal, S. L., Brown, W. E., Kramps J. A., Paradis, I. L., Dauber, J. H., Macpherson T. A., and Squeglia, N. 1988. “Identification, Cellular Localization, Isolation, and Characterization of Human Clara Cell-Specific 10 KD Protein.” *Journal of Histochemistry & Cytochemistry* 36 (1): 73–80.

Singh, M., and L. Johnson. 2006. “Using Genetically Engineered Mouse Models of Cancer to Aid Drug Development: An Industry Perspective.” *Clinical Cancer Research* 12 (18): 5312–28.

Soriano, P. 1999. “Generalized lacZ Expression with the ROSA26 Cre Reporter Strain.” *Nature Genetics* 21 (1): 70–1.

Sternberg, N., and Hamilton, D. 1981. “Bacteriophage P1 site-specific recombination: I. Recombination between *loxP* sites.” *Journal of Molecular Biology* 150 (4): 467–486.

- Stewart, S. A., and Weinberg, R. A.** 2000. "Telomerase and human tumorigenesis." *Seminars in Cancer Biology* 10 (6): 399–406.
- Stracci, F.** 2009. "Cancer screening, diagnostic technology evolution, and cancer control." *Methods in Molecular Biology* 471: 107–136.
- Stoffers, D. A., Zinkin, N. T., Stanojevic, V., Clarke, W. L., and Habener, J. F.** 1997. "Pancreatic Agenesis Attributable to a Single Nucleotide Deletion in the Human IPF1 Gene Coding Sequence." *Nature* 15 (1): 106–10.
- Stoffers, D. A., Heller, R. S., Miller, C. P., and Habener, J. F.** 1999. "Developmental Expression of the Homeodomain Protein IDX-1 in Mice Transgenic for an IDX-1 PromoterlacZ Transcriptional Reporter." *Endocrinology* 140 (11): 5374–5381.
- Sweetser, D. A., Hauff, S. M., Hoppe, P. C., Birkenmeier, E. H., and Gordon J.** 1988. "Transgenic Mice Containing Intestinal Fatty Acid-Binding Protein/human Growth Hormone Fusion Genes Exhibit Correct Regional and Cell-Specific Expression of the Reporter Gene in Their Small Intestine.pdf." *Proceedings of the National Academy of Sciences* 85: 9611–9615.
- Swindle, M. M., Makin, A., Herron, A. J., Clubb, F. J., and Frazier, K. S.** 2012. "Swine as Models in Biomedical Research and Toxicology Testing." *Veterinary Pathology* 49 (2): 344–56.
- Thomas, K. R., and Capecchi, M. R.** 1987. "Site-directed mutagenesis by gene targeting in mouse embryo-derived stem cells." *Cell* 51 (3): 503–512.
- Thyagarajan, B., Guimarães, M. J., Groth, A. C., and Calos, M. P.** 2000. "Mammalian Genomes Contain Active Recombinase Recognition Sites." *Gene* 244: 47–54.
- Tiffen, J. C., Bailey, C. G., Ng C., Rasko, J. E., and Holst, J.** 2010. "Luciferase Expression and Bioluminescence Does Not Affect Tumor Cell Growth in Vitro or in Vivo." *Molecular Cancer* 9: 299.
- Tokunaga, A., Anai, H., and Hanada, K.** 2016. "Mechanisms of Gene Targeting in Higher Eukaryotes." *Cellular and Molecular Life Sciences* 73 (3): 523–33.
- Tong, C., Huang, G., Ashton, C., Li, P., and Ying, Q-L.** 2011. "Generating Gene Knockout Rats by Homologous Recombination in Embryonic Stem Cells." *Nature Protocols* 6 (6): 827–44.
- Van Velkinburgh, J. C., Samaras, S. E., Gerrish, K., Artner, I., and Stein, R.** 2005. "Interactions between Areas I and II Direct Pdx-1 Expression Specifically to Islet Cell Types of the Mature and Developing Pancreas." *Journal of Biological Chemistry* 280 (46): 38438–44.
- Verrou, C., Zhang, Y., Zürn, C., Schamel, W. W. A., and Reth, M.** 1999. "Comparison of the Tamoxifen Regulated Chimeric Cre Recombinases MerCreMer and CreMer." *Journal of Biological Chemistry* 380 (12): 1435–1438.
- Vetere, A., Choudhary, A., Burns, S. M., and Wagner, B. K.** 2014. "Targeting the Pancreatic B-Cell to Treat Diabetes." *Nature Reviews Drug Discovery* 13 (4): 278–89.
- Walker, J. M., and Rapley, R.** eds. 2009. *Molecular Biology and Biotechnology*. 5th ed. Cambridge: Royal Society of Chemistry.
- Walrath, J. C., Hawes, J. J., Van Dyke, T., and Reilly, K. M.** 2010. "Genetically Engineered Mouse Models in Cancer Research." In *Advances in Cancer Research* 106: 113–64.

- Wert, S., Glasser, S. W., Korfhagen, T. R., and Whitsett, J.** 1993. "Transcriptional Elements from the Human SP-C Gene Direct Expression in the Primordial Respiratory Epithelium of Transgenic Mice." *Developmental Biology* 156 (2): 426–443.
- Whitelaw, C. B., Radcliffe, P. A., Ritchie, W. A., Carlisle, A., Ellard, F. M., Pena, R. N., Rowe, J., Clark, A. J., King, T. J., and Mitrophanous, K. A.** 2004. "Efficient Generation of Transgenic Pigs Using Equine Infectious Anaemia Virus (EIAV) Derived Vector." *FEBS Letters* 571 (1-3): 233–36.
- Whitsett, J. A., and Glasser, S. W.** 1998. "Regulation of Surfactant Protein Gene Transcription." *Biochimica et Biophysica Acta* 1408 (2-3): 303–311.
- Wiebe, P. O., Kormish, J. D., Roper, V. T., Fujitani, Y., Alston, N. I., Zaret, K. S., Wright, C. V. E., Stein, R. W., and Gannon, M.** 2007. "Ptf1a Binds to and Activates Area III, a Highly Conserved Region of the Pdx1 Promoter That Mediates Early Pancreas-Wide Pdx1 Expression." *Molecular and Cellular Biology* 27 (11): 4093–4104.
- Wikenheiser, K. A., Vorbroker, D. K., Rice, W. R., Clark, J. C., Bachurski, C. J., et al.** 1993. "Production of immortalized distal respiratory epithelial cell lines from surfactant protein C/simian virus 40 large tumor antigen transgenic mice." *Proceedings of the National Academy of Sciences* 90 (12): 11029-11033.
- Will, E., Klump, H., Heffner, N., Schwieger M., Schiedlmeier, B., Ostertag, W., Baum, C., and Stocking, C.** 2002. "Unmodified Cre recombinase crosses the membrane." *Nucleic Acids Research* 30 (12): e59.
- Worthley, D. L.** 2007, "Colorectal carcinogenesis: Road maps to cancer". *World Journal of Gastroenterology*, 13 (28): 3784-3791.
- Wu, G. D., Wang, W., and Traber, P. G.** 1992. "Isolation and Characterization of the Human Sucrase-Isomaltase Gene and Demonstration of Intestine-Specific Transcriptional Element." *The Journal of Biological Chemistry* 267 (11): 7863–7870.
- Wu, K-L., Gannon, M., Peshavaria, M., Offield, M. F., Henderson, E., Ray, M., Marks, A., Gamer, L. W., Wright, C. V. E., and Stein, R.** 1997. "Hepatocyte Nuclear Factor 3beta Is Involved in Pancreatic Beta-Cell-Specific Transcription of the Pdx-1 Gene." *Molecular and Cellular Biology* 17 (10): 6002–6013.
- Yandell, M., and Ence, D.** 2012. "A Beginner's Guide to Eukaryotic Genome Annotation." *Nature Reviews Genetics* 13 (5): 329–42.
- Zambrowicz, B. P., Imamoto, A., Fiering, S., Herzenberg, L. A., Kerr, W. G., and Soriano, P.** 1997. "Disruption of Overlapping Transcripts in the ROSA β geo 26 Gene Trap Strain Leads to Widespread Expression of β -Galactosidase in Mouse Embryos and Hematopoietic Cells." *Proceedings of the National Academy of Sciences* 94 (8): 3789-3794.
- Zhang, Y., Riesterer, C., Ayrall, A-M., Sablitzky, F., Littlewood, T. D., and Reth, M.** 1996. "Inducible site-directed recombination in mouse embryonic stem cells." *Nucleic Acids Research* 24 (4): 543–548.
- Zhang, J., Zhao, J., Jiang, W-j., Shan, X-w., Yang, X-w., and Gao, J-g.** 2012. "Conditional Gene Manipulation: Cre-Ating a New Biological Era." *Journal of Zhejiang University Science* 13 (7): 511–24.
- Zhao, L.H., Y.H. Zhao, H. Liang, T. Yun, X.J. Han, M.L. Zhang, X. Zhou, D.X. Hou, R.F. Li,**

and X.L. Li. 2015. "A Promoter Trap Vector for Knocking out Bovine Myostatin Gene with High Targeting Efficiency." *Genetics and Molecular Research* 14 (1): 2750–61.

Zhao, Z., J. Zuber, E. Diaz-Flores, L. Lintault, S. C. Kogan, K. Shannon, and S. W. Lowe. 2010. "p53 Loss Promotes Acute Myeloid Leukemia by Enabling Aberrant Self-Renewal." *Genes & Development* 24 (13): 1389–1402.

Zheng, E., Sage, M., Sheppard, E. A., Jurecic, V., and Bradley, A. 2000. "Engineering Mouse Chromosomes with Cre-*loxP*- Range, Efficiency, and Somatic Applications." *Molecular Cell Biology* 20 (2): 648–655.

8 Appendix

This chapter gives a detailed description of the construction of all vectors used during this work, as well as cell culture results.

pPGK-ERT²-Cre-ERT² functionality test in reporter cells

The tamoxifen-inducible Cre (ERT²-Cre-ERT²) was tested for Cre-mediated recombination of floxed sequences in the absence/presence of the inducer using mouse NIH-3T3 mT/mG and rat EAF mT/mG reporter cells (see Figure 59).

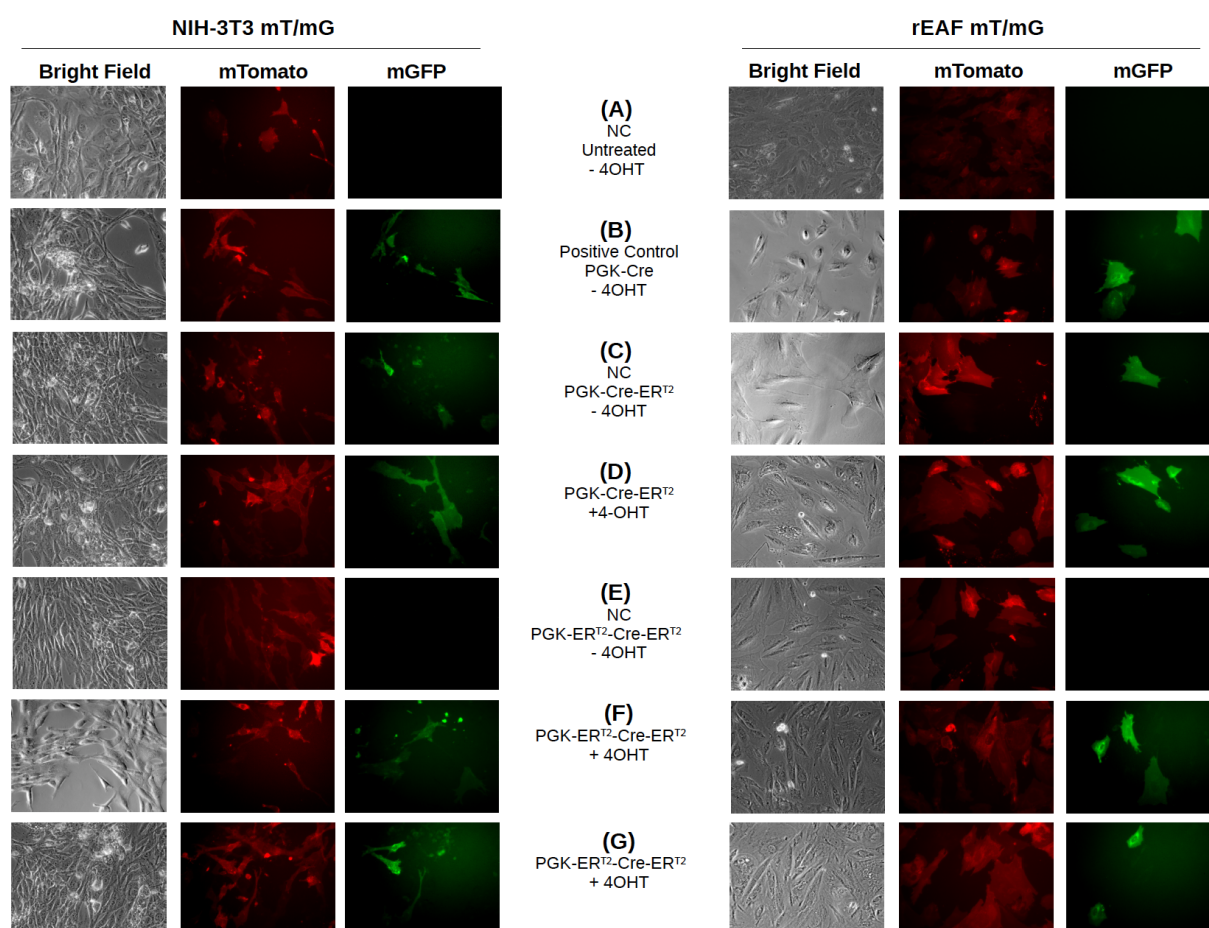


Figure 59: Functionality test of the pPGK-ERT²-Cre-ERT² and Cre-mediated recombination comparison between pPGK-Cre, pPGK-Cre-ERT² and PGK-ERT²-Cre-ERT² using mouse and rat reporter cells.

The reporter cells used were: mouse NIH-3T3 and rat EAF reporter cells. The cells express mTomato before 4-OHT induction, but after 4-OHT induction and Cre excision of the floxed mTomato sequence they express mGFP. Here, the pPGK-Cre-ERT² construct is leaky, and mGFP expression without 4-OHT induction was shown. In the other hand, the pPGK-ERT²-Cre-ERT² showed no background in the absence of the inducing agent. (A) Negative control: untreated cells; (B) positive control: transfected cells with pPGK-Cre; (C) transfected cells with pPGK-Cre-ERT² without 4-OHT induction; (D) transfected cells with PGK-Cre-ERT² and addition of 100nM of 4-OHT; (E): transfected cells with pPGK-ERT²-Cre-ERT² without 4-OHT induction; (F and G) transfected cells with pPGK-ERT²-Cre-ERT² and addition of 100nM of 4-OHT. Magnification of 20x.

Construction of SFTPC promoter

To amplify the 4.4 kb region of the SFTPC promoter by PCR, four overlapping fragments were amplified (with the oligonucleotides described in Table 23) and subcloned into pJET1.2, generating the pJET1.2+SPC-F1.1-R1.1; F4-R4; F3-R3 or F5-R5 vectors. Each vector was digested using restriction enzymes contained at the overlapping regions and then ligated to create the final pJET1.2_SFTPC vector containing the 4.4 kb fragment of the SFTPC promoter (see Figure 60).

Table 23: Oligonucleotides for the amplification of the porcine SFTPC 4.4 kb promoter

Oligonucleotides	Sequence 5' - 3'	Fragment and size
SP-C_F1.1 SP-C_R1.1 (<i>EcoRI</i>)	AGCCATTTGGTGCGGTCACA GCAGTGGCTCTGCATTGGCCT	2076 bp
SP-C_F4 SP-C_R4	GAGCGACAGCCTGAGAAAGGGC CTGCAAACCCAGCGTGCCG	1163 bp (overlapping with F1.1/R1.1 fragment)
SP-C_F3 SP-C_R3	AGTGGTGCACGCTGGAGGGA GGCGTCTGTGCCTGTGGACC	1510 bp (overlapping with F4/R4 fragment)
SP-C_F5- <i>SbfI</i> SP-C_R5-ex.1	GCACCTCATGCCTTTAGTAGTGCC CCTCCCCTGCTCATCCCCAAGT	510 bp (overlapping with F3/R3 fragment)

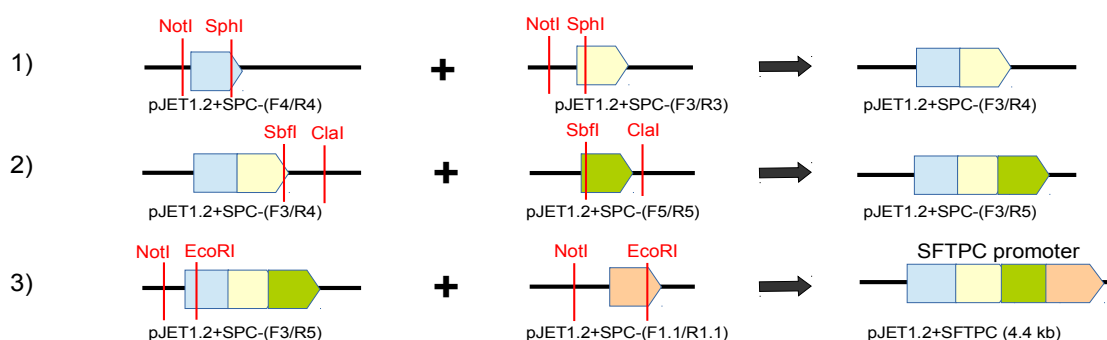


Figure 60: Localization of the amplified SFTPC promoter fragments and ligation into pJET1.2 cloning vector to generate the pJET1.2_SFTPC vector.

The pJET1.2+SPC-(F3-R3) and pJET1.2+SPC-(F4-R4) were digested using *NotI* and *SphI* restriction sites and ligated to create the pJET1.2+SPC-(F3-R4) vector. This was digested with *SbfI* and *ClaI* together with the pJET1.2+SPC-(F5-R5) vector to produce the pJET1.2+SPC-(F3-R5) vector. Then this and the pJET1.2+SPC-(F1.1-R1.1) were digested using *NotI* and *EcoRI* and ligated to generate the 4.4 kb SFTPC promoter (pJET1.2+SFTPC vector).

Cloning of the SFTPC promoter for dual luciferase assay

Two steps were necessary to make use of this reporter system. First it was necessary to generate more restriction sites 5' of SFTPC promoter to direct expression of the hRluc (*Renilla* luciferase) gene. Thus, the psiCHECK2 vector was double digested with *NheI* and *BamHI*, to isolate the transgenes, hRluc and hluc+ (firefly luciferase gene under the control of the HSV-TK, herpes simplex virus thymidine kinase promoter), from this vector sequence. Subsequently this fragment was cloned into the *BamHI-NheI* sites of the pSL1180 vector backbone (pSL1180_psiCHECK2). SFTPC promoter fragments, already subcloned into pJET1.2 vectors, were cloned into the pSL1180_psiCHECK2 vector. The cloning details and structures of the final vectors are shown in Figure 61.

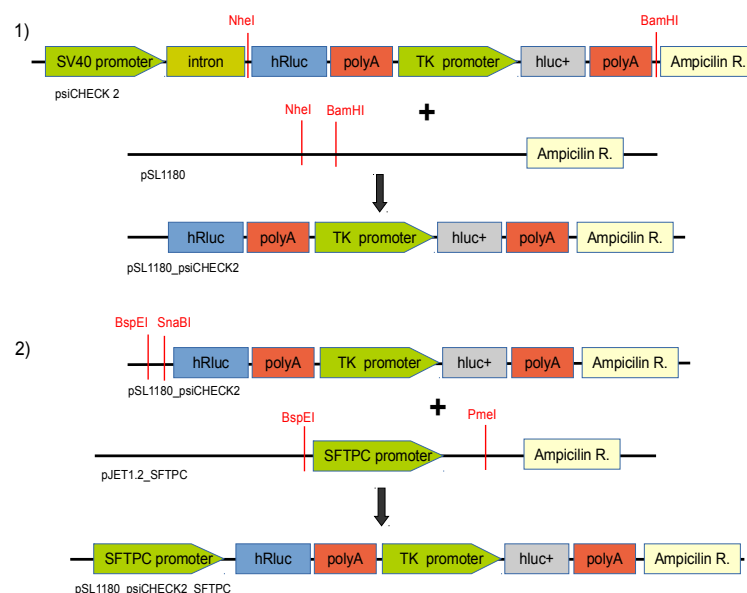


Figure 61: Schematic overview of psL1180_psiCHECK2 and psL1180_psiCHECK2_SFTPC vectors construction.

1) The original psiCHECK2 vector and the pSL1180 vector were cut with *NheI* and *BamHI* restriction enzymes and ligated, originating the pSL1180_psiCHECK2 vector. 2) The pJET1.2_SFTPC vector was cut with *BspEI* and *PmeI* restriction enzymes and was cloned into the pSL1180_psiCHECK2 vector into the *BspEI-SnaBI* sites to originate the final pSL1180_psiCHECK2_SFTPC vector.

Construction of ROSA26 gene targeting PDX-1 vector

In order to generate a porcine *ROSA26* gene targeting construct, carrying Cre recombinase driven by the PDX-1 promoter conventional cloning methods and based on the Gibson Assembly method (Gibson *et al.*, 2009) were used. The schematic diagram of the cloning steps to generate the psL1180_PDX-Cre_LSL_ROSA vector is indicate in Figure 62.

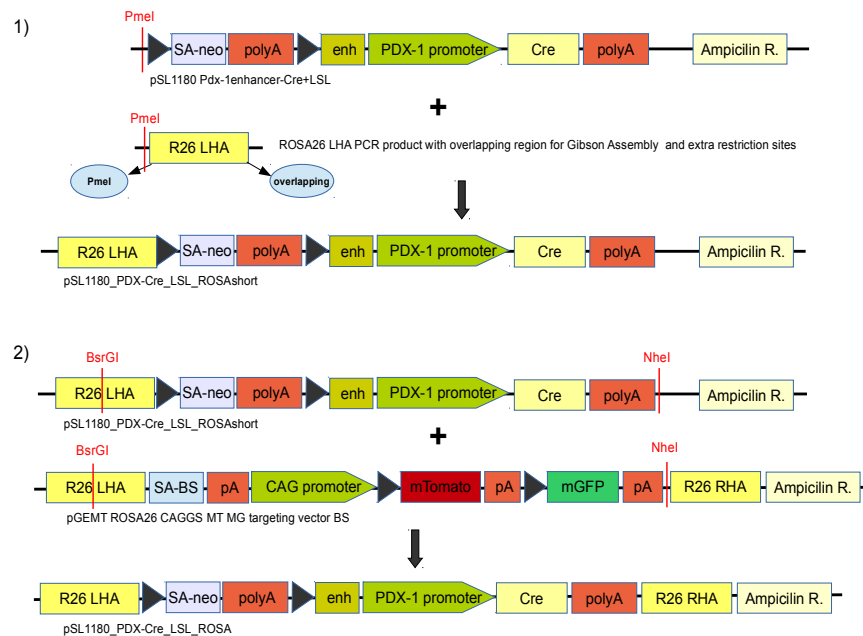


Figure 62: Schematic overview of the cloning steps to generate the gene targeting pSL1180_PDX-Cre_LSL_ROSA vector.

1) The pSL1180 Pdx-1enhancer-Cre+LSL vector was used to introduce the porcine *ROSA26* left homology arm by Gibson Assembly using a PCR product with a *PmeI* restriction site and an overlapping region. 2) The right homology arm of the porcine *ROSA26* locus was cloned into the pSL1180_PDX-Cre-LSL_ROSAshort vector, both cut with *BsrGI* and *NheI* restriction enzymes and the pSL1180_PDX-Cre-LSL_ROSA vector was obtained.

Construction of *ROSA26* tissue-specific Cre vectors for gene stacking

Transgenic dual fluorescent mTomato/mGFP reporter pigs were generated by Li S. *et al.*, 2014. These pigs carry a dual fluorochrome mTomato/mGFP cassette and prior Cre-recombination mTomato (red fluorescence) is expressed. After Cre-recombination mGFP (green fluorescence) is expressed and therefore, provide an indicator of tissue-specific Cre recombinase activity *in vivo*. Thus, gene stacking, an approach to add or replace at the same locus further transgenes, was used. Therefore, in order to generate a porcine *ROSA26* gene stacking construct, carrying Cre recombinase driven by the PDX-1 and the SFTPC promoters conventional cloning methods were used.

PDX-1 gene stacking vector

To generate the PDX-1 construct pSA-neo-PDX-Cre-R26-mT/mG to retarget at the *ROSA26* locus four cloning steps were necessary. All the steps with vectors used, restriction sites and originated vectors are indicated in Figure 63.

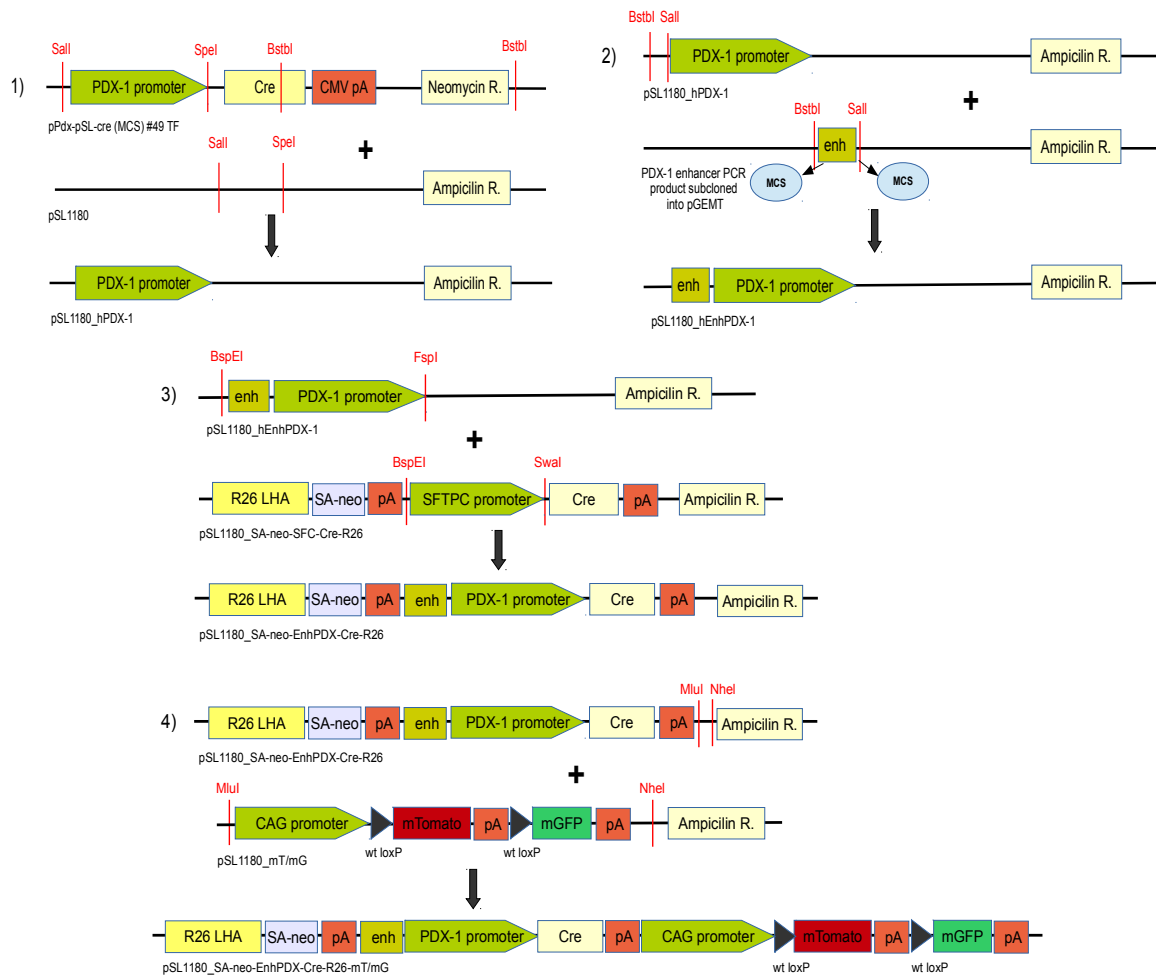


Figure 63: Molecular cloning schematic overview of the steps to generate the pSA-neo-PDX-Cre-R26-mT/mG vector.

To originate more restriction sites the PDX-1 promoter was cloned into the pSL1180 vector (1) and the PDX-1 enhancer was amplified by PCR and ligated with the pSL1180_hPDX-1 vector (2). Then the hEnhPDX-1 promoter was replaced by the SFTPC promoter from the pSL1180_SA-neo-SFC-Cre vector using *BspEI* and *SwaI* restriction sites (3). The pSL1180_mT/mG vector was cloned into the *MluI* - *AvrII* sites from the pSL1180_SA-neo-PDX-Cre-R26 vector to originate the final pSL1180_SA-neo-PDX-Cre-R26-mT/mG vector (4).

SFTPC gene stacking vector

Five cloning steps were necessary to generate the vector pSA-neo-SFC-Cre-R26-mT/mG for gene stacking strategy to retarget at the porcine *ROSA26* locus (see Figure 64).

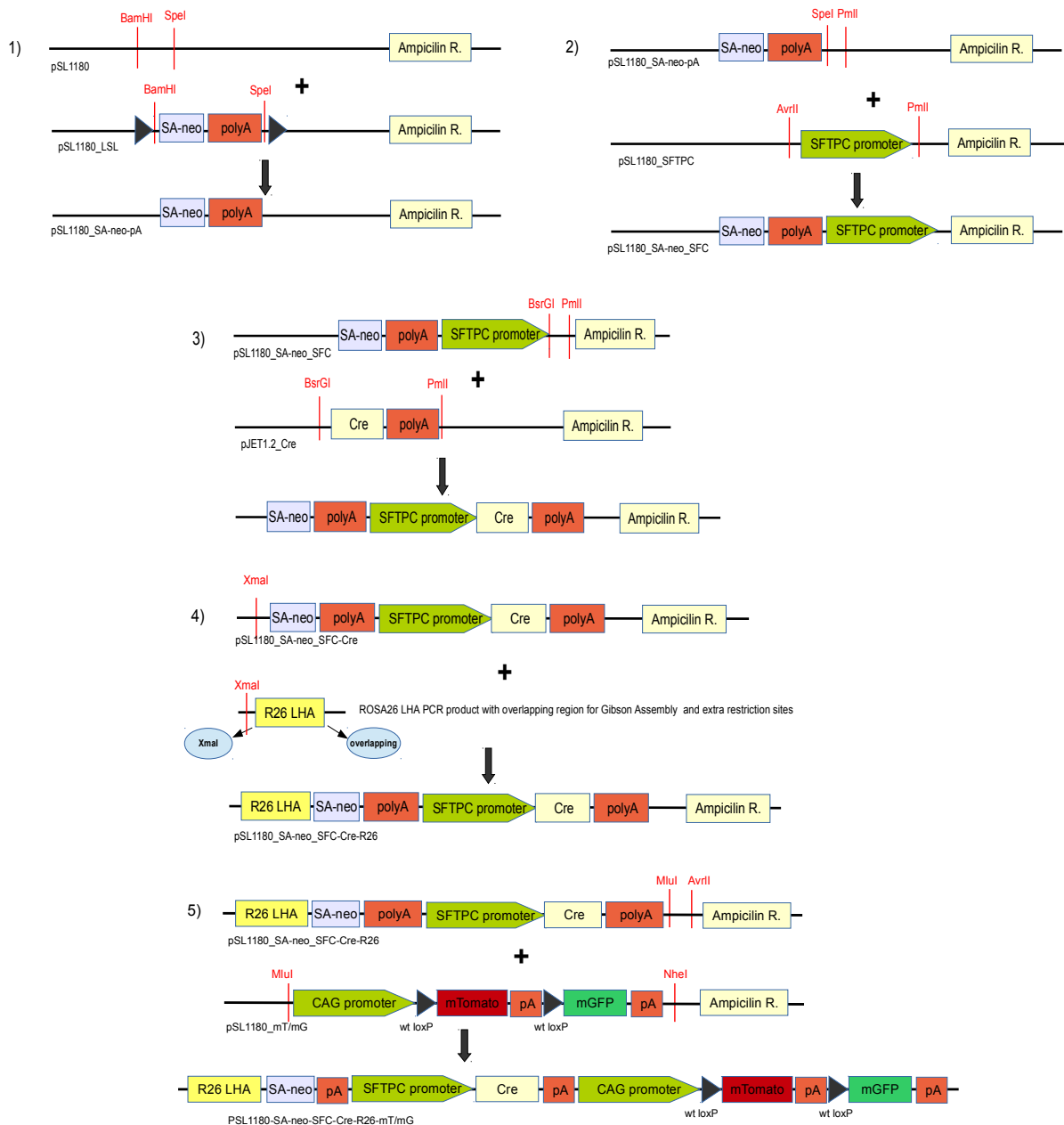


Figure 64: Schematic diagram of the cloning steps necessary to create the pSA-neo-SFC-Cre-R26-mT/mG vector.

1) The SA-neo cassette cut with *Bam*HI and *Spe*I restriction enzymes was cloned into the pSL1180 (pSL1180_SA-neo vector). 2) The porcine lung SFTPC promoter cut with *Avr*II and *Pml*I restriction enzymes was cloned into the *Spe*I-*Pml*I pSL1180_SA-neo vector (pSL1180_SA-neo-SFC). 3) The pJET1.2_Cre vector was cloned into the *Bsr*GI and *Pml*I sites from pSL1180_SA-neo-SFC vector, originating the pSL1180_SA-neo-SFC-Cre vector. 4) The porcine ROSA26 left homology arm was first amplified by PCR and cloned into the *Xma*I site of the pSL1180_SA-neo-SFC-Cre vector to originate the pSL1180_SA-neo-SFC-Cre-R26 vector. 5) The pSL1180_mT/mG vector was cloned into the *Mlu*I and *Avr*II sites from the pSL1180_SA-neo-SFC-Cre-R26 vector to originate the final pSL1180_SA-neo-SFC-Cre-R26-mT/mG vector.

Construction of iCre vectors

PGK-iCre and CAG-iCre vectors construction

The PGK promoter was cloned in order to drive the improved Cre (iCre) recombinase to compare the activity of the bacteriophage P1 Cre recombinase vector. Therefore, the coding sequence of Cre was replaced by the improved Cre, using the PGK-Cre and the pAAV-CAG-iCre (Addgene) vectors. The iCre cDNA, obtained from the pAAV-CAG-iCre plasmid, was isolated as a *Bam*HI and *Hind*III restriction fragment and placed under the control of the PGK promoter (see Figure 65-2).

The original pAAV-CAG-iCre plasmid was modified in order to eliminate the WPRE (woodchuck hepatitis virus post-transcriptional regulatory element) sequence using the restriction enzymes *Hind*III and *Sal*I (Figure 65-1).

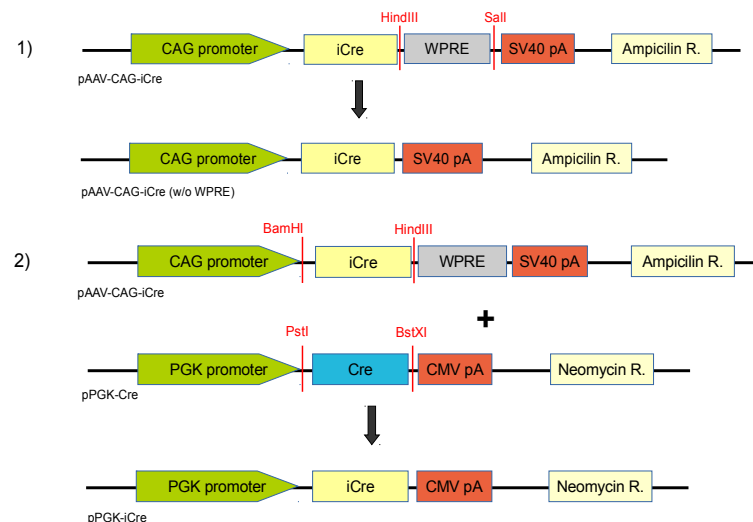


Figure 65: Schematic overview from molecular cloning steps of pPGK-iCre vector and pAAV-CAG-iCre (w/o WPRE) vector.

A) The WPRE sequence from the pAAV-CAG-iCre vector was removed after double digestion with *Hind*III and *Sal*I restriction enzymes and after a "fill-in" reaction to create blunt ends and then re-ligation was done. B) The same pAAV-CAG-iCre vector was also used in order to clone the iCre fragment into *Pst*I and *Bst*XI sites of the pPGK-Cre vector. This was done after creating blunt ends in order to replace the Cre recombinase for the improved Cre recombinase.

Modification of colon- and pancreas-specific Cre expression constructs

The codon-improved Cre recombinase sequence was used to replace the bacteriophage Cre recombinase coding sequence. In addition the sequence of the rabbit beta-globin intron (rb β G) was also cloned in some constructs, between the villin-1 or the PDX-1 specific-promoters and the iCre recombinase.

In this way the original villin-1 construct (mVil_CrehGHpA vector) and the PDX-1 construct (pSL1180 hPDX-1+enhancer w/o mutations, cloned by M.Sc. Heiko Guggemos) were used.

Villin-iCre and Villin-rb β G-iCre vectors construction

To create the changes cited above in the villin-1 vector (mVil_CrehGHpA), the Cre recombinase and the human growth hormone polyadenylation signal (hGH pA) coding sequences, were first isolated as a *Xma*I and *Aat*II restriction fragment. They were exchanged with the iCre recombinase and the simian virus 40 polyadenylation signal (SV40 pA) coding sequences, isolated as a *Bsp*EI and *Aat*II restriction fragment, from the pJet1.2_iCreSV40pA vector, to generate the pVillin_iCreSV40pA (see Figure 66).

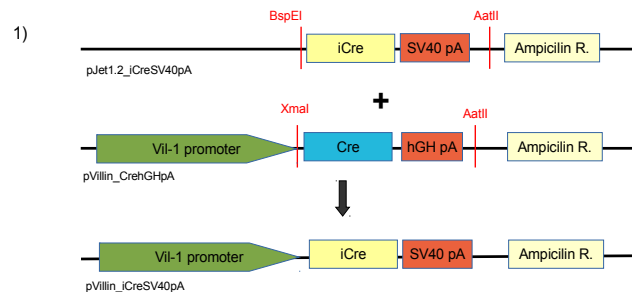


Figure 66: Schematic diagram of the cloning steps to create the pVillin_iCreSV40pA vector.

1) The mVil_CrehGHpA vector was cut with *Xma*I and *Aat*II restriction fragment to excise Cre and hGHpA. The vector was ligated with the *Bsp*EI and *Aat*II restriction fragment containing the iCre recombinase and the simian virus 40 polyadenylation signal (SV40 pA) coding sequence derived from the pJet1.2_iCreSV40pA vector. Thus, generating the pVillin_iCreSV40pA vector.

Furthermore, a similar construct was established, which contains the rabbit beta-globin intron. Therefore the vector pJet1.2_rb β G_iCreSV40pA was subjected to *Pml*I and *Aat*II restriction enzyme digestion in order to isolate the rb β G intron, the iCre recombinase and the SV40 pA signal coding sequences. These fragments were cloned into the mVil_CrehGHpA vector using *Sma*I and *Aat*II restriction fragment to obtain the pVillin_rb β G_iCreSV40pA (see Figure 67).

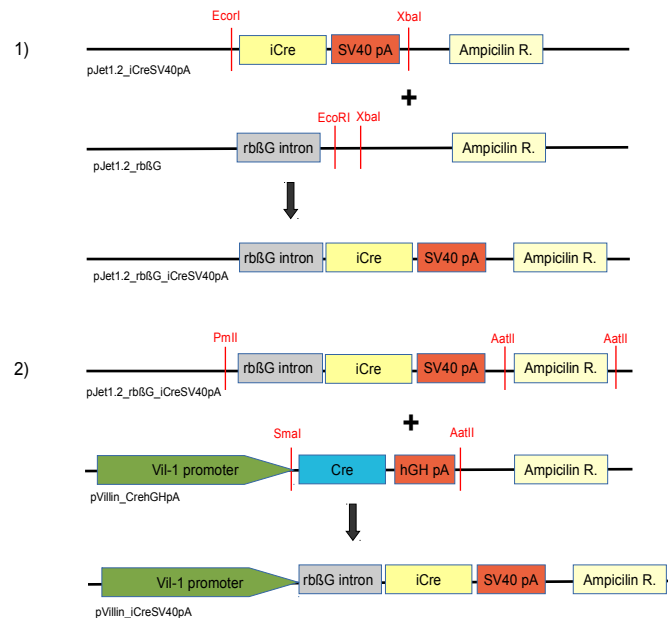


Figure 67: Schematic overview from molecular cloning steps of the pVillin_rbβG_iCre SV40pA vector.

1) To create a vector containing the rbβG intron, the iCre recombinase and the SV40 pA signal coding sequences, the iCre-SV40 pA were isolated as *EcoRI* and *XbaI* restriction sites and cloned upstream the rbβG intron (pJet1.2_rbβG vector). 2) The *PmlI* and *AatII* restriction enzymes cut up the rbβG intron, the iCre recombinase and the SV40 pA signal coding sequences from the pJet1.2_rbβG_iCreSV40pA vector. Thus, the Cre recombinase and the hGH pA, also isolated as a *SmaI* and *AatII* restriction fragment, from the mVil_CreGHpA vector, were replaced with those sequences, to obtain the pVillin_rbβG_iCreSV40pA.

PDX-iCre, PDX-rbβG-iCre and EnhPDX-rbβG-iCre vectors construction

Similar modifications were introduced into the PDX-1 constructs by M.Sc. Heiko Guggemos. Here, three different expression constructs were designed to direct pancreas-specific expression of iCre. These were:

- 1) the pEnhPDX-5'exon1_rbβG_iCreSV40pA plasmid, containing the human PDX-1 promoter region and enhancer, the 5' untranslated region of exon 1 and the iCre recombinase coding sequence;
- 2) the pHDX-5'exon1_rbβG_iCreSV40pA plasmid, same as vector number 1, but without the PDX-1 enhancer element;
- 3) the pHDX-5'exon1_iCreSV40pA, same as vector number 2, but without the rbβG intron.

To obtain the pSL1180_Enh-hPDX-5'exon1_rbβG_iCreSV40pA vector (Figure 68), first the sequence encoding for the renilla (from pHDX-5'exon1_rbβG_renilla vector), were changed by the sequences encoding the iCre recombinase and the SV40 pA signal (from pJet1.2_rbβG_iCreSV40pA vector), using *EcoRI* and *XbaI* restriction enzymes. Thus, generating the vector pJet1.2-hPDX-5'exon1_rbβG_iCreSV40pA. This vector was used to cut the 5'exon1, rbβG, iCre and SV40 pA signal coding sequences and to clone these fragments into the PDX-1 vector (pSL1180_hPDX-1+enhancer w/o mutations), using the *RsrII* and *XbaI*

restriction enzymes. After that the pSL1180_Enh-hPDX-5'exon1_rbβG_ iCreSV40pA construct was obtained (Figure 68).

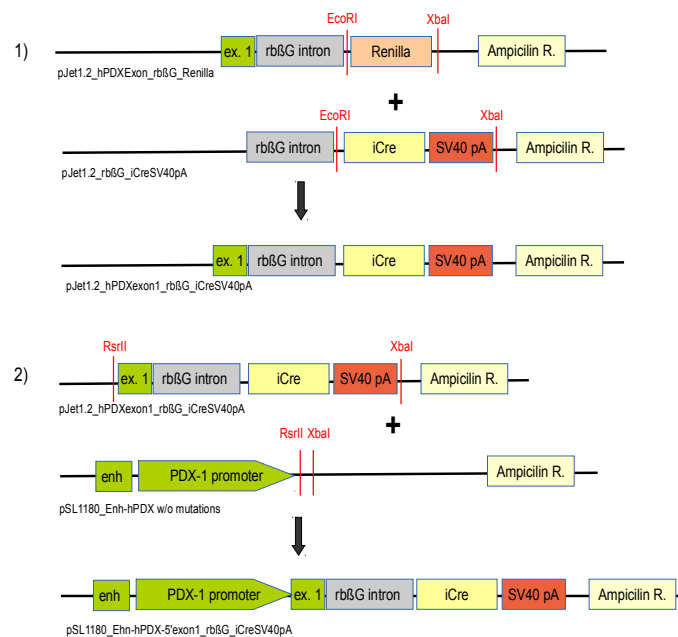


Figure 68: Schematic overview from molecular cloning steps of the pSL1180_Enh-hPDX-5'exon1_rbβG_iCreSV40pA vector.

1) The improved Cre (iCre) and the SV40 polyadenylation signal (SV40 pA) were used to replace the *renilla* from the pJet1.2_hPDXExon_rbβG_Renilla vector using *EcoRI* and *XbaI* restriction sites. 2) Thus, the PDX-1 exon1, the rabbit beta globin intron (rbβG) and the improved Cre-SV40pA were then cloned into the RsrII and XbaI restriction sites of the pSL1180_Enh-hPDX w/o mutations vector to generate the pSL1180_Enh-hPDX-5'exon1_rbβG_iCreSV40pA vector.

Further the pSL1180_Enh-hPDX-5'exon1_rbβG_iCreSV40pA construct was used to generate a vector without the PDX-1 enhancer, the pHPDX-5'exon1_rbβG_iCreSV40pA. Both restriction enzymes *PmeI* and *EcoRV* were used to excise the enhancer fragment and to make a religation (Figure 69-1). To produce a vector without the rbβG-intron, the PDX-1 promoter was cut with *EcoRI* and *BamHI* restriction endonucleases and inserted into same sites of the pSL1180_iCreSV40pA vector. Schematic representation of the pSL1180_hPDX-5'exon1_iCreSV40pA is shown in Figure 69-2.

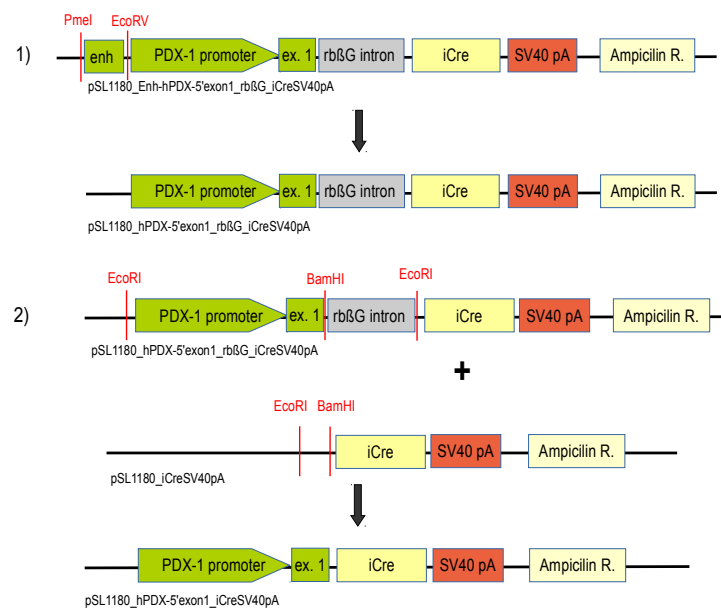


Figure 69: Schematic overview from molecular cloning steps of the pSL1180_hPDX-5'exon1_iCreSV40pA vector.

1) To eliminate the enhancer element from pSL1180_Enh-hPDX-5'exon1_rbβG_iCreSV40pA vector blunt enzymes *PmeI* and *EcoRV* were used and the vector was religated. 2) The pPDX-1 promoter and part of its exon1 were cut from the pSL1180_hPDX-5'exon1_rbβG_iCreSV40pA vector and cloned into the using *EcoRI* and *BamHI* sites from the pSL1180_iCreSV40pA vector. Thus, the pSL1180_hPDX-5'exon1_iCreSV40pA vector was obtained.

Generation of Cre recombinase vectors with 4-OHT binding domains

pPGK-Cre-ERT² vector construction

To generate the pPGK-Cre-ER^{T2} vector, the pSV40-βG-Cre-ER^{T2} vector was used to place the Cre-ERT² gene downstream of a PGK promoter. Thus, the Cre-ERT² gene, isolated as an *EcoRI* and *SacI* restriction fragment was cloned into the pSL1180 vector. Then, to place the Cre-ERT² under the control of the PGK promoter, they were digested with *BamHI* and *PmlI* restriction enzymes and cloned into the *BamHI* - *BstXI* sites of the pPGK-Cre vector (see Figure 70).

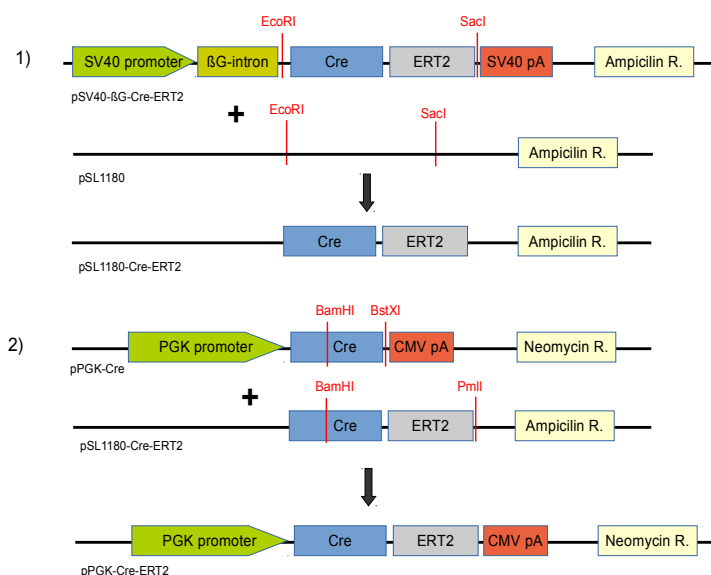


Figure 70: Schematic overview from two molecular cloning steps to generate the pPGK-Cre-ER^{T2} vector.

1) The Cre-ERT² gene, was isolated as an *EcoRI* and *SacI* restriction fragment and cloned into the same sites of the pSL1180 vector. 2) The pSL1180-Cre-ERT² vector was used to cut part of Cre and the ERT² coding sequences using *BamHI* and *PmlI* restriction enzymes. This fragment was clones into the *BamHI*-*BstXI* sites of the pPGK-Cre vector to originate the pPGK-Cre-ER^{T2} vector.

pPGK-ERT²-Cre-ERT² vector construction

To generate a Cre protein that contains a ligand binding domain at both of its termini, the previously designed PGK-Cre-ER^{T2} vector was modified by introducing another ER^{T2} at the N-termini of Cre coding sequence. The N-termini of ER^{T2} sequence as amplified by PCR and after 4 cloning steps the final construct was finished (see Figure 71).

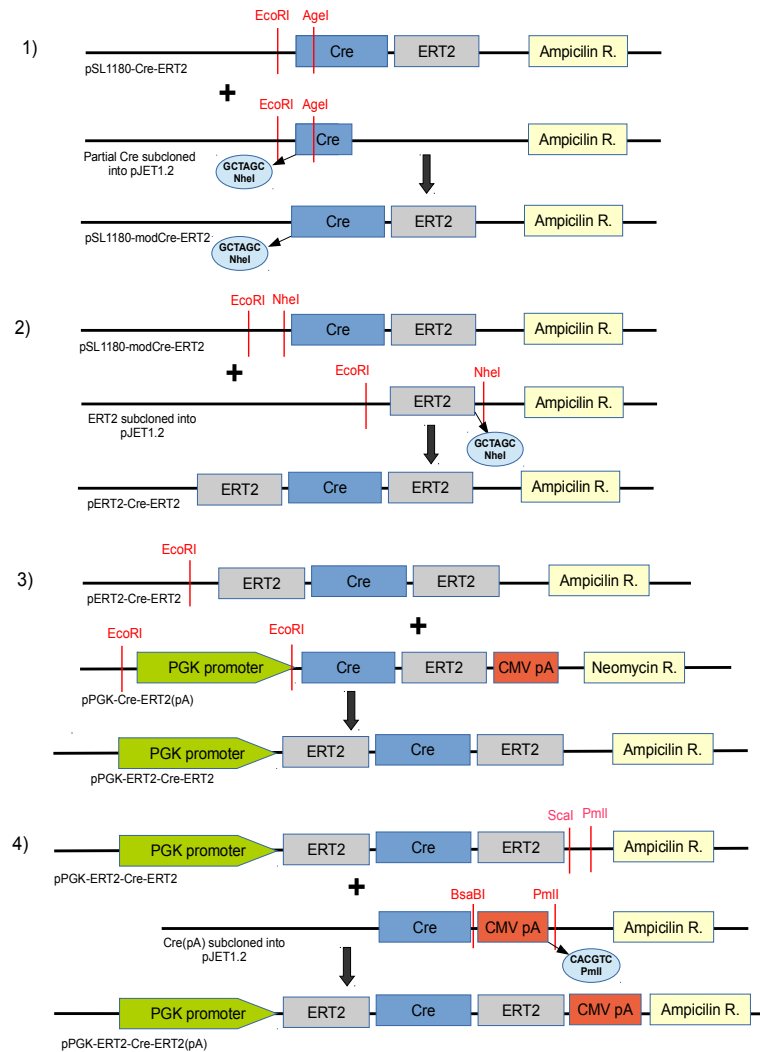


Figure 71: Schematic overview from four molecular cloning steps to generate the pPGK-ER^{T2}-Cre-ER^{T2} vector.

1) To create an *NheI* restriction site in front of Cre recombinase the PCR containing part of Cre and the *NheI* restriction site was used to replace part of Cre coding sequence from the pSL1180-Cre-ER^{T2} vector using *EcoRI* and *AgeI* restriction enzymes. 2) A ER^{T2} sequence amplified by PCR and also containing an extra *NheI* restriction site was placed in front of the modified pSL1180-Cre-ER^{T2} vector. 3) To place the ER^{T2}-Cre-ER^{T2} coding sequence under the control of the PGK promoter, digestion with *EcoRI* was made and cloned into *EcoRI* site of the pSL1180-ER^{T2}-Cre-ER^{T2} vector. 4) The CMV polyadenylation signal from the Cre(pA) vector was cut with *BsaBI* and *PmlI* and cloned into the *Scal*-*PmlI* sites of the pSL1180-ER^{T2}-Cre-ER^{T2} vector.

Sequencing alignments

PDX-Cre #357 pig

To sequencing the PDX-Cre pig, different primers were used. The primer were designed as:

- 3' junction: to sequence part of the right homology arm (RHA) until a point outside of the 3' prime of the porcine *ROSA26* locus.
- 5' junction: to sequence part of the intron 1 and the part of the left homology arm (LHA) of the porcine *ROSA26* locus;
- *lox2272* (left and right): to sequence both *lox2272* sites;
- Cre (forward and reverse): to cover the Cre recombinase coding sequence;

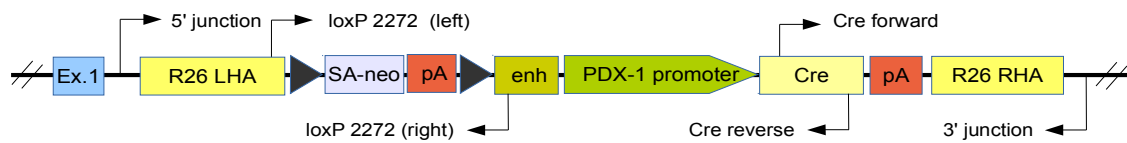


Figure 72: Localisation of the primers used for sequencing of the PDX-Cre #357 pig at the targeted porcine *ROSA26* locus.

5' junction forward primer is located in intron 1 of the porcine *ROSA26* locus; *lox2272* (left) forward is located at the end of the LHA; *lox2272* (right) reverse primer is located at the end of *PDX-1* enhancer element; Cre (forward) primer is located inside the Cre coding sequence; Cre (reverse) primer is located inside the Cre coding sequence and 3' junction reverse primer is located in a point outside of the porcine targeted locus.

3' junction

PDX-Cre pig	18655	AATACTACTATACAGAATTCACACAAGATCCCAACTTCTCTTAATCCCAGGGAGGTGTT	18714
Sequencing	528	AATACTACTATACAGAATTCACACAAGATCCCAACTTCTCTTAATCCCAGGGAGGTGTT	469
	18715	TAGGTTATTTCAATTCCTACTGTTAGCAAAGACTTTCTGCAACAGGAAAAGCAACTAAGG	18774
	468	TAGGTTATTTCAATTCCTACTGTTAGCAAAGACTTTCTGCAACAGGAAAAGCAACTAAGG	409
	18775	ATGAATAGTGACCAAGAGTAAACAAGAATTTACATGAAGTTTTTAATCAAAGACATCAG	18834
	408	ATGAATAGTGACCAAGAGTAAACAAGAATTTACATGAAGTTTTTAATCAAAGACATCAG	349
	18835	TTCTCTAGTAAAGAAGCCCAAACATCACCACCTTTCTGTACTGAATGAAAAATAAAATTT	18894
	348	TTCTCTAGTAAAGAAGCCCAAACATCACCACCTTTCTGTACTGAATGAAAAATAAAATTT	289
	18895	CTTTAAATATGGCTTGTGGTTCGCATACTTCATCTACAAGGCTCTTTGCTTCTATTTACA	18954
	288	CTTTAAATATGGCTTGTGGTTCGCATACTTCATCTACAAGGCTCTTTGCTTCTATTTACA	229
	18955	AATAGAAATGCTATTTAGTTCATGTATTAATCTGAATAACAGGTACATATTATGATTT	19014
	228	AATAGAAATGCTATTTAGTTCATGTATTAATCTGAATAACAGGTACATATTATGATTT	169
	19015	TTAAGGCAGATAGTAAACTTTCCCATAGATCTTAGGAGATTTGATCTTGTCTGTTGGGCAA	19074
	168	TTAAGGCAGATAGTAAACTTTCCCATAGATCTTAGGAGATTTGATCTTGTCTGTTGGGCAA	109
	19075	GCACTGTTTTACAGTGCTTCATTTTTTAAAGGTCAGGTAAGAACCTGACCAACTAAAT	19134
	108	GCACTGTTTTACAGTGCTTCATTTTTTAAAGGTCAGGTAAGAACCTGACCAACTAAAT	49
	19135	ATCAAAGCTGTATGGGCAATGAAATGTAACCTCATCCTCTGAT	19177
	48	ATCAAAGCTGTATGGGCAATGAAATGTAACCTCATCCTCTGAT	6

Figure 73: DNasequence alignment of 3' junction of the of the targeted porcine *ROSA26* locus from PDX-Cre pig.

Upper lane = PDX-Cre #357 pig; lower lane = sequencing results. Blue= part of right homology arm of the porcine *ROSA26* locus from PDX-Cre #357 pig. Red = point outside the homology arm of the porcine *ROSA26* locus from PDX-Cre #357 pig.

5' junction

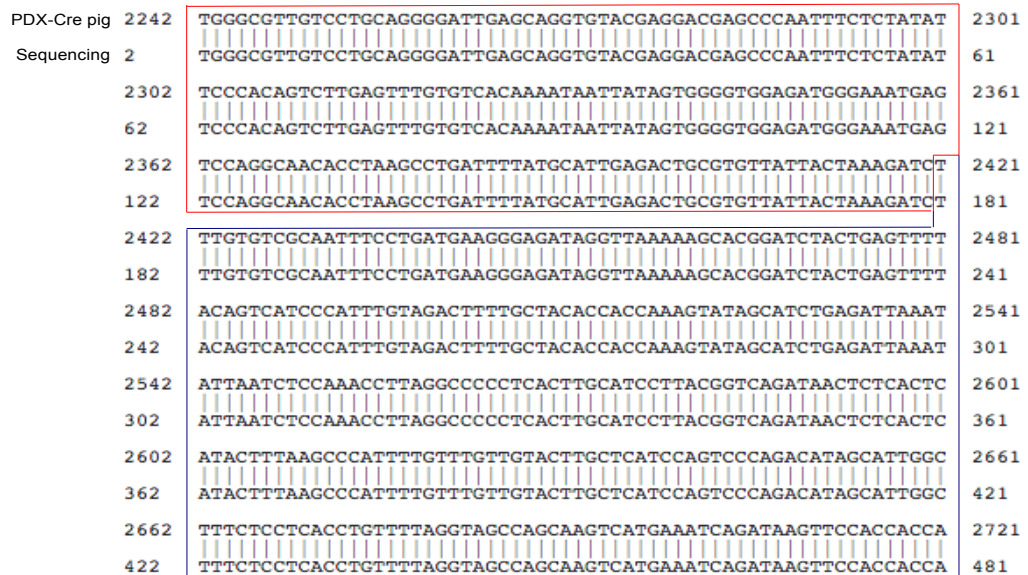


Figure 74: DNA sequence alignment of 5' junction of the of the targeted porcine *ROSA26* locus from PDX-Cre pig. Upper lane = PDX-Cre #357 pig; lower lane = sequencing results. Red = intron 1 of the porcine *ROSA26* locus from the PDX-Cre #357 pig. Blue = left homology arm of the porcine *ROSA26* locus from PDX-Cre #357 pig.

lox2272 (left)

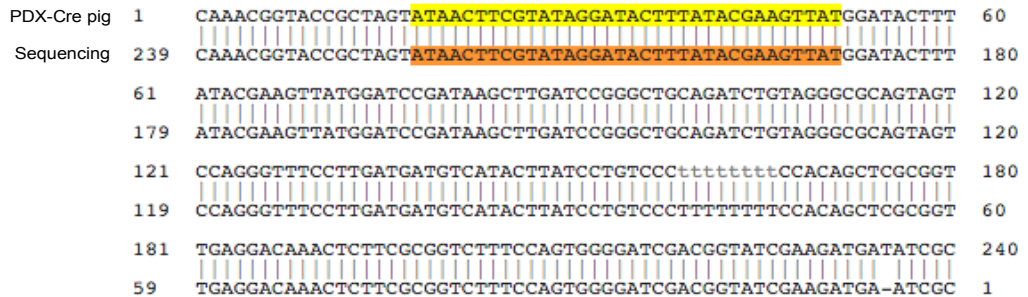


Figure 75: DNA sequence alignment of *loxP* 2272 (left) of the targeted porcine *ROSA26* locus from PDX-Cre pig. Upper lane = PDX-Cre #357 pig; lower lane = sequencing results. Yellow = *lox2272* site from the PDX-Cre #357 pig. Orange = *lox2272* site after sequencing.

lox2272 (right)

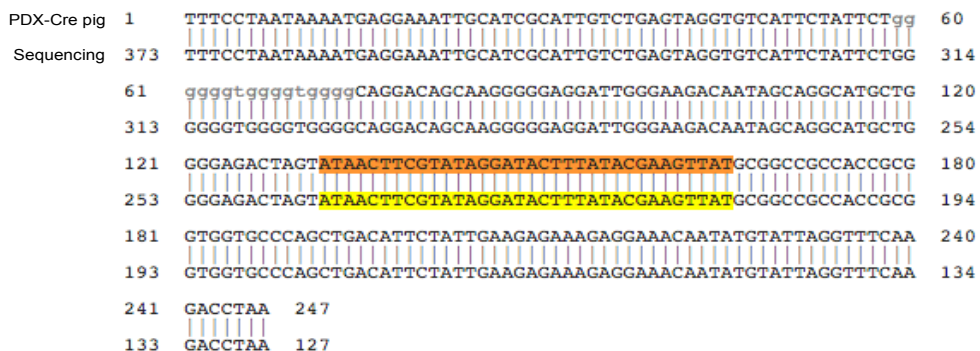


Figure 76: DNA sequence alignment of *lox2272* (right) of the targeted porcine *ROSA26* locus from PDX-Cre pig. Upper lane = PDX-Cre #357 pig; lower lane = sequencing results. Orange = *lox2272* site from the PDX-Cre #357 pig. Yellow = *lox2272* site after sequencing.

Cre (forward)

PDX-Cre pig	643	TCCATATTGGCAGAACGAAAACGCTGGTTAGCACCCGAGGTGTAGAGAAGGCACTTAGCC	702
Sequencing	1	TCCATATTGGCAGAACGAAAACGCTGGTTAGCACCCGAGGTGTAGAGAAGGCACTTAGCC	60
	703	TGGGGTAACTAACTGGTCGAGCGATGGATTTCCGTCTCTGGTGTAGCTGATGATCCGA	762
	61	TGGGGTAACTAACTGGTCGAGCGATGGATTTCCGTCTCTGGTGTAGCTGATGATCCGA	120
	763	ATAACTACCTGTTTTGCCGGGTGAGAAAAATGGTGTGCCGCGCCATCTGCCACCAGCC	822
	121	ATAACTACCTGTTTTGCCGGGTGAGAAAAATGGTGTGCCGCGCCATCTGCCACCAGCC	180
	823	AGCTATCAACTCGCGCCCTGGAAGGGATTTTGAAGCAACTCATCGATTGATTTACGGCG	882
	181	AGCTATCAACTCGCGCCCTGGAAGGGATTTTGAAGCAACTCATCGATTGATTTACGGCG	240
	883	CTAAGGATGACTCTGGTCAGAGATACCTGGCCTGGTCTGGACACAGTGCCCGTGTCCGAG	942
	241	CTAAGGATGACTCTGGTCAGAGATACCTGGCCTGGTCTGGACACAGTGCCCGTGTCCGAG	300
	943	CCGCGCGAGATATGGCCCGCTGGAGTTTCAATACCGGAGATCATGCAAGCTGGTGGCT	1002
	301	CCGCGCGAGATATGGCCCGCTGGAGTTTCAATACCGGAGATCATGCAAGCTGGTGGCT	360
	1003	GGACCAATGTAATAATGTGTCATGAACTATATCCGTAACCTGGATAGTGAACAGGGGCAA	1062
	361	GGACCAATGTAATAATGTGTCATGAACTATATCCGTAACCTGGATAGTGAACAGGGGCAA	420
	1063	TGGTGCCTGCTGCAAGATGGCGATTAGCTAAAAGGGCGAATTCAGCACACTGGCGGC	1122
	421	TGGTGCCTGCTGCAAGATGGCGATTAGCTAAAAGGGCGAATTCAGCACACTGGCGGC	480
	1123	CGTTACTAGATCATAATCAGCCATACCACATTTGTAGAGGTTTACTTGCTTT	1175
	481	CGTTACTAGATCATAATCAGCCATACCACATTTGTAGAGGTTTACTTGCTTT	533

Figure 77: DNA sequence alignment of Cre (forward) of the targeted porcine ROSA26 locus from PDX-Cre pig.
 Upper lane = PDX-Cre #357 pig; lower lane = sequencing results. Green = Cre recombinase coding sequence.

Cre (reverse)

PDX-Cre pig	1	TATGGCGCCGCTGCAGAAATCGCCCTTGCCACCATGGCACCCAGAAGAAGAGGAAGG	60
Sequencing	957	TATGGCGCCGCTGCAGAAATCGCCCTTGCCACCATGGCACCCAGAAGAAGAGGAAGG	898
	61	TGTCCAATTTACTGACCGTACACCAAAATTTGCCTGCATTACCGGTGATGCAACGAGTG	120
	897	TGTCCAATTTACTGACCGTACACCAAAATTTGCCTGCATTACCGGTGATGCAACGAGTG	838
	121	ATGAGGTTGCAAGAACCTGATGGACATGTTACGGGATCGCCAGGCGTTTTCTGAGCATA	180
	837	ATGAGGTTGCAAGAACCTGATGGACATGTTACGGGATCGCCAGGCGTTTTCTGAGCATA	778
	181	CCTGGAAAATGCTTCTGTCCGTTTGCCGGTCTGGGGCGCATGGTGAAGTTGAATAACC	240
	777	CCTGGAAAATGCTTCTGTCCGTTTGCCGGTCTGGGGCGCATGGTGAAGTTGAATAACC	718
	241	GGAAATGGTTTCCCGCAGAACCTGAAGATGTTCCGCGATTATCTTCTATATCTTCAGGCGC	300
	717	GGAAATGGTTTCCCGCAGAACCTGAAGATGTTCCGCGATTATCTTCTATATCTTCAGGCGC	658
	301	GCGGTCTGGCAGTAAAACTATCCAGCAACATTTGGGCCAGCTAAACATGCTTCATCGTC	360
	657	GCGGTCTGGCAGTAAAACTATCCAGCAACATTTGGGCCAGCTAAACATGCTTCATCGTC	598
	361	GGTCCGGGCTGCCACGACCAAGTGACAGCAATGCTGTTTCACTGGTTATGCGGCGGATCC	420
	597	GGTCCGGGCTGCCACGACCAAGTGACAGCAATGCTGTTTCACTGGTTATGCGGCGGATCC	538
	421	GAAAAGAAAACGTTGATGCCGGTGAACGTGCAAAACAGGCTCTAGCGTTCGAACGCACTG	480
	537	GAAAAGAAAACGTTGATGCCGGTGAACGTGCAAAACAGGCTCTAGCGTTCGAACGCACTG	478
	481	ATTTGACACAGGTTGTTCACTCATGAAAATAGCGATCGCTGCCAGGATATACGTAATC	540
	477	ATTTGACACAGGTTGTTCACTCATGAAAATAGCGATCGCTGCCAGGATATACGTAATC	418
	541	TGGCATTCTGGGGATTGCTTATAACACCCTGTACGTATAGCCGAAATGGCCAGGATCA	600
	417	TGGCATTCTGGGGATTGCTTATAACACCCTGTACGTATAGCCGAAATGGCCAGGATCA	358
	601	GGGTTAAAGATATCTCACCTACTGACGGTGGGAGAATGTTAATCCATATTGGCAGAACGA	660
	357	GGGTTAAAGATATCTCACCTACTGACGGTGGGAGAATGTTAATCCATATTGGCAGAACGA	298

Figure 78: DNA sequence alignment of Cre (reverse) of the targeted porcine ROSA26 locus from PDX-Cre pig.
 Upper lane = PDX-Cre #357 pig; lower lane = sequencing results. Orange and yellow = Kozak consensus sequence from PDX-Cre #357 pig and after sequencing, respectively. Pink = Nuclear localization signal of the SV40 large T antigen. Green = Cre recombinase coding sequence.

9 Acknowledgment

All work and all that exists is the result of a sum of efforts. Therefore, I would like to express my sincere thanks to all people who gave a little of themselves to support this realization.

Firstly, I would like to sincerely thank my research mentors Professor Dr. Angelika Schnieke, who gave me the opportunity to carry out my research work at the Livestock Biotechnology Institute at TUM in wonderful Freising and who was very helpful and supportive throughout my stay – thank you for the generous donation of your bike; Dr. habil. Tatiana Flisikowska and Dr. Anja Saalfrank, not only for the exceptional guidance but also for the friendship and patience they dedicated to every moment of support. Thank you for your expert advice and encouragement throughout this project, for always believing in me and for our shared time!

I also want to thank Dr. Alex Kind for the great discussions during our seminars and for correcting my PhD proposal, DAAD annual reports, abstracts and the thesis discussion chapter.

For reading this manuscript and for all comments, I would like to thank Professor Dr. Angelika Schnieke and Dr. habil. Tatiana Fliskowska. Special thanks go to Dr. Anja Saalfrank and Dr. Judy Kingman Ng, who provided corrections and excellent comments on my thesis.

Particular thanks go to Herr Dr. Fischer. Thank you for the encouraging words, continuous help, numerous advices, discussions and for always seeing things in a positive way! Thanks, also for your delicious Brazilian food recipes ideas and cooking for us! I also wish to express a special gratitude to Peggy Müller-Fliedner, and Marlene Stumbaum for providing me with a fantastic lab training, helping me in some difficult cloning steps (this goes also for Alexander Carrapeiro - thank you Alex) and our shared time in the lab and outside, as well as to Sulith Christan for keeping me well equipped in the lab, her advice on life and her positive vibe!

I am very grateful to Beate Rieblinger, Kilian Skowranek and Carolin Perleberg for our wonderful time at the chair, barbecues at the lake, nice evenings and friendship! I am very thankful for Denise Nguyen's support in onboarding, for the legendary parties organized by Dr. habil. Krzysztof Flisikowsky, for the invaluable assistance of Barbara Bauer and for the support of the colleagues of the Chair of livestock Biotechnology that have not been explicitly mentioned here. I also want to thank my students Aileen Elisabeth Seidl, Daniel Solvie, Chris Ludwig, Lisa-Marie Jordan, Tanja Stratz and Niko Seifert for their work and the nice time together.

This project would have been impossible without the support of the German Academic Exchange Service - DAAD, and the help of Maria José Salgado Martinez from DAAD.

Last but not least, thanks go to my mother Jussara, my father Rudolfo, my brothers Alexandre and Edwin Schulze and my husband Dr. Philipp Höfer for permanently encouraging and believing in me. They are most valuable to me and I dedicate this thesis to them.

10 Curriculum Vitae

Personal Information:

Name: Érica Alessandra Schulze

Date of birth: 05.04.1982

Place of birth: Curitiba - Brazil

Educational Background:

04/2012 – 12/2015*

*Experimental work

Ph.D. (Molecular biotechnology)

Chair of Livestock Biotechnology, Technical University of Munich, Germany

"Cre/loxP-mediated tissue specific activation of oncogene expression in pigs".

08/2007 – 10/2009

Master of Science (Bioprocess technology)

Department of Chemical Engineering, Federal University of Rio de Janeiro, Brazil

(12/2008 – 06/2009)

- Biotechnology Research Institute | National Research Council Canada, Montreal

"Production of recombinant adeno-associated viruses (rAAVs) in transfected HEK-293 cells cultured in suspension".

(01/2008 – 11/2008)

- Immunobiological Technology Institute (Bio-Manguinhos), Rio de Janeiro, Brazil

Cultivation and infection of Vero cells to produce dengue fever virus type 2 using adherent and suspension cultures and different types of cell culture media.

08/2003 – 08/2007

Bachelor of Science (Industrial pharmacy)

Department of Pharmacology, Federal University of Paraná, Curitiba, Brazil

(01/2007 – 07/2007)

- Immunobiological Technology Institute (Bio-Manguinhos), Rio de Janeiro, Brazil

"Cultivation and infection of Vero cells to produce yellow fever virus in cell culture flasks, spinner flasks and bioreactors using microcarriers".

08/2000 – 02/2003

Faculty of Nursing

Department of Nursing, Federal University of Paraná, Curitiba, Brazil

Professional Work:

03/2018

Global Product Manager - Vaccine

01/2017– 03/2018

Media Application Specialist - Biotechnology

- Sartorius Stedim Biotech, Göttingen, Germany

Support customers in cell culture media applications for the production of biopharmaceuticals and vaccines.

09/2016 – 12/2016

Research associate (Molecular Biology)

- Chair of Livestock Biotechnology, Technical University of Munich, Germany

Generation of porcine cell clones expressing an improved Cre recombinase driven by a pancreas-specific promoter.

10/2009 – 05/2011 Research associate (Animal cell technology)
 - Cell Culture Engineering Laboratory, Federal University of Rio de Janeiro, Brazil
Production of different recombinant proteins in mammalian cells.

Publications:

Saalfrank, A., Janssen, K-P., Ravon, M., Flisikowski, K., Eser, S., Steiger, K., Flisikowska, T., Müller-Fliedner, P., Schulze, E. A., Brönnner, C., et al. 2016. "A porcine model of osteosarcoma." *Oncogenesis*; 5(3):e210.

Chahal, P. S., Schulze, E. A., Tran, R., Montes, J., Kamen, A. A. 2014. "Production of adeno-associated virus (AAV) serotypes by transient transfection of HEK293 cell suspension cultures for gene delivery." *Journal of Virological Methods*; 196(2): 163–173.

Souza M. C., Freire M. S., Schulze E. A., Gaspar L. P., Castilho L. R. 2009. "Production of yellow fever virus in microcarrier-based Vero cell cultures." *Vaccine*; 27(46): 6420-6423.

Posters:

04/05/2016 – 07/05/2016 Chahal, P. S., Schulze, E. A., Bernier, A., Lanthier, S., Coulombe, N., Kamen, A., Gilbert, R. "Towards Large-Scale Manufacturing of Adeno-Associated Virus by Transient Transfection of HEK293 Suspension Cells in a Stirred Tank Bioreactor Using Serum-Free Medium". ASGCT 19th Annual Meeting. Washington D.C, USA.

25/09/2015 – 29/09/2015 Wander, C., Schulze, E. A., Flisikowska, T., Flisikowski, K., Saur, D., Wolf, E., Kind, A., and Schnieke, A. "The pig as a model for human cancer." 18th ECCO - 40th ESMO European Cancer Congress. Vienna, Austria.

28/10/2010 – 29/10/2010 Schulze, E. A., Gutierrez, E., Amable, P. R., Castilho, L. R. "Genetic modification of animal cells: experimental planning application to improve transfection efficiency." Anual Colloquium of Chemical Engineering. Rio de Janeiro, Brazil.

06/06/2010 – 11/06/2010 Schulze, E. A., Chahal, P., Medronho, R. A., Castilho, L. R., Fernandes, J., Kamen, A. A. "Production of serotype 6-derived recombinant adeno-associated virus in serum-free suspension cultures of HEK 293 cells. Vaccine Technology III. Puerto Vallarta, Mexico.

27/05/2009 – 30/05/2009 Chahal, P., Schulze, E. A., Tran, R., Montes, J., Grieger, J., Samulski, J., Kamen, A. "Manufacturing of Adeno-Associated viruses of different serotypes for gene therapy applications." ASGCT 12th Annual Meeting. California, USA.

01/06/2008 – 06/06/2008 Schulze, E. A., Sousa, M. C. O., Medronho, R. A., Freire, M. S., Castilho, L. R. "Comparison of dengue-2 virus production in vero cells under serum-free and serum containing conditions". Vaccine Technology II. Algarve, Portugal.

01/06/2008 – 06/06/2008 Sousa, M. C. O., Schulze, E. A., Gaspar, L. P., Castilho, L. dos R., Freire, M. S. "Production of yellow fever virus in vero cells grow in serum-free medium." Vaccine Technology II. Algarve, Portugal.

10/10/2007 – 11/10/2007 Schulze, E. A., Sousa, M. C. O., Freire, M. S., Castilho, L. dos R. "Comparison of yellow fever virus production in Vero cells using different cell culture serum-free media." XXIX Giulio Massarani Journey of Scientific, Cultural and Artistic Initiation of Federal University of Rio de Janeiro. Rio de Janeiro, Brazil.